ABSTRACT

Title: GENERALISATION AND BAYESIAN SOLUTION OF THE GENERAL RENEWAL PROCESS FOR MODELLING THE RELIABILITY EFFECTS OF IMPERFECT INSPECTION AND MAINTENANCE BASED ON IMPRECISE DATA

Andrew Guiseppe Jacopino, Doctor of Philosophy (Ph.D.) in Reliability Engineering, 2005

Directed By: Professor Ali Mosleh, Department of Mechanical Engineering

Common Stochastic Point Processes used in the analysis of Repairable Systems do not accurately represent the true life of a repairable component mainly due to the underlying repair assumption. Specifically, the Ordinary Renewal Process uses an as-good-as-new repair assumption while the Non-Homogenous Poisson Process uses an as-bad-as-old repair assumption. However, it is highly unlikely that any repairable system will readily fit into either repair assumption. Additionally, there is the possibility that any inspection or maintenance activity may actually worsen the system; worse-than-old. Regardless of the underlying repair assumptions and the limitation they impose on any solution, these point processes continue to be used to assist engineering and logistic decision making. While other solutions, mainly GRP based, have offered some resolution, no solution has sufficiently resolved the combined complexities of imperfect maintenance of multiple dependent failure

modes, imperfect inspections and data uncertainty, specifically unknown times to failure.

Accordingly, the solution offered here offers a model that can contend with all these factors through a Bayesian solution thereby allowing additional “soft-data” to be utilised during the analysis. The modelling scheme consisted of 10 cases divided into 2 main types; Type I with known failure times, and Type II with unknown failure times (data uncertainty). Each of the cases are incrementally modified through the addition of factors including imperfect maintenance of a single failure mode through to multiple dependent failure modes, and finally imperfect inspection. Generalisation of the GRP equations and Bayesian estimation models were developed for these cases. As a closed form solution to each of these cases is unavailable, numerical procedures were formulated. Specifically, an alternative Markov Chain sampling methods, Slice Sampling, was utilised to solve the Bayesian implementation of the needed extensions to the KIJIMA Type I GRP model with an underlying 2-parameter Weibull Time-To-Failure distribution.

Based on a number of examples the resulting models have shown the ability to accurately predict future failure trends. Furthermore, the model provides a number of insights into the results including relative maintenance effectiveness and the merit of optimising imperfect maintenance or inspection to maximise availability.

GENERALISATION AND BAYESIAN SOLUTION OF THE GENERAL RENEWAL PROCESS FOR MODELLING THE RELIABILITY EFFECTS OF IMPERFECT INSPECTION AND MAINTENANCE BASED ON IMPRECISE DATA

By

Andrew Guiseppe Jacopino.

Dissertation submitted to the Faculty of the Graduate School of the
University of Maryland, College Park, in partial fulfillment
of the requirements for the degree of
Doctor of Philosophy (Ph.D.)
in Reliability Engineering
2005

Advisory Committee:
Professor A. Mosleh, Chair
Professor M. Modarres
Associate Professor J. Bernstein
Associate Professor P. Sandborn
Professor G.B. Baecher, Dean's Representative

Preface

The following Dissertation has been written in *Australian* English and therefore the spelling throughout will be based on that found in the official *Australian* English Dictionary, the Macquarie Dictionary (www.macquariedictionary.com.au).

Dedication

Firstly my appreciation to Professor Ali Mosleh who had the vision to allow me to undertaken the last portion of this PhD via distance from Australia. I truly appreciate his perseverance and understanding with me in achieving this outcome especially given a number of dramatic changes in my personal circumstances during this time.

To my two “study buddies”, Tess and Remy, who have kept it all in perspective by tirelessly ignoring all facets of this research by sleeping under my desk throughout the period of study both in the USA and in Australia.

To my two children, Courtney and Connor, who have helped put it into perspective when there were problems.

Finally, my deepest thanks to my wife Nina, who has put up with the high and lows, the late nights on the computer and early morning calls to the USA, and the unaccompanied travel to the USA.

Acknowledgements

I would like to thank Dr Frank Groen (Prediction Technologies - http://www.prediction-technologies.com/index.htm) who gave his precious time to act as a mentor and an active participant in achieving this goal. Without his encouragement and support I wouldn't be where I am now.

I would also like to thank various personnel within the Royal Australian Air Force (RAAF) and the Defence Materiel Organisation (DMO) for allowing me opportunity to pursue this research and providing support. This includes Wing Commander Phil Tammen, Wing Commander Leon Phillips, Wing Commander Debbie Richardson, Squadron Leader David Haughton and Flight Lieutenant Ben Krutop.

Table of Contents

List of Tables

List of Figures

List of Equations

Chapter 1: Introduction

Repairable Item Models

Common Stochastic Point Processes used in the analysis of Repairable Systems do not accurately represent the true life of a repairable component due to the underlying repair assumption. Specifically, the Ordinary Renewal Process (ORP) uses an *as-good-as-new* repair assumption while the Non-Homogenous Poisson Process (NHPP) uses an *as-bad-as-old* repair assumption. However, it is highly unlikely that any repairable system will readily fit into either repair assumption. Additionally, there is the possibility that any inspection or maintenance activity may actually worsen the system; *worse-than-old*.

One model that can be used to address the repair assumption concern is the General Renewal Process (GRP), introduced by KIJIMA and SUMITA[1]. Simplistically GRP addresses the repair assumption by introducing the concept of *Virtual Age* into the Stochastic Point Processes to enable them to represent the full spectrum of repair assumptions[2]. The GRP model, sometimes referred to as *better-than-old-but-worse-*

---

1 KIJIMA, M. and SUMITA, U., "*A Useful Generalisation of renewal Theory: Counting Processes Governed by Non-Negative Markovian Increments*", Journal of Applied Probability, #23, 1986, pp. 71-88

2 Defined as "*A repairable system may end up in one of the five possible states after a repair: 1. as good as new; 2. as bad as old; 3. better than old but worse than new; 4. better than new; 5. worse than old.*", YANEZ, M., JOGLAR, F, and MODARRES, M., "*Generalized renewal process for analysis of repairable systems with limited failure experience*", Reliability Engineering and System Safety, Vol 77, USA, 2002, p167

than-new repair assumption, in its simplest form defines a single parameter, q, to represent the *Goodness of Repair*, or *Repair Effectiveness*.

While the concept of *Virtual Age* introduced by KIJIMA and SUMITA[3] in the form of a GRP model has started to make significant in-roads into the modelling and analysis of repairable items[4], there is little literature on the practical application, interpretation, or even applicability of this technique. Specifically, while the current engineering literature[5] discusses the method, based on a Maximum Likelihood Estimator (MLE) approach used to find a single q, they do not include any discussion on either the implementation of the method or interpretation of the results (e.g. What does q = 0.67 mean? What should I do and why should I care?). Consequently, without an understanding of the underlying GRP methodology and subsequent meaning and sensitivity of all the GRP variables, potentially there is the GRP model simply becomes a different type of 3-parameter Weibull equation for an analyst to use.

3 ibid

4 KAMINSKIY, M. and KRIVTSOV, V., *"A Monte Carlo Approach to Repairable System Reliability Analysis"* in *Probabilistic Safety Assessment and Management*, Springer-Verlag London Ltd, 1998, pp 1063-1068; YANEZ, et al, loc cit; METTAS, A. and ZHAO, W, Modeling and Analysis of Repairable Systems with General Repair, *2005 Proceedings Annual Reliability, Availability and Maintainability Symposium (RAMS06)*, Alexandria, VA, USA, 24-27 Jan 2005; JACK, N., "*Age Reduction Models for Imperfect Maintenance*", Mathematical Sciences Division, School of Informatics, University of Abertay, Dundee, Scotland; HURTADO, J.L., JOGLAR, F. and MODARRES, M., "*Generalized Renewal process: Models, Parameter Estimation and Applications to Maintenance Problems*", International Journal of Performability Engineering, Vol1, No. 1, July 2005, pp 37-50

5 ibid

While the current solutions from the engineering literature[6] offer resolution of the maintenance assumption, they do not address the full spectrum of complexities that exists in wider reliability community. Specifically, these complexities include the simultaneous ability to address:

- imperfect corrective and/or imperfect preventative maintenance for multiple failure modes existing in a single component including addressing failure mode dependencies (e.g. repair of failure mode 1 may effect the *Virtual Age* of failure mode 2 by making the future failure earlier or later);
- imperfect inspection for multiple failure modes for a single component;
- data uncertainty in terms of unknown failure times (i.e. observe a failure at next inspection but cannot establish exactly when the failure occurred within the inspection period); and
- use of "soft-data" (e.g. data from similar equipment such as previous models, engineering judgement, etc) as an input to model.

Although the limitations due to the underlying repair assumptions on any results is widely known, these point processes continue to be used to assist engineering and logistic decision making. Therefore, despite the best endeavours of both engineering and logistics staff to optimise the maintenance and spares philosophy, any solution will be suboptimal.

---

6 ibid

Accordingly, one of the main reasons for the increasing interest in GRP is the desire for a more accurate model which may lead to a reduced Total Cost of Ownership (TCO). One industry that is spending considerable resources in identifying and controlling their TCO is the aviation industry.

Total Cost of Ownership (TCO) in the Aviation Industry

The aviation industry acknowledges that aircraft can be directly influenced by the Reliability, Availability and Maintainability (RAM) Measures of Effectiveness (MOEs) to the extent that only 20% of the overall TCO is typically attributed to the "up-front" acquisition cost. In fact a recent detailed investigation by the Australian Defence Science and Technology Organisation (DSTO) found that over a 15 year aircraft life the acquisition cost of one fleet of aircraft was shown to be only 13%, with the other 87% in sustainment costs. This represents a significant amount of money. For example, the Australian Department of Defence (DOD) spends approximately 1 Billion Australian Dollars (AUD1B) (750 Million US Dollars), or 5.7% of the total annual Australian Defence budget of AUD17.5B (13.125 Billion US Dollars) on sustainment of their aircraft, which only total 283 fixed wing and 145 rotary wing aircraft of various complexity and age.

Moreover, one the major costs identified within the TCO is the management of Repairable Item(s) (RI) (components) which can be defined as "*An item which can be* *restored to perform all of its required functions by corrective maintenance.*"[7]. As part of the report DSTO found that of the 9.25% of the TCO could be attributed to the management of RIs. In this example the TCO was calculated as AUD8.1B and therefore the cost of managing RIs was a surprising AUD0.749B.

Repairable Item Management

Additionally, RI management can affect the Operational Availability[8] (A_o) of both individual aircraft and whole fleets by ensuring that a serviceable spare is available to the user within a prescribed timeframe. Clearly the key to ensuring that this occurs is to know the arising rate[9] in order to calculate the total number of spares based on a prescribed repair Turn-Around Time (TAT).

---

7 Military Standard 721C (MIL-STD-721C), Definitions of Terms for Reliability and Maintainability, 12 June 1981, pg 9

8 Operational Availability is defined as the percentage of time that an item is in a commitable state when considering both corrective and preventative maintenance, and spares and maintenance delays. These delays are typically referred to as Administrative and Logistics Delay Time (ALDT). Logistics Time Delay (LTD) is defined as the accumulated time during which a maintenance action cannot be performed due to the necessity to acquire maintenance resources, excluding any administrative delay. LDT includes time waiting for a Spare to become available, time waiting for an item of test equipment, time waiting for transportation, time waiting to use a facility, etc. LDT may also be referred to as Supply Delay Time. Administrative Delay Time (ADT) is defined as the accumulated time during which an action of corrective maintenance on a faulty item is not performed due to administrative reasons. Typical examples of ADT include time raising paperwork for the job, time assigning personnel priorities, Labour strike, time taken to travel to equipment site, time taken to complete paperwork to release equipment from maintenance, etc. Refer to ELBING, "An Introduction of Reliability and Maintainability Engineering", McGraw-Hill, USA, 1997, Section 11.1.3, pg 256, for further discussion.

9 It is important to note that arising rate has been deliberately used since RI management within the aviation industry is concerned whether an RI has been demanded by a user regardless of whether an actual failure has occurred. For example, consider a positive failure indicator by the aircraft maintenance Built In Test (BIT) which, after an investigation no failure can be found (typically referred to as Nil Fault Found (NFF)). In this case regardless that a failure didn't occur or couldn't be detected, the aircraft stopped (or couldn't start) flying and cause a maintenance action was required.

The reason for the interest in the optimal management of RIs from the aviation industry is divided into 2; those reasons that link to defence and those that link to commercial/civilian objectives.

Commercial Aviation Concerns with Traditional Repairable Item Management

Commercial aviation industry's focus is on A_o to maximise shareholder profits through optimal utilisation of the individual aircraft. To achieve this they will often purchase additional "insurance" spares to ensure that the ALDT, specifically the delay due to a lack of a spare, is minimised. However, the cost of these "insurance" spares, both in terms of initial purchase and on-going repairs if maintenance is required regardless of whether fitted (i.e calendar based), is a significant portion of the overall TCO. Accordingly, given the marginal profit margin that the commercial aviation industry operates under, especially post 11 September 2001, a more accurate model that realistically reflects the aviation environment is clearly warranted.

Defence Aviation Concerns with Traditional Repairable Item Management

Unlike commercial aviation organisations, defence aviation is not driven by profit, but rather the optimisation of operational capability[10] of the aircraft while achieving *Value For Money*.

[10] Operational Capability includes Systems Readiness (i.e. Availability), Mission Success (i.e. Mission Reliability), Logistics Footprint (i.e. support required to operate the aircraft such as maintenance staff, spares, test equipment, etc) and Demand Satisfaction Rate (i.e. availability of spares).

Life of an Aviation Repairable Item

Before cases (models) can be developed to support this approach it is important to understand the "life" of an aviation RI. As can be seen from Figure 1 the "life" of an RI has a significant amount of variation. From the time an RI has been manufactured, it is either installed on an operating aircraft, or is placed in a warehouse until such time that it is demanded by the organisation operating the aircraft. However, while on the aircraft, the RI can be subjected three further activities:

- an unscheduled failure resulting in a Correct Maintenance (CM) action;
- a scheduled servicing resulting in a Preventative Maintenance (PM) action; and
- the RI is removed to satisfy a higher demand on another aircraft (could be different type), typically referred to within the Aviation industry as "*Cannibalisation".*

While it is clear from Figure 1 that an RI can migrate between these states, an RI can been removed from the inventory (i.e. thrown away) if it becomes uneconomical to repair.

Summary of Aviation Industry's Need for a Realistic Repairable Item Model

Accordingly, given the complexity, dependence and low profit margin within the Aviation Industry the possibility of a reduction in TCO is a driving goal.

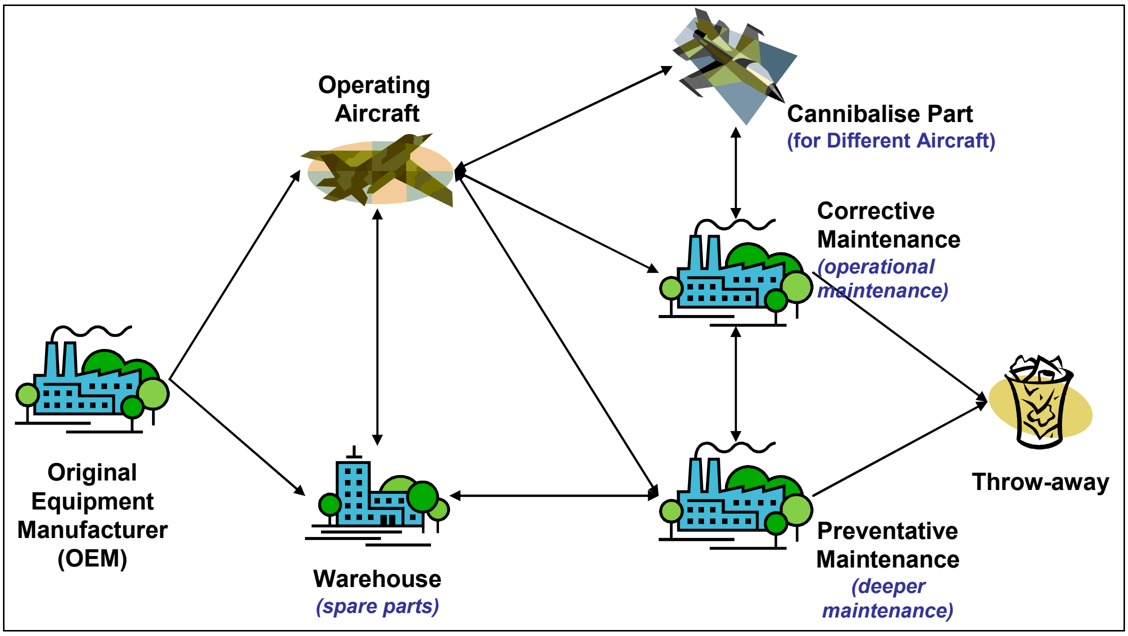

Figure 1: Life of an Aviation Repairable Item

The use of current Repairable Item models will result in a suboptimal solution to any spares modelling that may result in either:

- an aircraft being unavailable to conduct a mission awaiting a spare, or
- a higher TCO due to spare RIs that are not being utilised.

However, neither result is acceptable and accordingly, there is a need to construct a model that more realistically represents the life of a RI within the aviation environment. Any solution will need to address the combined complexities of imperfect maintenance of multiple dependent failure modes, imperfect inspections and data uncertainty, specifically unknown times to failure.

Area of Research

Table 1 provides the road-map of the research that was conducted and is now presented in this document.

Chapter 1: Introduction	Set the scene of the perceived need within the Aviation Industry to be solved.
Chapter 2: Description of Cases to be Modelled	Description of the life of an RI within the Aviation environment including the proposal of 2 case types; Case xA (known failure times) and Case xB (unknown failures times). These can be further divided as more realistic factors are introduced.
Chapter 3: Current Techniques for Analysis of Renewal Process	Description of Current techniques for analysis of RIs including KIJIM GRP equation. Also highlights possible alternative renewal process.
Chapter 4: Mathematical Set-up of Each Case	Described the mathematical setup including of the Cases from Chapter 3: Current Techniques for Analysis of Renewal Process
Chapter 5: Numerical Methods	Described the implementation of the *Slice Sampler* numerical analysis procedure.
Chapter 6: Role of 'q' in Analysis of Realistic Cases	Provides some rules of thumb to support insight into the behaviour of the GRP model for both the simple and complex cases will allow the reader to answer the traditional question of "so what?". Should I spend my limited budget on fixing imperfect inspection or imperfect maintenance?
Chapter 7: Examples	Review of a number of examples including real data for Cases 1A and Cases 4A.
Chapter 8: Conclusion	Conclusion and summary

Table 1: Road-map of the Dissertation

Chapter 2: Description of Cases to be Modelled

Review of the Life of an Aviation Repairable Item

Before examining the specific modelling requirements of each of the cases we need to revisit the life of a Repairable Item within the Defence Aviation environment as described in Chapter 1: Introduction and Figure 1. Based on this description it is possible to construct a flowchart that represents the "life" of an RI including imperfect inspection, imperfect corrective and imperfect preventative maintenance. This flowchart is provided at Figure 2.

Overall Case Assumptions

Before examining the specific modelling requirements of each of the cases there are a number of assumptions that apply to all the cases. These general assumptions are listed in Table 2.

• Only valid for a single component (e.g. single serial number from a fleet) • Only 2 states observable; serviceable and unserviceable (i.e. failed) • When considering multiple failure modes, only the failure that was discovered in the failed state is repaired, with no repair of other failures regardless of state (e.g. whether in failed state or not).

Table 2: Common Model Assumptions for all Cases

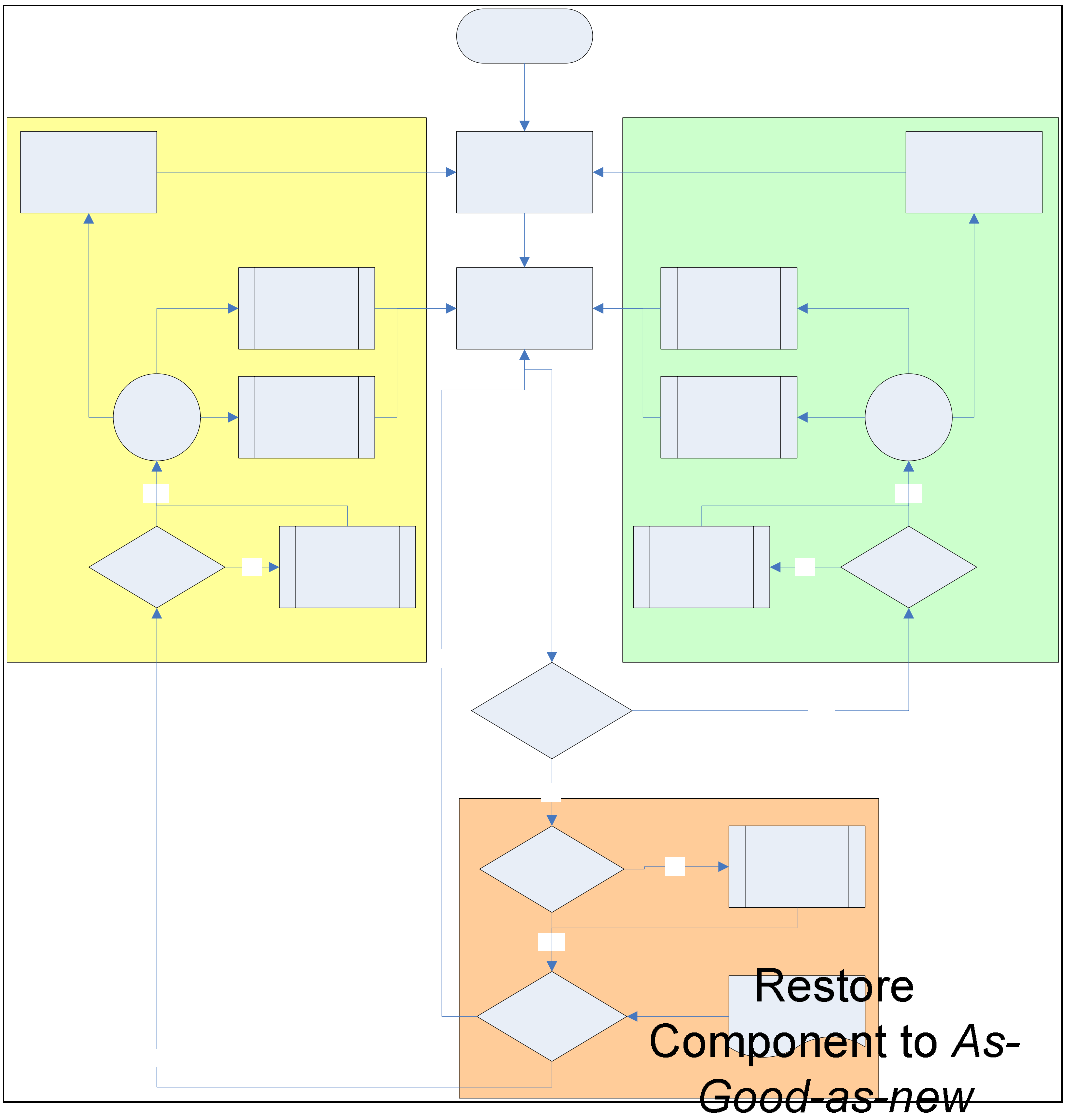

Figure 2: Flowchart of the Life of an Aviation Repairable Item

Case Types

There are two distinct case types; for the purposes of the modelling; labelled *Case A* and *Case B*. The differences between *Case A* and *Case B* are detailed in Table 3.

Case A	Case B
Case A represents components with Known Failure Times. These models are representative of components where a failure can be observed and repaired as they occur (e.g. avionics with an automatic Built In Test (BIT)[11]). This definition is similar to the concept of an *evident* under Reliability Centred Maintenance (RCM) logic[12].	*Case B* represents components with Unknown Failure Times. These models are representative of components where a failure is not observable during operation. Failure is only observed, and therefore repaired, during scheduled inspection points. This definition is similar to the concept of a *hidden failure* under RCM logic[13].

Table 3: Description of Case Types

<u>*Case 1*</u>

Case 1 represents the simplest model whereby data for a single failure mode is observed. Once the failure has been observed it is repaired instantaneously, noting that since there is only a single failure mode, there is no need to model the impact of the maintenance (and inspection) on the other failure modes. Case 1 is further divided along the lines of the Case Types listed above. Specifically:

Case 1A – Known Failure Times. This is representative of equipment that is constantly monitored for failures through BIT, etc and repaired during After-Flight

11 *Automatic built-in test (ABIT). A subset of BIT which is initiated automatically when subsystem electrical power is turned on; or iterative testing and monitoring, is non-interruptive to (following the initial power-up tests) and invisible to the user, it provides continuous normal system operation except when an operator-relevant fault is detected and reported; detects and isolates each fault to the corresponding level of maintenance.* Definition from para 3.1.41, Military Standard 1309D – Definitions of Terms of Testing, Measurement and Diagnostics dated 12 February 1992, pg 4 – 5.

12 Evident Failure – "*A failure mode whose effects will on their own eventually and inevitably become evident to the operating crew under normal circumstances.*" Definition from Defence Standard (DEFSTAN) 02-45 (NES 45), *Requirements for the Application of Reliability-Centred Maintenance Techniques to HM Ships, Submarines, Royal Fleet Auxiliaries and other Naval Auxiliary Vessels - Category 2*, Issue 2, UK Ministry of Defence, 14 July 2000, B-7.

13 Hidden Failure – A failure mode that will not, on its own, become evident to the operating crew under normal circumstances. Definition from DEFSTAN 02-45 (NES 45), op cit, B-6.

(AF), Turn-Around (TA) or rectification maintenance actions. A pictorial representation of both the real and virtual time for Case 1A is shown in Figure 3.

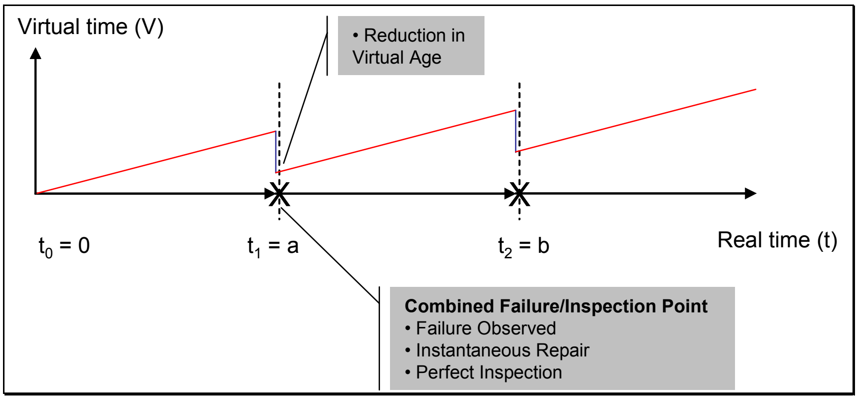

Figure 3: Diagram of Case 1A

Case 1B – Unknown Failure Times. Representative of equipment that is not monitored for failures or the failure will not, on its own, become evident to the operating crew under normal circumstances. Inspection, and the corresponding Before Flight (BF), AF, TA and/or rectification maintenance action, occurs at fixed (scheduled) intervals and is assumed to be perfect (e.g. inspection process does not 'age' the equipment). Furthermore, it is assumed that the component cannot accumulate any further 'age' from the time of failure, until the inspection (observation) and maintenance. A pictorial representation of both the real and virtual time for Case 1B is shown in Figure 4.

<u>Case 2</u>

Case 2 differs from Case 1 by including the modelling of multiple independent failure modes. Again, once the failure has been observed it is repaired instantaneously.

While multiple failure modes are included and therefore the 'age' of each of the independent failure mode must be tracked, the assumption of independence means that there is no need to model the impact of the maintenance (and inspection) on the other failure modes (refer to Cases 3 – 5). Furthermore, the inspection process is still to be assumed perfect (e.g. inspection process does not 'age' the equipment); refer to Case 4 – 5 for imperfect inspection. In comparison with Case 1, there is clearly an increased data requirement to support Case 2, including accuracy of assigning failures to specific failure modes. Case 2 is further divided along the lines of the Case Types listed above. Specifically:

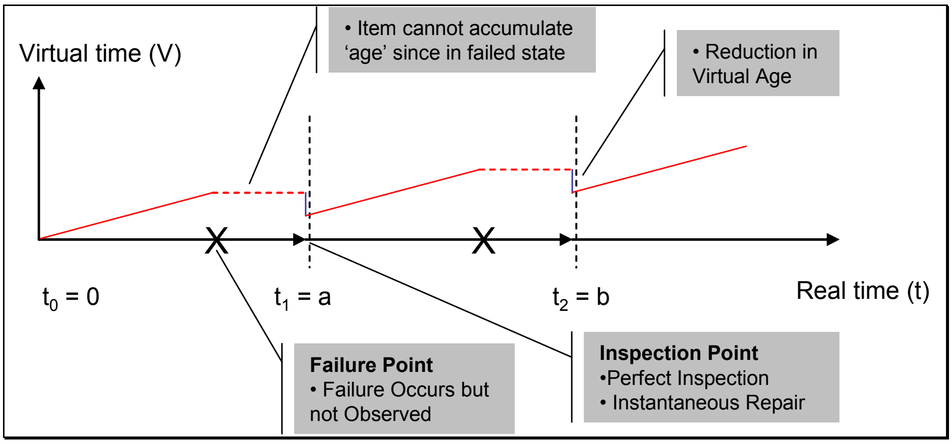

Figure 4: Diagram of Case 1B

Case 2A – Known Failure Times. Similar to Case 1A, Case 2A is representative of equipment that is constantly monitored for failures through BIT, etc and repaired during AF, TA and/or rectification maintenance action and where failure modes can be analysed separately and then combined in the GRP simulation. A pictorial representation of both the real and virtual time for Case 2A is shown in Figure 5.

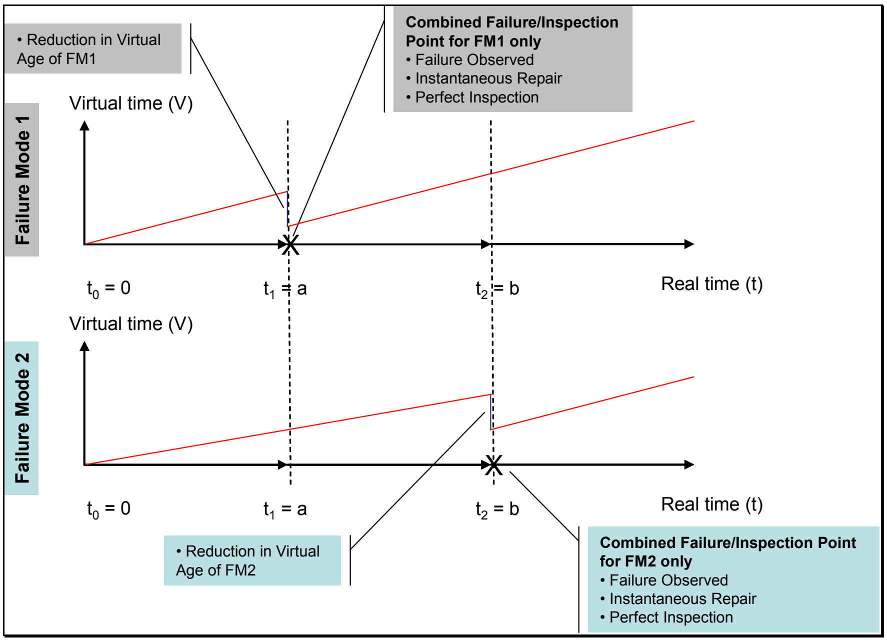

Figure 5: Diagram of Case 2A

Case 2B – Unknown Failure Times. Similar to Case 1B, Case 2B is representative of equipment that is not monitored for failures (e.g. failure can occur without observing). Inspection, and the corresponding BF, AF, TA and/or rectification action, occurs at fixed (scheduled) intervals in this scenario. A pictorial representation of both the real and virtual time for Case 2B is shown in Figure 6.

Case 3

Case 3 differs from Case 2 by modelling multiple dependent failure modes. In this case, the multiple failure modes will impact the 'age' of each of the other failure mode. Accordingly, in addition to the independent failure mode, the interaction between each failure mode must be tracked. Furthermore, the inspection process is still to be assumed perfect (e.g. inspection process does not 'age' the equipment);

refer to Case 4 – 5 for imperfect inspection. Case 3 is further divided along the lines of the Case Types listed above. Specifically:

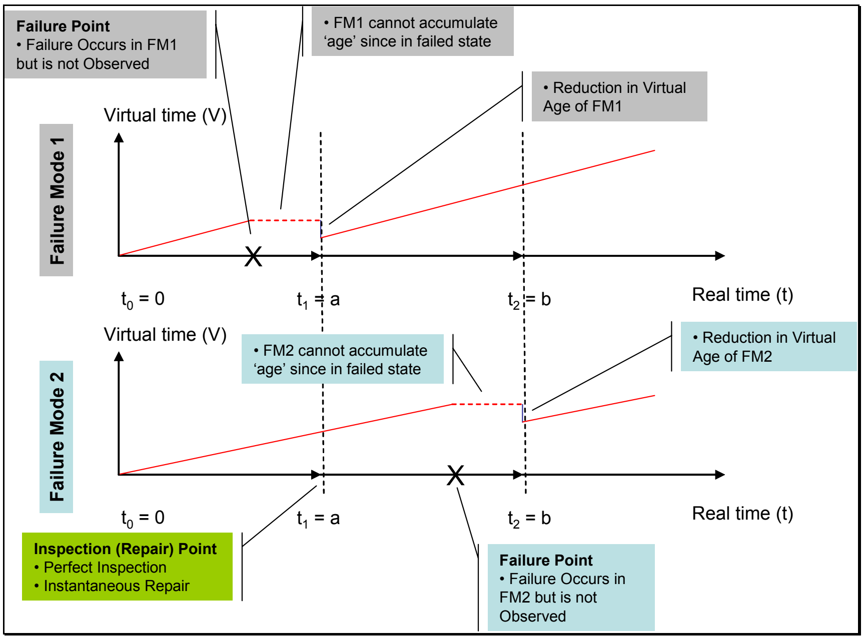

Figure 6: Diagram of Case 2B

Case 3A – Known Failure Times. This is representative of equipment that is constantly monitored for failures through BIT, etc and repaired during AF, TA and/or rectification action and where failure modes can be analysed separately and then combined in the GRP simulation. A pictorial representation of both the real and virtual time for Case 2B is shown in Figure 7.

Case 3B – Unknown Failure Times. Case 3B is representative of equipment that is not monitored for failures (e.g. failure can occur without observing). Inspection, and the corresponding BF, AF, TA and/or rectification action, occurs at fixed (scheduled) intervals in this scenario. A pictorial representation of both the real and virtual time for Case 2B is shown in Figure 8.

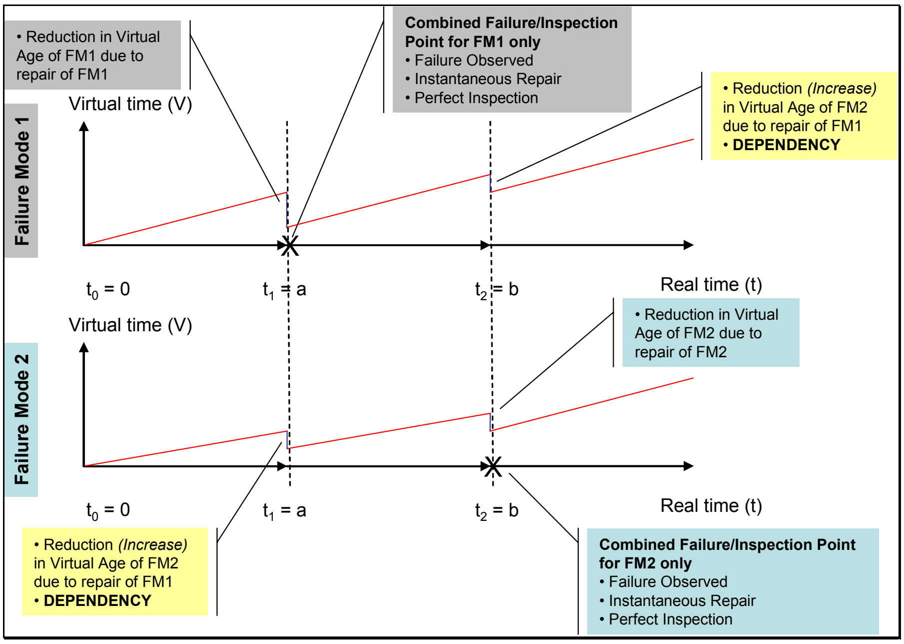

Figure 7: Diagram of Case 3A

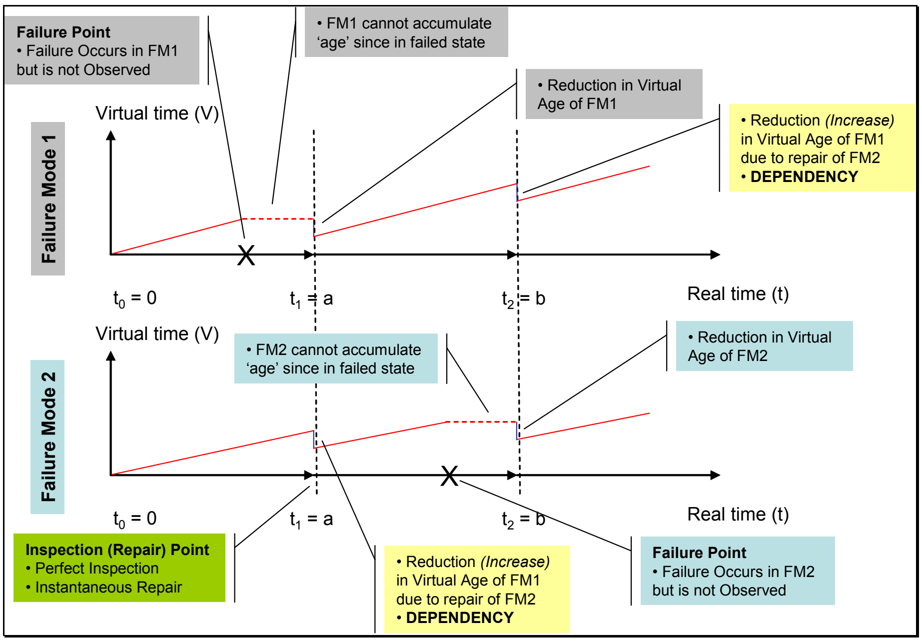

Figure 8: Diagram for Case 3B

Case 4

Case 4 builds on Case 3 by explicitly including modelling of where inspection process can 'age' a different failure mode that did not fail and/or was not repaired. In this case, in addition to tracking each of the multiple failure modes and their individual impact (i.e. aging) on each of the other failure modes, it is important to track the impact of the inspection process on each of the failure modes. Case 4 is further divided along the lines of the Case Types listed above. Specifically:

Case 4A – Known Failure Times. Case 4A is representative of equipment that is constantly monitored for failures through BIT, etc and repaired during AF, TA and/or rectification action and where failure modes can be analysed separately and then combined in the GRP simulation. A pictorial representation of both the real and virtual time for Case 2B is shown in Figure 9.

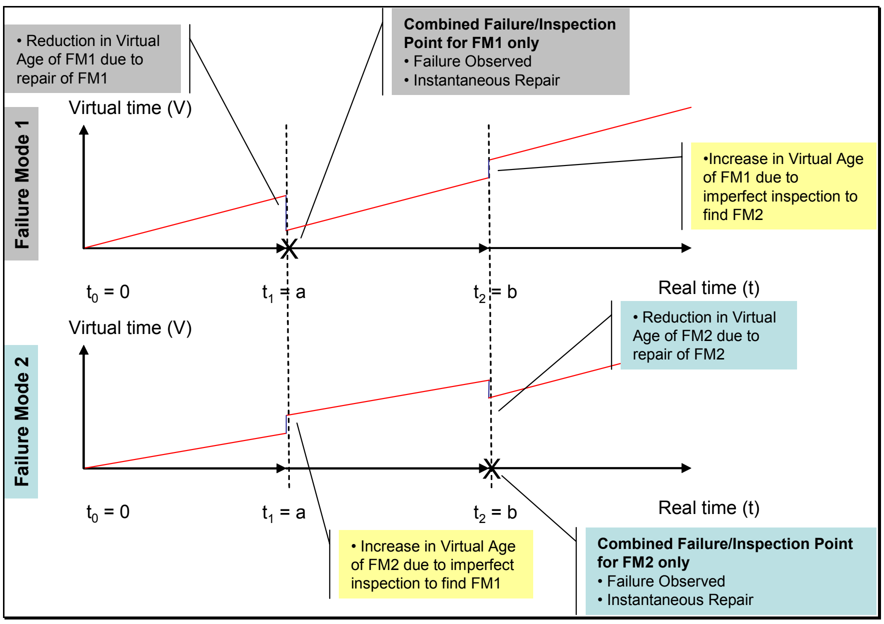

Figure 9: Diagram for Case 4A

Case 4B – Unknown Failure Times. Representative of equipment that is not monitored for failures (e.g. failure can occur without observing). Inspection, and the corresponding AF/TA/rectification action, occurs at fixed (scheduled) intervals. Furthermore, the inspection process is perfect (e.g. inspection process does not 'age' the equipment). A pictorial representation of both the real and virtual time for Case 2B is shown in Figure 10.

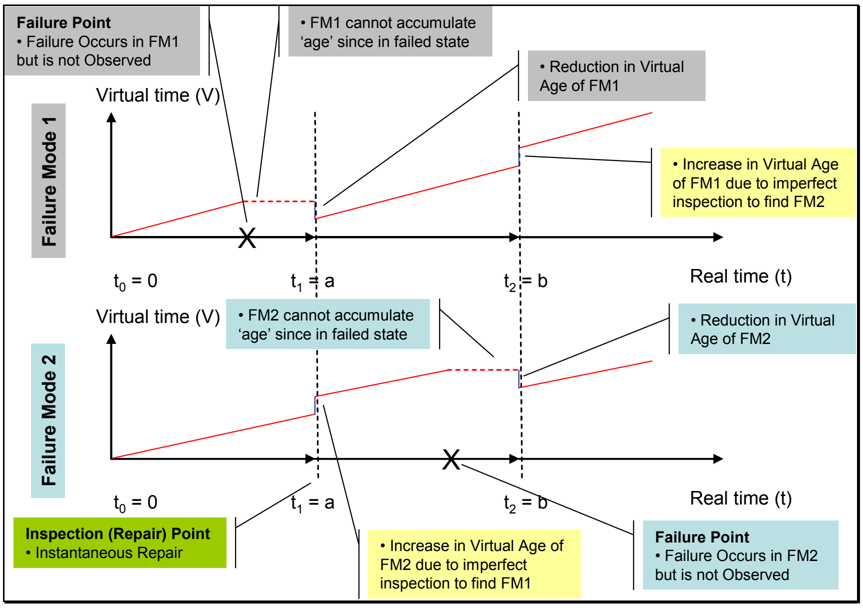

Figure 10: Diagram for Case 4B

<u>*Case 5*</u>

Case 5 builds on Case 4 by modelling where the inspection process can 'age' a different failure mode that did not fail and/or wasn't repaired. This is representative of the case where any repair action is delayed from the failure discovery point, and is very common within the aviation industry since one of their prime objectives is to ensure that flights are completed on schedule. Within the RAAF the process of delaying the repair of a known failure in a component is called a Carried Forward

Unserviceability (CFU). A CFU is only allowed on certain components that do not affect safety, and can only be authorised by specifically appointed personnel. In this case, the model must track each of the multiple failure modes and their individual impact (i.e. aging) on each of the other failure modes, the impact of the inspection process on each of the failure modes, and the impact of any delay on other failure modes. Case 5 is the most data intensive. Case 5 is further divided along the lines of the Case Types listed above. Specifically:

Case 5A – Known Failure Times. This is representative of equipment that is constantly monitored for failures through BIT, etc and repaired during the AF, TA and/or rectification action and where failure modes can be analysed separately and then combined in the GRP simulation. A pictorial representation of both the real and virtual time for Case 2B is shown in Figure 11.

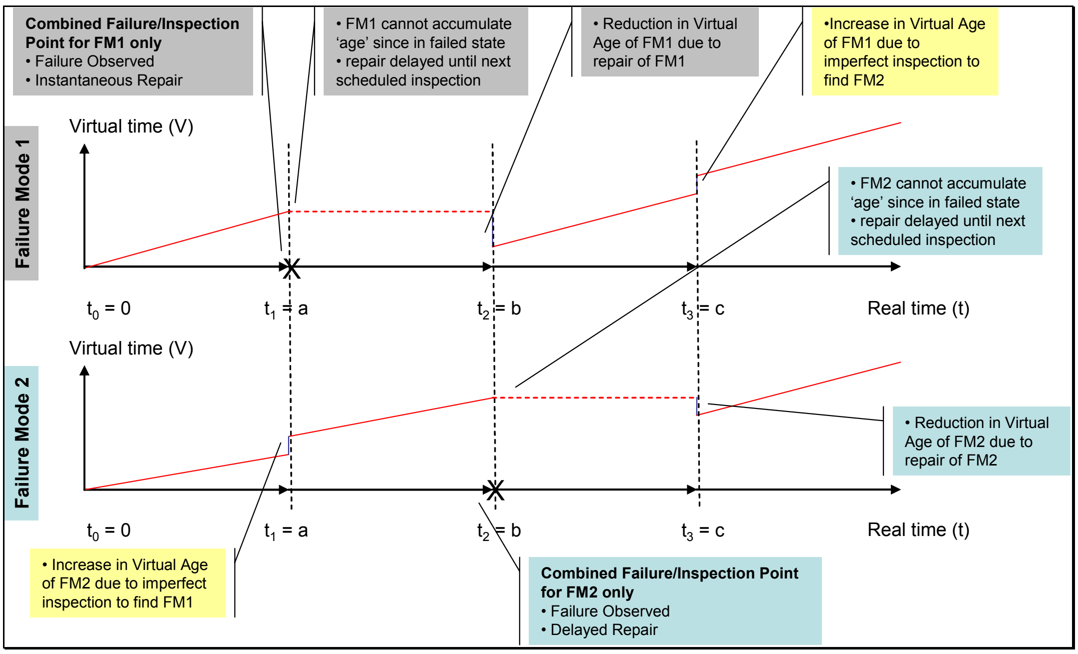

Figure 11: Diagram for Case 5A

Case 5B – Unknown Failure Times. Case 5B is representative of equipment that is not monitored for failures (e.g. failure can occur without observing). Inspection, and the corresponding BF, AF, TA and/or rectification action, occurs at fixed (scheduled) intervals. A pictorial representation of both the real and virtual time for Case 2B is shown in Figure 12.

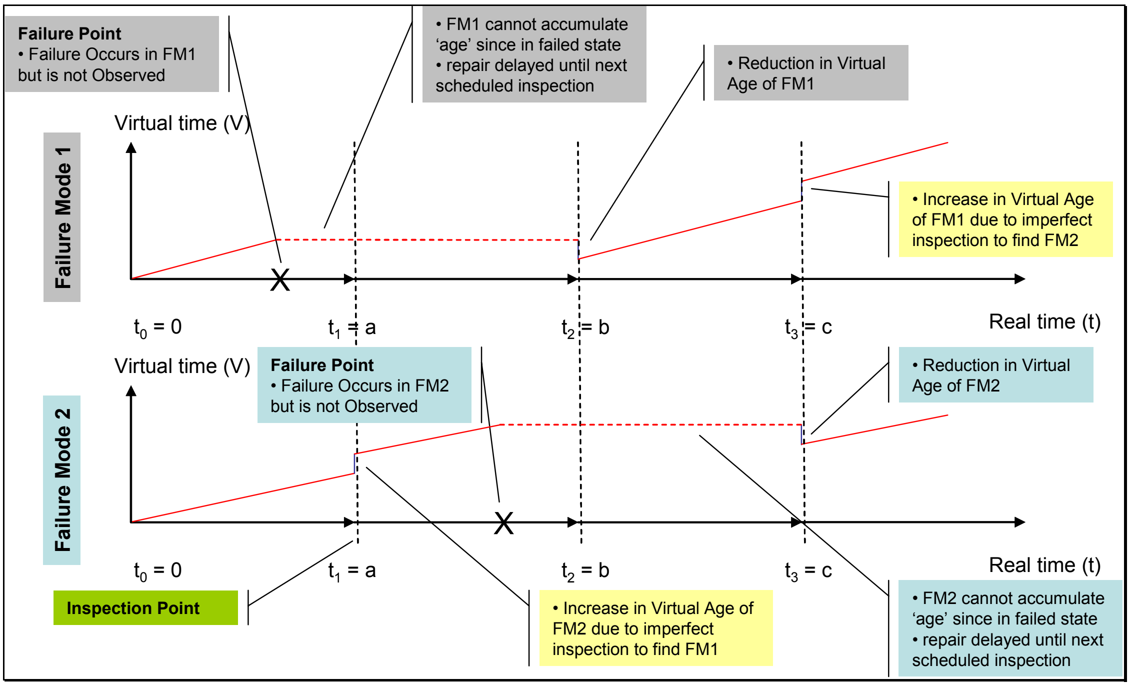

Figure 12: Diagram for Case 5B

Summary of Case

A summary of the model assumptions for each of cases detailed above is provided in Table 4.

	Single Failure Mode Instantaneous Repair Perfect Inspection **CASE 1**	**Multiple Independent Failure Modes** Instantaneous Repair Perfect Inspection **CASE 2**	Multiple **Dependent** Failure Modes Instantaneous Repair Perfect Inspection **CASE 3**	Multiple Dependent Failure Modes Instantaneous Repair **Imperfect Inspection** **CASE 4**	Multiple Dependent Failure Modes **Delayed Repair** Imperfect Inspection **CASE 5**
CASE A **Known Failure Times** (**failure observed** and repair as occurs)	**Case 1A** Representative of equipment that is constantly monitored for failures through BIT, etc and repaired during AF/TA /rectification action	**For Cases 2 – 5:** 1. only repair failure mode that was discovered in the failed state (e.g. no repair of other failures regardless state) 2. Increased data requirement from Case 1 to support the assignment of failures to specific failure modes			
		Case 2A Representative of case where failure modes can be analysed separately and then combined in the GRP simulation.	**Case 3A** Representative of the case where failure modes will impact (e.g. 'age') other failure modes.	**Case 4A** Representative of case where inspection process can 'age' a different failure mode that did not fail and/or was not repaired. Considered the most representative case of realistic aviation operations	**Case 5A** Representative of the case where any repair action is delayed from the failure discovery point. This case is common within the aviation industry to ensure that flights are completed on schedule.
CASE B **Unknown Failure Times** (**failure non-observable** and repaired at scheduled inspection point)	**Case 1B** Representative of equipment that is not monitored for failures (e.g. failure can occur without observing). Inspection, and AF/TA/ rectification action, occurs at fixed intervals.	**Case 2B** As above but unknown failure times.	**Case 3B** As above but unknown failure times.	**Case 4B** As above but unknown failure times.	**Case 5B** As above but unknown failure times.

Table 4: Summary of Model Assumptions for Cases

Chapter 3: Current Techniques for Analysis of Renewal Process

Reason for GRP Model

Repairable systems are generally not replaced by new systems following the occurrence of a failure; rather, they are repaired and put into operation again (e.g. cars, aircraft, etc). Clearly this sequence of *use, failure and repair*, can be continued *ad infinitum* until either (1) the system can no longer be repaired, or (2) the cost of the repair exceeds a certain threshold such as the cost of replacing the component with a new one. The later is generally referred to as uneconomic fleet the next day. The distinction is important from a predictive modelling point of view. Generally speaking, for the non-repairable items, the basis is the TTF distributions and all respective probabilistic and statistical procedures related to such distributions. On the other hand, the basic mathematical models for the repairable items require consideration of at least two random processes, used as models for failure and repair processes. The differences extends to such notions as *failure rate* (applicable to repairable items,) whereas in the case of repairable systems the appropriate measure is *rate of occurrence of failures* (ROCOF), which has a different meaning than the failure rate.

With this is mind, traditional repairable item models such as the Homogenous Poisson Process (HPP), Non-Homogenous Poisson Process (NHPP) and the Ordinary Renewal Process (ORP) are used extensively. Furthermore, these techniques are widely available in commercial software packages. A detailed review of the HPP, NHPP and ORP repairable item models can be found in many Reliability Engineering textbooks[14].

While HPP, NHPP and ORP solutions have also been used in repairable system analysis for many years, they suffer problems due to their model assumptions. For example, the HPP model can only be used to model an item with an exponential failure time distribution where the ROCOF is assumed to be constant, regardless of the age of the item. However, this assumption makes it impossible to model aging effects due to the memorylessness of the exponential function.

The repair assumption in the ORP is based on any repair activity restoring the item to new, regardless of the age of the item. This assumption is called *perfect repair assumption,* or as *good-as-new*.

In contrast, the NHPP model offers the opposite extreme where the repair assumption is based on the premise that any repair activity restores the item exactly to the state (i.e., age) just prior to the failure. This assumption is called the *minimal repair assumption*, *same-as-old,* or *as-bad-as-old*. Furthermore, the NHPP can be used with any underlying failure time distribution (e.g., Weibull and Lognormal) which result in time-dependent ROCOF, capable of representing aging effects. However, as HOYLAND and RAUSAND point out:

---

14 ASHER, H. and FEINGOLD, H., *loc it*; MODARRES, M., KAMINSKIY, M. and KRIVTSOV, V., loc cit; ELBING, *"An Introduction of Reliability and Maintainability Engineering"*, McGraw-Hill, USA, 1997; HOYLAND, A. and RAUSAND, M., loc cit.

> *"An NHPP is not a realistic model when the failed parts to be replaced have been in operation for a long time. For the NHPP to be realistic, the parts put into service should be identical to the old ones and hence should be aged outside the system under identical conditions for the same period of time."* [15]

Additionally, HOYLAND and RAUSAND also argue that "[t]*he minimal repair assumption is . . . often applicable, and the NHPP may be accepted as a realistic model, at least as a first-order approximation"* [16] for the analysis of a complex system based on the following argument:

> *". . . consider a system consisting of a large number of components. Suppose that a critical component fails and causes a system failure and that this component is immediately replaced by a component of the same type, thus causing negligible system downtime. Since only a small fraction of the system is replaced, it seems natural to assume that the system's reliability after the repair is essentially the same as immediately before the failure. In other words, the assumption of* ***minimal repair*** *is a realistic approximation.*
>
> *A car is a typical example of a repairable system. Usually the operating time of a car is expressed in terms of the mileage indicated on the speedometer. Repair actions will not usually imply extra mileage. The repair 'time' is thus negligible. Many repairs are accomplished by*

---

15 HOYLAND, A. and RAUSAND, M., op cit, pp 314-315

16 ibid

adjustments and replacement of single components. The minimal repair assumption is therefore often applicable, and the NHPP may be accepted as a realistic model, at least as a first-order approximation.“ [17]

While the ORP and NHPP can be used to approximate a solution, a realistic repair activity is somewhere in between these two models depending on a number of factors including overall age of the component, number of repairs, effectiveness of the repair, skill of the technicians, etc. This is sometimes referred to as *better-than-old-but-worse-than-new* repair assumption. Furthermore, while it is clear that neither the NHPP nor the ORP adequately reflect this more realistic repair assumption, they represent the maximum and minimum conditions of the model.

A more realistic model for the case of realistic maintenance is the so-called *General Renewal Process (GRP),* introduced by KIJIMA and SUMITA in 1986[18] allowing the *goodness of repairs* to be modelled from *as-good-as-new* (i.e. ORP) to *same-as-old* (i.e. NHPP). In the simplest form of GRP, a single parameter, q, represents the *goodness of repairs*, or *Repair Effectiveness.* Unfortunately, there is no closed form solution to the GRP model equation, and even the numerical integration approaches are difficult to apply. Instead, a numerical method is required to undertake this replacement KAMINSKIY and KRIVTSOV[19] proposed a Monte Carlo (MC) simulation based solution which has been adopted by a software tool. Although the

---

17 ibid

18 KIJIMA, M. and SUMITA, U., loc cit.

19 KAMINSKIY, M. and KRIVTSOV, V., loc cit.

study was aimed at the component model, the tool can be equally applied to any repairable object such as a system, subsystem, or component based purely on the data availability. YANAS, et al and

A summary of the various repairable item models, their underlying distribution, repair effectiveness and ability to model aging effects is provided in Table 5.

Repairable Item Model	**Underlying Reliability Distribution**	**Repair Effectiveness Assumption**	**Assessment of System Aging**
HPP	Exponential only	N/A	N/A
Renewal Process (RP)	Any distribution	As good as new (q = 0)	N/A
NHPP	Any distribution (usually Weibull)	As good as old, q =1(as it was just before a failure)	Applicable
GRP	Any distribution	Any ($0 \leq q \leq 1$)	Applicable

Table 5: Summary of Repairable Item Models

<u>*Formulation of GRP Model*</u>

Aging effects can be modelled through the reduction of ROCOF during the lifetime of a system/component. This concept of *Virtual Age (VA)* was introduced by KIJIMA and SUMITA[20] in 1986 and is now referred in most literature to as GRP.

The GRP model allowing the *goodness of repairs* to be modelled from *as-good-as-new* (i.e. ORP) to *same-as-old* (i.e. NHPP). The variation between the two repair assumptions is achieved through this notion of *VA*.

[20] KIJIMA, M. and SUMITA, U., loc cit.

Let A_n be the VA of the item immediately after the n^{th} repair. If $A_n = y$, then the product has the time to $(n + 1)^{th}$ failure X_{n+1}, which is distributed according to the cumulative distribution function (CDF) shown in Equation 1.

$$F(X|A_n = y) = \frac{F(X+y) - F(y)}{1 - F(y)}$$

Equation 1: CDF of the GRP Model

where $F(X)$ is the CDF of the Time-To-First-Failure (TTFF) distribution of a new item. The *Real Age* of a component is the sum where $S_0 = 0$ is shown in Equation 2.

$$S_n = \sum_{i=1}^{n} X_i$$

Equation 2: Real Age of a Component under the GRP Model

KIJIMA[21] introduced 2 models for *virtual age*, typically referred to as the KIJIMA Type I and Type II equations, whose construct is shown in Equation 3.

$$V_i = V_{i-1} + A_i \cdot Y_i - KIJIMA\_Type\_I$$
$$V_i = A_i \cdot (Y_i - V_{i-1}) - KIJIMA\_Type\_II$$

Equation 3: KIJIMA Type I and Type II Virtual Age Equations for GRP Model

where A_i may be a random variable.

Note that throughout the study A_i is assumed = constant = q.

21 KIJIMA, M., loc cit.

One method of understanding the concept of *virtual age* for both the KIJIMA Type I and Type II GRP model is through the plotting of real age versus *virtual age* for varying q. This can be seen in Figure 13 where an item is exposed to a series of operation, failure and renewals. In this case let t_k, be the time of the k^{th} failure, x_k represent the *virtual age* immediately after restoration, and y_k represent the *virtual age* immediately before the k^{th} failure.

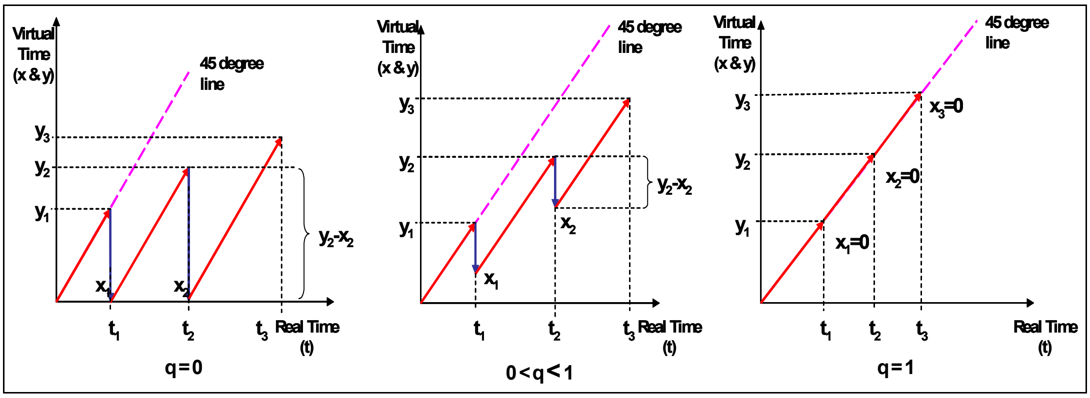

Figure 13: Virtual Age versus Real Age for Varying *q* Values

From Figure 13 it is possible to find an expression for t_k, in terms of x_k and y_k as follows:

$$t_{k+1} = t_k + (y_{k+1} - x_k)$$

Equation 4: Expression for t_k, in terms of x_k and y_k

The expected number of failures in the interval (0, t] for both the KIJIMA Type I and Type II GRP models, called the Cumulative Intensity Function (CIF), is given by a solution of the GRP equation[22] as shown in Equation 5.

[22] KIJIMA, M. and SUMITA, U., loc cit

$$H(t) = E[N(t)] = \int_0^t \left\{ g(\tau|0) + \int_0^\tau h(x) g(\tau - x|x) dx \right\} d\tau$$
$$where$$
$$g(t|x) = \frac{f(t+qx)}{1-F(qx)}; t, x \geq 0$$

Equation 5: CIF of the GRP

Where Equation 5 is the conditional PDF such that $g(t|0) = f(t)$, and $F(t)$ and $f(t)$ are the CDP and PDF of the TTFF distribution.

Unfortunately, as previously highlighted there is no closed form solution to this equation, and even the numerical integration approaches are difficult to apply. The numerical integration approach(es) can be found in .

The GRP model is very useful when realistically modelling repairable items since it has the flexibility to model various repair assumptions; i.e. *better-than-old-but-worse-than-new* repair assumption. For example, if $q = 0$, the solution of the GRP corresponds to the solution of an ORP model with the *as-good-as-new* repair assumption. Conversely, if $q = 1$, the solution of the GRP corresponds to the solution of a NHPP, that is the *same-as-old* repair assumption. While development of the GRP model is relatively intuitive the only concern is in the parameter estimation, especially q, and the simulation of a result.

Limitations of KIJIMA GRP Model

DAGPUNAR[23] states that the limitation of KIJIMA Type I GRP model is that any reduction in virtual age on the i^{th} repair affects only the most recent operating time Y_i. Thus, the state of an item (i.e. operating time) cannot undergo any major improvement through the introduction of better repair techniques, modification of the item, etc since the item will still have a large virtual age, but only a small recent operating time. Furthermore, under a failure rate increasing to infinity the KIJIMA Type I GRP model (with the exception of $A_i = 0$) will result in zero operating times in the limit. In order to eliminate the limitation of the KIJIMA Type I GRP model, DAGPUNAR[24] proposes the *TYPE III* model as follows.

Let the initial age of the item is $S_0 = s$, a specified value. Let the repair function $\varphi(w)$, the *virtual age* immediately after the i^{th} repair be defined in Equation 6.

$$
\begin{aligned}
&V_i = \varphi \cdot \left(Y_i + V_{i-1}\right) \\
&\textit{where} \\
&V_o = s
\end{aligned}
$$

Equation 6: Type III Virtual Age Equations for GRP Model

Furthermore, it is assumed that repair does not age the item, i.e. $0 \leq \varphi(w) \leq w$, or equivalently as shown in Equation 7.

---

23 DAGPUNAR, J.S., *"Renewal-type Equations for a General Repair Process"*, Quality and Reliability Engineering International, Vol 13, No 4, July-Aug. 1997, p. 235-45

24 ibid

$$V_i \leq \sum_{j=1}^{i} Y_j$$

Equation 7: Virtual Age of Type III GRP Equation

In the case of the *TYPE III* model the solution is shown in Equation 8.

$$H(t,s) = E[N(t,s)] = \int_0^t \left\{ 1 + H[t-y, \phi(s+y)] \frac{f(s+y)}{\bar{F}(s)} \right\} dy$$

Equation 8: CIF of the Type II GRP Model

where the general repair function *{φ(w): w ≥ 0}*, initial age of the item *s*, and the TTFF is *y*.

Similar to the KIJIMA Type I and Type II GRP models, there is no closed form solution to this equation, and even the numerical integration approaches are difficult to apply, therefore a MC based solution offered by KAMINSKIY and KRIVTSOV[25], YANEZ, et al[26], METTAS, et al[27] or JACK[28] approach can be used. HURTADO et al[29] provided an alternative approach to the MLE through the application of a Genetic Algorithm (GA) to solve the GRP equation. However, the *Type III* model introduced by DAGPUNAR has not been examined as part of this study.

25 KAMINSKIY, M. and KRIVTSOV, V., loc cit.

26 YANEZ, M., JOGLAR, F, and MODARRES, M., loc cit.

27 METTAS, A. and ZHAO, W, loc cit.

28 JACK, N., loc cit.

29 HURTADO et al, loc cit.

Simulation of General Renewal Process (GRP)

Introduction into GRP Simulation

In order to study both the KIJIMA Type I and Type II GRP models it was necessary to develop a simulation tool. This was completed using the programming feature of MathCad® software; specifically MathCad® Professional 12. The setup of both GRP simulation tools was based on the similar work completed by Dr Frank Groen[30] using a straight MC simulation (i.e. a simulation without any constraints). It is then possible to undertake the studies based on the simulated CIF data from the KIJIMA Type I and Type II GRP models. The simulation method and study techniques are provided in the following paragraphs.

Simulation of the GRP Model

Setup of the KJIMA Type I GRP model was based Dr Frank Groen's work[31] as follows:

> *Straight MC Simulation*
>
> *The following algorithm is proposed to perform the straight MC simulation, i.e. simulation without any constraints. Let t_k, the time of the k-th failure be known. The time of the next failure t_{k+1} is then found as*

[30] GROEN, F., *"Supplement to 'Bayesian Data Analysis for General-Renewal Process'"*, Technical Paper, University of Maryland, 2003

[31] ibid

$$
\begin{aligned}
&x_k = q \cdot t_k \\
&\ln R_k = -\left(\frac{x_k}{\alpha}\right)^{\beta} \\
&u \in \langle 0,1 \rangle \\
&y_{k+1} = \alpha\left(-\ln u - \ln R_k\right)^{1/\beta} \\
&t_{k+1} = t_k + (y_{k+1} - x_k)
\end{aligned}
$$

- *x_k represents the virtual age immediately after restoration*
- *y_k represents the virtual age immediately before the k^{th} failure*
- *$ln(R_k)$ represents the natural log of the reliability at virtual age x_k*
- *u represents a standard uniform random sample*

The only subtraction in this algorithm takes place in the last line. Given the expected values of y_{k+1} and x_k, this should normally not be a problem. Furthermore, in the worst case scenario where q = 1, the value of $ln(R_k)$ will increase by 1 on average for every iteration of k. The value of $ln(R_k)$ should therefore stay small enough for the addition in the second to last line not to pose a problem. The algorithm can therefore be used for high values of k.

However, derivation, including assumptions, of the MC equations was not included in the paper. Therefore, the following derivations are provided in support of the use of these equations.

From these equations it is possible to iteratively find the time of next failure, t_{k+1}, using values for the virtual age immediately after restoration, x_k, and the virtual age immediately before the $(k+1)^{th}$ failure, y_{k+1}. Specifically, the time of next failure, t_{k+1}, is shown in Equation 9.

$$t_{k+1} = t_k + \left(y_{k+1} - x_k\right)$$

Equation 9: Time of Next Failure, t_{k+1}, for GRP Equation

The derivation of this relationship was previously shown.

To find the expression for t_{k+1}, the expressions for x_k and y_{k+1} need to be determined. However, given both the expressions for x_k and y_{k+1} are dependent on the method of calculating the virtual age, the expressions for x_k and y_{k+1} will be different for the KIJIMA Type I and Type II models.

The expression for y_{k+1} can be found by rewriting the previously defined CDF for the GRP model as shown in Equation 10.

$$F\left(X \middle| A_n = y\right) = \frac{F(X+y) - F(y)}{1 - F(y)} = \frac{F'(t_{k+1}) - F(t_k)}{1 - F(t_k)} = \frac{R(t_k) - R'(t_{k+1})}{R(t_k)}$$

Equation 10: Expression for y_{k+1}

where $R(t_k)$ is the reliability just after the k^{th} failure/renewal and $R'(t_{k+1})$ is the reliability just before the $(k+1)^{th}$ failure.

However, since $F(X|A_n = y)$ is a Failure Distribution we know that $F(X|A_n = y) = U$ where $U \in$ <0,1> and thus the CDF can be re-written as shown in Equation 11.

$$\begin{aligned}
&F\left(X \middle| A_n = y\right) = U = \frac{R(t_k) - R'(t_{k+1})}{R(t_k)} = 1 - \frac{R'(t_{k+1})}{R(t_k)} \\
&\Rightarrow \frac{R'(t_{k+1})}{R(t_k)} = 1 - U = U' \\
&\Rightarrow R'(t_{k+1}) = R(t_k) \cdot U' \\
&\therefore \ln\left[R'(t_{k+1})\right] = \ln\left[R(t_k) \cdot U'\right] = \ln\left[R(t_k)\right] + \ln\left[U'\right]
\end{aligned}$$

Equation 11: CDF of GRP Model

where $U \in$ <0,1>, then $U' = 1 - U$ where $U' \in$ <0,1>.

Now since $R'(t_{k+1})$ is defined as the reliability just before the $(k+1)^{th}$ failure, and using a Weibull Distribution as the underlying TTF distributions, it is possible to derive the equation for the virtual age immediately before the $(k+1)^{th}$ failure, y_{k+1}, as shown in Equation 12.

$$
\begin{aligned}
&\ln[R'(t_{k+1})] = \ln[R(t_k)] + \ln[U'] \\
&\Rightarrow \ln\left[e^{-\left(\frac{y_{k+1}}{\alpha}\right)^{\beta}}\right] = \ln\left[e^{-\left(\frac{x_k}{\alpha}\right)^{\beta}}\right] + \ln[U'] \\
&\Rightarrow -\left(\frac{y_{k+1}}{\alpha}\right)^{\beta} = -\left(\frac{x_k}{\alpha}\right)^{\beta} + \ln[U'] \\
&\Rightarrow \frac{y_{k+1}}{\alpha} = \left[\left(\frac{x_k}{\alpha}\right)^{\beta} - \ln[U']\right]^{\frac{1}{\beta}} \\
&\therefore y_{k+1} = \alpha \cdot \left[\left(\frac{x_k}{\alpha}\right)^{\beta} - \ln[U']\right]^{\frac{1}{\beta}}
\end{aligned}
$$

Equation 12: Virtual Age Immediately Before the $(k+1)^{th}$ Failure

We now have expression for y_{k+1} as a function of x_k, which as previously mentioned is dependent on whether a KIJIMA Type I or Type II GRP model is being simulated. Therefore, we now need to find an expression for x_k for both the KIJIMA Type I and Type II GRP model.

Simulation of the KIJIMA Type I GRP Model

From the original KIJIMA Type I expression for virtual age provided in Equation 3, it is possible to derive an expression for x_k as shown in Equation 13.

$$
\begin{aligned}
&x_k = x_{k-1} + q \cdot (T_k) = x_{k-1} + q \cdot (t_k - t_{k-1}) \\
&\Rightarrow [x_{k-2} + q \cdot (t_{k-1} - t_{k-2})] + q \cdot (t_k - t_{k-1}) \\
&\Rightarrow \{x_{k-3} + q \cdot (t_{k-2} - t_{k-3})\} + [q \cdot (t_{k-1} - t_{k-2})] + q \cdot (t_k - t_{k-1}) \\
&\Rightarrow x_0 + q \cdot (t_1 - t_0) + \cdots + q \cdot (t_{k-2} - t_{k-3}) + q \cdot (t_{k-1} - t_{k-2}) + q \cdot (t_k - t_{k-1}) \\
&\therefore x_k = x_0 - q \cdot t_0 + q \cdot t_k
\end{aligned}
$$

Equation 13: Virtual Age Immediately After Restoration, x_k, for KIJIMA Type I GRP Equation

However, assuming the initial assumptions that t_0 = 0, x_0 = 0 and q = constant the final expression for x_k for the KIJIMA Type I model is shown in Equation 14.

$$
\begin{aligned}
&x_k = x_0 - q \cdot t_0 + q \cdot t_k \\
&\therefore x_k = q \cdot t_k
\end{aligned}
$$

Equation 14: Simplified Virtual Age Immediately After Restoration, x_k, for KIJIMA Type I GRP Equation

Now substituting y_{k+1} and x_k it is possible to solve for t_{k+1} for the simplified straight MC equation for simulation of a KIJIMA Type I GRP model as shown in Equation 15.

$$
\begin{aligned}
&t_{k+1} = t_k + (y_{k+1} - x_k) \\
&\Rightarrow t_k + \left[\left(\alpha \cdot \left[\left(\frac{q \cdot t_k}{\alpha} \right)^{\beta} - \ln[U'] \right]^{\frac{1}{\beta}} \right) - (q \cdot t_k) \right] \\
&\therefore t_{k+1} = t_k \cdot (1 - q) + \alpha \cdot \left[\left(\frac{q \cdot t_k}{\alpha} \right)^{\beta} - \ln(U') \right]^{\frac{1}{\beta}}
\end{aligned}
$$

Equation 15: Time of Next Failure, t_{k+1}, for KIJIMA Type I GRP Equation

An interesting observation of the final expression of t_{k+1} is that it is **only** dependent on t_k, the previous TTF. Thus the prediction of any future TTF value is only dependent on the previous TTF value, whether found through actual data, simulation or by approximation.

While the original straight MC equations developed by Dr Frank Groen[32] were implemented to find the mean and distribution of the number of failures/renewals (ie CIF) for a given *t*, the implementation used throughout this study was based on finding the mean and distribution of the TTF to the kth failure.

Simulation of the KIJIMA Type II GRP Model

Similar to the KIJIMA Type I GRP expression, from the expression for the virtual age for KIJIMA Type II previously defined it is possible to derive an expression for x_k as provided in Equation 16.

$$
\begin{aligned}
& x_k = q \cdot \left[x_{k-1} + \left(t_k - t_{k-1}\right)\right] \\
& \Rightarrow q \cdot \left\{q \cdot \left[x_{k-2} + \left(t_{k-1} - t_{k-2}\right)\right]\right\} + q \cdot \left(t_k - t_{k-1}\right) \\
& \Rightarrow q^2 \cdot x_{k-2} + q^2 \cdot \left(t_{k-1} - t_{k-2}\right) + q \cdot \left(t_k - t_{k-1}\right) \\
& \Rightarrow q \cdot \left\{q \cdot \left[x_{k-2} + \left(t_{k-1} - t_{k-2}\right)\right]\right\} + q \cdot \left(t_k - t_{k-1}\right) \\
& \Rightarrow q^k \cdot x_0 + q^k \cdot \left(t_1 - t_0\right) + \cdots + q^2 \cdot \left(t_{k-1} - t_{k-2}\right) + q \cdot \left(t_k - t_{k-1}\right) \\
& \Rightarrow q^k \cdot t_1 + \cdots + q^2 \cdot \left(t_{k-1} - t_{k-2}\right) + q \cdot \left(t_k - t_{k-1}\right) \\
& \therefore x_k = q^k \cdot t_1 + \cdots + t_{k-2} \cdot \left(q^3 - q^2\right) + t_{k-1}\left(q^2 - q\right) + t_k \cdot q
\end{aligned}
$$

Equation 16: Virtual Age Immediately After Restoration, x_k, for KIJIMA Type II GRP Equation

[32] ibid

However, assuming the initial assumptions that $t_0 = 0$, $x_0 = 0$ and q = constant the final expression for x_k for the KIJIMA Type II GRP model is shown in Equation 17.

$$
\begin{aligned}
x_k &= q^k \cdot t_1 + \cdots + t_{k-2} \cdot \left(q^3 - q^2\right) + t_{k-1}\left(q^2 - q\right) + t_k \cdot q \\
&\Rightarrow \sum_{i=1}^{k-1} \left[t_{(k-i)} \cdot \left(q^{i+1} - q^i\right)\right] + t_k \cdot q \\
\therefore x_k &= \sum_{i=1}^{k-1} \left[t_{(k-i)} \cdot q^i \cdot (q-1)\right] + t_k \cdot q
\end{aligned}
$$

Equation 17: Simplified Virtual Age Immediately After Restoration, x_k, for KIJIMA Type II GRP Equation

Substituting for y_{k+1} and x_k it is possible to solve for t_{k+1} for the simplified straight MC equation for simulation of a KIJIMA Type II GRP model as follows:

$$
\begin{aligned}
t_{k+1} &= t_k + \left(y_{k+1} - x_k\right) \\
&\Rightarrow t_k + \left[\left(\alpha \cdot \left[\left(\frac{x_k}{\alpha}\right)^{\beta} - \ln[U']\right]^{\frac{1}{\beta}}\right) - x_k\right] \\
\therefore t_{k+1} &= t_k + \left[\left(\alpha \cdot \left[\left(\frac{\sum_{i=1}^{k-1}\left[t_{(k-i)} \cdot q^i \cdot (q-1)\right] + t_k \cdot q}{\alpha}\right)^{\beta} - \ln[U']\right]^{\frac{1}{\beta}}\right) - \left(\sum_{i=1}^{k-1}\left[t_{(k-i)} \cdot q^i \cdot (q-1)\right] + t_k \cdot q\right)\right]
\end{aligned}
$$

Equation 18: Time of Next Failure, t_{k+1}, for KIJIMA Type II GRP Equation

Unlike the expression for t_{k+1} for the KIJIMA Type I GRP model, the expression for the KIJIMA Type II GRP model is dependent on all previous values of t_k. Any future prediction of t_{k+1} will require that all previous values of t_k be known, and therefore increase the data requirements for actual failure data, simulation of data or the use of an approximation technique. This requirement also significantly increases the complexity of the prediction model of the KIJIMA Type II GRP model compared to the KIJIMA Type I GRP model.

Furthermore, from the simplification of x_k for both the KIJIMA Type I and Type II GRP models it is clear that the virtual age immediately after renewal (i.e. x_k) of the KIJIMA Type I GRP model will always be greater than the KIJIMA Type II GRP model, except where q=1.

Discussion of GRP Equation Parameters

Given the utilisation of a 2-parameter Weibull distribution as the underlying Time-To-Failure distribution, the resulting Time of Next Failure, t_{k+1}, for the KIJIMA Type I GRP Equation as shown in Equation 15 relies on the following three parameters:

- GRP Equation Scale Parameter (α)
- GRP Equation Shape Parameter (β)
- GRP Equation Repair Effectiveness Parameter (q)

Each parameter will be examined separately in order to establish their nature, characteristic and role.

GRP Equation Scale Parameter (α)

The scale parameter (α) of a KIJIMA Type I GRP equation with an underlying 2-parameter Weibull distribution "influences both the mean and spread, or dispersion, of the distribution."[33]. The scale parameter (α) is also called the *characteristic life* of the component.

GRP Equation Shape Parameter (β)

The shape parameter (β) of a KIJIMA Type I GRP equation with an underlying 2-parameter Weibull distribution provides an "insight into the behaviour of the failure process"[34]. For example, if $\beta = 1$, $\lambda(t)$ is constant and the distribution is identical to the exponential distribution. In general terms, if $\beta < 1$, there is a decreasing failure rate (DFR), if $\beta = 1$ there is a constant failure rate (CFR) and therefore identical to the exponential distribution, while if $\beta > 1$, there is an increasing failure rate (IFR). A summary of the effect of the shape parameter is shown in Table 6.

Consequently, and quite logically, as the shape parameter (β) increases, the TTF decreases.

---

33 ELBING, C., "*An Introduction of Reliability and Maintainability Engineering*", McGraw-Hill, USA, 1997, pg 63

34 ibid

Value of Shape Parameter	Property
$0 < \beta < 1$	Decreasing Failure Rate (DFR)
$\beta = 1$	Constant Failure Rate (CFR)
$1 < \beta < 2$	Increasing Failure Rate (IFR), Concave
$\beta = 2$	Rayleigh Distribution (linear)
$\beta > 2$	IFR, Convex
$3 \leq \beta \leq 4$	IFR, Approaches normal distribution, symmetrical

Table 6: Effect of Shape Parameter on GRP Equation[35]

GRP Equation Repair Effectiveness Parameter (q)

The nature, characteristic and role of the GRP Equation Repair Effectiveness Parameter (q) requires significant discussion, which is held in Chapter 6: Role of 'q' in Analysis of Realistic Cases.

HURTADO et al[36] provided an alternative to the MLE approached used by KAMINSKIY et al[37], YANEZ, et al[38], METTAS, et al[39] and JACK[40] to solve the single failure mode with perfect inspection via a Genetic Algorithm (GA).

---

35 ELBING, C., op cit, Table 4.1, pg 64

36 HURTADO et al, loc cit.

37 KAMINSKIY, M. and KRIVTSOV, V., loc cit.

38 YANEZ, M., JOGLAR, F, and MODARRES, M., loc cit.

39 METTAS, A. and ZHAO, W, loc cit.

40 JACK, N., loc cit.

Additionally, HURTADO et al[41] solves the GRP equation where the underlying TTF distribution can be assumed to be a 2-parameter Weibull or lognormal.

Alternative Renewal Process Models

While the focus of the research was based on the utilisation of GRP a number of alternative renewal process models were reviewed. Each of these models varied in terms of assumptions (e.g. perfect maintenance and inspection, etc), their intended use (e.g. optimisation of throughput based on condition-based maintenance, etc) and level of complexity (e.g. low – simple closed equations).

Estimation and Testing in an Imperfect Inspection Model

The Estimation and Testing in an Imperfect Inspection Model developed by SRIVASTAVA and YANHONG[42] was intended to estimate p (failure probability between successive inspection; expf(λT)) and β in order to determine whether imperfect-inspection is occurring. To do this the model makes the following assumptions:

- inspection duration is negligible,
- failed component is replaced by a new,

---

41 HURTADO et al, loc cit.

42 SRIVASTAVA, M. S. and YANHONG, W., Estimation & Testing in an Imperfect-inspection Model, *IEEE Transactions on Reliability*, v 42, n 2, Jun, 1993, p 280-286

- system of n components which have IID exponential life distribution with rate λ,
- inspection process is otherwise benign, and
- all components can be considered as either *new* or in a *state of undetected failure* after an inspection and subsequent replacement of the detected failures.

Overall, the imperfect-inspection model works through the probability of detecting a failure = β, where $0 < \beta \leq 1$, therefore allowing undetected failures to remain in the system after each inspection. The solution to this model was found through application of an approximate likelihood filtering of a Markov Chain. This method uses a first order autoregressive binomial model as an approximation of the original model where $\beta_{estimate}$ is small. In more general situations [i.e. when the assumption of exponential component life distribution does not hold], this approach can be quite complicated. However, we recommend using the autoregressive binomial models as a replacement. This results in the model being considered medium complexity since the solution requires MLE numerical solution and simulation.

Hybrid Maintenance Model with Imperfect Inspection for a System with Deterioration and Poisson Failure

The Hybrid Maintenance Model with Imperfect Inspection for a System with Deterioration and Poisson Failure developed by HOSSEINI, KERR and RANDALL[43] was intended to provide a comparison between break-down, planned scheduled maintenance, and condition-based maintenance to determine which provides better throughput. To do this the model makes the following assumptions:

- no preventative maintenance, and
- perfect inspection

The solution to the model was through the use of a state based solution using generalised stochastic Petri-Net where condition-based maintenance is undertaken (i.e. no preventative maintenance), subject to deterioration-failures and to Poisson-failures. Specifically the model uses two types of failures:

- ***Deterioration failure*** – a process where the important parameters of a system gradually worsen. If left unattended, the process leads to a deterioration failure. Sometimes called "*hard faults*" since they occur instantaneously in any deterioration stage and are generally unpredictable, so that a failure cannot be prevented and inevitability should be restored

43 HOSSEINI, M.M., KERR, R.M., RANDALL, R.B., Hybrid Maintenance Model with Imperfect Inspection for a System with Deterioration and Poisson Failure, *Journal of the Operational Research Society*, 50, 12, Dec 1999, p 1229-1243

by a corrective action. This is represented by a multi-state continuous-time Markov deterioration process.

- ***Poisson failure*** – a failure for which the failure-rate is constant. Sometimes called “soft faults” (trend faults), as they grow gradually with time, and lead to a predictable situation that lends itself to condition monitoring (i.e. inspection).

Furthermore, the model uses two types of restoration (repair/replace):

- ***minimal maintenance*** – limited effort and effect – for deterioration model, minimal maintenance restores the system to the previous deterioration state; and
- ***major maintenance*** – the system is restored to *as-goods-as-new*

Finally, after an inspection, based on the degree of deterioration, a minimal maintenance, or major maintenance, or no action is taken where:

- a deterioration failure is restored by major repair
- a Poisson failure is restored by minimal repair

Overall, the model is based on Hard Faults occurring instantaneously in any deterioration stage. These faults are generally unpredictable with the emphasis of the model on the maximisation of the system throughput, and optimal inspection policy within this strategy and optimal inter-inspection time are obtained. Due to the required use of a Petri-Net simulation to find a solution the complexity of this model is considered high.

Inspection, Maintenance and Replacement Models

The Inspection, Maintenance and Replacement Models developed by ABDEL-HAMEED[44] was intended to establish the optimal replacement level that yields the policy that simultaneously minimises (1) total discounted cost of maintenance and replacements and (2) long-run-average cost of maintenance and replacements per unit time. To do this the model makes the following assumptions:

- failure is detected only by inspection,
- perfect inspection,
- replacements are done using new and identical devices, and
- time to make the replacement is negligible.

Overall the model is based on based on *semi-Markov* damage from deterioration of the device subject to *inspection* and *imperfect maintenance*. The complexity of this model is considered low since there is a closed form solution.

---

44 ABDEL-HAMEED, M., Inspection, Maintenance and Replacement Models, *Computers & Operations Research*, Vol 22, No. 4, Apr, 1995, pp 435-441

Modelling of Inspection Reliability

The Modelling of Inspection Reliability developed by WALL[45] intended to provide a review of the reliability of the inspection process including how to model this process. The review of reliability of the inspection process, specifically:

- Probability of Detection (POD), and
- Probability of False Indication (PFI).

Furthermore, WALL discussed the definition and method of experimentally measuring POD and PFI. WALL also attempted to model, including the various approaches, of POD and PFI through theoretical estimation in lieu of measurement as a cost-effective means of progression. Finally, WALL discussed the validation of the models. Unfortunately, while WALL provides a comprehensive review of POD and PFI there is very little quantitative substance to the review and no model is provided.

Continuous-Time Predictive-Maintenance Scheduling for a Deteriorating System

The Continuous-Time Predictive-Maintenance Scheduling for a Deteriorating System was developed by GRALL, DIEULLE, BÉRENGUER and ROUSSIGNOL[46]. This method was intended to establish the optimal inspection and preventative-replacement decision in order to balance the cost caused by failure and unavailability

---

45 WALL, M., Modelling of Inspection Reliability, *IEEE*, 1996

46 GRALL, A., DIEULLE, L., BÉRENGUER, C., ROUSSIGNOL, M., Continuous-Time Predictive-Maintenance Scheduling for a Deteriorating System, *IEEE Transactions on Reliability*, Vol 51, No.2, June 2002

on an infinite horizon (i.e. steady state). It was based on 2 maintenance decision variables; (1) the preventative replacement threshold and (2) inspection schedule based on the system state. To do this the model makes the following assumptions:

- Perfect inspection – each inspection reveals instantaneously, and without error, the true state of the system
- Failure is detected only by inspection. Hence, if the system fails, it remains failed until the next inspection, and therefore active alarmed systems are not considered. The focus is on passive or inaccessible systems or structures whose failures are not obvious to the user and can be difficult to characterise and identify
- The time to make the replacement is negligible
- After a maintenance action, the system is as-good-as-new (i.e. perfect maintenance/repair)

Overall the model is based on the following decision variables that have to be jointly optimised to minimise the long-term cost of the maintained device:

- preventative-replacement threshold M, and
- inspection schedule

However, the model does not assume that the system is regularly inspected; irregular inspection dates are allowed; the next inspection depends on the system state revealed by the current inspection. Furthermore, the deterioration within the model is based on the Gamma function which describes a positive, increasing jump processes with statistically independent stationary increments. Due to the required use of numerical integration to allow the optimisation of the various factors, the complexity of this model is considered high.

Renewal Process in Reliability Engineering Software

Through the course of the research it was clear that interest in "realistic" modelling of the renewal process, mainly for repairable items (or systems) was increasing. This trend is evidenced by the increasing number of journal and conference papers. While some of the most interesting model that can take into account imperfect inspection and maintenance are discussed above, there was a similar change in reliability engineering software. The software allows repairs to components to be effected by a "repair factor", which is essentially the same as the KIJIMA 'q' value (refer to Chapter 3: Current Techniques for Analysis of Renewal Process). Consequently, the "repair factor" creates a KIJIMA Type I or Type II model.

Software that includes a "repair factor" are as follows:

- AvSIM+ (v9.0) by Isograph (refer to http://www.isograph-software.com/avsover.htm). While AvSIM+ does allow the user to enter a value for the "repair factor", it does not provide a technique for calculating the "repair factor".

- Weibull++ (v7) by Reliasoft (refer to http://www.reliasoft.com/Weibull/index.htm). Similar to the AvSIM+ product the Weibull++ (v7) product allows the user to enter a value for the "repair factor". However, unlike the AvSIM+ product the Weibull++ (v7) product also includes a 'q' parameter estimator based on a Maximum Likelihood Estimator (MLE) approach as described in METTAS et al[47].
- Bayesian Reliability Assessment Tool (BRASS) (V1.2) by Prediction Technologies (refer to http://www.prediction-technologies.com/products/brass.htm)

Summary of Renewal Process Models

While there are many renewal process models that vary in terms of their underlying assumptions, intended use and level of complexity these alternative models appear unable to improve on the GRPs mechanism for allowing the inclusion of imperfect inspection and maintenance.

Accordingly, the GRP model was selected as the underlying renewal process model given its ability to contend with both imperfect inspection and maintenance and therefore capable of the realistic study of RIs.

---

47 METTAS, A. and ZHAO, W, loc cit.

Chapter 4: Mathematical Set-up of Each Case

Introduction

Generic Model

Modelling of the various cases involves two distinct steps as illustrated in Figure 14; *Parameter Estimation* and *CIF simulation*.

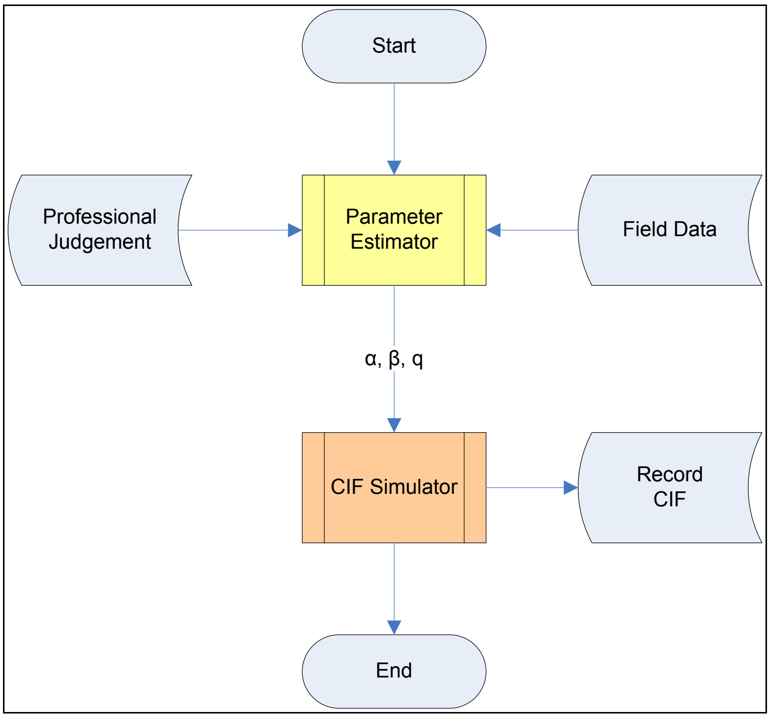

Figure 14: Generic Mathematic Set-up of Cases

For simplicity each model component will be examined separately. Furthermore, although the individual cases have some factors in common, there are also a number of differences in each step and therefore the solution to individual cases will be examined separately.

Model Time

At first glance there appears to be only two timeframes within these models; operating time and virtual time. However, the ability of a component to be in a failed state without being discovered (e.g. Case xB and Case 5A) there is a requirement to introduce a third timeframe; aircraft time. The reader should note that this generic reference to "time" equally represents other aviation "times" such as number of engine starts, landings, hull pressurisations, etc. Accordingly, in the modeling of all the cases detailed in Chapter 2: Description of Cases to be Modelled, three "time" clocks are used to monitor the "times" involved:

- Operational hours,
- Virtual hours, and
- Airframe hours.

Treatment of Uncertain and Soft Data

Before examining the mathematical set-up each individual case, it is important to discuss how to treat *uncertain* and *soft* data.

General Methodology for the Treatment of Uncertain Data

The standard Bayes Theorem is provided at Equation 19.

$$\pi(x|E) = \frac{L(E|x) \cdot \pi_0(x)}{\int L(E|x) \cdot \pi_0(x) \cdot dx}$$

Equation 19: Standard Form of Bayes Theorem

Here $\pi(x \mid E)$ = probability of observing x given the evidence (E)

$L(E \mid x)$ = likelihood of the evidence (E) given the variable x

π_0 = prior distribution of x

Additionally, the evidence, and specifically in this case the uncertain data, can be defined as shown in Equation 20.

$$E = \{E_i, w_i\}$$

Equation 20: Format of Uncertain Data/Evidence

Here E_i = i^{th} piece of evidence

w_i = belief or "weight" of the i^{th} evidence

Given the form of the uncertain data provided at Equation 20 it is possible to modify Equation 19. Specifically there are three methods as described in MOSLEH[48] of making allowance for the uncertain data as follows:

[48] MOSLEH, A., ENRE655 – Advanced Reliability Modelling Course Notes; University of Maryland, USA, 2005

Method 1 – Weighted Likelihood Method

The first method of treating uncertain data is through the modification of the likelihood function L (E | x) from Equation 19. There are two techniques for modifying the likelihood function as shown in Equation 21 and Equation 22.

$$\pi(x|E) = \frac{\left[\sum_{i=1}^{n} L(E|x)\cdot \Pr(E_i)\right]\cdot \pi_0(x)}{\int\left[\sum_{i=1}^{n} L(E|x)\cdot \Pr(E_i)\right]\cdot \pi_0(x)\cdot dx} = \frac{\left[\sum_{i=1}^{n} L(E|x)\cdot w_i\right]\cdot \pi_0(x)}{\int\left[\sum_{i=1}^{n} L(E|x)\cdot w_i\right]\cdot \pi_0(x)\cdot dx}$$

Equation 21: Weighted Likelihood Function – Product Technique

Where there are *n* pieces of evidence.

$$\pi(x|E) = \frac{\prod_{i=1}^{n}\left[L(E|x)\right]^{w_i}\cdot \pi_0(x)}{\int\prod_{i=1}^{n}\left[L(E|x)\right]^{w_i}\cdot \pi_0(x)\cdot dx}$$

Equation 22: Weighted Likelihood Function – Power Technique

Method 2 – Weighted Posterior Method

The second method of treating uncertain data is through the modification of the posterior function as shown in Equation 23.

$$\pi(x|E_i) = \frac{L(E_i|x)\cdot \pi_0(x)}{\int L(E_i|x)\cdot \pi_0(x)\cdot dx}$$

$$\pi(x|E) = \sum_{i=1}^{n}\pi(x|E_i)\cdot \Pr(E_i) = \sum_{i=1}^{n}\pi(x|E_i)\cdot w_i$$

Equation 23: Weighted Posterior Technique

Method 3 – Weighted Data

The third method of treating uncertain data is through the modification of the individual evidence, or data, as shown in Equation 24.

$$\overline{E} = \sum_{i=}^{n} E_i \cdot w_i$$
$$\pi\left(x \middle| \overline{E}\right) = \frac{L\left(\overline{E} \middle| x\right) \cdot \pi_0(x)}{\int L\left(\overline{E} \middle| x\right) \cdot \pi_0(x) \cdot dx}$$

Equation 24: Weighted Data Technique

Each of the three methods for treating uncertain data have differing advantages and disadvantages. Consequently, the selection of the method for implementation should be made with these in mind.

Implementation of the Treatment of Uncertain Data in GRP Equation

Throughout the research one area that I concentrated on was uncertainty in the failure times, t_i, defined as Case xB, in Table 3. Here the likelihood function was constricted when t_i is uncertain and then integrated over a range of times. Furthermore, the management of the uncertain failure times assumed equal weighting (i.e. relevance)

However, it is possible to modify the solution offered in the research to allow different weighting (i.e. relevance) for different portions of the data. Specifically, the technique used throughout the research could be modified as shown in Equation 25 to allow for different weighting (i.e. relevance) for different portions of the data.

$$
\begin{aligned}
&L = \left[L\left(E_i | x\right)\right]^{w_i}\\
&\text{where } 0 \le w_i \le 1 \text{ and}\\
&w_i = 0 \Rightarrow \text{data is not relevant}\\
&w_i = 1 \Rightarrow \text{data is fully relevant}
\end{aligned}
$$

Equation 25: Implementation of Weighted Likelihood Function – Power Technique

Additionally other *soft data* can be introduced into the GRP equation through the *prior distribution* as described in Role of the Prior Distribution.

Selection of Method for the Treatment of Uncertain Data in GRP Equation

Given each of the three methods for treating uncertain data have differing advantages and disadvantages, and the possible use of introducing *soft data* via the *prior distribution*, the nature of the data uncertainty will determine how the Bayesian GRP solution is modified.

Case 1A

Parameter Estimator for Case 1A

The estimation of α, β and q for Case 1A is relatively simple using the Slice Sampling technique described in Chapter 5: . The reader should note that rather sample from a distribution for x = (x_1, x_2, . . . , x_n) by applying a single variable slice sampler, it is possible to sample from the multivariate distribution. This technique is referred to by NEAL[49] as *multivariate slice sampling*. Since the number of parameters (n) in Case

49 NEAL, R. M., loc cit.

1A = 3, this technique is not overly burdensome in either complexity or computation time. A high level process map of the estimator model used is provided in Figure 15.

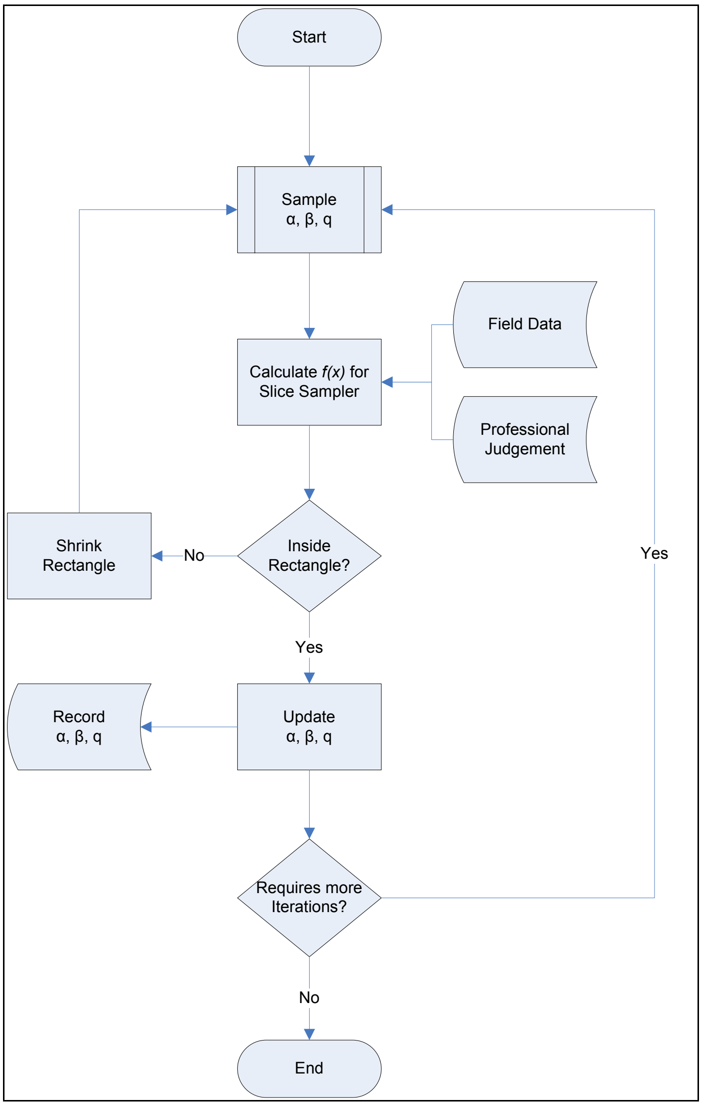

Figure 15: Estimation Process for Case 1A

CIF Simulator for Case 1A

The simulation of the simple GRP (Case 1A) was previously provided in JACOPINO, A., GROEN, F. and MOSLEH, A[50]. However, for clarification the equation for simulating a KIJIMA Type I GRP equation is provided in Equation 26.

$$t_{k+1} = t_k \cdot (1-q) + \alpha \cdot \left[\left(\frac{q \cdot t_k}{\alpha} \right)^{\beta} - \ln(U') \right]^{\frac{1}{\beta}}$$

$$where$$

$$U' = 1 - \langle 0,1 \rangle$$

Equation 26: KIJIMA Type I GRP TTF Simulation Equation

Please refer to Chapter 3: Current Techniques for Analysis of Renewal Process or JACOPINO, et al[51] for additional discussion on the TTF simulation of GRP equations.

<u>Case 1B</u>

Parameter Estimator for Case 1B

In Case 1B the estimator now needs to take into account data uncertainty of the times to failure by including the inspection intervals in order to bound when a failure could have occurred. Accordingly, the equations now include the intervals as auxiliary

---

50 JACOPINO, A., GROEN, F. and MOSLEH, A., *Behavioural Study of the General Renewal Process*, Reliability, Availability and Maintainability Symposium, Los Angles, CA, USA, 2004

51 ibid.

variables as shown in Equation 27 where I_i and I_{i-1} is the most recent i^{th} and $(i-1)^{th}$ inspection interval.

$$\Pi\left(t_i \middle| \alpha, \beta, q, t_{i-1}, I_i, I_{i-1}\right)$$

Equation 27: Auxiliary Variable Equation including Inspection Intervals

Graphically, using the underlying Weibull pdf, this appears as shown in Figure 16.

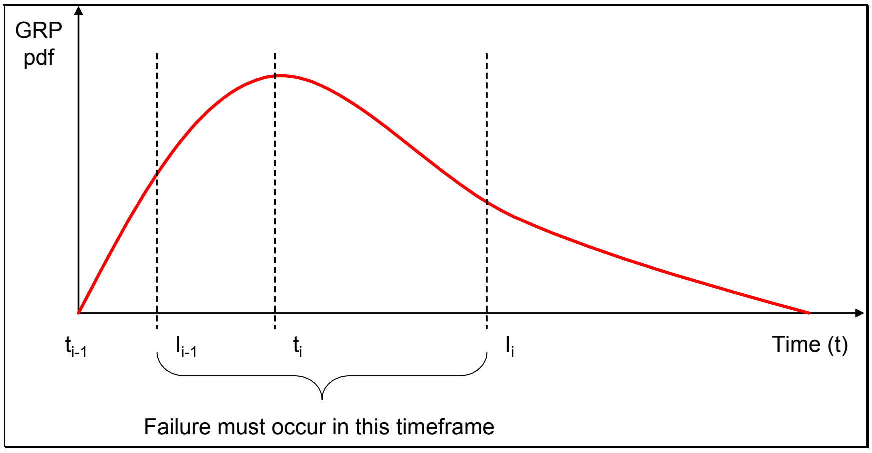

Figure 16: Inspection Interval and Underlying Weibull pdf

Here the pdf for the slice sampler for Case 1B is of the form provided in Equation 28.

$$\Pi = \frac{pdf(X_i)}{R(Y_{i-1}) - R(Y_i)} \cdot \frac{R(X_{i-1}) - R(Y_{i-1})}{R(X_{i-1})}$$

$$where$$

$$X_i = t_{i-1} \cdot q + t_i - t_{i-1}$$

$$X_{i-1} = t_{i-2} \cdot q + t_{i-1} - t_{i-2}$$

$$Y_i = X_i + I_i - t_i = t_{i-1} \cdot q + I_i - t_{i-1}$$

$$Y_{i-1} = t_{i-1} \cdot q + I_{i-1} - t_{i-1}$$

Equation 28: Slice Sampler f(x) for Case 1B

The use of the auxiliary variables and the KIJIMA Type I model in which the next TTF, t_i, is only dependant upon the previous TTF, t_{i-1}, allows the simplification of Equation 27 as shown in Equation 29:

Given

$$\alpha, \beta, \mathrm{q} \mid t_1, t_2, t_{3,} \ldots$$

$$t_1 \mid \alpha, \beta, \mathrm{q}, t_2, t_{3,} \ldots$$

$$t_2 \mid \alpha, \beta, \mathrm{q}, t_1, t_{3,} \ldots$$

Then

$$f(x) = \pi(t_1 \mid \alpha, \beta, q) \cdot \pi(t_2 \mid \alpha, \beta, q, t_1) \cdot \pi(t_3 \mid \alpha, \beta, q, t_2) \cdot \pi(t_4 \mid \alpha, \beta, q, t_3) \ldots$$

Equation 29: Simplification of Auxiliary Variable Equation for Case 1B

Consequently, to find t_2, only need $\Pi(t_1 \mid \alpha, \beta, q)$ x $\Pi(t_2 \mid \alpha, \beta, q, t_1)$, and to find t_3, only need $\Pi(t_3 \mid \alpha, \beta, q, t_2)$ x $\Pi(t_2 \mid \alpha, \beta, q, t_1)$, etc

Therefore, *f(x)* for the slice sampler for each time is as shown in Equation 30 and Equation 31.

$$f(x = t_1) = \Pi_0(\alpha, \beta, q) \cdot h(t_1 \mid \alpha, \beta, q, t_1, I_1)$$

where

$$h(t_1 \mid \alpha, \beta, q, t_1, I_1) = \frac{\frac{\beta}{\alpha} \cdot \left(\frac{t_1}{\alpha}\right)^{\beta - 1} \cdot e^{-\left(\frac{t_1}{\alpha}\right)^{\beta}}}{1 - e^{-\left(\frac{I_1}{\alpha}\right)^{\beta}}}$$

Equation 30: f(x) for t_1 for Case 1B

$$f(x = t_2 \ldots t_n) = \Pi_0(\alpha, \beta, q) \cdot h(t_2 \mid \alpha, \beta, q, t_2, t_1, I_2, I_1)$$
$$where$$
$$h(t_1 \mid \alpha, \beta, q, t_1, I_1) = \frac{\frac{\beta}{\alpha} \cdot \left(\frac{t_2 - t_1 + q \cdot t_1}{\alpha} \right)^{\beta - 1} \cdot e^{-\left(\frac{t_2 - t_1 + q \cdot t_1}{\alpha} \right)^{\beta}}}{e^{-\left(\frac{I_1 - t_1 + q \cdot t_1}{\alpha} \right)^{\beta}} - e^{-\left(\frac{I_2 - t_1 + q \cdot t_1}{\alpha} \right)^{\beta}}} \cdot \frac{e^{-\left(\frac{q \cdot t_1}{\alpha} \right)^{\beta}} - e^{-\left(\frac{I_1 - t_1 + q \cdot t_1}{\alpha} \right)^{\beta}}}{e^{-\left(\frac{q \cdot t_1}{\alpha} \right)^{\beta}}}$$

Equation 31: f(x) for $t_2 \ldots t_n$ for Case 1B

CIF Simulator for Case 1B

The GRP simulator for Case 1B must be taken into account the delay from the time of failure to the time of inspection (and instantaneous repair). Therefore, the simple GRP simulation found in JACOPINO, et al[52] and can be modified as shown in Equation 32.

$$t_{i+1} = I_i(1 - q) + \alpha \cdot \left[\left(q \cdot \frac{I_i}{\alpha} \right)^{\beta} - \ln(1 - U) \right]^{\frac{1}{\beta}}$$
$$where$$
$$U = \langle 0,1 \rangle$$

Equation 32: CIF Simulation Equation for Case 1B

Case 2A

Case 2A is relatively simple. In this situation the independent data sources for each of the particular failure mode are analysed using the estimator in Case 1A. The key to this technique is the assumption of independence and the use of multiple ‘clocks’ to independently simulate and compare the TTF of each of the individual failure

52 JACOPINO, et al, loc cit.

modes. A process map describing the mathematical set-up of the Case 2A model is provided in Figure 17.

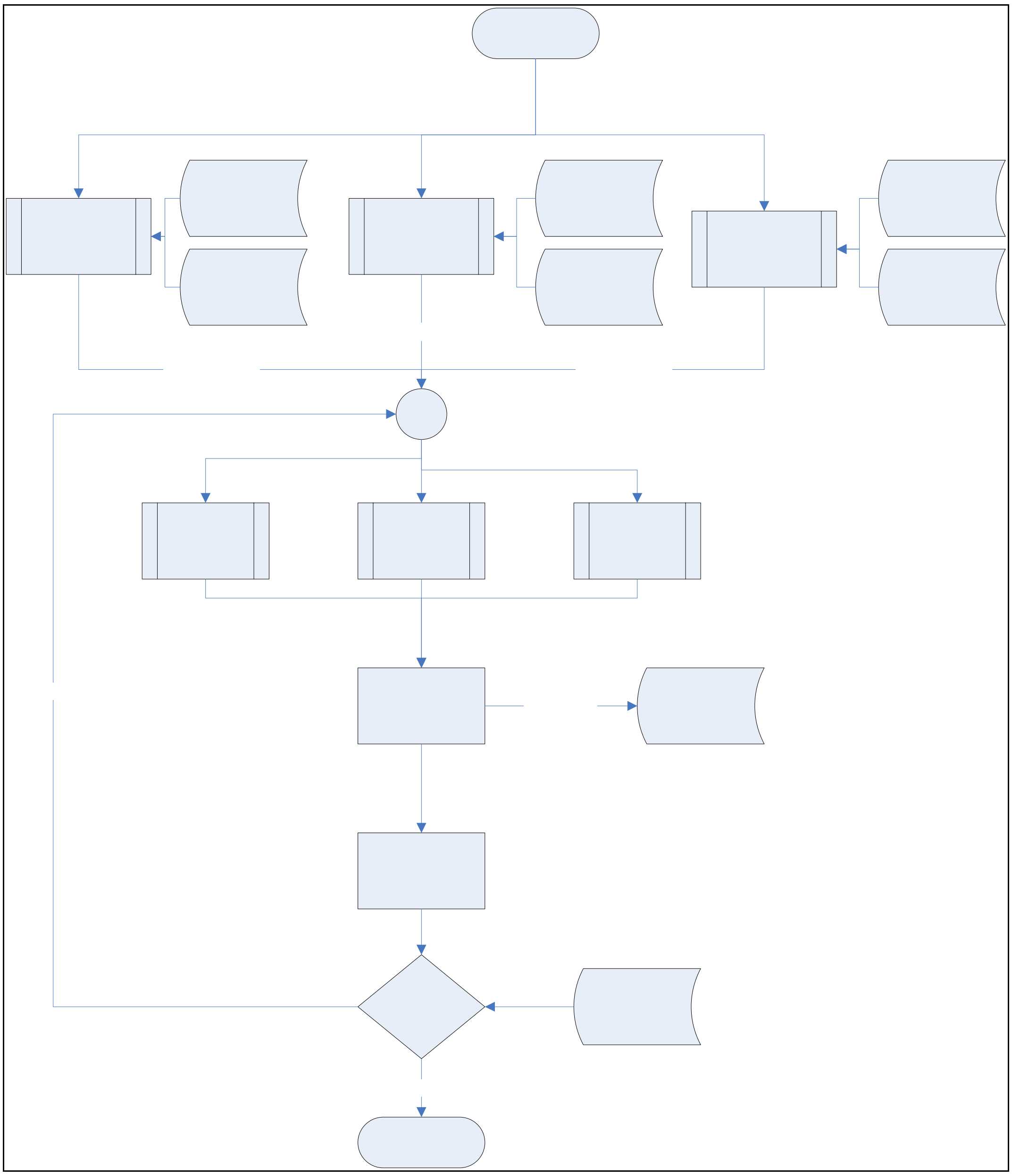

Figure 17: Process Map for Case 2A Model

Failure
Fiel

Slice Sampler
Parameter for

Parameter Estimator for Case 2A

In Case 2A the parameter estimator for each failure mode is assumed to be independent and therefore the solution is the same as for Case 1A. However, for Case 2A the output from the parameter estimator are series of <*α, β, q*> parameters sets for each failure mode.

CIF Simulator for Case 2A

Similar to the parameter estimator the CIF simulator uses multiple independent Case 1A CIF simulators. However, the technique, typically referred to as "competing failure modes[53]" is then used to identify which failure mode fails (and therefore is renewed) next.

Case 2B

The model set-up for Case 2B is the same as for Case 2A, however, the individual (and independent) estimators and simulators for each failure model corresponds to the Case 1B solutions. Again, the key to modelling Case 2B is through the assumption of independent simulation and comparison of multiple 'clocks', representing each failure mode, in order to determine the TTF of the overall component.

53 NELSON, W. B., *Accelerated Testing : Statistical Models, Test Plans, and Data Analysis*, Wiley Series in Probability and Statistics, Wiley-Interscience, USA, 1990

Parameter Estimator for Case 2B

Here the parameter estimator for each failure mode is assumed to be independent from each other and therefore is the same as for Case 1B. Again, the output from the Case 2B parameter estimator is a number of $<\alpha, \beta, q>$ parameters sets for each failure mode.

CIF Simulator for Case 2B

Similar to the Case 2B parameter estimator the CIF simulator uses multiple independent Case 1B CIF simulators where a "competing failure mode" model is then used to identify which failure mode fails (and therefore is renewed) next.

Case 3A

Introduction

Case 3A introduces dependent failure modes into the previous Case 2A solution. The dependency between failure modes is achieved through the use of additional q variables which represent both the effect of the maintenance action on the failure mode undergoing direct maintenance (i.e. in a failed state), and also the indirect effect on the other failure modes. Consequently, each direct and indirect failure mode relationship requires a variable. For example, considering two dependent failure modes results in the variables listed in Equation 33.

$$\begin{bmatrix} \alpha_{FM1} & \beta_{FM1} & q_{FM1-Direct\_CM} & q_{FM1-Indirect\_CM} \\ \alpha_{FM2} & \beta_{FM2} & q_{FM2-Indirect\_CM} & q_{FM2-Direct\_CM} \end{bmatrix}$$

Equation 33: Variable Set-up for Case 3A/3B

As can be seen from Equation 33 each additional failure mode will increase the number of variables to be solved. For example, while a two failure mode solution requires 8 parameters, a 4 failure mode solution requires 24 parameters.

Again in Case 3A, inspection is assumed perfect and therefore only associated with corrective maintenance actions. However, unlike Case 1A – 2B the dependent relationship makes it possible for the virtual age of the indirect failure mode to be advanced after maintenance actions (i.e. *worse-than-old* where $q > 1$). For example, in a 2-dependent failure mode model, if failure mode 1 incurs some corrective maintenance, then while failure mode 1 will be restored, the virtual age of failure mode 2 will be effected by $q_{FM1\text{-}Indirect}$ and may be worse than before the maintenance action.

Estimator for Case 3A

The parameter estimator for Case 3A uses the same *f(x)* defined in Case 2A at Equation 28 noting that the input data must now include:

- failure by failure mode, and
- when the Preventative Maintenance actions are scheduled to occur.

However, unlike Case 2A, when a maintenance action occurs the *Virtual Age* for all failure modes are updated including the potential for making the indirect failure modes *worse-than-old*. In Case 3A the results from the parameter estimation are a series of $<\alpha_i, \beta_i, q_{i\text{ – Direct Corrective Maintenance}}, q_{i\text{ – Indirect Corrective Maintenance}}>$ parameter sets. A process map describing the mathematical set-up of the Case 3A model is provided in Figure 18.

Simulator for Case 3A

The CIF simulator for Case 3A uses a similar technique to the CIF simulator for Case 2A. However, unlike Case 2A when a Corrective Maintenance action occurs the virtual age of **all** failure modes is adjusted based on the time when an individual failure mode failed and therefore which direct and indirect q's need to be applied. As before, the next simulated TTF for these various failure modes are then combined via the completing failure mode technique. A process map describing the mathematical set-up of the Case 3A model is provided in Figure 19.

Case 3B

Simular to the difference between Case 2A and Case 2B, Case 3B only varies the Case 3A parameter estimator through the change in *f(x)* to include the inspection intervals as defined boundaries. Consequently the data required for Case 3B must include the inspection times. Furthermore, similar to Case 3A the model includes a number of new parameters to represent both the direct and indirect application of q.

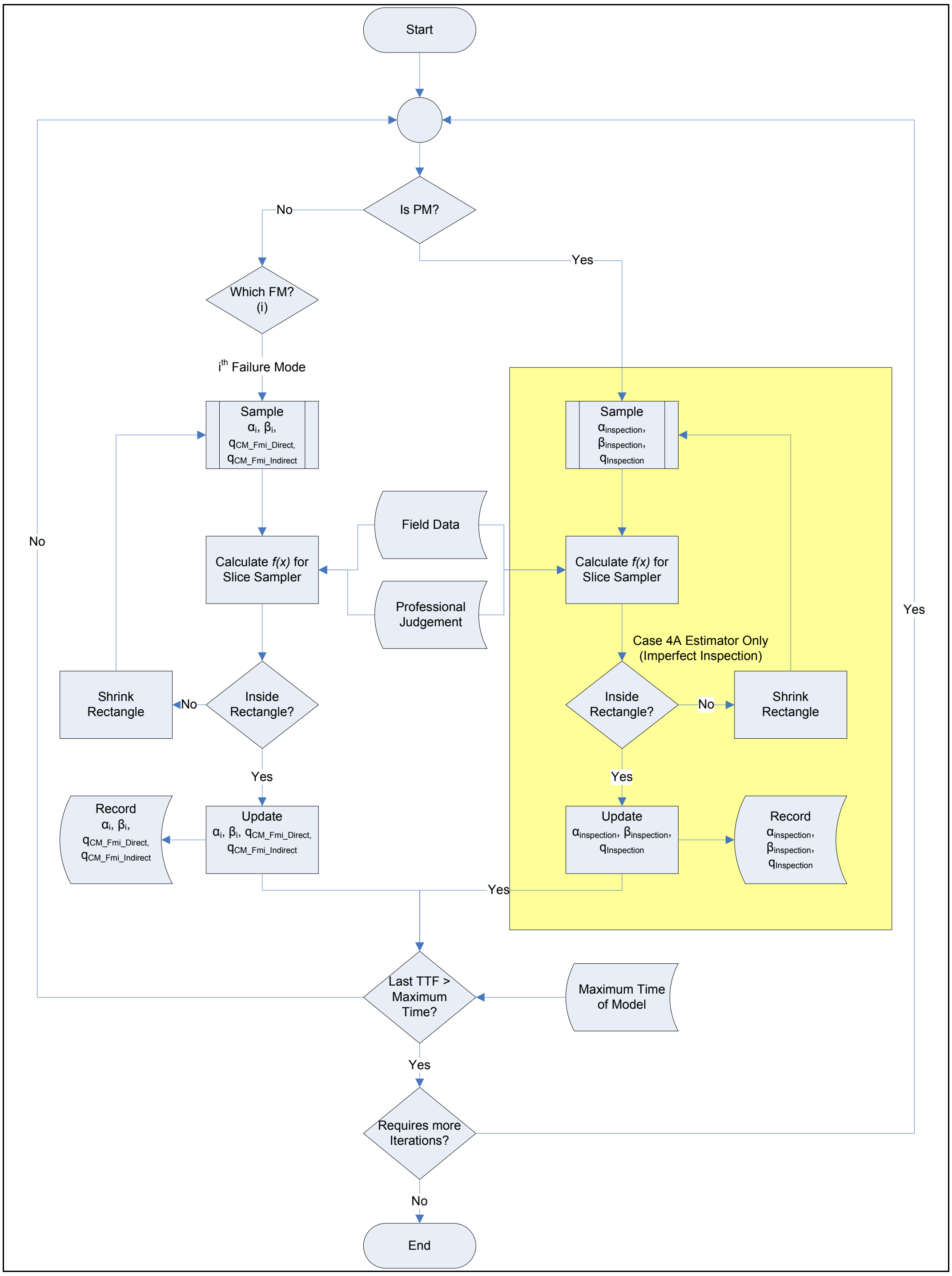

Figure 18: Process Map for Case 3A/4A/5A Parameter Estimator

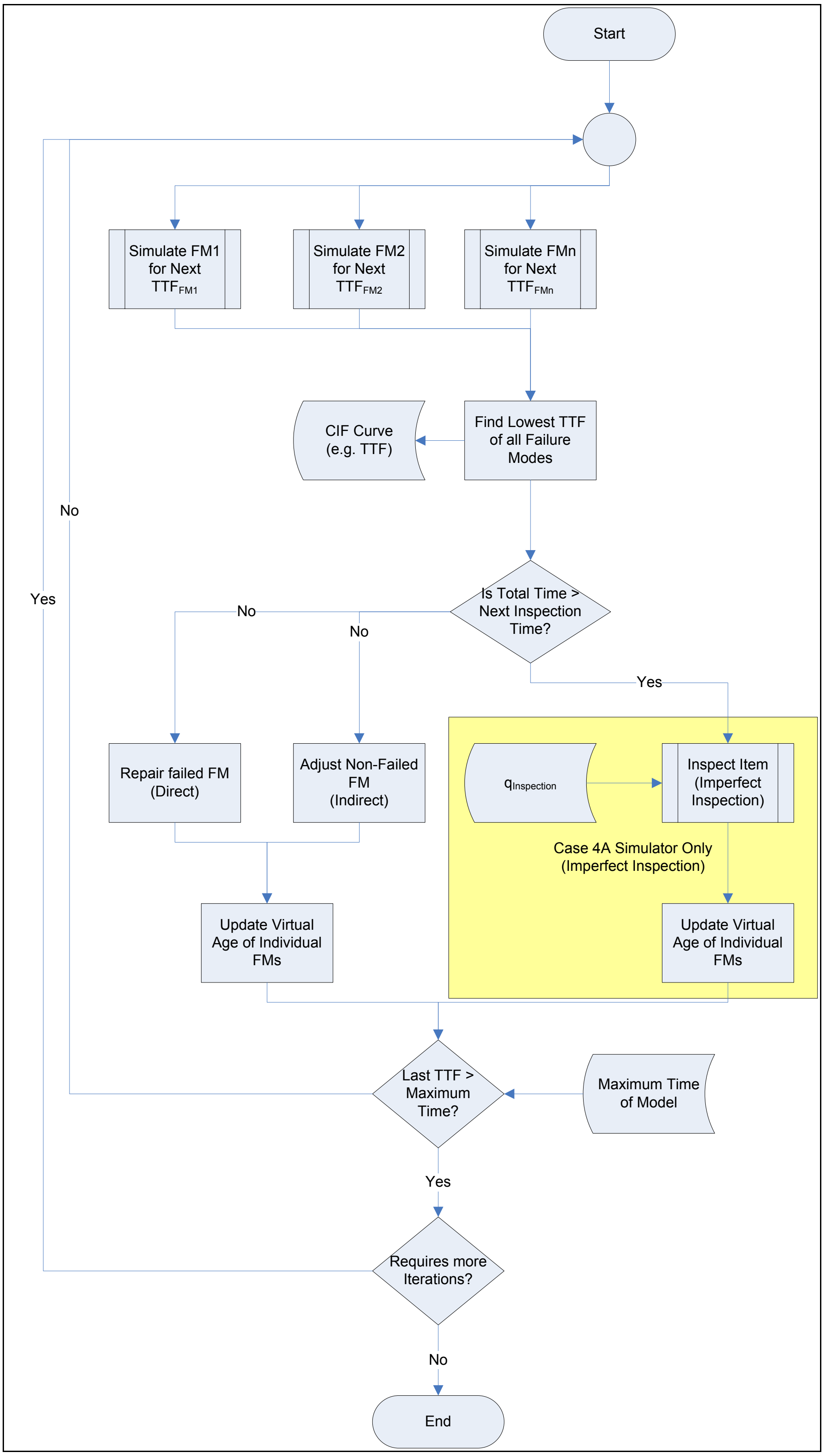

Figure 19: Process Map for Case 3A/4A TTF Simulator

Case 4A

Introduction

Case 4A introduces *Imperfect Inspection* in the Preventative Maintenance actions to the previous Case 3A model of imperfect maintenance of multiple dependent failure modes. The modelling of the *Imperfect Inspection* is achieved through the use of additional *q* variables which represent the effect of the inspection activity on each of the failure modes. For example, considering 2 dependent failure mode with *Imperfect Inspection* results in the variables listed in Equation 34.

$$\begin{bmatrix} \alpha_{FM1} & \beta_{FM1} & q_{FM1-Direct\_CM} & q_{FM1-Indirect\_CM} & q_{FM1-Inspection} \\ \alpha_{FM2} & \beta_{FM2} & q_{FM2-Indirect\_CM} & q_{FM2-Direct\_CM} & q_{FM2-Inspection} \end{bmatrix}$$

Equation 34: Variable Set-up for Case 4A/4B

As can be seen from Equation 34 each additional failure mode will increase the number of variables to be solved. For example, while a 2 failure mode solution requires 10 parameters, a 4 failure mode solution requires 28 parameters.

Similar to Case 3A the maintenance actions and inspection makes it possible for the *Virtual Age* of the failure mode to be advanced (i.e. *worse-than-old* where $q > 1$).

Estimator for Case 4A

The parameter estimator for Case 4A is the same as in Case 3A except that if a preventative maintenance action, including inspection occurs, the $q_{inspection}$ is re-evaluated. Again, when either a corrective or preventative maintenance action occurs the virtual age for all failure modes are updated including the potential for making the failure modes *worse-than-old*. In Case 4A the results from the parameter estimation are a series of <α_i, β_i, $q_{i\text{ – Direct Corrective Maintenance}}$, $q_{i\text{ – Indirect Corrective Maintenance}}$, $q_{i\text{ – Preventative Maintenance}}$> parameter sets. A process map describing the mathematical set-up of the Case 4A model is provided in Figure 18.

Simulator for Case 4A

The CIF simulator for Case 4A uses a similar technique to the CIF simulator for Case 3A. However, unlike Case 3A when a Preventative Maintenance action occurs, including inspection, the *Virtual Age* of **all** failure modes is adjusted. As before, the next simulated TTFs for these various failure modes are then combined via the completing failure mode technique. A process map describing the mathematical set-up of the Case 4A model is provided in Figure 19.

Case 4B

Simular to the difference between Case 3A and Case 3B, Case 4B only varies the Case 4A parameter estimator through the change in *f(x)* to include the inspection intervals as defined boundaries. Consequently the data required for Case 4B must include the inspection times. Furthermore, similar to Case 4A the model includes a number of new parameter to represent both the dependency of the corrective maintenance action and imperfect maintenance.

Case 5A

Introduction

Case 5A introduces delays in maintenance actions from the point of discovery of the failure. While the modelling of Case 5A uses the same variable as Case 4A (refer to Equation 34) the actual set-up of the Case 5A parameter estimator and TTF simulator are different.

Estimator for Case 5A

The parameter estimator for Case 5A is the same as in Case 5A expect that delays can be observed between the detection of a failure and the maintenance action. Again, when either a corrective or preventative maintenance action occurs the virtual age for all failure modes are updated including the potential for making the failure modes *worse-than-old*. In Case 5A the results from the parameter estimation are a series of $<\alpha_i, \beta_i, q_{i\text{ – Direct Corrective Maintenance}}, q_{i\text{ – Indirect Corrective Maintenance}}, q_{i\text{ – Preventative Maintenance}}>$ parameter sets. A process map describing the mathematical set-up of the Case 4A model is provided in Figure 18.

Simulator for Case 5A

The CIF simulator for Case 5A uses a similar technique to the CIF simulator for Case 4A. However, unlike Case 4A a delay in the maintenance action can be introduced where the virtual age of **all** failure modes is adjusted. As before, the next simulated TTF for these various failure modes are then combined via the competing failure mode technique. A process map describing the mathematical set-up of the Case 5A model is provided in Figure 20.

Case 5B

Simular to the difference between Case 4A and Case 4B, Case 5B only varies the Case 5A parameter estimator through the change in *f(x)* to include the inspection intervals as defined boundaries. Consequently the data required for Case 5B must include the inspection times. Furthermore, similar to Case 5A the model includes a number of new parameter to represent both the dependency of the corrective maintenance action and imperfect maintenance.

Most Likely Case for Aviation Industry

While 10 cases have been presented to satisfactorily model reality, there are 2 cases that are most representative. Specifically, Cases 4A and 4B are considered the most representative since they are flexible in terms of failure modes and associated dependencies.

Cases 5A and 5B are not considered the most representative for the aviation industry since the major systems are all monitored for failures. While there are some RIs and circumstances where a failure may not be repaired for a period of time (called a Carried Forward Unserviceability (CFU) with Australian Defence aviation areas) these items, by definition, are not safety critical. Accordingly, while they are legitimate part of the aircraft, given there is insufficient resources for all Case 5A and Case 5B RIs they are not considered a high priority for RI analysis.

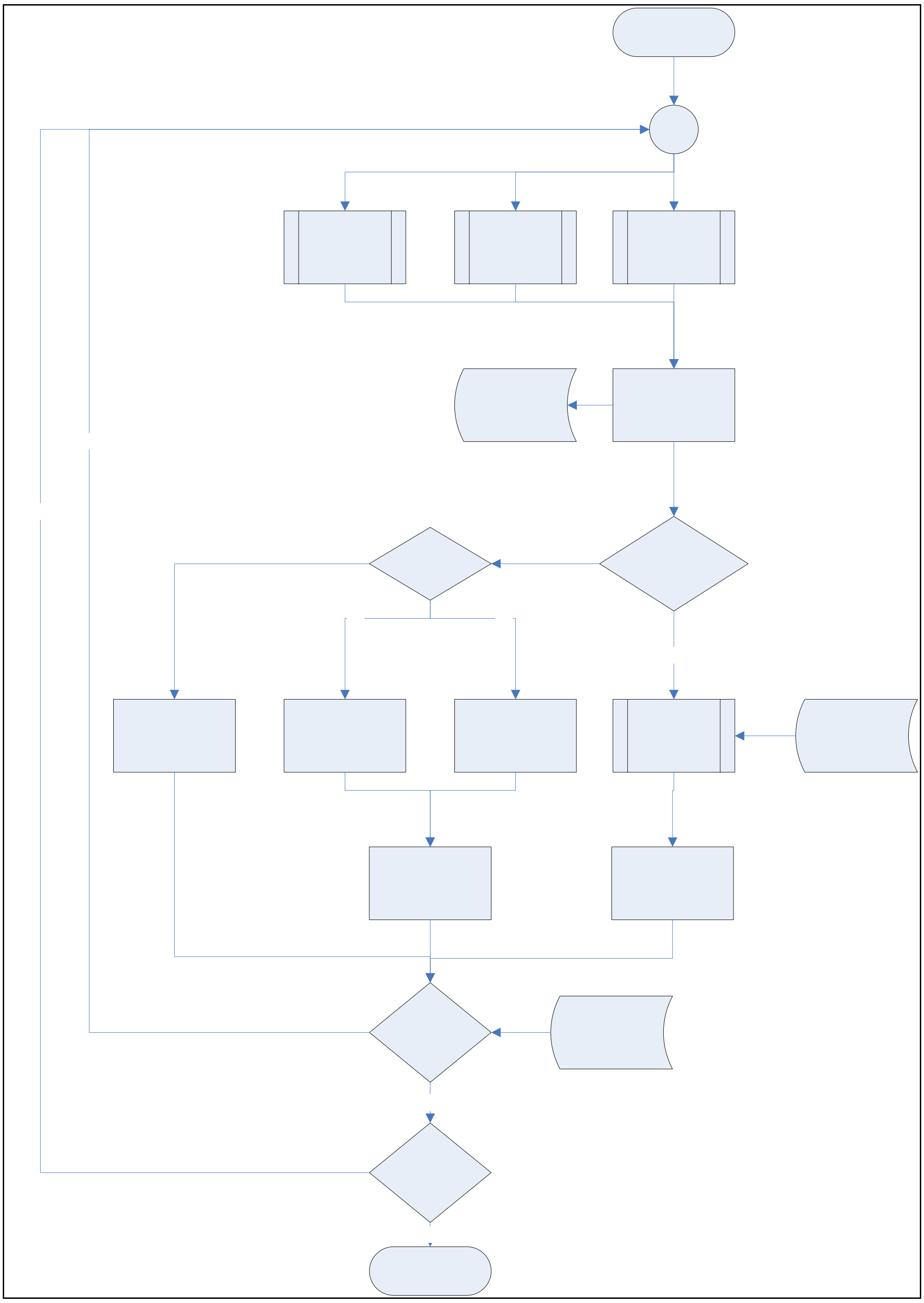

Figure 20: TTF Simulator for Case 5A

Chapter 5: Numerical Methods

Introduction

As discussed in Chapter 3: Current Techniques for Analysis of Renewal Process, unfortunately there is no closed form solution to the GRP equation. Accordingly, a numerical method is needed to estimate the various parameters of the GRP equation. Initially, a Markov Chain Monte Carlo (MCMC) method, such as Gibbs sampling or the Metropolis-Hastings algorithm, was considered to sample from the complex, multivariate distribution defined by the cases in Chapter 2: Description of Cases to be Modelled. However, both these MCMC methods have a number of disadvantages with their use and consequently an alternative MCMC sampler developed by NEAL[54], typically referred to as the *Slice Sampling* method, was utilised.

The aim of this chapter is threefold. Firstly, this chapter will provide a background on the *Slice Sampling* method including comparison with other MCMC methods. Secondly, this chapter will describe the implementation of the *Slice Sampling* method, including describing the role of $f(x)$ on the final result. Finally, this chapter will examine the effects of autocorrelation, a common problem in MCMC samplers, and discuss the solution utilised throughout the research.

---

[54] NEAL, R. M., loc cit

Posterior Density Function for Bayesian GRP Equation

According to Bayes Theorem, the probability distribution for known failure times (i.e. Case xA) can be represented as shown in Equation 35.

$$\pi(\alpha,\beta,q|E)=\frac{\hat{L}(E|\alpha,\beta,q)\cdot\pi_0(\alpha,\beta,q)}{\iiint\limits_{\alpha,\beta,q}\hat{L}(E|\alpha,\beta,q)\cdot\pi_0(\alpha,\beta,q)}$$

Equation 35: Posterior Density Function for Case xA

Here, the posterior density function is the normalised product of the general likelihood function *L(E | α, β, q)* and the prior distribution $\pi_0(\alpha, \beta, q)$. The general likelihood function *L(E | α, β, q)* describes the probability of observing evidence *E*, given that *α*, *β* and *q* are the true parameters of the GRP model.

Additionally, Equation 35 can be modified for the case where there is uncertainty in the failures time (i.e. Case xB) which are defined as (t_1, . . . ,t_{n+1}), where t_i is the time of the i^{th} failure and *n* is the number of failure observed at the time of last observation. In this case the general likelihood function $L(E \mid \alpha, \beta, q, (t_1, \ldots, t_{n+1}))$ describes the probability of observing evidence *E*, given that *α*, *β*, *q* and $(t_1, \ldots, t_{n+1})$ are the true parameters of the GRP model. The equation for the probability distribution for Case xB is provided in Equation 36.

$$\pi(\alpha,\beta,q|E)=\frac{\hat{L}(E|\alpha,\beta,q,(t_1\ldots t_n))\cdot\pi_0(\alpha,\beta,q)}{\iiint\limits_{\alpha,\beta,q,(t_1\ldots t_n)}\hat{L}(E|\alpha,\beta,q,(t_1\ldots t_n))\cdot\pi_0(\alpha,\beta,q)}$$

Equation 36: Posterior Density Function for Case xB

In both equations the evidence is either of known failure times or unknown failure times (but known inspection intervals).

General Likelihood Function for Bayesian GRP Equation

GROEN[55] showed that the GRP failure density of the i^{th} failure could be represented as shown in Equation 37.

$$f\left(\tau_i \middle| \alpha, \beta, q, \tau_{i-1}\right) = \frac{1}{R_W\left(q \cdot \tau_{i-1} \middle| \alpha, \beta\right)} \cdot f_W\left(\tau_i - \tau_{i-1} + q \cdot \tau_{i-1} \middle| \alpha, \beta\right)$$
$$where$$
$$R_W(t) = e^{-\left(\frac{t}{\alpha}\right)^{\beta}}$$
$$f_W(t) = \frac{d}{dt} R_W(t) = \frac{\beta}{\alpha} \cdot \left(\frac{t}{\alpha}\right)^{\beta-1} \cdot e^{-\left(\frac{t}{\alpha}\right)^{\beta}}$$

Equation 37: GRP Failure Density of the i^{th} Failure

While Equation 37 describes the influence of individual failures, the data will be represented as a sequence of failure times ($t_1, \ldots, t_{n+1}$). Therefore, Equation 37 can be utilised to find some function *g(x)* which represents the probability density of a particular sequence ($t_1, \ldots, t_{n+1}$) as shown in Equation 38.

$$g(x) = \pi\left[\left(t_1 \ldots t_{n+1}\right) \middle| \alpha, \beta, a\right]$$

Equation 38: Probability Density of a Particular Failure Sequence

---

55 GROEN, F., "*Bayesian Framework for General Renewal Process Modelling Report*", Technical Paper, University of Maryland, 2002

However, the density function at Equation 38 using the fact that Equation 14 showed that for a KIJIMA Type I GRP equation that the i^{th} failure is only dependant on the $(i\text{-}1)^{th}$ failure. Accordingly, Equation 38 can be constructed iteratively as shown in Equation 39.

$$g(x) = \pi\left[(t_1 \ldots t_{n+1})\middle|\alpha, \beta, a\right] = \pi(t_1)\cdot \pi(t_2|t_1)\cdots \pi(t_n|t_{n-1})\cdot \pi(t_{n+1}|t_n)$$

Equation 39: Probability Density of a Particular Sequence Failure Sequence

Computation of the Posterior Density Function

Unfortunately the either Case xA or Case xB the general likelihood function and consequently the posterior density function at Equation 35 and Equation 36 are mathematically intractable. Therefore, a numerical method, such as the Gibbs sampler or Metropolis-Hastings algorithm, is required to provide a representation of the posterior distribution in the form of a set of samples $< \alpha_i, \beta_i, q_i >$, where $i = 1, \ldots, n$, and α_i, β_i, q_i are realistations of the parameter values. Indeed GROEN[56] has implemented a Metropolis-Hastings algorithm as a solution to the Case 1A Posterior Density function.

However, there has been considerable research published on the commonly used MCMC methods, specifically the Metropolis-Hastings algorithm and Gibbs sampler, regarding their individual limitations as follows:

[56] ibid

Gibbs Sampler. It is acknowledged that once a method for sampling from all required conditions using a Gibbs sampler is found, no further tuning of the parameters is required in order to produce the final MC sampler. However, to achieve this, a method for sampling the multi-variate GRP distribution with data uncertainty needs to be devised. As will be shown, this is not a trivial exercise.

Metropolis-Hastings Algorithm. The Metropolis-Hastings Algorithm is similar to the Gibbs sampler requiring an appropriate "proposal" distribution to ensure sampling can take place, and again, this would need to be completed to all sampling of the non-standard multi-variate GRP distribution.

Accordingly, given these acknowledged limitations a simpler, alternative Numerical Method was sought.

Slice Sampling Markov-Chain Monte-Carlo (MCMC) Sampling Technique

Concept of the Slice Sampling Technique

The concept of the *Slice Sampling* technique is described by NEAL[57] as follows:

"Suppose we wish to sample from a distribution for a variable, *x*, taking values in some subset of $\Re^n$, whose density is proportional to some function

57 NEAL, R. M., op cit, pg 706

$f(x)$.We can do this by sampling uniformly from the $(n+1)$-dimensional region that lies under the plot of $f(x)$. This idea can be formalized by introducing an auxiliary real variable, y, and defining a joint distribution over x and y that is uniform over the region $U = \{(x, y) : 0 < y < f(x)\}$ below the curve or surface defined by $f(x)$. That is, the joint density for (x, y) is [shown in Equation 40]

$$p(x, y) = \begin{cases} 1/Z, & \text{if } 0 < y < f(x), \\ 0 & \text{otherwise} \end{cases}$$

$$\text{where } Z = \int f(x)dx$$

Equation 40: Slice Sampler Joint Density for *(x, y)*

The marginal density for x is then [shown in Equation 41].

$$p(x) = \int_0^{f(x)} \left(\frac{1}{Z}\right) dy = \frac{f(x)}{Z}$$

Equation 41: Slice Sampler Marginal Density for x

To sample for x, we can sample jointly for (x, y), and then ignore y.

Generating independent points drawn uniformly from U may not be easy, so we might instead define a Markov chain that will converge to this uniform distribution. Gibbs sampling is one possibility: We sample alternately from the conditional distribution for y given the current x, which is uniform over the interval $(0, f(x))$, and from the conditional distribution for x given the current y, which is uniform over the region $S = \{x : y < f(x)\}$, which I call the "slice" defined by y. Generating an independent point drawn uniformly from S may still be difficult, in which case we can substitute some update for x that leaves the uniform distribution over *S* invariant. Higdon (1996) has interpreted the standard Metropolis-Hastings algorithm in these terms. Beyond this, however, reducing the problem to that of updating *x* so as to leave a *uniform* distribution invariant allows us to use various tricks that would not be valid for a non-uniform distribution."[58]

Single Variable Slice Sampling Method

The single variable slice sampling method uses an iterative process to replace the current value, x_0, with a new value, x_1, through a three step procedure:

"(a) Draw a real value, y, uniformly from (0, $f(x_0)$), thereby defining a horizontal "slice": $S = \{x : y < f(x)\}$. Note that x_0 is always within S.

(b) Find an interval, I = (L, R), around x_0 that contains all, or much, of the slice.

(c) Draw the new point, x_1, from the part of the slice within this interval."[59]

NEAL[60] describes four schemes for finding the interval at step 2. However, the use of the GRP equation with an underlying 2-parameter Weibull TTF equation limits the

58 NEAL, R. M., op cit, pg 710

59 NEAL, R. M., op cit, pg 712

60 NEAL, R. M., op cit, pg 714

possible values of x such that the interval, I = (L, R), can be set to this boundary. The limitation of each of the parameters is described in Table 7.

Variable Interval Lower Bound (L)	Variable Interval Upper Bound (R)
Weibull Scale Parameter ($\alpha_{min} \leq \alpha \leq \alpha_{max}$)	
Since a rule of thumb for an estimate of α for a component is typically equal to the Time To First Failure (TTFF), t_1, then: $0 \leq \alpha_{min}$	Although a rule of thumb for an estimate of α for a component is typically equal to the TTFF, t_1, it is recommended that: $\alpha_{max} \leq 2 \times t_1$
Weibull Shape Parameter ($\beta_{min} \leq \beta \leq \beta_{max}$)	
Realistically a β value of less than 0.5 for a physical component is unrealistic. Therefore: $0.5 \leq \beta_{min}$	A β value of greater than 5 for a physical component is unrealistic. However, to allow the *Slice Sampler* the greatest freedom with the space, *S*, therefore: $\beta_{max} \leq 10$
Repair Effectiveness Parameter ($q_{min} \leq q \leq q_{max}$)	
The set-up of the Virtual Age of a component using the Type I KIJIMA GRP equation therefore defines 'q' as: $0 \leq q_{min}$. Otherwise, if $q < 0$, the result is *better-than-new*[61].	The set-up of the Virtual Age of a component using the Type I KIJIMA GRP equation allows 'q' to be considered $1 < q$ (i.e. *worse-than-old*). However, to allow the use of Interval implementation of the Slice Sampler method $q_{max} \leq 1.5$ Although this could be set higher.
Time To Failure (TTF) ($I_{i-1} \leq t_i \leq I_i$) *(Case xB only)*[62]	
Given the set-up of Case xB includes periodic inspection points, the TTF by definition cannot be before the previous inspection point (I_{i-1}): $I_{i-1} \leq t_i$	Given the set-up of Case xB includes periodic inspection points, the TTF by definition cannot be after the next inspection point (I_i): $t_i \leq I_i$

Table 7: Parameter Intervals for Slice Sampler

61 While from a modelling perspective allowing $q < 0$ (i.e. *better-than-new*) is valid since the maintenance activity may modify the component (i.e. through a modification program), it has not been considered as part of the research.

62 The TTF for Case xA are not parameters for the Slice Sampler method since they Case xA assumes the sequence of TTFs are known.

Multivariate Slice Sampling Method

NEAL describes a number of techniques for using the *Slice Sampling* method to sample from multivariate distributions for $x = (x_1, \ldots, x_n)$. The two main choices are either:

Option 1 – Update each variable (x_i) in turn by sampling from a multivariate distribution using the single-variable *Slice Sampling* method. This is simply the sequential application of the single-variable *Slice Sampling* method described above. Option 1 was implemented for solving Case xB (unknown failure times) utilising the interval bounds as described above.

Option 2 – Apply the idea of the *Slice Sampling* method directly to the multivariate distribution. NEAL refers to this technique as *Multivariate Slice Sampling with Hyperrectangles* and describes this process as:

> "We can generalize the single-variable slice sampling methods of Section 4 to methods for performing multivariate updates by replacing the interval $I = (L, R)$ by an axis-aligned hyperrectangle $H = \{x : L_i < x_i < R_i$ for all $i = 1, \ldots, n\}$. Here, L_i and R_i define the extent of the hyperrectangle along the axis for variable x_i. The procedure for finding the next state, $x_1 = (x_{1,1}, \ldots, x_{1,n})$, from the current state, $x_0 = (x_{0,1}, \ldots, x_{0,n})$, parallels the single-variable procedure:

(a) Draw a real value, y, uniformly from $(0, f(x_0))$, thereby defining the slice $S = \{x : y < f(x)\}$.

(b) Find a hyperrectangle, $H = (L_1, R_1)\times\cdots\times(L_n, R_n)$, around x_0, which preferably contains at least a big part of the slice.

(c) Draw the new point, x_1, from the part of the slice within this hyperrectangle.

When all the variables have bounded ranges we might set H to the entire space, but this may be inefficient, since S is likely to be much smaller."[63]

Option 2 was implemented for the solution of Case xA (known failure times) since the boundary conditions imposed on the parameters did not result in a comparatively large S compared with the computation time required for other techniques. Specifically, rather than sequentially update α, then β, then q, each iteration updates a single combination of $< \alpha, \beta, q >$ and thereby reduces computation time required.

Implementation of the Slice Sampling Method

Implementing the *Slice Sampling* method required three factors:

1. development of a continuous distribution, $f(x)$, that is proportional to the density;

63 NEAL, R., op cit, pg 721

2. development of a prior distribution that adequately addresses the prior knowledge of the various parameters; and
3. advice on the initial guess values for each of the parameters.

As previously discussed, *f(x)* is the key to the use of the *Slice Sampling* method and accordingly, a significant proportion of the research went into verifying a *f(x)*, originally proposed by GROEN[64] for use in a Metropolis-Hastings algorithm solution, that adequately represented the individual Case xA and xB scenarios. This *f(x)* is based on a likelihood estimator for the Bayesian GRP Algorithm described in GROEN[65].

Role of the Prior Distribution

The role of the *Prior Distribution* in any Bayesian Analysis is to represent the relevant prior knowledge, including subjective judgement, regarding the characteristics of the parameter and its distribution.

The *prior* distribution, shown in Equation 34, is made up of a vector of q's which could relate to the direct maintenance of individual failure modes, the indirect (or dependent) impact on failure modes not undergoing maintenance or inspection. This set-up allows the analyst to use their professional judgement to pick the shape and the range of the individual *priors.*

---

64 GROEN, F., *"Bayesian Framework for General Renewal Process Modelling Report"*, loc cit

65 ibid

In the case of the GRP equation with an underlying 2-parameter Weibull distribution the *Prior Distribution* reflects the analyst's knowledge, including subjective judgement, regarding the Weibull Scale (α) and Shape (β) parameters, and the specific GRP parameter(s) (q).

Furthermore, analyst has the ability to assume that (initially) each of the prior distributions are independent and therefore the prior distribution can be written as shown in Equation 42.

$$\pi_0(\alpha, \beta, q) = \pi_0(\alpha) \cdot \pi_0(\beta) \cdot \pi_0(q)$$

Equation 42: General Independent Form of Prior Distribution

However, given the set-up of the equations the posterior function of $\pi_0(\alpha, \beta, q)$ is no longer independent.

The *Prior Distribution* is used in conjunction with a MCMC sampler in order to generate the *Posterior Distribution* of the GRP equation. Additionally, the *Prior Distribution* was developed conscious of one of the objectives of the parameter estimator; specifically to limit the requirement of the analyst to *tune* the algorithm to the individual data.

Weibull Scale Parameter (α) Prior

At the beginning of the research it was expected that a *prior distribution* for the Weibull Scale Parameter (α) (i.e. $\pi_0(\alpha)$) would be established based on the judgement of the analyst, utilising a lognormal Probability Density Function (pdf) of the form shown at Equation 43.

$$\pi_0(\alpha) = \frac{1}{\alpha} \cdot e^{-\frac{1}{2}\left(\frac{\ln\alpha - \mu_t}{\sigma_t}\right)^2}$$

Equation 43: Lognormal PDF for Weibull Scale Parameter (α)

Although Equation 43 is a lognormal distribution, based on the relationship between the lognormal distribution and some other parameters shown in Equation 44 it is possible to elicit a range of values, including a confidence, from the analyst. For example, if the analyst is 90% confident that $100 \leq \alpha \leq 150$ then μ_α and σ_α can be calculated.

$$\mu_\alpha = \ln\left[\frac{\mu_{\alpha\_t}}{\sqrt{\ln\left(1+\left(\frac{\sigma_{\alpha\_t}{}^2}{\mu_{\alpha\_t}{}^2}\right)\right)}}\right]$$

$$\sigma_\alpha = \sqrt{\ln\left[1+\left(\frac{\sigma_{\alpha\_t}{}^2}{\mu_{\alpha\_t}{}^2}\right)\right]}$$

$$where$$

$$\mu_{\alpha\_t} = \frac{\alpha_{high\_guess} + \alpha_{low\_guess}}{2}$$

$$\sigma_{\alpha\_t} = \frac{1}{\Phi(Confidence)} \cdot \left(\frac{\alpha_{high\_guess} - \alpha_{low\_guess}}{2}\right)$$

Equation 44: Calculation of Weibull Scale Parameter Prior

However, given one of the objectives of the analysis was to be able to conduct the analysis without *tuning* it was decided to make the prior distribution of α uniform. Accordingly, $\pi_0(\alpha) = 1$.

Furthermore, it was observed to have only limited impact on the final results; a testament to the *Slice Sampling* technique. One reason for the limited impact on the final result is due to the boundaries (i.e. I = (L, R)) utilised by the *Slice Sampler*. Specifically, that whether the parameter estimation is undertaken with a non-informative prior the parameter boundaries defined in Table 7 shall effectively restrict the possible parameter set of the space (*S*).

Weibull Shape Parameter (β) Prior

Unlike the Weibull Scale Parameter (α) and the GRP Parameter (q), it is possible to define a prior distribution for the Weibull Shape Parameter (β)) (i.e. $\pi_0(\beta)$) due to the physical nature of the equipment under assessment. Specifically, for technical equipment β can be described within a finite boundary, $0 \leq \beta \leq 10$, and therefore represented with a *prior distribution* based on a modified lognormal pdf where $\mu_\beta=0.63$ and $\sigma_\beta=0.5$. This result is shown in Equation 45 and shown graphically in Figure 21.

$$\pi_0(\beta) = \frac{1}{\beta} \cdot e^{-\frac{1}{2}\left(\frac{\ln\beta - 0.63}{0.5}\right)^2}$$

Equation 45: Lognormal PDF for Weibull Shape Parameter (β)

Of interest, although both the prior and the interval boundary allowed $0.5 \leq \beta \leq 10$, in reality, in all the cases run β never exceeded 6. Again, this results is a testament to the *Slice Sampling* method.

GRP Parameter (q) Prior

The original intent of the GRP Parameter, *q*, constrains it to the boundary of q = 0 (*as-good-as-new* restoration) to q = 1 (*as-bad-as-old* restoration). However, this would ignore two of the five cases defined in YANEZ, et al[66]; *better-than-new* (i.e. $q < 0$) and *worse-than-old* (i.e. $q > 1$). Given that *q* is an abstract construct of the GRP concept it may not have a direct physical representation.

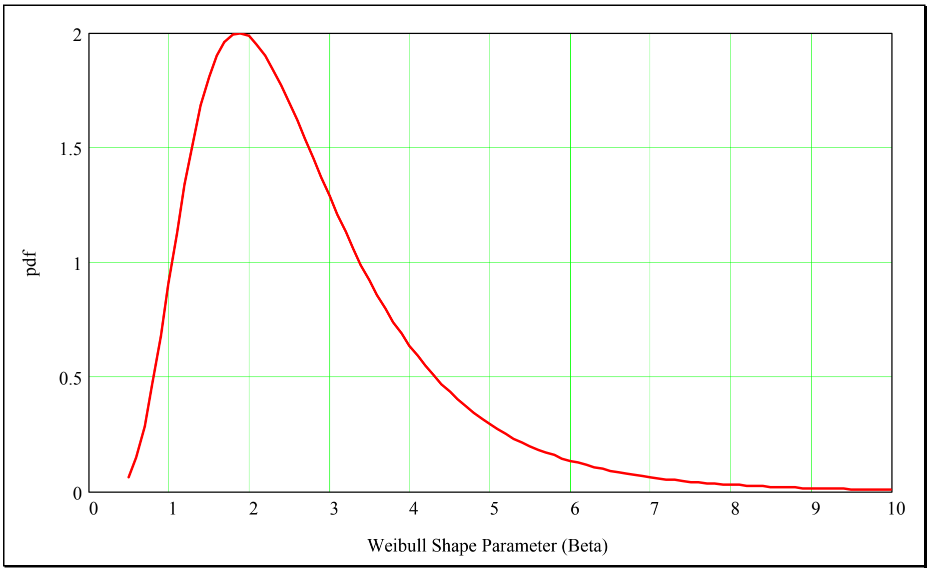

Figure 21: Prior Distribution of Weibull Shape Parameter

---

66 YANEZ et al, op cit, pg 167

Accordingly, there are circumstances where q > 1 where imperfect maintenance action(s) cause the component to be left in a worse condition than before the maintenance action. Furthermore, while there are also cases where q < 0 (i.e. *better-tan-new*) this is due to the incorporation of an modification and/or Engineering Change Proposal (ECP) program, this was considered outside the scope of the research. Therefore, the model uses $0 \leq q \leq 1.5$.

Moreover, given one of the objectives of the research was reduce the requirement to *tune* the algorithm it was decided to make the prior distribution of q uniform across the interval $0 \leq q \leq 1.5$. Accordingly, $\pi_0(q) = 1$.

Combined GRP Prior Distribution

Accordingly, the final prior equation was developed and is shown in Equation 46.

$$\pi_0(\alpha,\beta,q) = 1 \cdot \left(\frac{1}{\sigma_\beta} \cdot e^{-\left(\frac{1}{2}\cdot\left(\frac{\ln\beta-\mu_\beta}{\sigma_\beta}\right)^2\right)} \right) \cdot 1 = 2 \cdot e^{-\left(\frac{1}{2}\cdot\left(\frac{\ln\beta-0.63}{0.5}\right)^2\right)}$$

Equation 46: Prior for f(x) for both Case xA and xB

The prior equation is the same for both Case xA and xB, and reflects the knowledge of the GRP parameters (i.e. α, β and q).

Sensitivity of the Combined GRP Prior Distribution

It is possible to review the sensitivity of the model to the prior. To do this the USS Halfbeak example (refer to Case 1A Solution – USS Halfbeak) was revisited and a GRP Parameter (*q*) Prior introduced based on the lognormal prior equation and relationship shown in Equation 43 and Equation 44. Three prior values of *q* were then examined, simplistically representing the analysts judgement that *q* = high (i.e. *as-bad-as-old* repairs), *q* = low (i.e. *as-good-as-new* repairs) and *q* = constant = non-informative. A summary of these three cases and their respective values is provided in Table 8 and shown graphically in Figure 22.

	Analyst Low *q* guess	**Analyst High *q* guess**	**Analyst Confidence**	**Calculated μ_q**	**Calculated σ_q**
***q* = low**	0	0.4	90%	-1.847	0.69
***q* = non-informative**	0	1.5	100%	-	-
***q* = high**	06	1.0	90%	-0.242	0.193

Table 8: Summary of *q* Prior Distribution

The parameter estimator was re-run against the data utilising 51 data points in the parameter estimator, but then comparing the output from the CIF simulator with all 71 data point. A graphical representative of the variation in CIF is shown is Figure 23. From Figure 23 it is obvious that the *q* prior had very little effect on the outcome. However, logically this is to be expected since by definition a Bayesian prior should have less and less impact as “real” data becomes available. In this case, since 51 data points are being used the influence of the *q* prior in the parameter estimator should be very little, which Figure 23 illustrates.

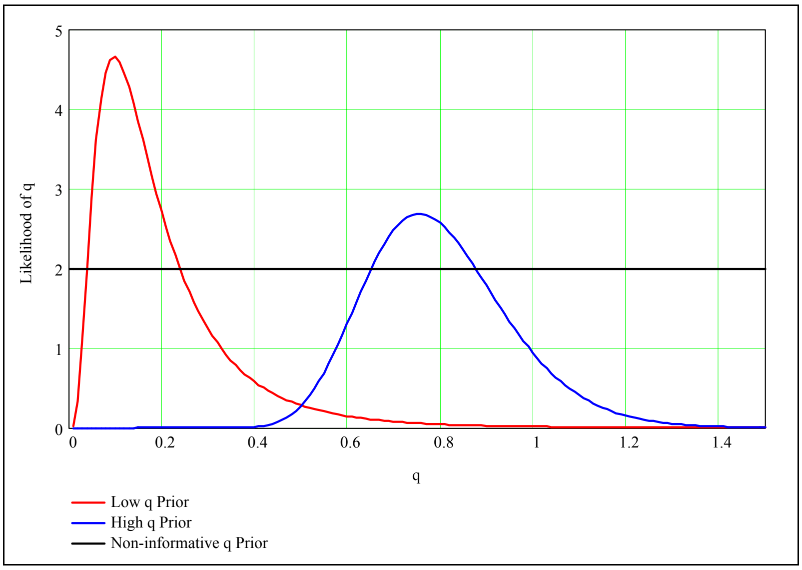

Figure 22: Prior *q* Values as Input to *USS Halfbeak* Sensitivity Analysis

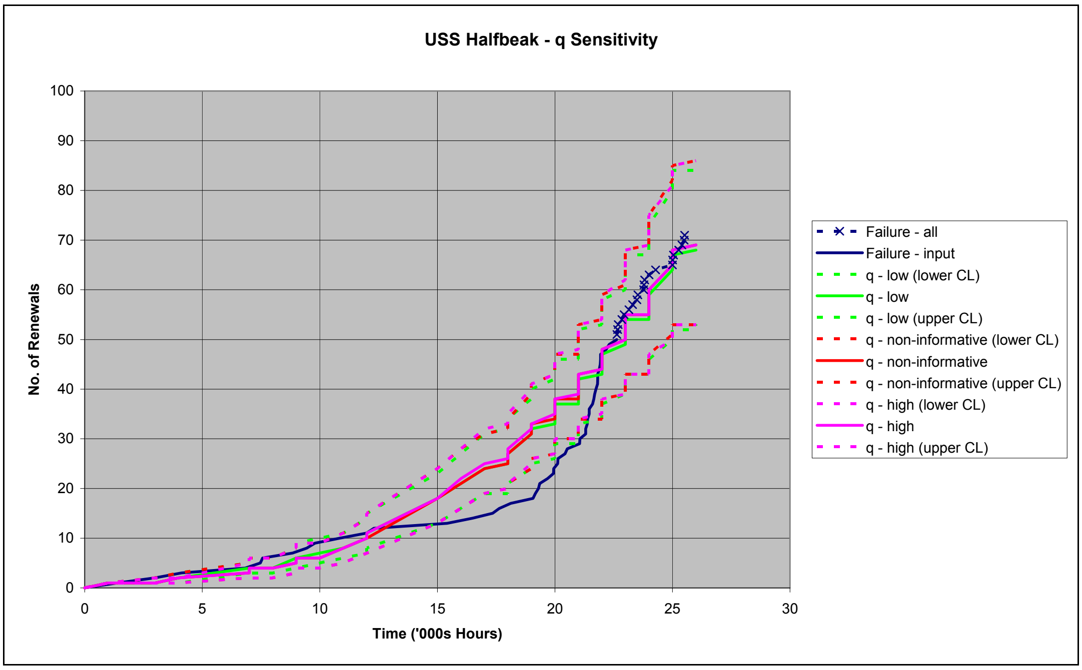

Figure 23: Sensitivity Analysis of Bayesian Prior for q on USS Halfbeak Data

f(x) for Case 1A – 2A

The *f(x)* for Case xA is based on the unnormalised posterior density function originally proposed by Dr Frank Groen[67] for use in a Metropolis-Hastings algorithm solution as shown in Equation 47.

$$\pi(X) = \pi(\alpha, \beta, q, \{t_1 \ldots t_n\}) = \hat{L}(E|\alpha, \beta, q, \{t_1 \ldots t_n\}) \cdot \pi_0(\alpha, \beta, q)$$

Equation 47: Unnormalised Posterior Density Function for Case xA

The prior distribution was based on the understanding of the expected values of each parameter (i.e. α, β and q (and t_i where $i = 0 \ldots n$ for Case xB)) and is discussed in Role of the Prior Distribution.

Using the equation for finding the probability density of a particular failure sequence is it possible to find *f(x)* for use in the *Slice Sampler* method for Cases 1A – 2A. The resulting *f(x)* is provided at Equation 48.

$$f_{Case1A-2A}(x) = \Pi_0(\alpha, \beta, q) \cdot \prod_{i=0}^{n} \frac{\left(\frac{\beta}{\alpha}\right) \cdot \left(\frac{t_i - t_{i-1} + q \cdot t_{i-1}}{\alpha}\right)^{\beta-1} \cdot e^{\left\{-\left(\frac{t_i - t_{i-1} + q \cdot t_{i-1}}{\alpha}\right)^{\beta}\right\}}}{e^{\left\{-\left(\frac{q \cdot t_{i-1}}{\alpha}\right)^{\beta}\right\}}}$$

Equation 48: *f(x)* for Case 1A – 2A

67 ibid

Here the TTF is represented by a sequence of failure times ($t_1, \ldots, t_{n+1}$), where t_i is the time of the i^{th} failure and n is the number of failures observed at the time of last observation.

f(x) for Case xB

Case xB refer to those cases where there is uncertainty on the exact failure time of the i^{th} failure. In lieu of an exact failure time it is known that the i^{th} failure occurred between two known inspection times, I_{j-1} and I_j, where $j = 1, \ldots, m$ representing the inspection intervals.

While the *f(x)* for Case xB is based on the unnormalised posterior density function originally proposed by GROEN[68] for use in a Metropolis-Hastings algorithm solution as shown in Equation 47, additional *auxiliary variables* had to be included. Specifically, Equation 38 was modified to include the additional auxiliary variables, known inspection times (I), as shown in Equation 49.

$$\pi(X) = \pi(\alpha, \beta, q, [t_1 \ldots t_n]) = \hat{L}(E|\alpha, \beta, q, [t_1' \ldots t_n']) \cdot \pi_0(\alpha, \beta, q)$$

Equation 49: Probability Density of a Particular Failure Sequence including Inspection Points

Again, the prior distribution was based on the understanding of the expected values of each parameter (i.e. α, β and q (and t_i where $i = 0 \ldots n$ for Case xB)) and is discussed in Role of the Prior Distribution.

68 ibid

Using the equation for finding the probability density of a particular failure sequence as shown in Equation 49 is it possible to find *f(x)* for use in the *Slice Sampler* method for Cases 1B-2B, and is shown in Equation 50. Furthermore, due to the fact that by definition t_0=0, therefore *f(x)* for $t_{i=1}$ can be simplified.

Again, the TTF is represented by a sequence of failure times ($t_1, . . . ,t_{n+1}$), where t_i is the time of the i^{th} failure and n is the number of failures observed at the time of last observation.

f(x) for Case 3A-4A-5A and 3B-4B-5B

Cases 3A-5A and Cases 3B-5B now include multiple dependent failure modes and imperfect inspections. Accordingly, a new *f(x)* needs to be found.

Firstly consider that any of the failure modes, including the inspection, can independently cause the component to fail through the application of separate sets of failure mechanisms (e.g. Failure Mode 1 = fatigue, Failure Mode 2 = corrosion). This relationship can be represented via a *series* arrangement based on the assumption that the underlying TTF distribution of each failure mode is a 2-parameter Weibull. For example, a component with 2 dependent Failure Modes including imperfect inspection is shown in Figure 24.

$$f_{Case3B-5B}(x) = \begin{cases} \Pi_0(\alpha,\beta,q) \cdot \dfrac{\left(\dfrac{\beta}{\alpha}\right) \cdot \left(\dfrac{t_1}{\alpha}\right)^{\beta-1} \cdot e^{\left\{-\left(\frac{t_1}{\alpha}\right)^{\beta}\right\}}}{1 - e^{\left\{-\left(\frac{q \cdot t_1}{\alpha_j}\right)^{\beta}\right\}}} & i = 1 \\ \Pi_0(\alpha,\beta,q) \cdot \displaystyle\prod_{i=2}^{n} \dfrac{\left(\dfrac{\beta}{\alpha}\right) \cdot \left(\dfrac{t_i - t_{i-1} + q \cdot t_{i-1}}{\alpha}\right)^{\beta-1} \cdot e^{\left\{-\left(\frac{t_i - t_{i-1} + q \cdot t_{i-1}}{\alpha}\right)^{\beta}\right\}}}{e^{\left\{-\left(\frac{I_{i-1} - t_{i-1} + q \cdot t_{i-1}}{\alpha}\right)^{\beta}\right\}} - e^{\left\{-\left(\frac{I_i - t_{i-1} + q \cdot t_{i-1}}{\alpha}\right)^{\beta}\right\}}} \cdot \dfrac{\left(\dfrac{\beta}{\alpha}\right) \cdot \left(\dfrac{q \cdot t_{i-1}}{\alpha}\right)^{\beta_j - 1} \cdot e^{\left\{-\left(\frac{I_{i-1} - t_{i-1} + q \cdot t_{i-1}}{\alpha}\right)^{\beta}\right\}}}{1 - e^{\left\{-\left(\frac{q \cdot t_{i-1}}{\alpha}\right)^{\beta}\right\}}} & i = 2 \ldots n \end{cases}$$

Equation 50: *f(x)* for Cases 1B-2B

In this concept the Weibull Scale (α) and Weibull Shape (β) parameter for each maintenance event remains the same regardless of the action (i.e. corrective, preventative or an inspection). However, a different q applies to each of the different maintenance action types, reflecting the variation in repair assumption (e.g. *as-good-as-new*, *worse-than-old*, etc) made possible through the GRP concept of *Virtual Age*. Additionally, in the case of the multiple dependent failure modes (Cases 4A-5A and 4B-5B), the dependent q does not represent a physical activity, but rather as a method of affecting a 'jump' in the *Virtual Age* of an individual failure mode by increasing, decreasing or leaving the dependent q values unchanged.

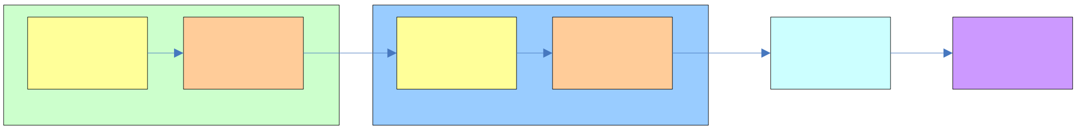

Figure 24: Reliability of Component with 2-dependent Failure Modes and Imperfect Inspection

Given the *series* arrangement the overall reliability of the component is simply the product of distribution the individual failure modes. Therefore, using the equation for finding the probability density of a particular failure sequence as shown in Equation 39 and the relationship of the various dependent failure modes as shown in Figure 24, it possible to find *f(x)* for Cases 3A-5A and Cases 3B-5B.

Firstly, we need to modify Equation 37 given the underlying TTF distribution is a 2-parameter Weibull distribution. Therefore, for a series system it is possible to find the GRP failure density of the ith failure for a component with multiple dependent failure modes and imperfect inspection as shown in Figure 24.

$$R_{component}(t) = \prod_{j=1}^{r} e^{\left\{-\left(\frac{t}{\alpha_j}\right)^{\beta j}\right\}} = e^{\left\{-\sum_{j=1}^{r}\left(\frac{t}{\alpha_j}\right)^{\beta_j}\right\}}$$

$$f_{component}(t) = \prod_{j=1}^{r}\left\{\left(\frac{\beta_j}{\alpha_j}\right)\cdot\left(\frac{t}{\alpha_j}\right)^{\beta j-1}\cdot e^{-\left(\frac{t}{\alpha_j}\right)^{\beta_j}}\right\} = \sum_{j=1}^{r}\left(\frac{\beta_j}{\alpha_j}\right)\cdot\left(\frac{t}{\alpha_j}\right)^{\beta_j-1}\cdot e^{\left\{-\sum_{j=1}^{r}\left(\frac{t}{\alpha_j}\right)^{\beta_j}\right\}}$$

Equation 51: GRP Failure Density of the ith Failure for a Component with Multiple Dependent Failure Modes and Imperfect Inspection

Here *j* represents the number of failure modes including dependent failure modes and imperfect inspection failure modes where $j = 1 \ldots r$.

Accordingly, the results from Equation 51 can be inserted into Equation 39 resulting in *f(x)* for use in the *Slice Sampler* method for Cases 3A-4A-5A as shown in Equation 52.

$$f_{Case3A-5A}(x) = \Pi_0(\alpha,\beta,q)\cdot\prod_{i=0}^{n}\frac{\sum_{j=1}^{r}\left(\frac{\beta_j}{\alpha_j}\right)\cdot\left(\frac{t_i - t_{i-1} + q_j \cdot t_{i-1}}{\alpha_j}\right)^{\beta_j - 1}\cdot e^{\left\{-\sum_{j=1}^{r}\left(\frac{t_i - t_{i-1}+q_j \cdot t_{i-1}}{\alpha_j}\right)^{\beta_j}\right\}}}{e^{\left\{-\sum_{j=1}^{r}\left(\frac{q_j \cdot t_{i-1}}{\alpha_j}\right)^{\beta_j}\right\}}}$$

Equation 52: *f(x)* for Cases 3A–5A

Similarly, this same substitution can be made to the Case xB *f(x)* previously provided in Equation 50, and can be found at Equation 54.

The key to the practical implementation of this approach is the identification and recording of the failure mode (mechanism) for each maintenance event and must be able to indicate whether the action was corrective, preventative or an inspection, and what, if any, failure mode (mechanism) was observed. Fortunately, the Failure Reporting And Corrective Action System (FRACAS) of most complex technical equipment will include this information. This knowledge is then used in deciding which *q* is then applied to the *f(x)*. For example, consider a component with two failure modes, which are dependent and are also exposed to imperfect inspections. Therefore, using the equation for finding the probability density of a particular failure sequence (based on the times to failure) as shown in Equation 39 it is possible to calculate *f(x)* as shown in Equation 53.

$$f(x) = f(x)_{FM1} * f(x)_{FM1} * f(x)_{Inspection} * f(x)_{FM1} * f(x)_{FM2} \ldots$$

where

$$f(x)_{FM1} = f(\alpha_{FM1}, \beta_{FM1}, q_{FM1}) + f(\alpha_{FM2}, \beta_{FM2}, q_{fFM2\text{ due to }FM1})$$

$$f(x)_{FM2} = f(\alpha_{FM2}, \beta_{FM2}, q_{FM2}) + f(\alpha_{FM1}, \beta_{FM1}, q_{fFM1\text{ due to }FM2})$$

$$f(x)_{Inspection} = f(\alpha_{FM1}, \beta_{FM1}, q_{Inspection\text{ of }FM1}) + f(\alpha_{FM2}, \beta_{FM2}, q_{Inspection\text{ of }FM2})$$

Equation 53: Implementation of Calculation of *f(x)* for Cases 3A/B – 5A/B

Initial Guess Values for *Slice Sampler*

The implementation of the *Slice Sample* method required initial values of the various parameters, α, β and q, for both Case xA nad xB, and ($t_{1\ guess}, \ldots, t_{n\ guess}$) for Case xB only. While it is possible to mechanise these initial values, given the emphasis of this technique on using *soft-data* the concept of allowing the analyst to select these initial values was included. As a result, Table 9 provides a recommended method for determining the guess values for use in the GRP *Slice Sampler*.

Auto-correlation and Interleaving Effects

Introduction

Given most MCMC sampling techniques suffer from the effect of auto-correlation, as part of the analysis of the Slice Sampling technique it was important to examine both Case xA and xB parameter estimation output. Specifically, to examine this output was correlated and what the impact this had on the output and the recommended solution.

$$
f_{Case3B-5B}(x)=\begin{cases}
\Pi_0(\alpha,\beta,q)\cdot\prod_{i=0}^{Input\_Data}\dfrac{\sum_{j=1}^{r}\left(\dfrac{\beta_j}{\alpha_j}\right)\cdot\left(\dfrac{t_1}{\alpha_j}\right)^{\beta_j-1}\cdot e^{-\left\{-\sum_{j=1}^{r}\left(\frac{t_1}{\alpha_j}\right)^{\beta_j}\right\}}}{1-e^{\left\{-\sum_{j=1}^{r}\left(\frac{q_j\cdot t_1}{\alpha_j}\right)^{\beta_j}\right\}}} & i=1\\
\Pi_0(\alpha,\beta,q)\cdot\prod_{i=0}^{Input\_Data}\dfrac{\sum_{j=1}^{r}\left(\dfrac{\beta_j}{\alpha_j}\right)\cdot\left(\dfrac{t_i-t_{i-1}+q\cdot t_{i-1}}{\alpha_j}\right)^{\beta_j-1}\cdot e^{\left\{-\sum_{j=1}^{r}\left(\frac{t_i-t_{i-1}+q\cdot t_{i-1}}{\alpha_j}\right)^{\beta_j}\right\}}}{e^{\left\{-\sum_{j=1}^{r}\left(\frac{I_{i-1}-t_{i-1}+q\cdot t_{i-1}}{\alpha_j}\right)^{\beta_j}\right\}}-e^{\left\{-\sum_{j=1}^{r}\left(\frac{I_i-t_{i-1}+q\cdot t_{i-1}}{\alpha_j}\right)^{\beta_j}\right\}}}\cdot\dfrac{\sum_{j=1}^{r}\left(\dfrac{\beta_j}{\alpha_j}\right)\cdot\left(\dfrac{q\cdot t_{i-1}}{\alpha_j}\right)^{\beta_j-1}\cdot e^{\left\{-\sum_{j=1}^{r}\left(\frac{I_{i-1}-t_{i-1}+q\cdot t_{i-1}}{\alpha_j}\right)^{\beta_j}\right\}}}{1-e^{\left\{-\sum_{j=1}^{r}\left(\frac{q\cdot t_{i-1}}{\alpha_j}\right)^{\beta_j}\right\}}} & i=2\ldots n
\end{cases}
$$

Equation 54: *f(x)* for Cases 3B-5B

Auto-correlation

As part of the simulation of the Slice Sampler parameter estimator and GRP simulator, a step was included to determine whether the parameter estimation output was being observed.

Weibull Scale Parameter ($\alpha_{min} \leq \alpha \leq \alpha_{max}$)
A rule of thumb for an estimate of α for a component is typically equal to the TTFF, t_1.
$\alpha_{guess} = t_1$ or α_{guess} = MTBF if $\beta \approx 1$
Weibull Shape Parameter ($\beta_{min} \leq \beta \leq \beta_{max}$)
Unless a β value is known or assumed, it is recommended that the initial guess be:
$\beta_{guess} = 1$ (i.e. constant failure rate)
Repair Effectiveness Parameter ($q_{min} \leq q \leq q_{max}$)
Unless q is known or assumed, it is recommended that the initial guess be:
$q_{guess} = 0.5$ (i.e. between *as-good-as-new* and *as-bad-as-old*)
Time To Failure (TTF) ($t_{i-1} \leq t_i \leq t_{i+1}$) (Case xB only)
Unless t_i is known or assumed, it is recommended that the initial guess be:
$t_{i\ guess} = (I_i - I_{i-1}) / 2$

Table 9: Recommended Guess Values for the GRP Parameters

Using the *USS Grampus* dataset[69] for the case xA and one simulated result for case xB, it was possible to investigate whether parameter estimation output was correlated over a range of lag 1 to lag 30. Given that LAW and KELTON[70] recommended that while there may be no appreciable correlation at lags 1 or 2, there may be a dependence at lag 3 due to some anomaly of the generator. The graph of the correlation for lag 1 to lag 30 of the outcome of the parameter estimation output for both the Case xA can be seen in Figure 25. While the fact that output was correlated was not unexpected, the duration of the correlation (e.g. even at lag 5) was surprising.

69 Additional details for the Grampus dataset can be found in Chapter 8

70 LAW, A.M. and KELTON, *Simulation Modelling and Analysis*, 3rd Ed., McGraw-Hill Higher Education, USA, 2000

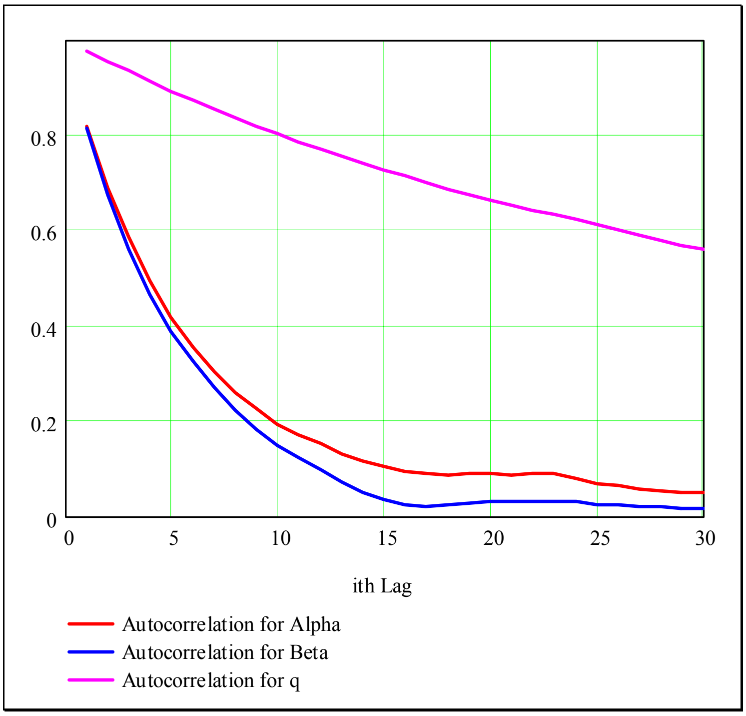

Figure 25: Correlation Graph for Case xA (10,000 iterations)

Interleaving

Given the clear indication that the output from the parameter estimation was strongly correlated, an *interleaving* technique was included within the algorithm. The aim of the interleave is to only record the i^{th} value from the MCMC and therefore reduce the effect of correlation. While it is clear that some form of interleaving is required, the significant issue is to what extent. From Figure 25 it is clear that there is still correlation at high levels of lag (e.g. 10), however, this needs to be offset by the reduction in efficiency of the MCMC sampler. Accordingly, an interleave value of at least 10 was selected for use throughout the research. An example of the impact of the inclusion of interleaving on the individual parameters and the final output is shown in Figure 26 and Figure 27.

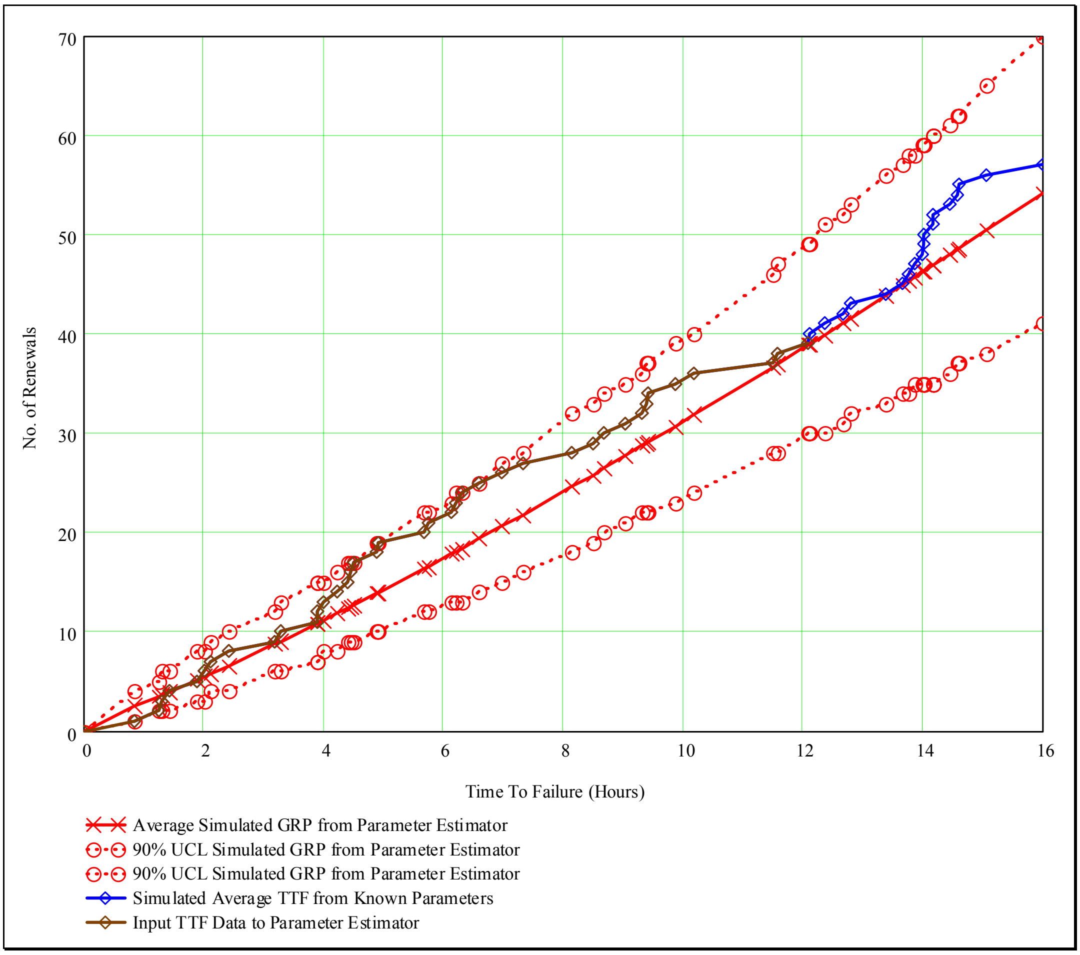

Figure 26: Analysis of *Grampus* Data with No Interleaving

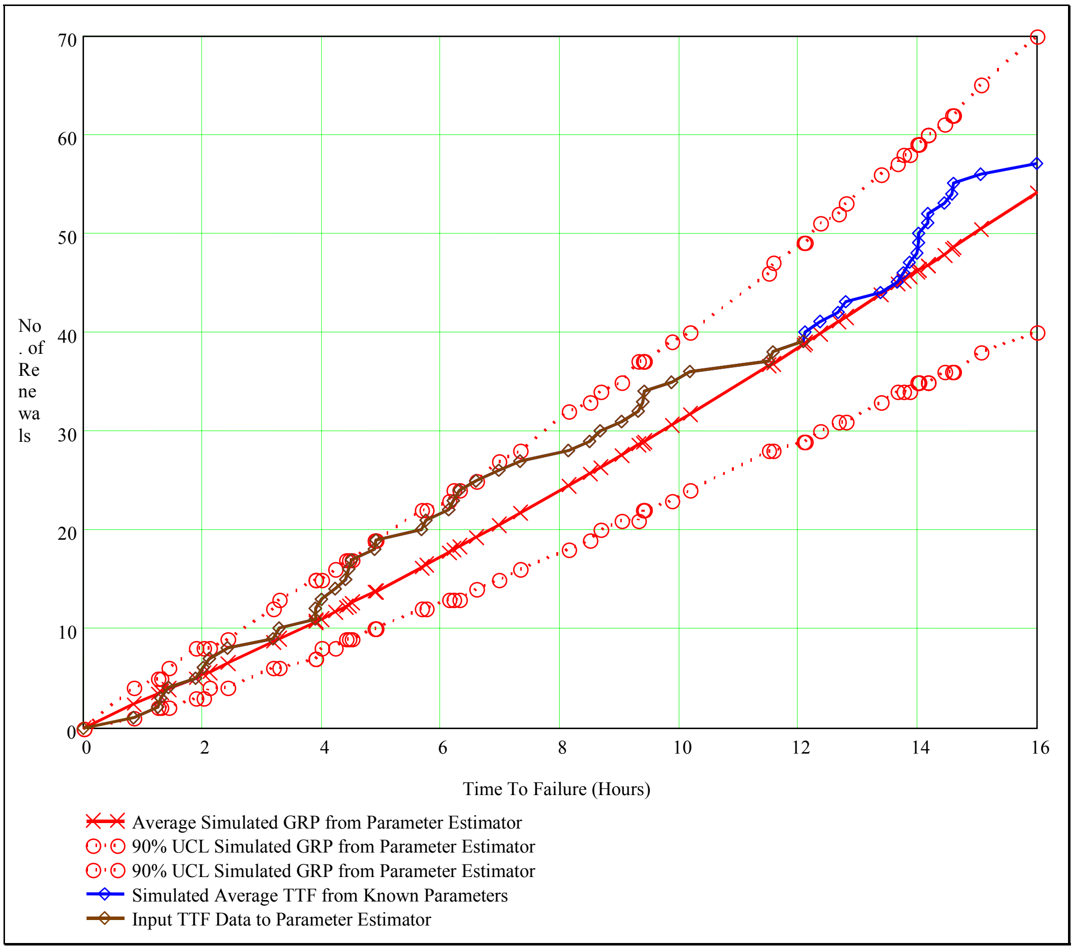

Figure 27: Analysis of *Grampus* Data with Interleaving = 5

Chapter 6: Role of 'q' in Analysis of Realistic Cases

While the General Renewal Process (GRP), including it's unique identifier *q*, are becoming more common in engineering literature[71] and even in some reliability software packages[72], neither provides guidance on the use and/or interpretation of *q*. For example, if $q = 0.7$, should there be concern that maintenance is not efficient? Furthermore, if the maintenance is undertaken by a third party under a performance based contract, should a portion of the payment be withheld given the apparent lack of "goodness of repair".

Accordingly, it is the intent of this chapter to provide some insight into the use and interpretation of *q*.

The chapter begins with some findings on the effect on the Cumulative Intensity Function (CIF) in response to changes in α, β and q. This initial review is based on a simple component with a single failure mode with no inspection and/or preventative maintenance. Unlike the rest of the study, this phase examined both the KIJIMA Type I GRP model, which is the basis of the research, and the KIJIMA Type II GRP model. The second section is a review of the effect on the CIF based purely on the effect of the *q* related to inspection/preventative maintenance compared with the *q*

---

71 KAMINSKIY, M. and KRIVTSOV, V., loc cit; YANEZ, M., et al, loc cit; METTAS, A. et al, loc cit, JACK, N., loc cit, HURTADO, et al, loc cit.

72 Software that include a parameter estimator for *q* includes Reliasoft's "Weibull++ (Version 7) and Prediction Technology's BRASS (Version 1.1).

related to the actual corrective maintenance actions. The third section expands the second section by examining the effect of multiple dependent failure modes with both imperfect inspection/preventative maintenance and imperfect corrective maintenance.

<u>Effect of q on a Corrective Maintenance Regime with a Single Failure Mode</u>

Set-up

Table 10 provides the values of α, β and q, the number of renewals and number of realisations that were used throughout the study, including the range of values of β and q used in the sensitivity study. The initial value of α = 2.84 was based on an estimated results for a complex system using a KIJIMA Type I GRP estimation model. The research was based on a different but related area of study.

	Single/Poisson Distribution	Sensitivity Study Variation in q	Sensitivity Study Variation in β
α	2.84	2.84	2.84
β	1.5	1.5	$1 \leq \beta \leq 2$
q	0.6	$0 \leq q \leq 1$	0.6
Number of Renewals	161	161	161
Number of Realisations	10, 000	10, 000	10, 000

Table 10: Setup of Variables during MC Simulation

A sensitivity study of the Weibull distribution scale parameter, α, was not undertaken since any variation in α will only result in a linear translation in the time of the CIF curve of both the KIJIMA Type I and Type II GRP model.

Output from CIF Simulator

Figure 28 and Figure 29 illustrate the output from the MathCad® model including showing the mean, and the upper and lower 95% CL values for all 10,000 realisations. Additionally, Figure 28 and Figure 29 shows four of the 10,000 possible realisations as an illustration of the MC simulation methodology.

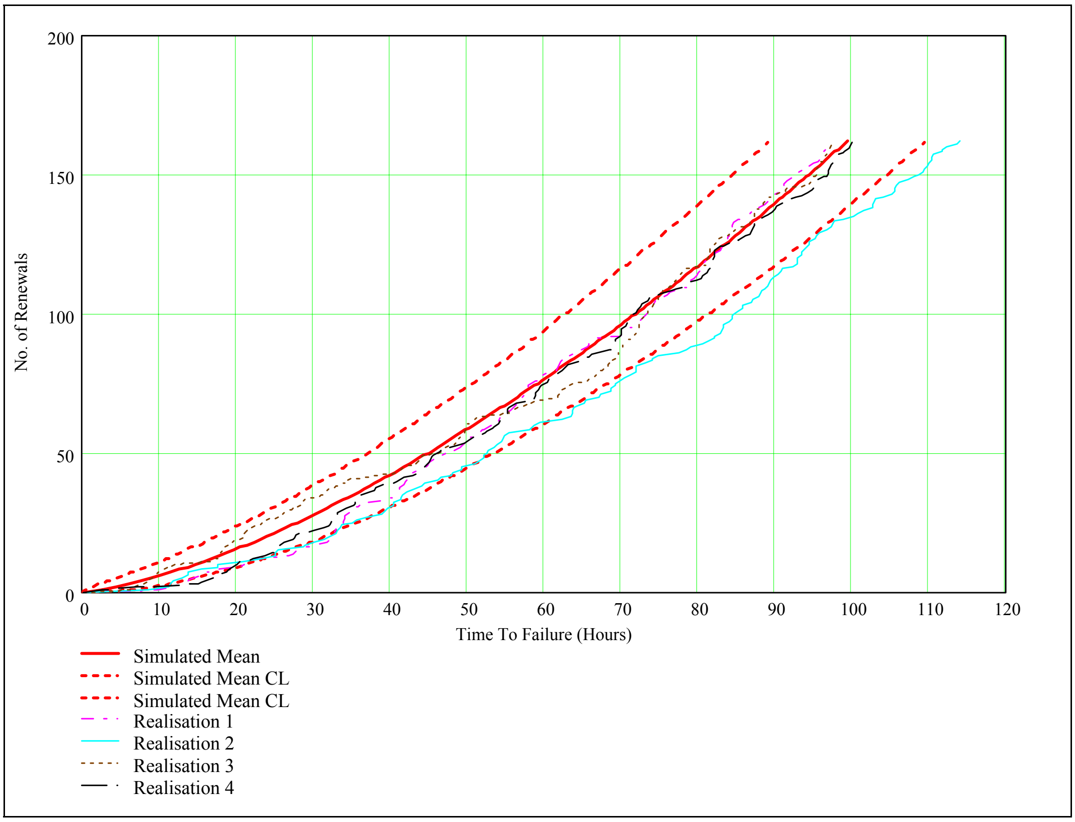

Figure 28: Simulation of KIJIMA Type I Model - Mean, 95%CL and Realisations (α = 2.84, β = 1.5, q = 0.6)

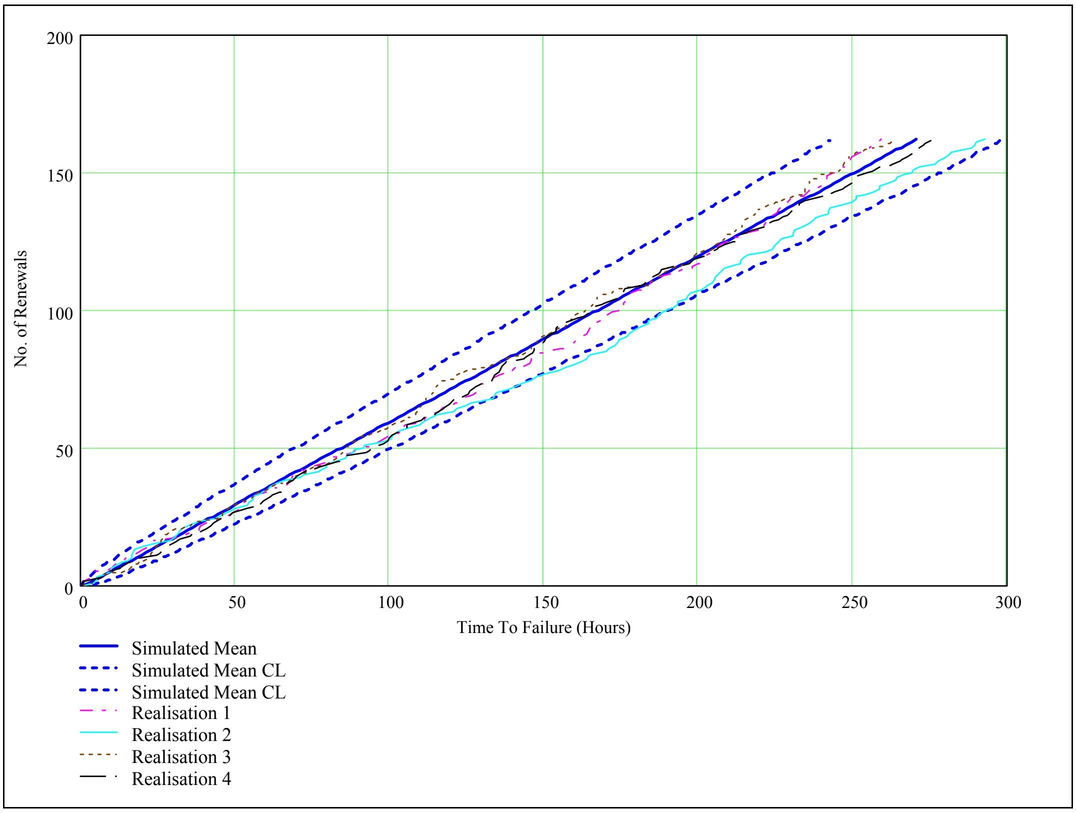

Figure 29: Simulation of KIJIMA Type II Model - Mean, 95%CL and Realisations (α = 2.84, β = 1.5, q = 0.6)

Results from the Comparison between the KIJIMA Type I and Type II GRP Model

The first part of the study involved examining the CIF curve versus Time-To-Failure (TTF) from the KIJIMA Type I and Type II GRP models over a large number of renewals; in this case 161 renewals. Both models used $\alpha = 2.84$, $\beta = 1.5$, $q = 0.6$ and *total number of realisations* = 10,000.

From Figure 30 and Figure 31 it is possible to observe the differences in output as a function of the number of renewals from the KIJIMA Type I and Type II GRP models. Three conclusions could be drawn from these observations.

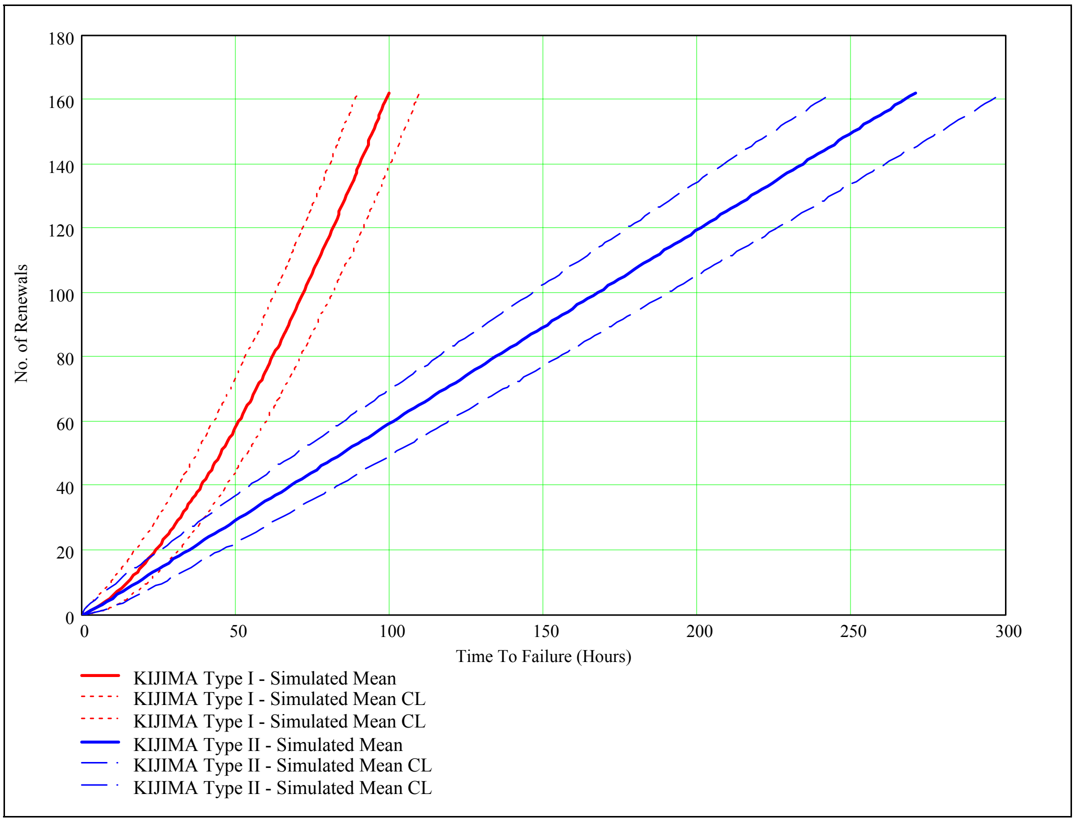

Figure 30: Comparison of Simulated Output from KIJIMA Type I and Type II Models (α = 2.84, β = 1.5, q = 0.6)

Remembering that the implementation of the MC simulation used throughout this study was based on finding the mean and distribution of the TTF to the kth failure/renewal it is possible to observe that at low numbers of renewals (i.e. < 10) the TTF of the KIJIMA Type I and Type II GRP models are almost identical. For example, TTF based on the mean values of the 10,000 realisations for the 8th failure is 12.587 hours for the KIJIMA Type I GRP model. This compares with 14.654 hours for the KIJIMA Type II GRP model. The similarity can be better seen in Figure 31.

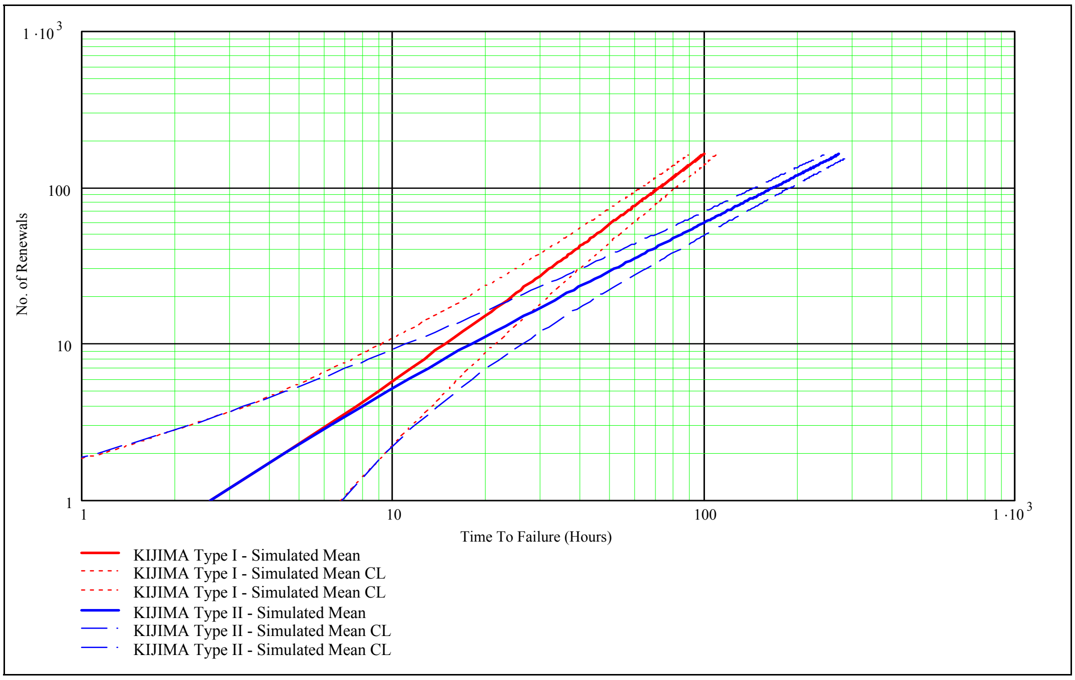

Figure 31: Log-Log Scale Comparison of Simulated Output from KIJIMA Type I and Type II Models (α = 2.84, β = 1.5, q = 0.6)

Secondly, at higher number of renewals the outputs from the two GRP models vary considerably. This observation confirms DAGPUNAR's[73] notion that under a failure rate increasing to infinity the KIJIMA Type I GRP model (with the exception of q = 0) will result in zero operating times (i.e. the item will fail immediately after renewal) in the limit. For example, the TTF based on the mean values of the 10,000 realisations for the 50th failure is 50.9 hours for the KIJIMA Type I GRP model compared with 101 hours for the KIJIMA Type II GRP model which is a significant difference. This variation can be better observed in Figure 30 and Table 11.

73 DAGPUNAR, J.S., loc cit

No of Failures/Renewals	GRP Type I	GRP Type II
5	8.9	9.6
10	14.8	18
20	24	34.6
40	38.6	67.8
60	50.9	101
80	61.8	134.2
100	71.9	167.5
150	94.4	250.56

Table 11: Comparison of Simulated Output from KIJIMA Type I and Type II Models (α = 2.84, β = 1.5, q = 0.6)

Thirdly, it was possible to observe that the CIF curve for the KIJIMA Type II GRP model becomes a straight line at higher numbers of renewals. This observation agrees with KIJIMA's initial findings where it was noted that output of the KIJIMA Type II GRP *"grows linearly for large n* [renewals]*"*[74]. The linearity indicates that the virtual age for the KIJIMA Type II GRP model becomes constant, or is at equilibrium, at higher numbers of renewals. The reason for this equilibrium can be seen from Equation 17, the equation for x_k, where as k (the number of renewals) increases, the impact on each additional renewal becomes smaller since x_k is a function of $q^k(1-q)$.

While this difference is hardly surprising, the knowledge of the performance and variation between the two models at high number of renewals is a very important consideration in model selection. Specifically, the selection of the GRP model type

74 KIJIMA, M., op cit, p100

should be representative of the physical failure mode(s) that the component/system will undergo over the appropriate number of renewals.

Consider a complex system consisting of a number of sub-systems and components which are purely mechanical, purely electrical/electronic or a hybrid of both elements. An example of such a system is an modern aircraft with purely mechanical components such as landing gear and engines, purely electrical/electronic components such as the flight computer, or hybrid components such as control actuators which combine both the electronic controllers and the mechanical (actually hydraulic) actuators. While, such complex systems can be modelled using the KIJIMA Type I GRP model, it results in the case where at the limit of renewals the system will have zero operating time. From a physical understanding of the system, it is possible to see that this may not be the case. In the example of the modern aircraft so long as the airframe remains within the fatigue life the aircraft can remain operational with non-zero operating times for a large number of renewals. For example, some the B-52 operating with the United States Air Force (USAF) have been in service for more than 50 years and remain operational.

However, there are cases where the KIJIMA Type I GRP model can be used and is appropriate; mainly in purely mechanical systems/components. For example, consider a hydraulic ram that is subjected to corrosion. Typically the maintenance and repair process includes cleaning using either mechanical or chemical abrasives. As the hydraulic ram undergoes many renewals, at some point in time there is sufficient *wear*[75] of the ram to result in permanent leaks since the diameter of the ram is now less than seal tolerance. Therefore, the hydraulic ram will continuously fail regardless of whether a renewal is undertaken, and will therefore have a zero operating time.

Based on these observations it is possible to make recommendations on model selection based on the item to be modelled. For example, based on the observations a logical conclusion would be as follows:

- a complex system such as an aircraft or car should be modelled using the KIJIMA Type II GRP model, and
- individual components should be modelled using the KIJIMA Type I GRP models.

While these recommendations offer some guidance on model selection, it is important that the type of model is representative of the physical failure mode(s) that the component/system will undergo over the appropriate number of renewals. Ultimately model choice should be at the discretion of the analyst.

---

75 *wear* can be defined as *'. . . as the undesirable cumulative change in dimensions brought about by the gradual removal of discrete particles from contacting surfaces in motion, due to predominately mechanical action. It should be further recognised that corrosion often interacts with the wear process to change the character of the surfaces of wear particles through reaction with the environment. Wear is, in fact, not a single process but a number of different processes that may take place independently or in combination.'* from COLLINS, J.A. *"Failure of Materials in Mechanical Design – Analysis, Prediction, Prevention"*, 2nd Ed., John-Wiley & Sons, USA, 1993

Results for GRP Type I from Sensitivity Study of a Variation in q ($0 \leq q \leq 1$) for $\beta = 1.5$

The first part of the sensitivity study examined the impact on the CIF curve from the KIJIMA Type I GRP model due to a variation in q from $0 \leq q \leq 1$, where β = constant = 1.5.

It was observed for the KIJIMA Type I GRP model that as q increased from $0 \leq q \leq 1$, while β = constant = 1.5, the CIF curve increased. This can be seen in Figure 32 and Figure 33. Interestingly, it was also observed that the MTBF of the KIJIMA Type I GRP model is very sensitive to variation of low values of q (i.e. $0 \leq q \leq 0.2$). This can again be seen in Figure 32 and Figure 33.

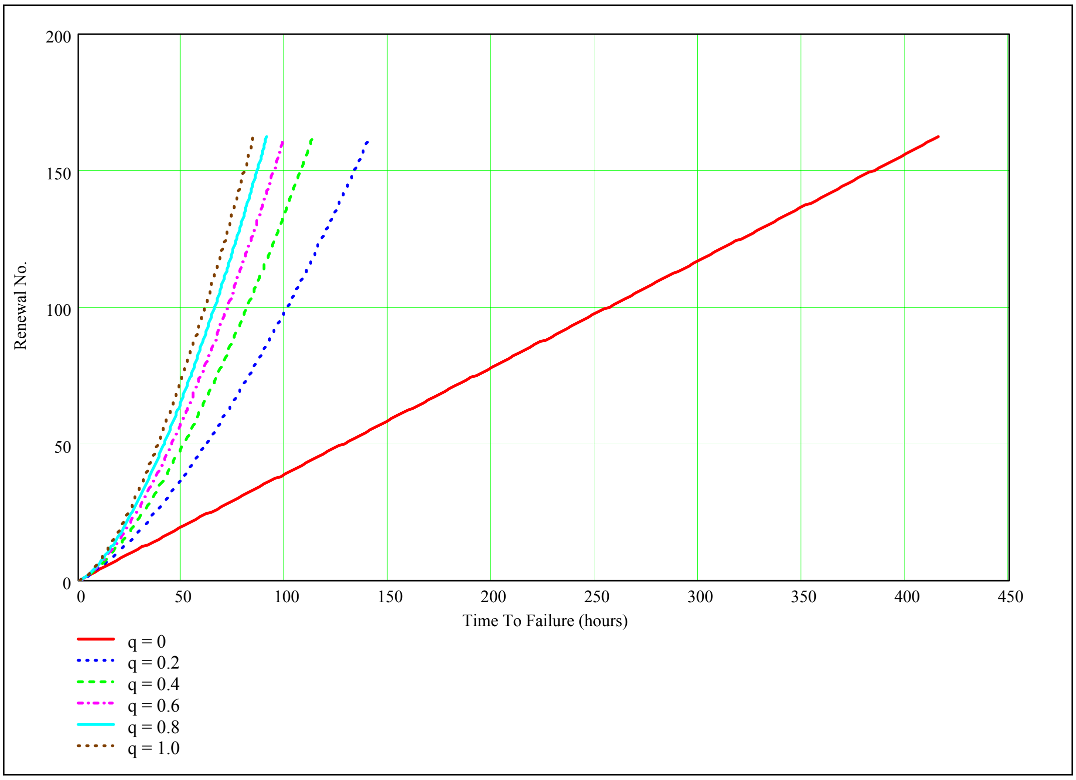

Figure 32: Simulated KIJIMA Type I Model (β = 1.5, q = 0, 0.2, 0.4, 0.6, 0.8, 1)

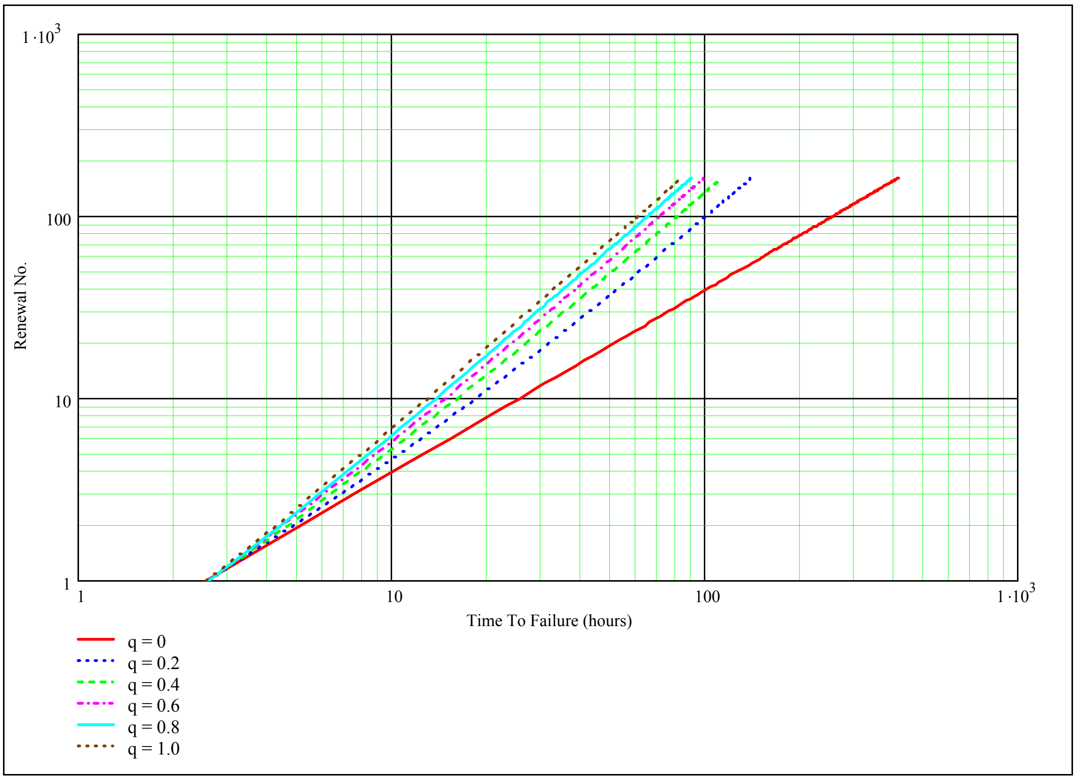

Figure 33: Log-Log Simulated KIJIMA Type I (β = 1.5, q = 0, 0.2, 0.4, 0.6, 0.8, 1)

Results for KIJIMA Type II GRP model from Sensitivity Study of a Variation in q (0 ≤ q ≤ 1) for β = 1.5

The first part of the sensitivity study also examined the impact on the CIF curve from the KIJIMA Type II GRP model due to a variation in q from $0 \leq q \leq 1$, where β = constant = 1.5.

It was observed for the KIJIMA Type II GRP model that as q increased from $0 \leq q \leq 1$, while β = constant = 1.5, the CIF curve increased. This can be seen in Figure 34 and Figure 35. This observation agrees with KIJIMA's initial findings where it was noted that the difference between the output of the model for $q = 1$ compared to $q < 1$

"is big, especially for large n [renewals]*"*[76]. However, unlike the KIJIMA Type I GRP model which was sensitive to low values of q (i.e. $0 \leq q \leq 0.2$), the KIJIMA Type II GRP model was more sensitive to variation of higher values of q (i.e. $0.8 \leq q \leq 1$). This can again be seen in Figure 34 and Figure 35.

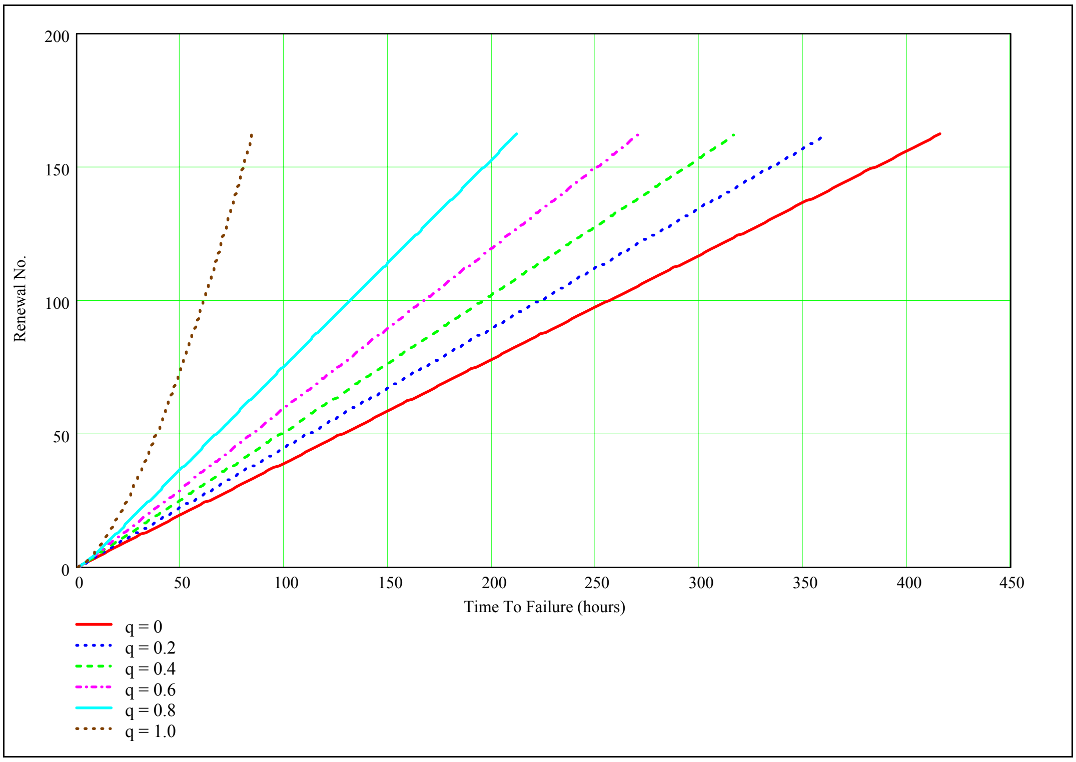

Figure 34: Simulated KIJIMA Type II Model (β = 1.5, q = 0, 0.2, 0.4, 0.6, 0.8, 1)

[76] KIJIMA, M., op cit, p101

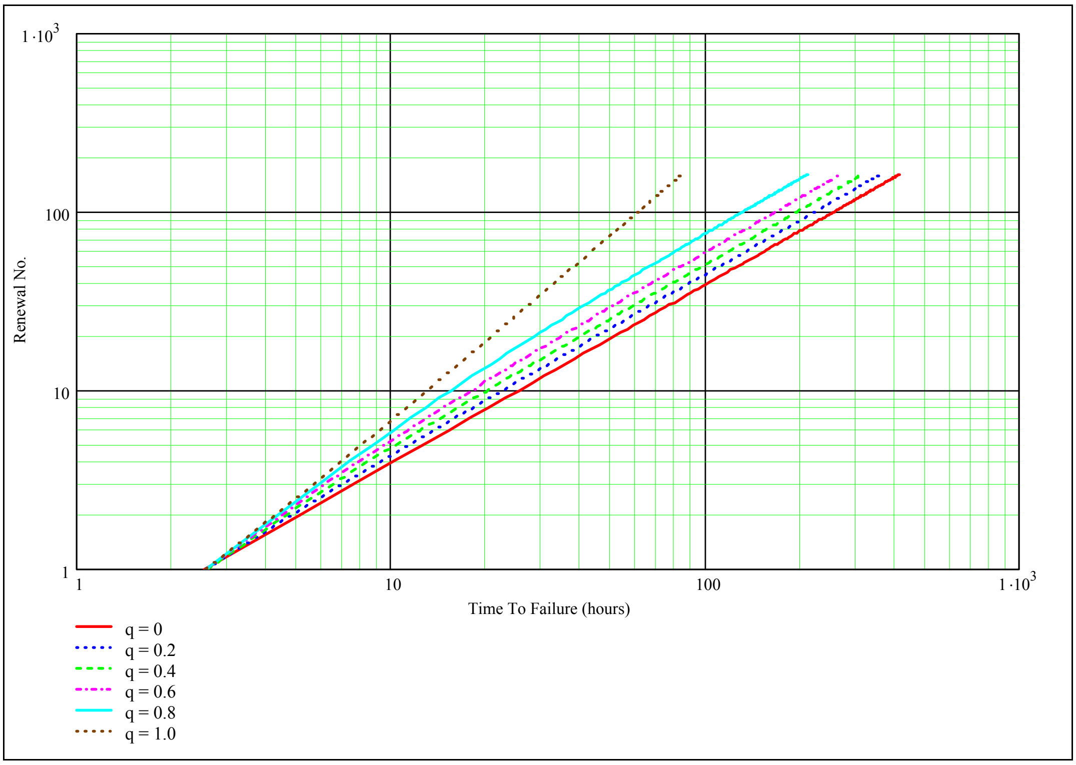

Figure 35: Log-Log Simulated KIJIMA Type II Model (β = 1.5, q = 0, 0.2, 0.4, 0.6, 0.8, 1)

Results for KIJIMA Type I GRP model from Sensitivity Study of a Variation in β ($1 \leq \beta \leq 2$) for q = 0.6

The second part of the sensitivity study examined the impact on the CIF curve from the KIJIMA Type I GRP model due to a variation in β from $1 \leq \beta \leq 2$, where q = constant = 0.6.

It was observed for the KIJIMA Type I GRP model that as β was increased from $1 \leq \beta \leq 2$, while q = constant = 0.6, the CIF curve increased. This can be seen in Figure 36 and Figure 37. The increase of the CIF curve as a result of an increasing β value was expected given that the underlying TTF distribution is Weibull, and therefore any increase in β in a TTF distribution should result in a higher CIF.

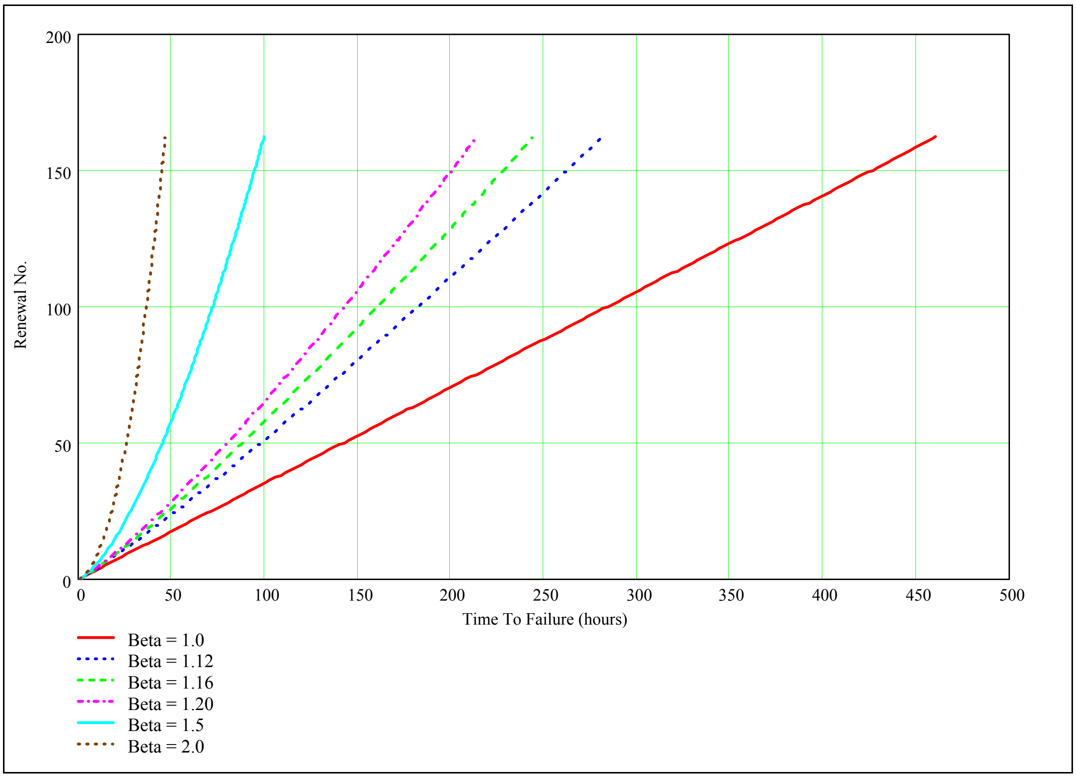

Figure 36: Simulated KIJIMA Type I Model (q = 0.6, β = 1, 1.12, 1.16, 1.2, 1.5, 2)

Interestingly, the KIJIMA Type I GRP model was very sensitive to any change in the value of β. In fact there were noticeable variations in the shape of the CIF curve for a change in β of 0.04. This is counter-intuitive since variation of β where $1.2 \leq \beta \leq 1.4$ in a typical Weibull TTF distribution would be generally considered to have minimal effect on the Weibull Hazard Rate (which can be considered equivalent to the GRP CIF) and therefore considered the same value. For example, a variation of ±0.2 in the estimation of β of a Weibull TTF distribution through probability plotting is not considered significant to the final model output. However, clearly from Figure 36 and Figure 37 this is not the case for the KIJIMA Type I GRP model. Therefore, the accurate selection of β is very important, especially for the prediction of future values.

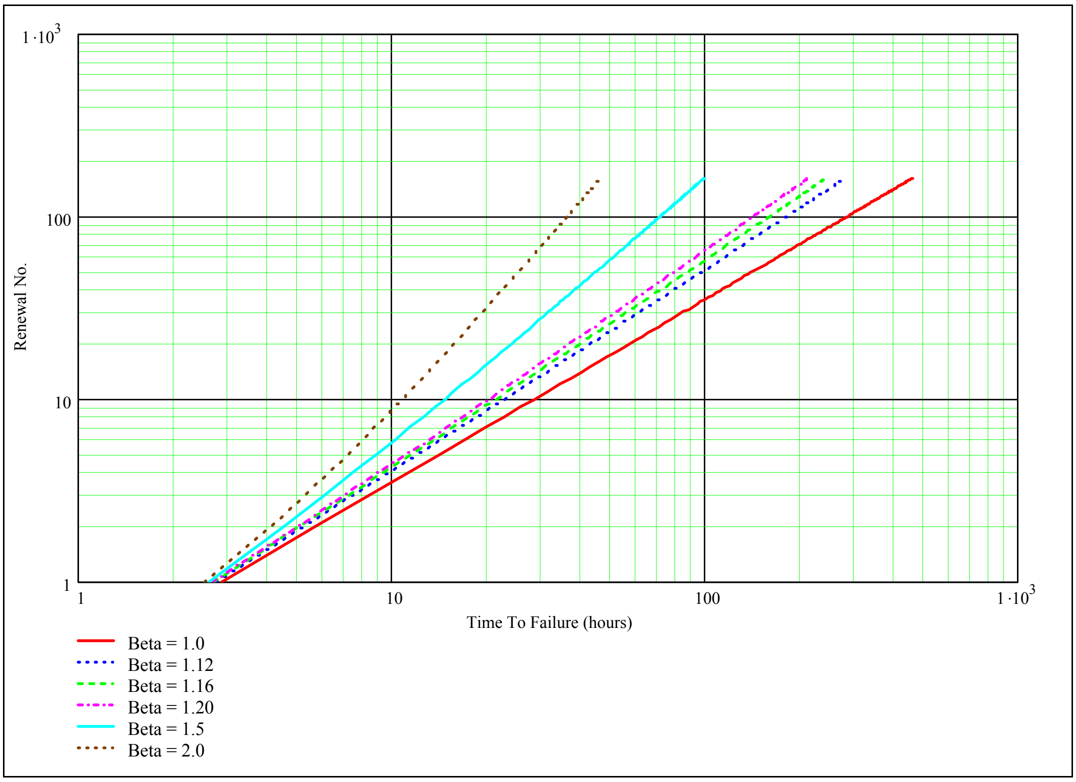

Figure 37: Log-Log Simulated KIJIMA Type I Model (q = 0.6, β = 1, 1.12, 1.16, 1.2, 1.5, 2)

Results for KIJIMA Type II GRP model from Sensitivity Study of a Variation in β ($1 \leq \beta \leq 2$) for q = 0.6

The second part of the sensitivity study also examined the impact on the CIF curve from the KIJIMA Type II GRP model due to a variation in β from $1 \leq \beta \leq 2$, where q = constant = 0.6.

It was observed for the KIJIMA Type II GRP model that as β was increased from $1 \leq \beta \leq 2$, while q = constant = 0.6, the CIF curve increased. This can be seen in Figure 38 and Figure 39.

Similar to the KIJIMA Type I GRP model, the KIJIMA Type II GRP model was sensitive to any change in the value of β. However, it was observed that the KIJIMA Type II GRP model was less sensitive to variation of β than the KIJIMA Type I GRP model.

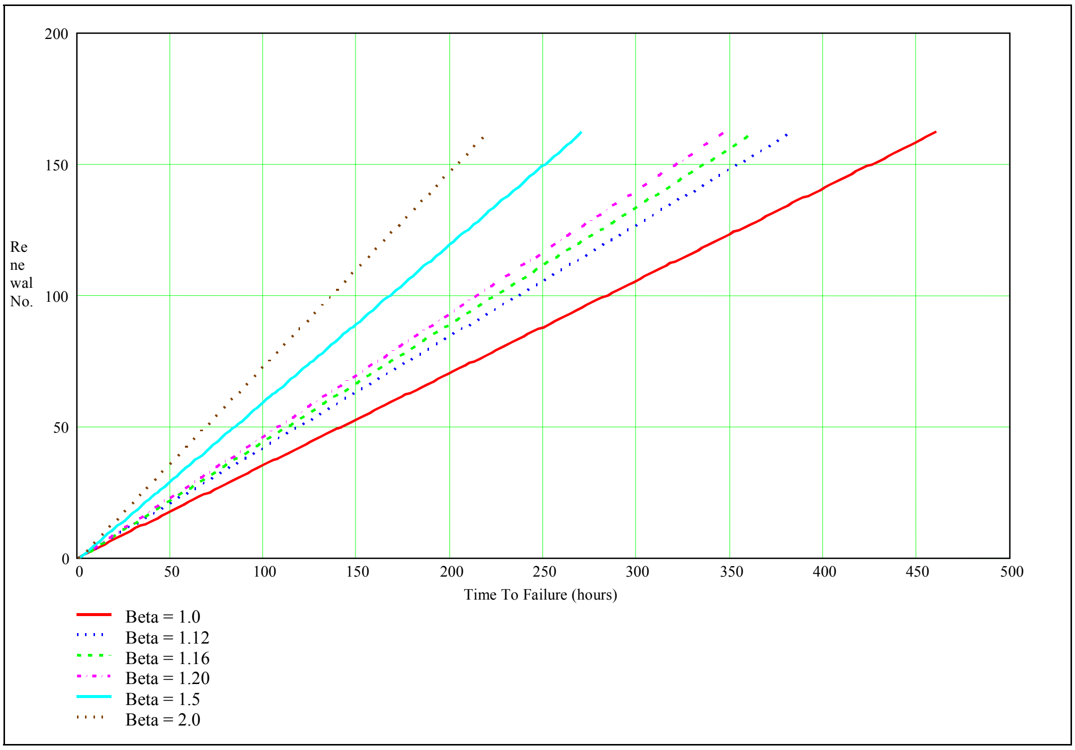

Figure 38: Simulated KIJIMA Type II Model (q = 0.6, β = 1, 1.12, 1.16, 1.2, 1.5, 2)

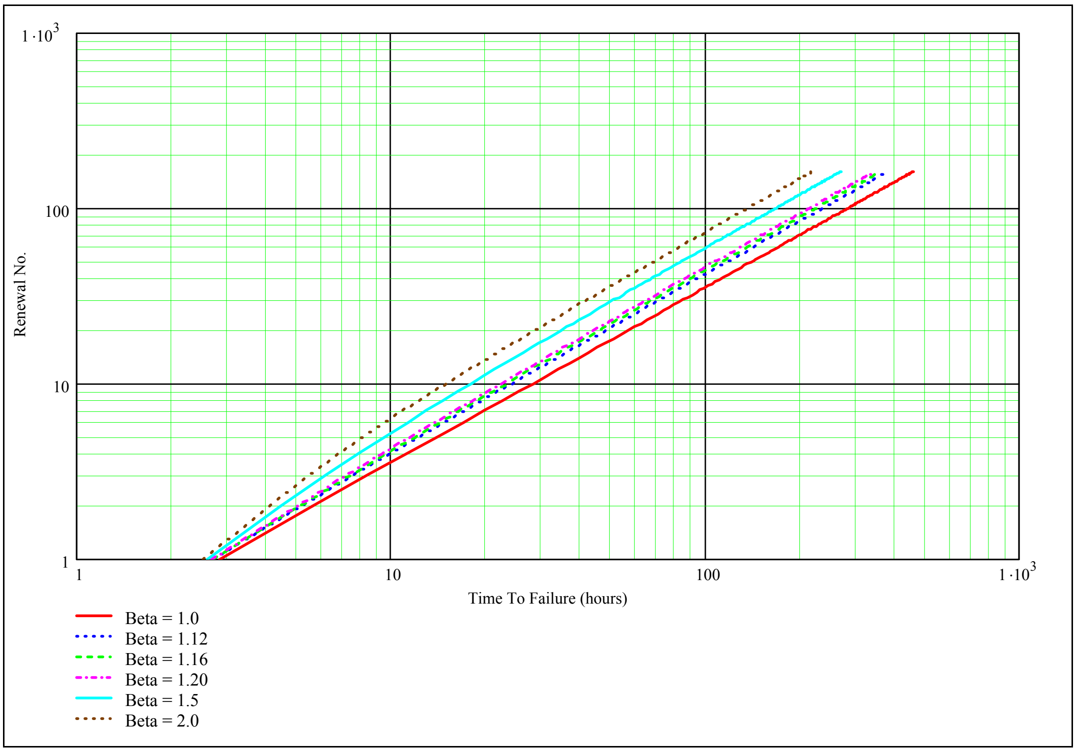

Figure 39: Log-Log Simulated KIJIMA Type II Model (q = 0.6, β = 1, 1.12, 1.16, 1.2, 1.5, 2)

Effect of 'q' on Combined Preventative/Inspection and Corrective Maintenance Regime with a Single Failure Mode for KIJIMA Type I GRP Equation

Set-up

Table 12 provides the values of α, β, $q_{Inspection}$ and $q_{Maintenance}$, the maintenance interval, the number of renewals and number of realisations that were used throughout the study, including the range of values of β, $q_{Inspection}$ and $q_{Maintenance}$ used in the sensitivity study. The initial value of α = 150 is based on the value used for Failure Mode 1 for Case Study 4A. As before, a sensitivity study of the Weibull distribution scale parameter, α, was not undertaken since any variation in α will only result in a linear translation of the CIF curve.

	Sensitivity Study Variation in β	Sensitivity Study Variation in $q_{Inspection}$	Sensitivity Study Variation in $q_{Maintenance}$
α	150	150	150
β	β = 0.75, 1.0, 1.5, 2.25, 3.5	1.5	1.5
$q_{Inspection}$	0.5	q = 0, 0.25, 0.5, 0.75, 1, 1.25, 1.5	0.5
$q_{Maintenance}$	0.7	0.7	q = 0, 0.25, 0.5, 0.75, 1, 1.25, 1.5
Inspection Interval	Every 400 hours	Every 400 hours	Every 400 hours
Number of Renewals	16	16	16
Number of Realisations	10, 000	10, 000	10, 000

Table 12: Setup of Variables during Study on the Effect of 'q' on Combined Preventative/Inspection and Corrective Maintenance Regime with a Single Failure Mode

Results from Sensitivity Study of a Variation in β (0.75 ≤ β ≤ 3.5)

This part of the review examined the impact on the CIF curve from the KIJIMA Type I GRP model with a separate periodic inspection and maintenance regime due to a variation in β from 0.75 ≤ β ≤ 3.5, where α = constant = 150, $q_{inspection}$ = constant = 0.5, $q_{maintenance}$ = constant = 0.7.

It was observed for the KIJIMA Type I GRP model that as β increased the CIF curve increased, which was as expected given the previous findings. This variation can be seen in Figure 40. As before, the increase of the CIF curve as a result of an increasing β value was expected given that the underlying TTF distribution is Weibull, and therefore any increase in β in a TTF distribution should result in a higher CIF.

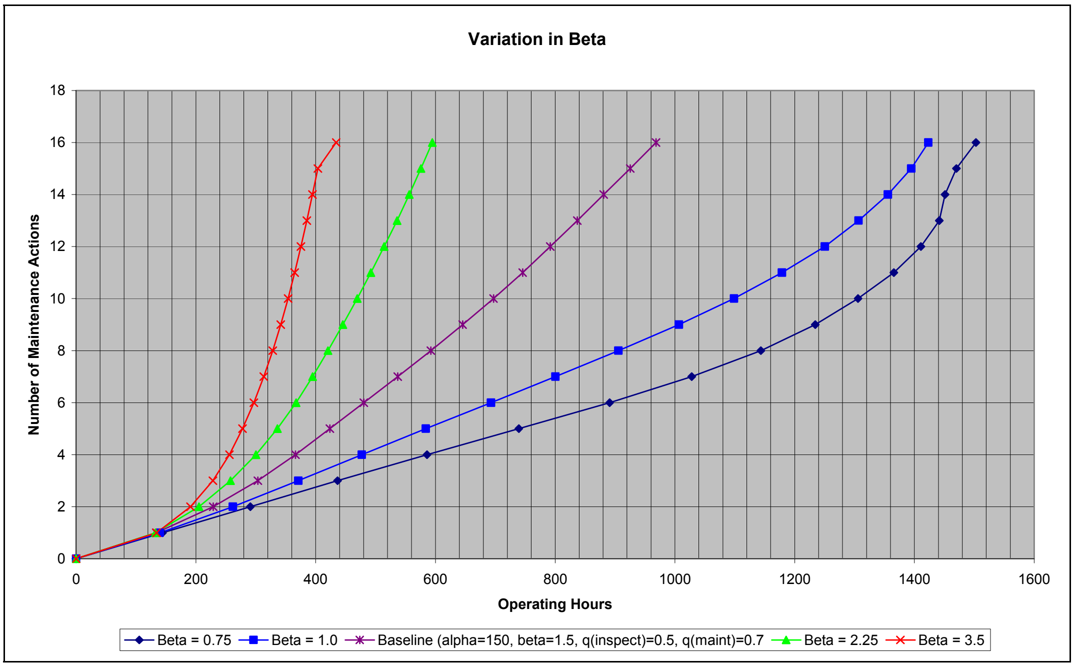

Figure 40: Results from Sensitivity Study of a Variation in β on Combined Preventative/Inspection and Corrective Maintenance Regime with a Single Failure Mode for KIJIMA Type I GRP Equation

Similar to the previous study, the KIJIMA Type I GRP model with a separate periodic inspection and maintenance regime appeared sensitive to small changes in the value of β away from β = 1.0. However, major changes of β > 2.0 appeared to have less impact. For example the difference in CIF between β = 1 and β = 1.5, compared with β =1.5 and β = 2.25, and with β = 2.25 and β = 3.5 decreased with increasing β.

Results from Sensitivity Study of a Variation in $q_{inspection}$ ($0 \leq q_{inspection} \leq 1.5$)

This part of the review examined the impact on the CIF curve from the KIJIMA Type I GRP model with a separate periodic inspection and maintenance regime due to a variation in $q_{inspection}$ from $0 \leq q_{inspection} \leq 1.5$, where α = constant = 150, β = constant =

1.5, $q_{maintenance}$ = constant = 0.7 and scheduled maintenance interval every 400 operating hours.

It was observed for the KIJIMA Type I GRP model that as $q_{inspection}$ increased the CIF curve increased, which was as expected given the previous findings. This variation can be seen in Figure 40. While there was change in the CIF curve due to changes in $q_{inspection}$ the relatively small change, especially for higher $q_{inspection}$ values, was unexpected. Moreover, the apparent limited effect of $q_{inspection} > 1$ (i.e. *worse-than-old*) was surprising. However, in further review these results appear quite logical for one main reason. In this example given the value of the underlying 2-parameter Weibull TFF there were more corrective maintenance tasks (i.e. unscheduled failures) than preventative maintenance activities. Therefore, there will be comparatively less preventative maintenance actions, and consequently less impact on the *Virtual Age* (VA) over the observation time in comparison with corrective maintenance actions (e.g. dominate failure mode).

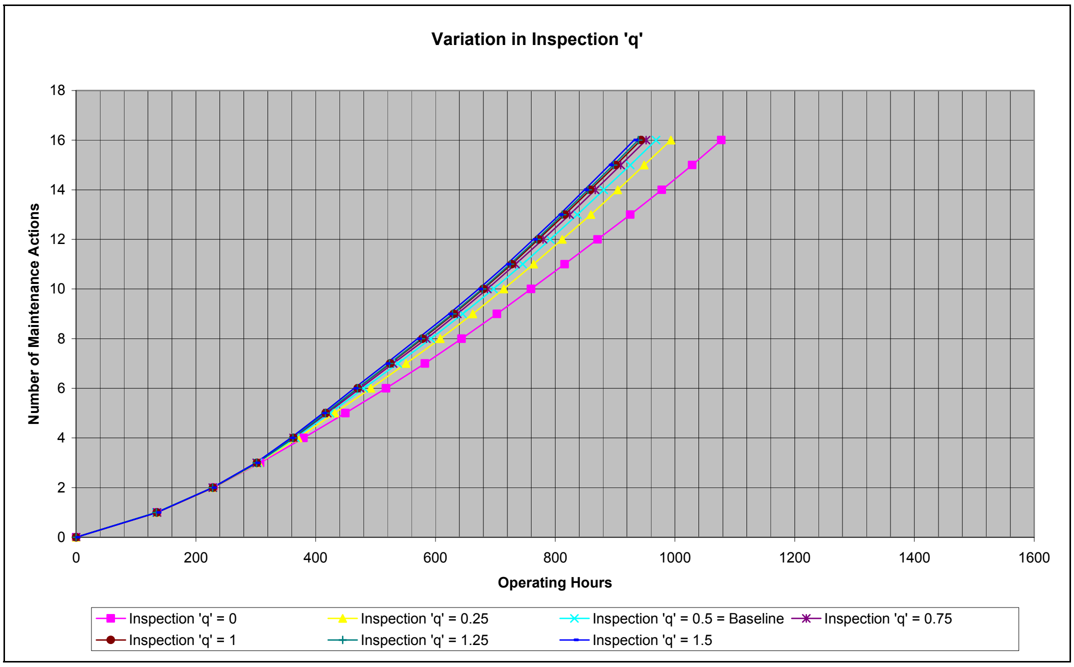

Figure 41: Results from Sensitivity Study of a Variation in $q_{inspection}$ on Combined Preventative/Inspection and Corrective Maintenance Regime with a Single Failure Mode for KIJIMA Type I GRP Equation

Results from Sensitivity Study of a Variation in $q_{maintenance}$ ($0 \leq q_{maintenance} \leq 1.5$)

This part of the review examined the impact on the CIF curve from the KIJIMA Type I GRP model with a separate periodic inspection and maintenance regime due to a variation in $q_{maintenance}$ from $0 \leq q_{inspection} \leq 1.5$, where α = constant = 150, β = constant = 1.5, $q_{inspection}$ = constant = 0.5 and a scheduled maintenance interval every 400 operating hours.

It was observed for the KIJIMA Type I GRP model that as $q_{maintenance}$ increased the CIF curve increased, which was as expected given the previous findings. This variation can be seen in Figure 42. Unlike the change in the CIF due to a change $q_{inspection}$, a change in the CIF curve due to changes in $q_{maintenance}$ were significant, especially for lower higher $q_{maintenance}$ values. Based on the previous findings this was expected given the impact on the VA.

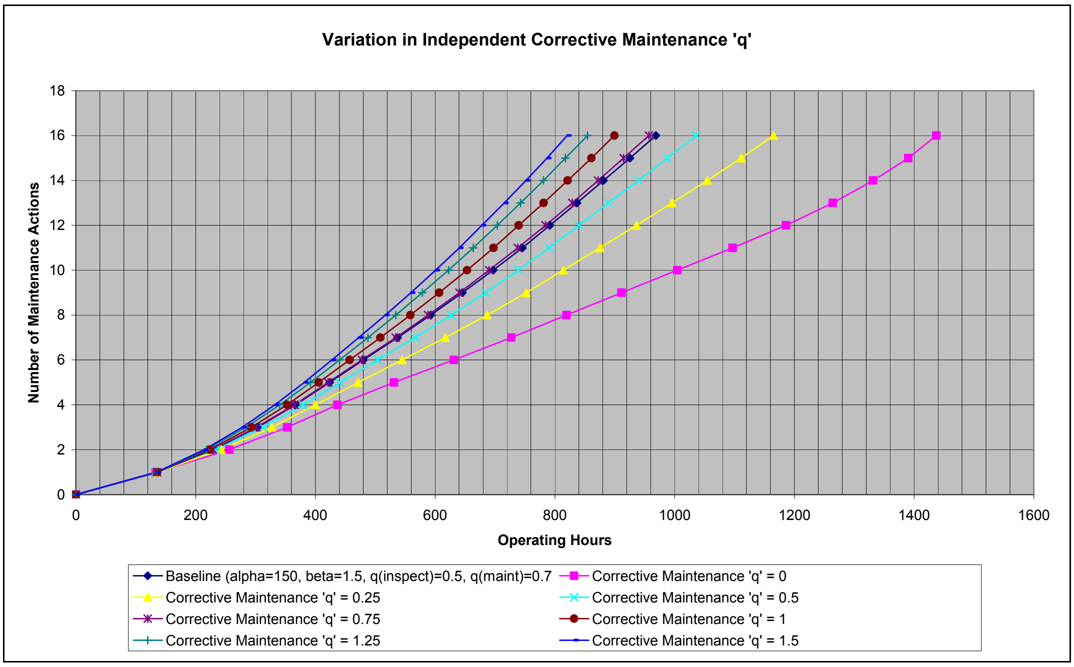

Figure 42: Results from Sensitivity Study of a Variation in $q_{maintenance}$ on Combined Preventative/Inspection and Corrective Maintenance Regime with a Single Failure Mode for KIJIMA Type I GRP Equation

Combined Results from Sensitivity Study

Figure 43 provides a summary of the three sensitivity studies completed on the Combined Preventative Maintenance/Inspection and Corrective Maintenance Regime with a Single Failure Mode for KIJIMA Type I GRP Equation. Specifically the sensitivity study on the variation of:

- Inspection/Preventative Maintenance *q*;
- Independent Corrective Maintenance *q*; and
- Inspection/Preventative Maintenance Interval

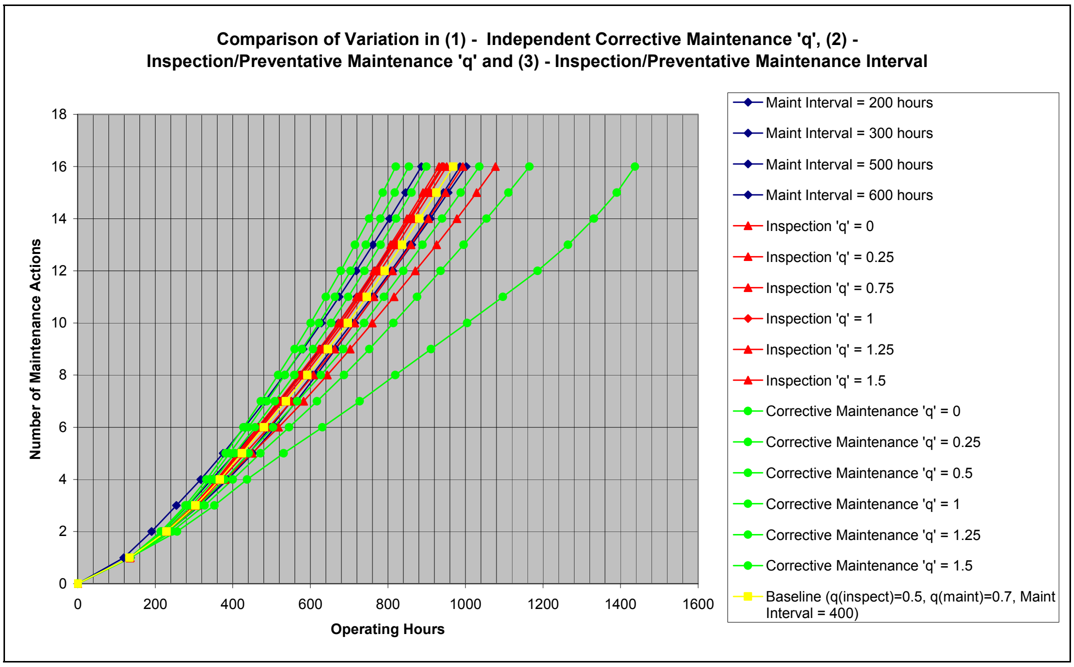

Figure 43: Summary of Results from Sensitivity Study for a Combined Preventative/Inspection and Corrective Maintenance Regime with a Single Failure Mode for KIJIMA Type I GRP Equation

The rationale for this comparison is to provide further insight into the behaviour of the KIJIMA Type I GRP Equation. Furthermore, based on these insights this research provides guidance on the decision making process by highlighting where to concentrate resources to assist the achievement of an organisational goal (e.g. increased reliability or decreased TCO for the same reliability).

From Figure 43 it is clear that the CIF curve is most sensitive to the q related to the corrective maintenance actions; especially at low (i.e. $q_{maintenance} < 0.5$). Surprisingly, there is little sensitivity, indicated by the lack of spread in CIF curves, due to variation in either preventative maintenance/inspection or maintenance interval. Furthermore the apparent limited effect of $q_{inspection} > 1$ (i.e. *worse-than-old*) and reducing the maintenance interval by half (i.e. 400 hours to 200 hours) was unexpected. However, in further review these results appear quite logical for one main reason. In this example, given the value of the underlying 2-parameter Weibull TFF, there are more corrective maintenance tasks (i.e. unscheduled failures) than preventative ones. Therefore, even if a preventative maintenance action does occur, given there are significantly less over the observation time the corrective maintenance q will dominate on the VA of the component.

Accordingly, in this example the guidance for a decision maker would be to concentrate resources (i.e. personnel and/or funding) on lower the corrective maintenance q. However, this will be highly dependent on the setup of each case and it is strongly recommended that each case undertake a sensitivity study similar to that conducted in this chapter.

Effect of 'q' on Combined Preventative/Inspection and Corrective Maintenance Regime with a Multiple Dependent Failure Modes for KIJIMA Type I GRP Equation

Set-up

Table 13 provides the values of α, β, $q_{Inspection}$ and $q_{Maintenance}$ for each Failure Mode including the dependency, the maintenance interval, number of renewals and number of realisations that were used throughout the study. Additionally, Table 13 includes the range of values of α β, $q_{Inspection}$ and $q_{Maintenance}$ used in the sensitivity studies. The initial values for both Failure Modes 1 and 2 are based on the research provided in Case Study 4A. However, unlike previous analysis, a sensitivity study of the Weibull distribution scale parameter, α, was undertaken given there is a significant difference (100%) in the α values corresponding to each of the different Failure Modes.

Results from Sensitivity Study of a Variation in α

This part of the review examined the impact on the CIF curve of a variation in either α value of Failure Mode 1 or 2.

It was observed for the KIJIMA Type I GRP model that as α increased the CIF curve decreased. This variation can be seen in Figure 44. As before, the decrease of the CIF curve as a result of an increasing α value was expected given that the underlying TTF distribution is Weibull, and therefore any increase in α in a TTF distribution should result in a lower CIF curve. However, of interest is the difference in variation of the CIF curve between Failure Mode 1 and 2. Specifically, a 50% increase/decrease for variation of α of Failure Mode 1 had a larger variation in the CIF curve than the same 50% increase/decrease for Failure Mode 2.

The reason for the difference in variation is similar to that discussed in the previous findings. Specifically, that a slight variation in the *dominant* failure mode will have comparatively larger impact on the CIF curve. In this example, the *dominant* Failure Mode **is** Failure Mode 1 whose α value (e.g. 150 hours) is 50% of the Failure Mode 2 α value (e.g. 300 hours).

	α_{FM1}	α_{FM2}	β_{FM1}	β_{FM2}	q_{I_1}	q_{I_2}	q_{M_1}	q_{M_2-}	q_{M_1-}	q_{I_2}

								1	2	
Baseline	150	300	1.5	3.5	0.5	1.0	0.7	0.2	1.2	0.2
α_{FM1}	75, 150, 225									
α_{FM2}		150, 300, 450								
β_{FM1}			0.75, 1.0, 1.5, 2.25							
β_{FM2}				1.0, 1.75, 3.5, 5.25						
q_{I_1}					(1)[77]					
q_{I_2}						(1)				
q_{M_1}							(1)			
q_{M_2-1}								(1)		
q_{M_1-2}									(1)	
q_{I_2}										(1)
Inspection Interval	Every 400 hours									
Number of Renewals	16									
Number of Realisations	10, 000									

Table 13: Setup of Variables during Study on the Effect of *q* on Combined Preventative/Inspection and Corrective Maintenance Regime with a Multiple Dependent Failure Modes

77 Consists of varying the specific ‘q’ across a range of specified values; 0, 0.25, 0.5, 0.75, 1, 1.25, 1.5

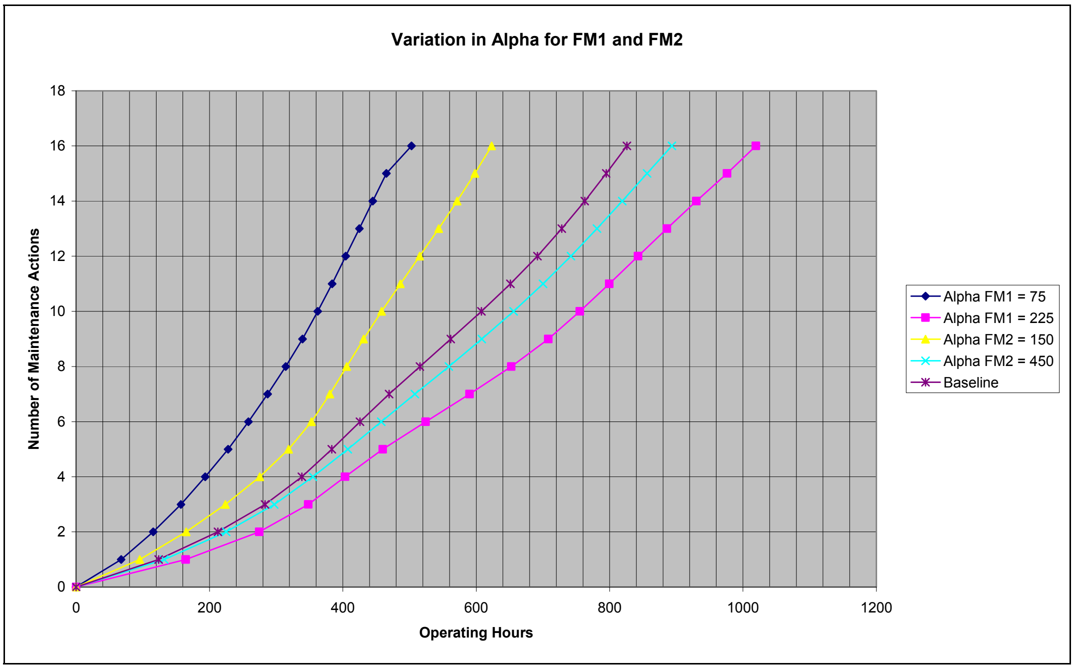

Figure 44: Results from Sensitivity Study of a Variation in α on Combined Preventative/Inspection and Corrective Maintenance Regime with a Multiple, Dependent Failure Modes

Results from Sensitivity Study of a Variation in β

This part of the review examined the impact on the CIF curve due to a variation in either β value of Failure Mode 1 or 2.

It was observed for the KIJIMA Type I GRP model that as β increased the CIF curve increased, which was as expected given the previous findings. This variation can be seen in Figure 45. As before, the increase of the CIF curve as a result of an increasing β value was expected given that the underlying TTF distribution is Weibull, and therefore any increase in β in a TTF distribution should result in a higher CIF curve. However, of interest is the difference in variation of the CIF curve between Failure Mode 1 and 2. Specifically, that a change in the β value for Failure

Mode 2 had an insignificant change on the CIF curve compared to changes in Failure Mode 1.

The initial reason for the difference in variation is the similar to that discussed was presented in the previous section. Specifically that slight variation to the failure modes will have comparatively larger impact on the CIF curve. However, in this example, the *dominant* failure mode **is** failure mode 1 whose β value (e.g. 1.5) is much smaller than failure mode 2 (e.g. 3.5 hours). So why is the smaller β dominant? Again, this is linked to the notion that the dominant failure mode is the one with the most renewals, and therefore α plays a more significant role, rather than β.

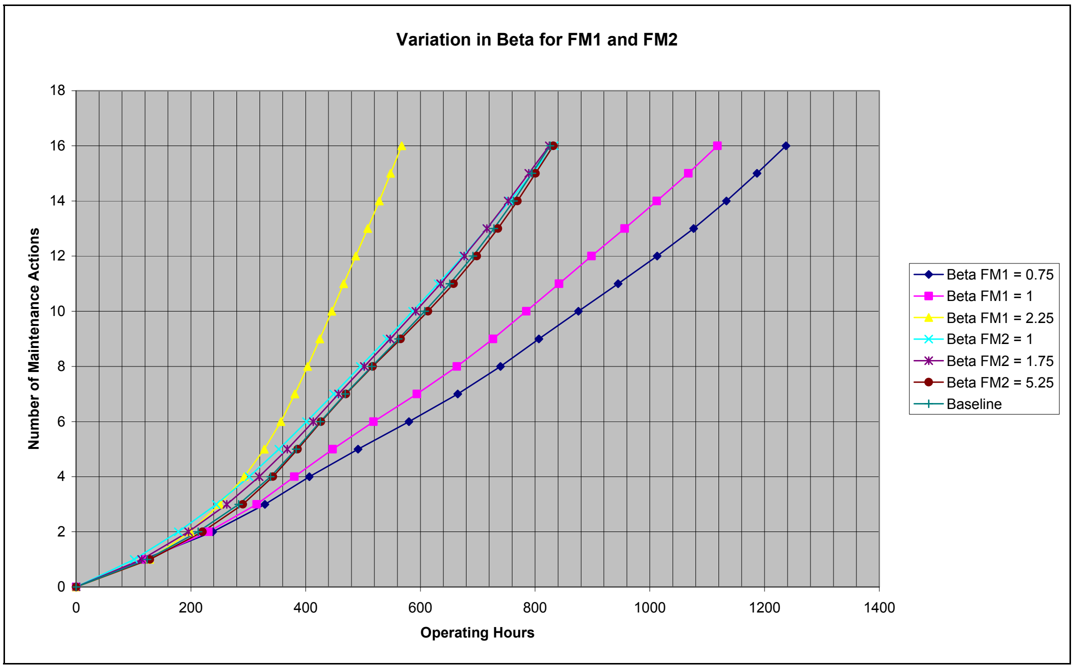

Figure 45: Results from Sensitivity Study of a Variation in β on Combined Preventative/Inspection and Corrective Maintenance Regime with a Multiple, Dependent Failure Modes

Furthermore, similar to the previous study, the KIJIMA Type I GRP model appeared sensitive to small changes in the value of β away from $\beta = 1.0$. This can be seen in Figure 45 where the variation of the CIF curve compared with the β value of Failure Mode 1.

Results from Sensitivity Study of a Variation in $q_{inspection}$ ($0 \leq q_{inspection} \leq 1.5$)

This part of the review examined the impact on the CIF curve from the KIJIMA Type I GRP model due to a variation in $q_{inspection}$ from $0 \leq q_{inspection} \leq 1.5$ for both Failure Mode 1 and 2.

It was observed for the KIJIMA Type I GRP model that as $q_{inspection}$ for failure mode 2 increased the CIF curve increased, which was as expected given previous findings. This variation can be seen in Figure 46. However, of most interest was the observation of no variation in the CIF curve due to variation in $q_{inspection}$ for failure mode 1. The absence of variation can be seen in Figure 47.

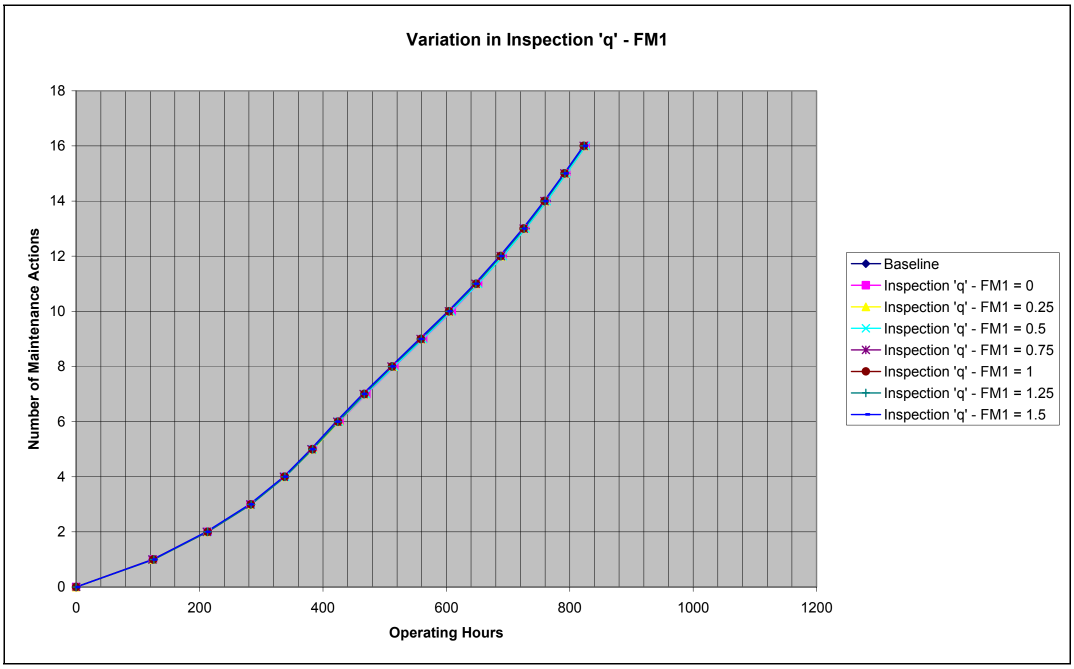

Figure 46: Results from Sensitivity Study of a Variation in $q_{inspection}$ for Failure Mode 1 on Combined Preventative/Inspection and Corrective Maintenance Regime with a Multiple, Dependent Failure Modes

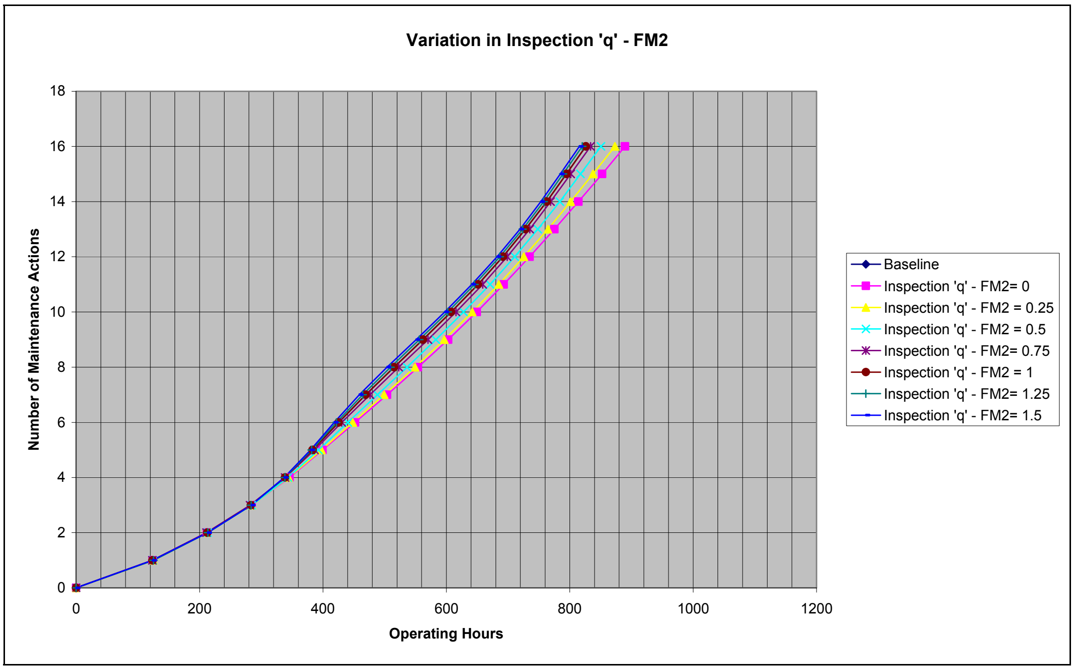

Figure 47: Results from Sensitivity Study of a Variation in $q_{inspection}$ for Failure Mode 2 on Combined Preventative/Inspection and Corrective Maintenance Regime with a Multiple, Dependent Failure Modes

While there was change in the CIF curve due to changes in $q_{inspection}$ for Failure Mode 2 as single failure mode example, the relatively small change, especially for higher $q_{inspection}$ values, was unexpected. Furthermore the apparent limited effect of $q_{inspection}$ > 1 (i.e. *worse-than-old*) was surprising. However, in further review these results appear quite logical for one main reason. In this example given the value of the underlying 2-parameter Weibull TFF there are more corrective maintenance tasks (i.e. unscheduled failures) than preventative ones. Therefore, even if a preventative maintenance action does occur, the significantly lower numbers over the observation time mean that corrective maintenance q will dominate.

Results from Sensitivity Study of a Variation in $q_{\mathrm{maintenance}}$

This part of the review examined the impact on the CIF curve from the KIJIMA Type I GRP model due to a variation in $q_{maintenance}$ from $0 \leq$, $q_{maintenance} \leq 1.5$ for both Failure Modes. This part of the review also examined the impact on the CIF due to variation in the dependent 'q' value which affected the failure mode.

It was observed for the KIJIMA Type I GRP model that as $q_{maintenance}$ increased, regardless of the Failure Mode or dependency, the CIF curve increased, which was predictable given the previous findings. This variation can be seen in Figure 48, Figure 49, Figure 50 and Figure 51. Unlike the change in the CIF due to a change $q_{inspection}$, a change in the CIF curve due to changes in $q_{maintenance}$ were significant, especially for lower higher $q_{maintenance}$ values. Based on the previous findings this was expected.

Again, the difference in effect of the variation across the four $q_{maintenance}$ values can be attributed to the impact of the *dominant* Failure Mode. Specifically that slight variations to the direct and dependent q for the *dominant* Failure Mode will have comparatively larger impact on the CIF curve. This can be observed since the difference in the CIF due to the same variation in $q_{maintenance}$ on Failure Mode 1 is larger than for Failure Mode 2, or indeed the dependent Failure Mode 2 due to 1, or Failure Mode 2 due to 1.

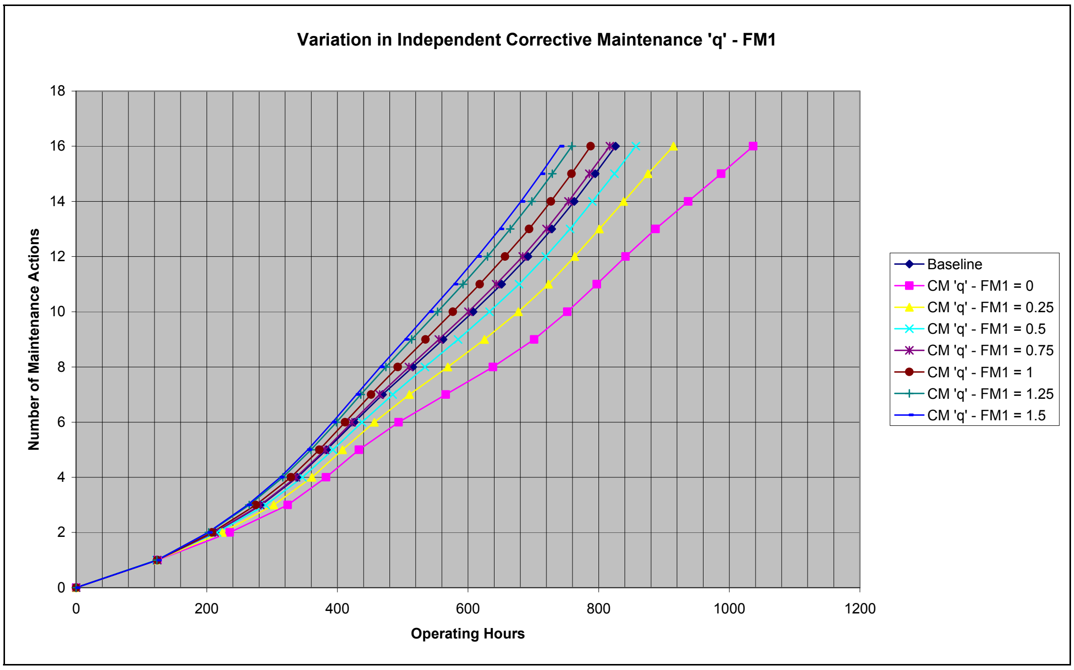

Figure 48: Results from Sensitivity Study of a Variation in $q_{maintenance}$ for Failure Mode 1 on Combined Preventative/Inspection and Corrective Maintenance Regime with a Multiple, Dependent Failure Modes

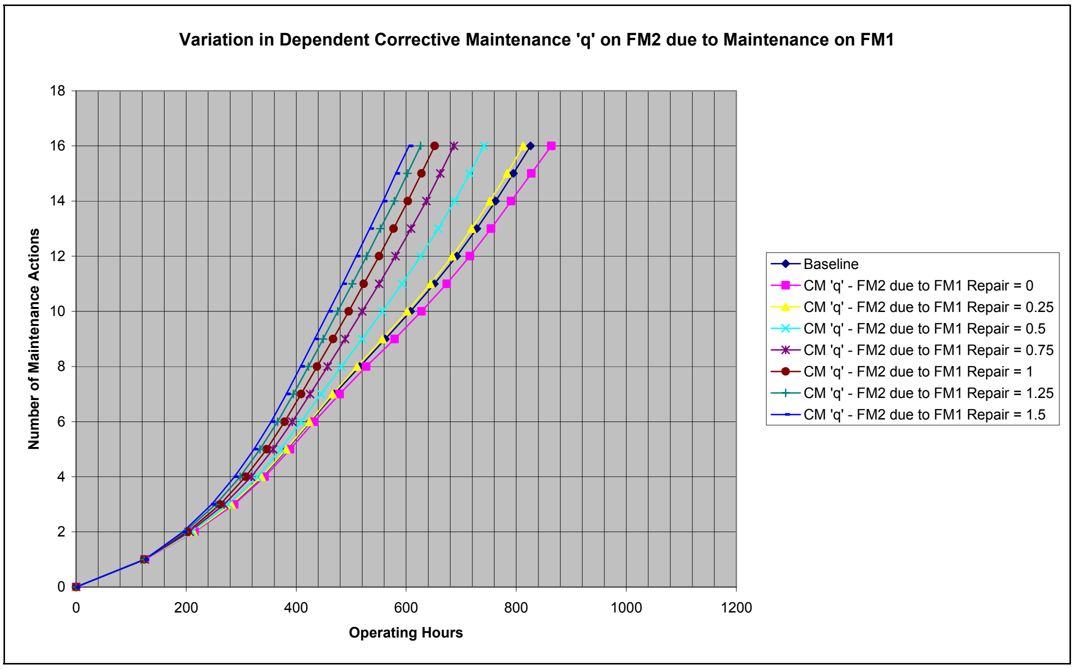

Figure 49: Results from Sensitivity Study of a Variation in $q_{maintenance}$ for Failure Mode 2 based on a Repair to Failure Mode 1 on Combined Preventative/Inspection and Corrective Maintenance Regime with a Multiple, Dependent Failure Modes

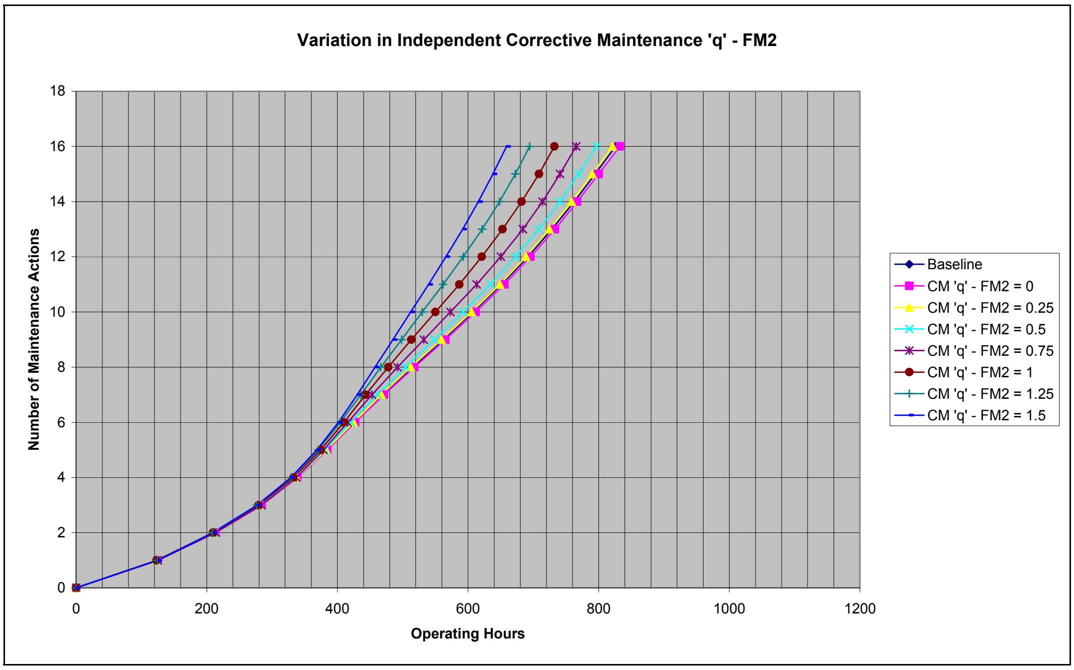

Figure 50: Results from Sensitivity Study of a Variation in $q_{maintenance}$ for Failure Mode 2 on Combined Preventative/Inspection and Corrective Maintenance Regime with a Multiple, Dependent Failure Modes

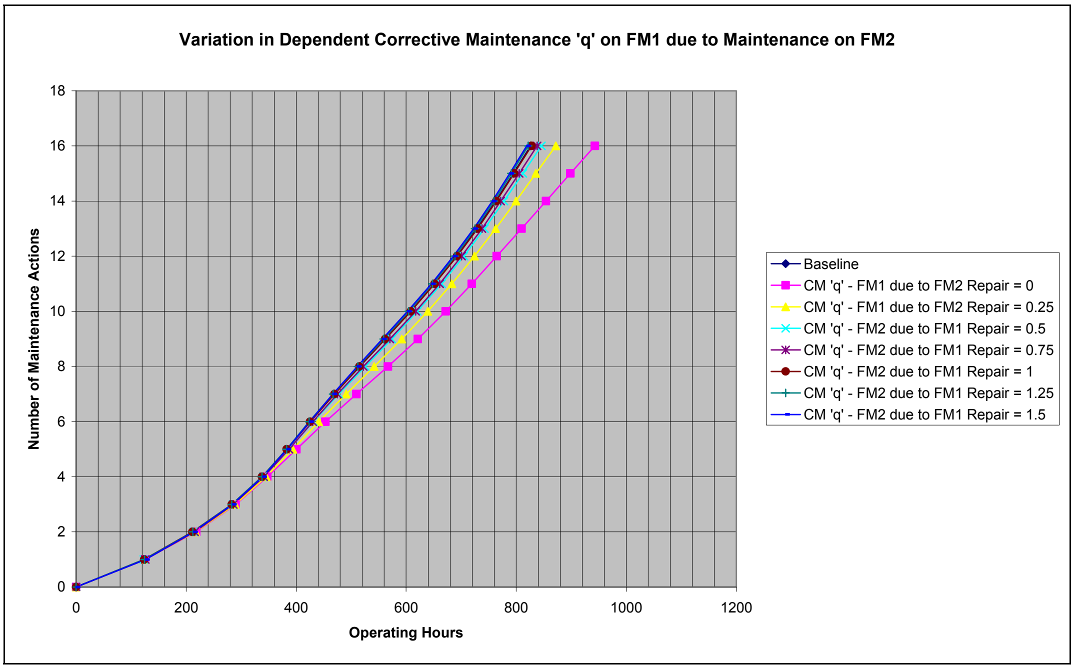

Figure 51: Results from Sensitivity Study of a Variation in $q_{maintenance}$ for Failure Mode 1 based on a Repair to Failure Mode 2 on Combined Preventative/Inspection and Corrective Maintenance Regime with a Multiple, Dependent Failure Modes

Representative Links to the GRP Parameters

Set-up

While it is clear that the various parameters of the GRP equation have a symmetric impact on the CIF curve they are also representative of other, more tangible factors. Indeed, while the original intent of the research was to use data from the Australian Defence Force aviation sector to compare and contrast the use and variation of *q,* the access to fleet wide specific serial number data, and the detailed operating environment, was very difficult. In isolation this behaviour may appear contrary to the highly regulated nature of the aviation industry, however, this lack of serial number level data is quite common across the defence, commercial and civil aviation practices.

Accordingly, it was not possible to undertake any detailed study on the variation of the GRP parameters due to operations factors such as:

- Geographic location,
- Maintenance facility/staff,
- Maintenance tools/manuals/procedures,
- Incorporation of a design change/modification, or
- Mission profile.

Notwithstanding, it is quite possible to hypothesise mapping the GRP parameters, especially q, to some operations factors. This can be seen in Table 14.

Cause Mechanism	**Parameter to be Adjusted**
Operational Flight Profile (i.e. mission profile)	**α, q**
Climate (i.e. location of the base)	**α**
Introduction of new technology (i.e. replacement/modification of existing item):	
• Removal of Failure Mode(s)	**α**
• Increase repairability	**q**
Inspection/Maintenance Training/Proficiency	**q**
Inspection/Maintenance Procedures	**q**

Table 14: Cause Mechanism verses Parameter Adjustment

Summary of Role of 'q'

The research into the behaviour of the KIJIMA Type I and Type II models have provided some useful insights into their implementation and interpretation as follows:

a. At low number of renewals (i.e. < 10), there is little difference between the KIJIMA Type I and Type II models.

b. At high numbers of renewals (i.e. > 40), there is a significant difference between the KIJIMA Type I and Type II models. For example at t = 40 hours there is almost 100% difference in CIF. Refer to Table 11.

c. At high numbers of renewals (i.e. > 40) the CIF curve of the KIJIMA Type II model approaches a straight line.

d. As β and q increased the TTF decreased for both KIJIMA Type I and Type II models.

e. TTF of the KIJIMA Type I GRP model is:

   i. very sensitive to variation of low values of q (e.g. $0 \leq q \leq 0.2$); and

   ii. very sensitive to variation in the value of β. In fact there were noticeable variations in TTF for a change in β of 0.04.

f. TTF of the KIJIMA Type II GRP model is:

   i. very sensitive to variation of high values of q (e.g. $0.8 \leq q \leq 1.0$); and

   ii. sensitive to variation in the value of β; although the β - sensitivity observed for the KIJIMA Type II GRP model is less than with the KIJIMA Type I GRP model.

g. The selection of either the KIJIMA Type I or Type II should ensure that the chosen model is representative of the physical failure mode(s) that the component/system will undergo over the appropriate number of renewals. For example, based on the observations the following guidance is recommended:

    i. complex systems such as an aircraft or car should be modelled using the KIJIMA Type II GRP model, and

    ii. individual components should be modelled using the KIJIMA Type I GRP model.

h. When examining the effect on multiple q, whether representing change $q_{inspection}$ or $q_{maintenance}$, there is a significant difference in effect based on the link to the *dominant* failure mode. In this circumstance, the *dominant* failure mode is the one that results in the most renewals. Specifically slight variations to the *dominant* failure mode will have comparatively larger impact on the CIF curve. Therefore, any resources (i.e. personnel and/or funding) consideration should be assigned to "fixing" the *dominant* failure mode.

Chapter 7: Examples

Introduction

The original intent of this research was to examine real Repairable Item (RI) data from the Defence aviation environment. Unfortunately, it is very difficult to get the life of a single RI (e.g. serial number) from the current Maintenance Management System, a common problem within the aviation industry. That said, some data has been obtained for components. Due to the number of cases it is impossible to demonstrate the output from the model, and therefore a representative sample will be shown for illustrative purposes. The following cases will be used to illustrate the process:

1. Case 1A – 2 sets of data from USS *Grampus* and USS *Halfbeak* Number 4 Main Propulsion Diesel Engine from MEEKER and ESCOBAR[78];
2. Case 4A (Single Failure Mode) – 2 sets of data representing Serial No 1244 and Serial No 10484 for Valve Housings (Part No 710085-1), from 1 of the 4 Allison T56A-14 turbo-propeller engines of the Lockheed P-3C Orion Maritime Patrol aircraft.
3. Case 4A (2 Failure Modes) – simulated data for use in this model.

[78] ibid

<u>Case 1A Solution – USS Grampus</u>

Background

Given the challenge with access to data, alternative sources of data were required. Consequently RI from the commonly quoted repairable item data source, USS *Grampus* and USS *Halfbeak* Number 4 Main Propulsion Diesel Engine from MEEKER and ESCOBAR[79], were used as the input data for a Case 1A (single FM, Instantaneous Repair, Perfect Inspection). To allow comparison of the model, the parameter estimator use the first two thirds of the data set, while the simulator predicted the whole data set. A copy of the USS *Grampus* and USS *Halfbeak* Number 4 Main Propulsion Diesel Engine is provided at Appendix 1 – Case 1A Data.

Parameter Estimation

The estimator was run for 5,000 iterations with an interleave value of 5 resulting in 1,000 parameter sets of α, β and q. An initial guess of α = 1, β = 1and q = 0.5 was used. The results from the parameter estimator for α, β and q, including the variation over their individual space, can be seen in Figure 52 and Figure 53.

---

[79] ibid

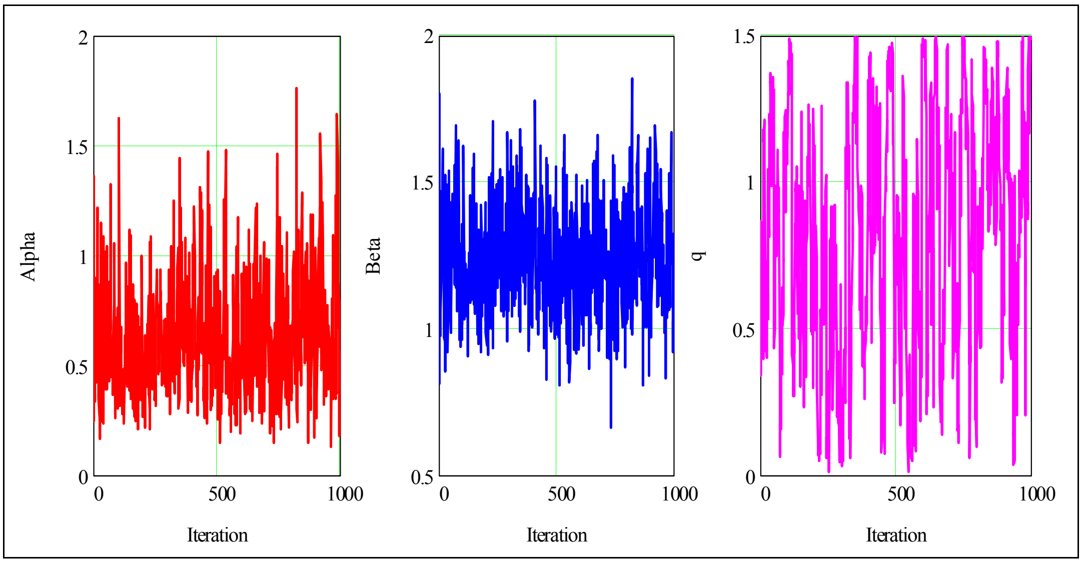

Figure 52: Variation in Parameter Set for USS Grampus (Case 1A)

Of specific interest the results from the parameter estimator α, β and q were converted to illustrate the areas of highest likelihood for each of the parameters as shown in Figure 54.

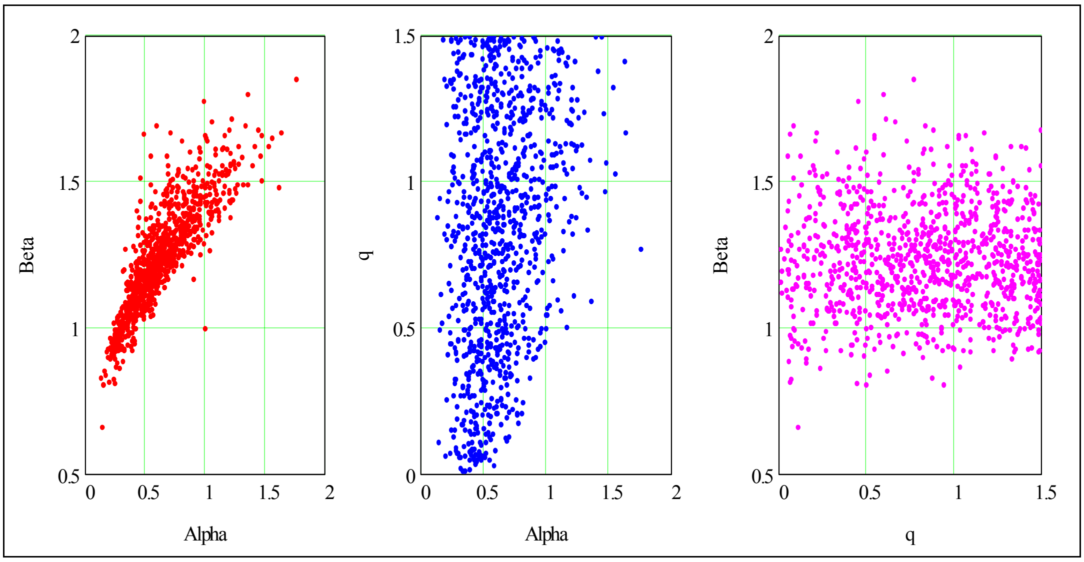

Figure 53: Parameter Set for USS Grampus (Case 1A)

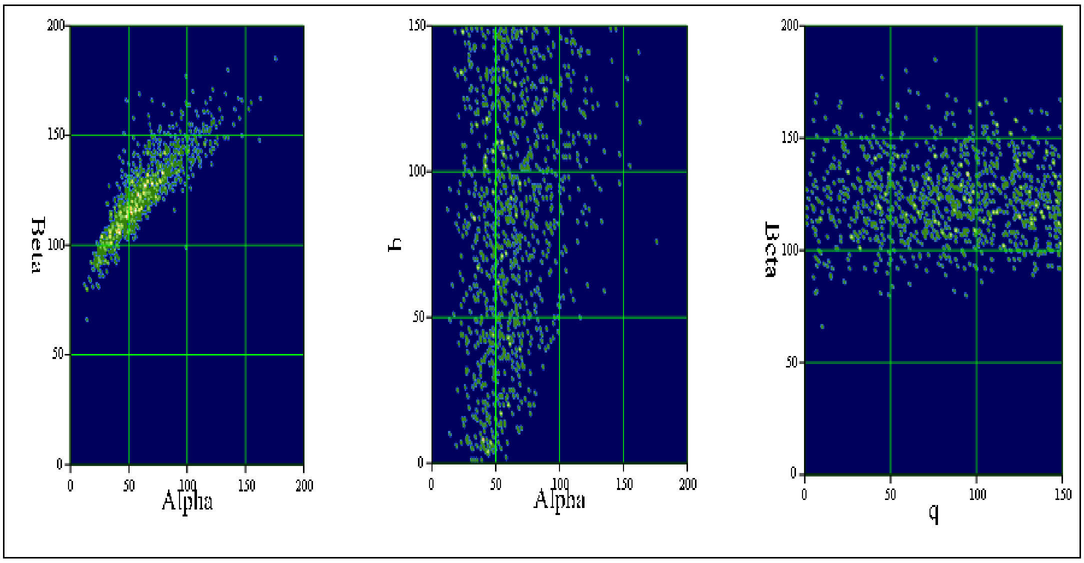

Figure 54: Parameter Set for USS Grampus (Case 1A)

As part of the results from the parameter estimator for α, β and q each of the parameters were assumed to be normally distributed and a mean and standard deviation calculated including Pearson's r correlation coefficient. The resulting values are provided in Table 15.

Additionally, for comparative purposes the data provided at Appendix 1 – Case 1A Data was also analysed using an ORP (2-parameter Weibull model) and NHPP (Power Law model). These values are also provided in Table 15.

Parameter	KIJIMA Type I GRP Equation			ORP (2-parameter Weibull)	NHPP (Power Law)
	Mean	Standard Deviation	Pearson's r Correlation Coefficient		
α	0.631	0.263	0.09	0.553	0.418
β	1.237	0.178	0.018	1.22	1.088
q	0.828	0.409	0.188	n/a	n/a

Table 15: Summary of Parameter Estimators for USS *Grampus* Data

CIF Simulation

Each of set from the parameter estimator were then simulated 100 times and the averages recorded resulting in 1,000 CIF curves. The 1,000 CIF curves were then averaged to find the average CIF curve for all parameter sets, and the non-parametric 90 percentile upper and lower confidence limits. The resulting CIF curve is provided at Figure 55.

As can been seen from Figure 55, the results accurately predict the additional five5 data points, and the non-parametric 90 percentile upper and lower confidence limits effectively bound the simulated data.

Case 1A Solution – USS Halfbeak

Background

Given the problems encountered with access to data, alternative sources of data were required. Consequently RI from the commonly quoted repairable item data source, USS *Halfbeak* Number 4 Main Propulsion Diesel Engine from MEEKER and ESCOBAR[80], was used as the input data for a Case 1A (single FM, Instantaneous Repair, Perfect Inspection). To allow comparison of the model to the data the first two thirds of the data set was used by parameter estimator, while the simulator predicted the whole data set. A copy of the USS *Halfbeak* Number 4 Main Propulsion Diesel Engine is provided at Appendix 1 – Case 1A Data.

---

80 MEEKER, W.Q. and ESCOBAR, L.A., Statistical Methods for Reliability Data, Wiley-Interscience, USA, 1998

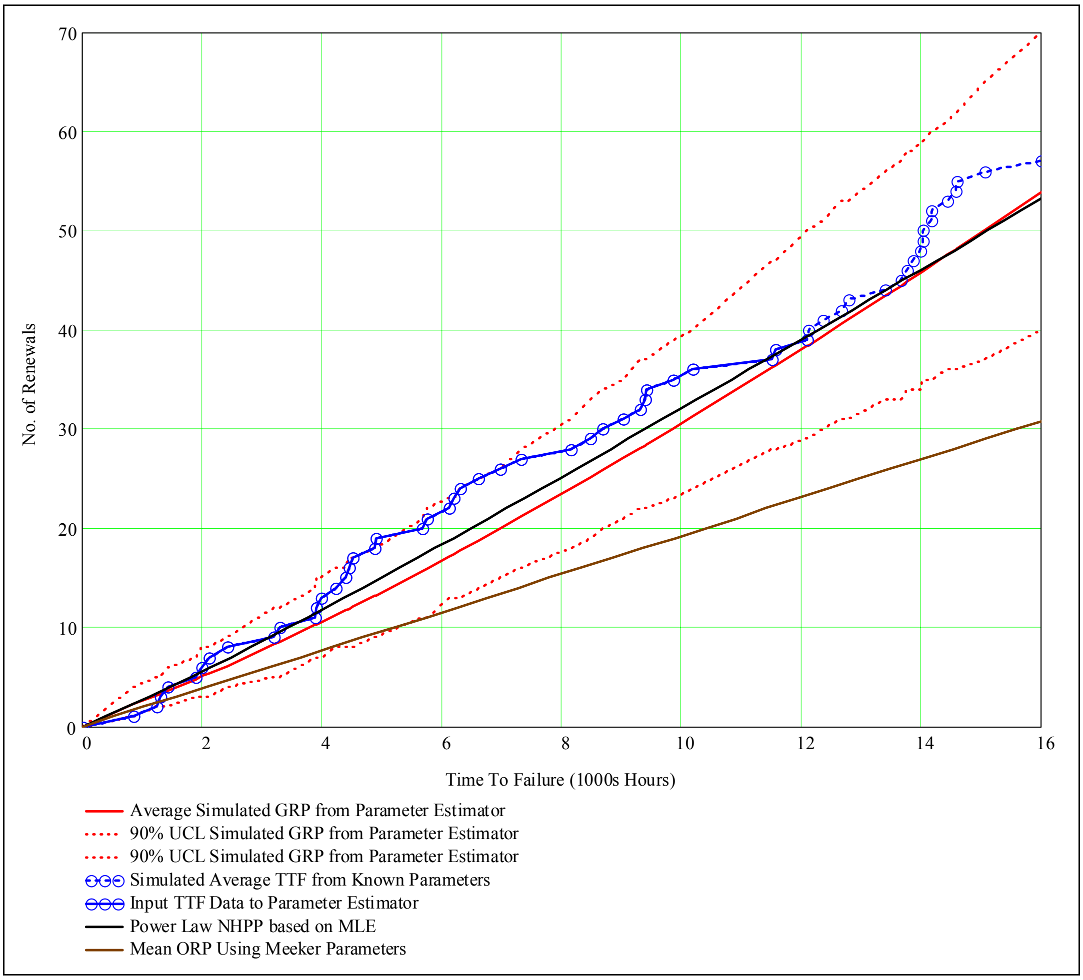

Figure 55: CIF Curve for USS *Grampus* (Case 1A)

Parameter Estimation

The estimator was run for 1,000 iterations with an interleave value of 1 resulting in 1,000 parameter sets of α, β and q. An initial guess of $\alpha = 1$, $\beta = 1$and $q = 0.5$ was used. The results from the parameter estimator for α, β and q, including the variation over their individual space can be seen in Figure 56 and Figure 57.

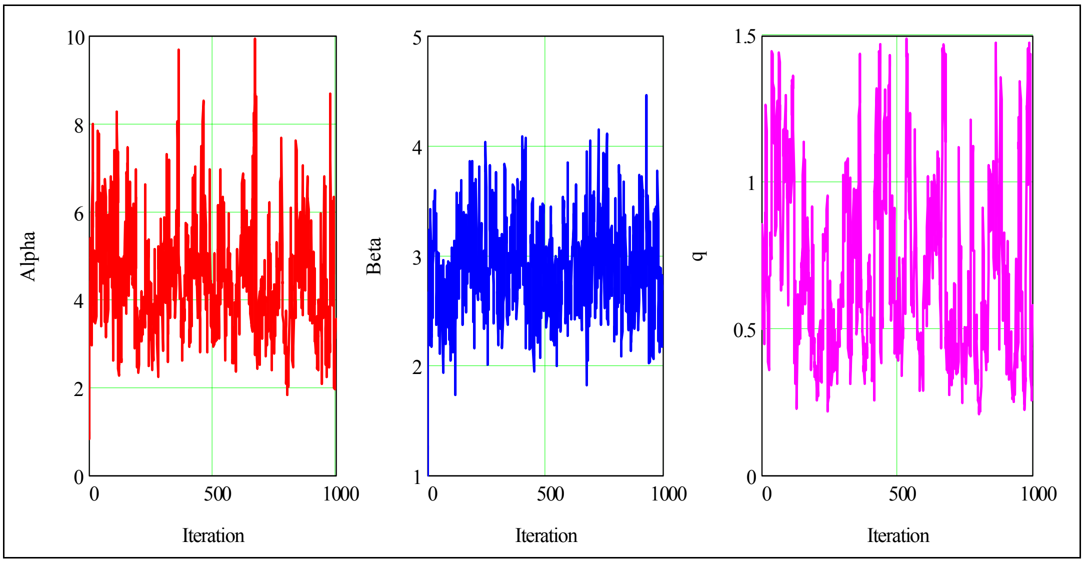

Figure 56: Variation in Parameter Set for USS *Halfbeak* (Case 1A)

Of specific interest the results from the parameter estimator for α, β and q were converted to illustrate the areas of highest likelihood for each of the parameters as shown in Figure 57.

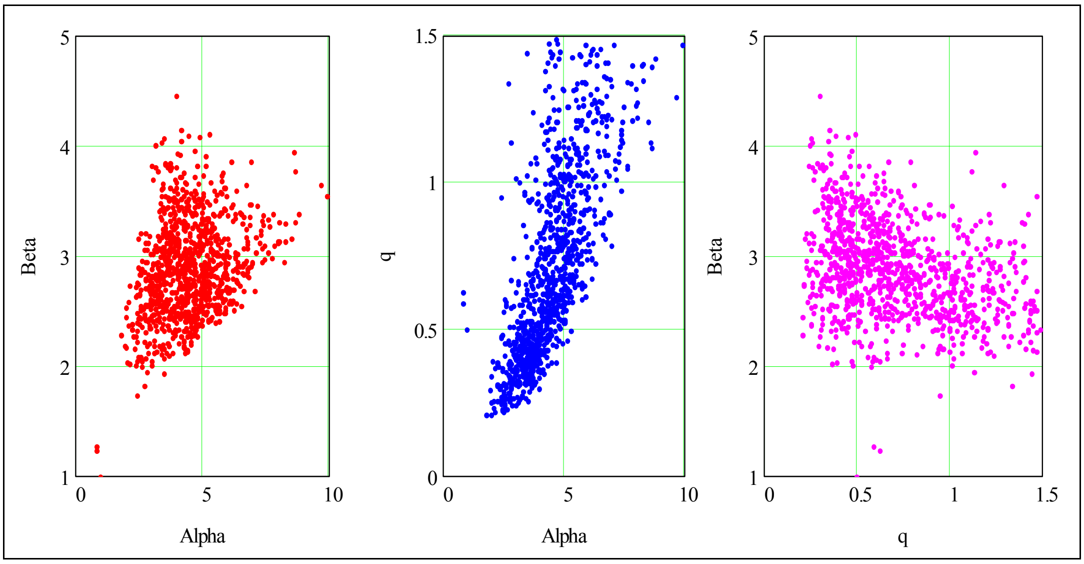

Figure 57: Parameter Set for USS *Halfbeak* (Case 1A)

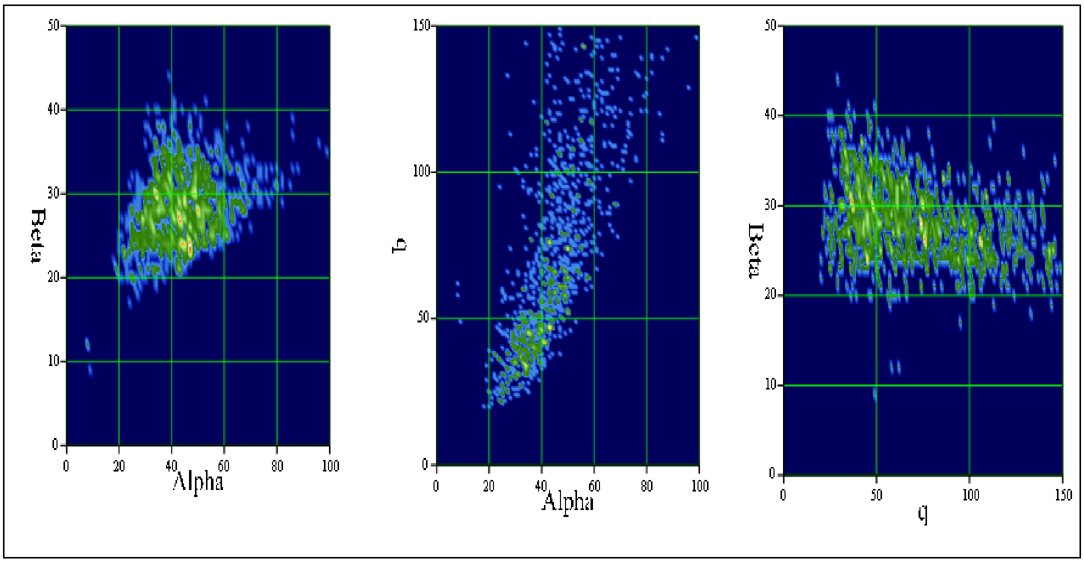

Figure 58: Parameter Set for USS *Halfbeak* (Case 1A)

As part of the results from the parameter estimator for α, β and q each of the parameters were assumed to be normally distributed and a mean and standard deviation calculated including Pearson's r correlation coefficient. The resulting values are provided in Table 16.

Additionally, for comparative purposes the data provide at Appendix 1 – Case 1A Data was also analysed using an ORP (2-parameter Weibull model) and NHPP (Power Law model). These values are also provided in Table 16.

Parameter	KIJIMA Type I GRP Equation			ORP (2-parameter Weibull)	NHPP (Power Law)
	Mean	Standard Deviation	Pearson's r Correlation Coefficient		
α	4.48	1.26	-0.1	5.45	5.362
β	2.881	0.435	0.025	2.76	2.717
q	0.71	0.316	-0.108	n/a	n/a

Table 16: Summary of Parameter Estimators for USS *Halfbeak* Data

CIF Simulation

Each of set from the parameter estimator were then simulated 100 times and the averages recorded, resulting in 10,000 CIF curves. The 10,000 CIF curves were then averaged to find the average CIF curve for all parameter sets, and the non-parametric ninety percentile upper and lower confidence limits. The resulting CIF curve is provided at Figure 59.

As can been seen from Figure 59, the results accurately predict the additional 5 data points, and the non-parametric ninety percentile upper and lower confidence limits effectively bound the simulated data.

Comparison of Case 1A Results from USS Grampus vs USS Halfbeak

One area of interest was the comparison of the results from the parameter estimation, specifically the q value from any real data. The value and trend over time of q highlights a number interesting outcomes. For example, the ability to compare and contrast the parameter estimator values from identical repairable items (i.e. same part number but different serial number) may be able to predict future changes due to various factors such as location (i.e. temperature, humidity, etc), maintenance facility/staff, maintenance tools/manuals/procedures, incorporation of a design change/modification, mission profile, etc.

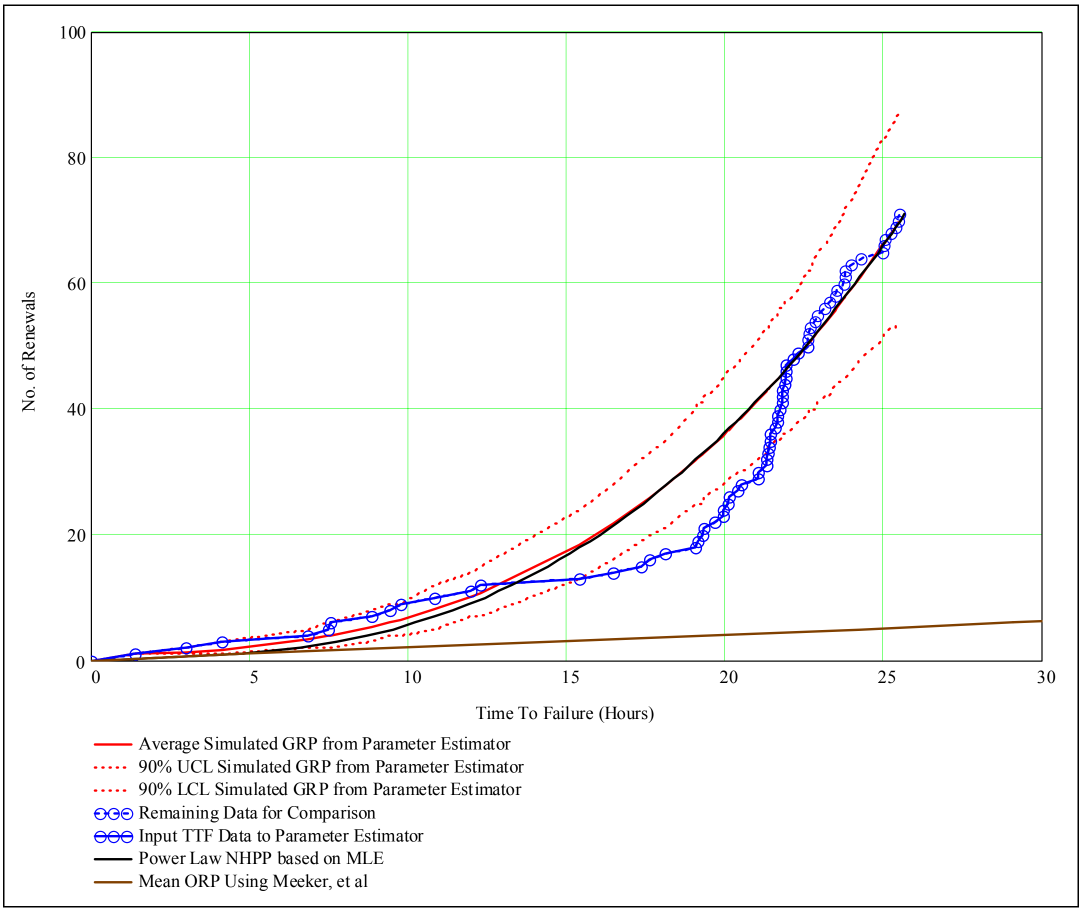

Figure 59: CIF Curve for USS Halfbeak (Case 1A)

Based on the assumption that the uncertainty in the actual values of α, β and q are normally distributed it was possible to compare the various GRP parameters previously listed in Table 15 and Table 16 as shown in Figure 60, Figure 61 and Figure 62. Additionally, the ORP and NHPP parameter estimations provided in Table 15 and Table 16 as shown in Figure 60 and Figure 61.

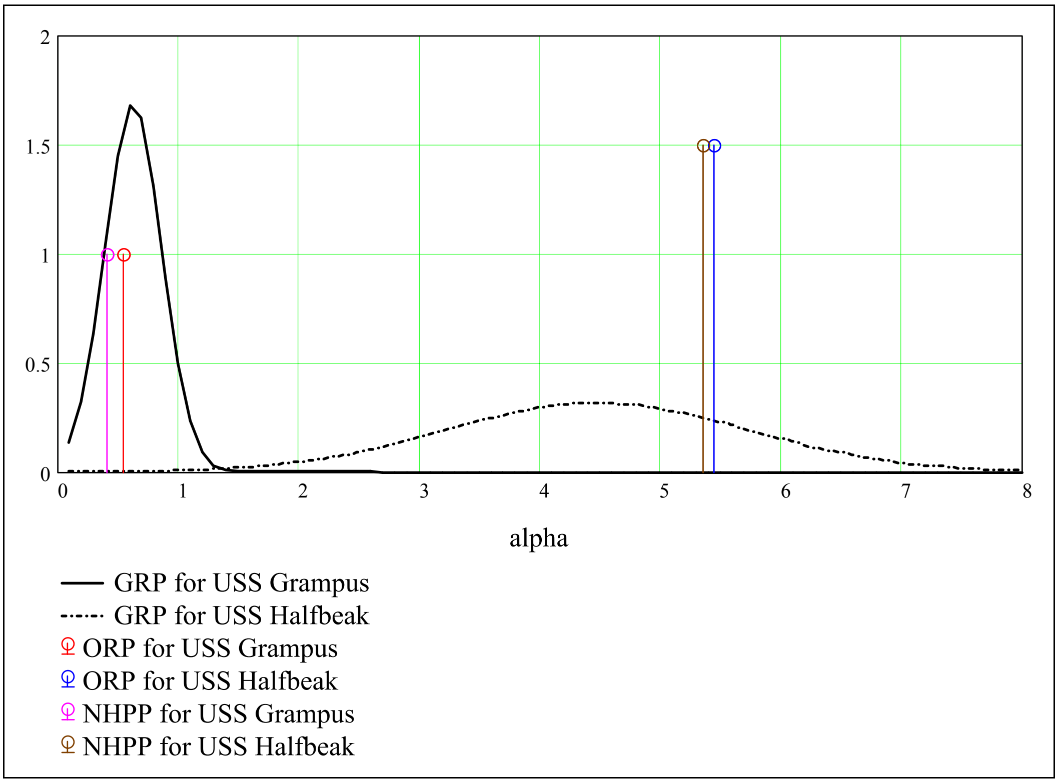

Figure 60: Comparison of α for USS *Grampus* & USS *Halfbeak*

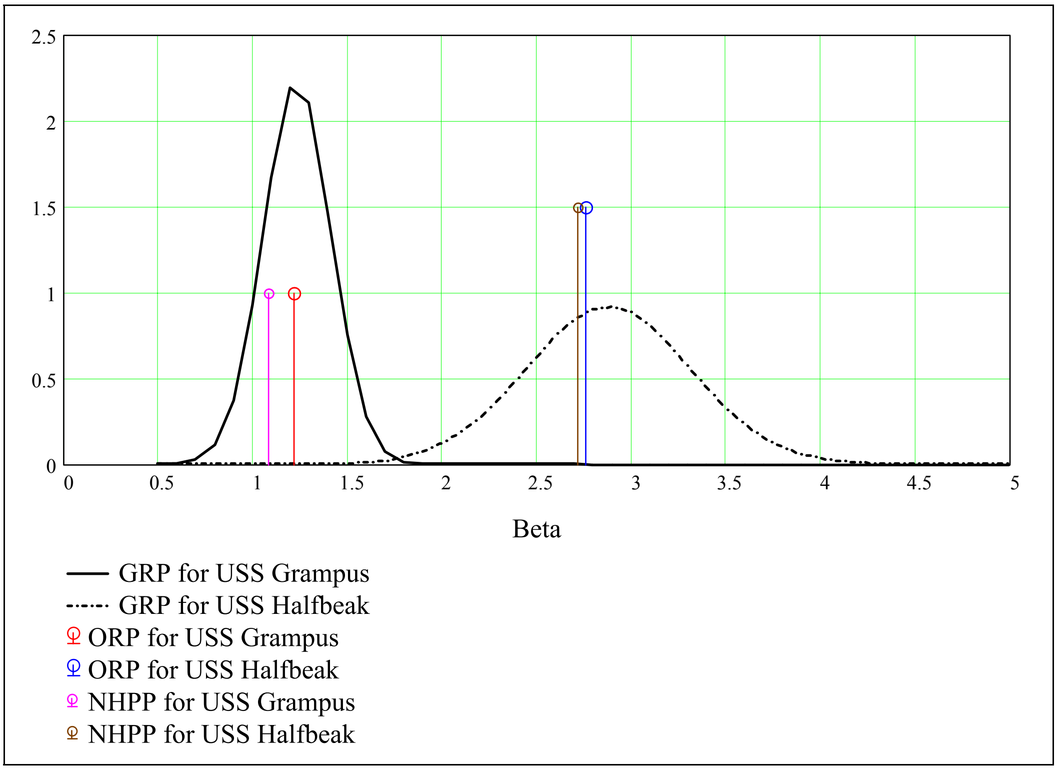

Figure 61: Comparison of β for USS *Grampus* & USS *Halfbeak*

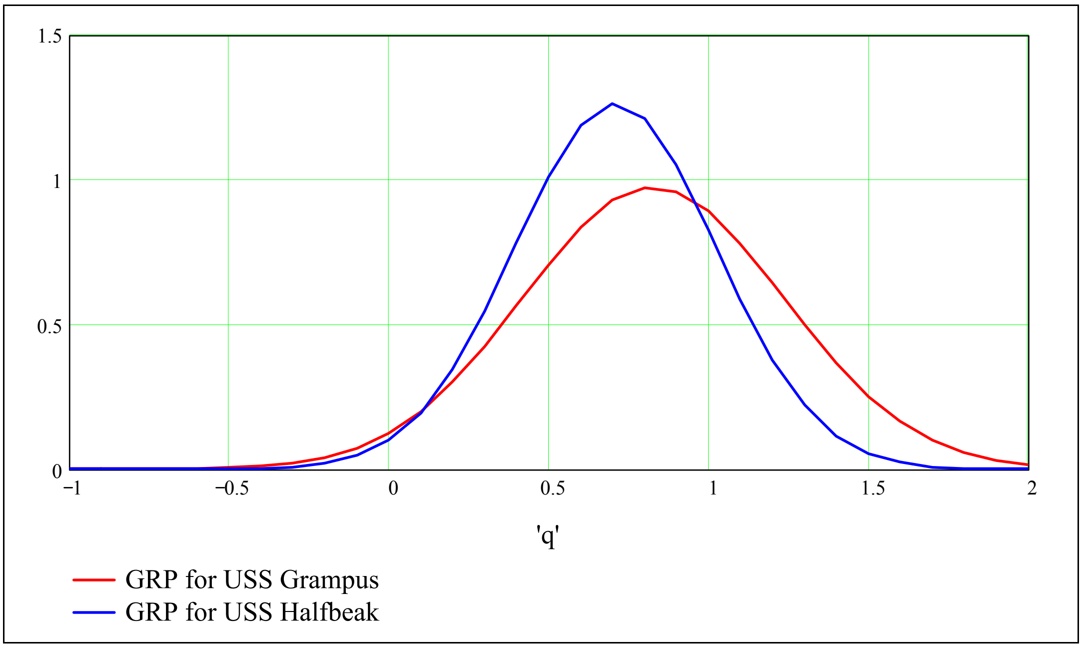

Figure 62: Comparison of 'q' for USS *Grampus* & USS *Halfbeak*

Of specific interest was the variation in q as a representative of the *goodness of repair* as shown in Figure 62.

For USS *Grampus* the q averaged 0.828 based on an initial guess of 0.5 entered into the parameter estimator and a non-informative Bayesian prior. Accordingly, the value of q close to $q = 1$ (i.e. *as-bad-as-old*) indicated that the repair to the engine does not significantly rejuvenate the engine (i.e. reduce the *Virtual Age* (VA) of the engine). However, the $\beta \approx 1$ shows a constant, if very slightly increasing failure rate.

Conversely, for USS *Halfbeak* the q averaged 0.71, again based on a guess of 0.5 and a non-informative Bayesian prior. This result and distribution can be seen in Figure 62 and leaves the impression that the maintenance effectiveness of the USS *Halfbeak* repairs were higher than for the USS *Grampus*. However, given the findings from

Chapter 6: Role of ‘q’ in Analysis of Realistic Cases (i.e. KIJIM GRP Type I is less sensitive to exact values of q for $q > 0.2$) then this difference is academic. Rather both these engines should be treated similarly. Furthermore, the key to this comparison is the value of β which varies significantly between the two systems; USS *Grampus* - $\beta =$ and USS *Halfbeak* - $\beta =$. Again the Chapter 6: Role of ‘q’ in Analysis of Realistic Cases highlighted that the KIJIMA Type I equation was very sensitive to small variation in β.

Case 4A Solution – Valve Housing (Part No 710085-1) Serial No 1244 and 10484

As part of this study various aircraft System Project Offices (the organization responsible for the sustainment of particular weapon systems) were approached for component level data. The Royal Australian Air Force (RAAF) Maritime Patrol System Project Office (MPSPO) provided the following data on the Valve Housing (Part No 710085-1), from 1 of the 4 Allison T56A-14 turbo-propeller engines of the Lockheed P-3C Orion Maritime Patrol Aircraft.

Background on Lockheed P-3C Orion Maritime Patrol Aircraft

The RAAF operates 19 Lockheed AP-3C Orion Maritime Patrol Aircraft in a variety of missions including Anti-Submarine Warfare (ASW), Anti-Surface Warfare (ASuW), Search and Survivor Supply (SASS)[81] and Surface Surveillance roles. The

[81] This differs from the more known Search and Rescue (SAR) role since being a fixed wing aircraft (in comparison with a rotary wing helicopter) the Lockheed P-3C Orion Maritime Patrol aircraft cannot actually rescue personnel.

original P-3C Orion was designed in 1960's and 1970's and the RAAF has been operating them since 1978 resulting in an average age of 23 years[82]. While the RAAF has undertaken modifications over the years, the basic aircraft has essentially remained the same. Furthermore, while the AP-3C Orion aircraft are based at RAAF Base Edinburgh in Adelaide, South Australia, they have a significant deployment schedule throughout the South Pacific, the South East Asian Archipelago and in more recent times, the Middle East. Each of these deployment regions has different climate conditions. More information on the RAAF AP-3C can be found at http://www.defence.gov.au/raaf/organisation/technology/aircraft/orion.htm.

Figure 63: Lockheed AP-3C Orion Maritime Patrol Aircraft

82 CROWLEY, C. K., 'Meeting the Ageing Aircraft Challenge – A Life Cycle Management Philosophy for Optimizing Safety, Effectiveness And Economy – From "'Lust To Dust"', University College, Australian Defence Force Academy, University of New South Wales, Canberra, September 2004, Table 1.1, pg20

Background on Valve Housing (Part No 780085-1)

The Valve Housing comprises the top part of the propeller control assembly of the Allison T56A-14 turbo-propeller engine. The Valve Housing contains the "brains" of the propeller, and is located in the top section of the propeller afterbody. It is a very complex hydro-mechanical assembly, the components of which sense the pilot's command and the propellers condition and then converts any disparity between the two into hydraulic actuation to restore the balance. The valve housing incorporates the following sub assemblies:

- Fly-weight sensing governor,
- Alpha shaft,
- Beta shaft,
- Main and standby regulator valve,
- Feather valve, and
- Backup valve.

Other functionality that is contained in the valve housing includes Engine RPM Governor, reverse blade angle control, Beta schedule, Airstart switch, Auxiliary pump cutout switch and beta light and pitchlock reset switch. A picture of the valve housing is provided at Figure 64.

The Valve Housing is considered *safety critical* since some of the consequences of the identified failure modes are assessed as *catastrophic*. Accordingly, there is prescribed preventative maintenance which, based on the current maintenance policy, is an Overhaul (OH) at 5500 Engine Hours.

Previous Data Review on Valve Housing (Part No 780085-1)

In 1982 a review of maintenance policy for the valve housing concluded that change to the maintenance policy from OH on condition to OH at 3850 engine hours was warranted. Then in 1988 the maintenance policy this was changed to OH at 4500 engine hours to align with the RAAF C130H aircraft which utilises the same engine/propeller configuration. During 1990 a request to change the lifing policy to align the valve housing with the Hub and Blade was rejected for lack of supporting data. In 1991 the Valve Housing was re-lifed twice, firstly to 5000 engine hours and then to 5500 engine hours.

Between July 1993 and July 1998 there have been 203 recorded removals of valve housings, 92 of which have been failures, 55 of which occurred in flight. Only 10 items were recorded as being removed for OH after reaching the stated maintenance OH life.

Removed for access (to the pump housing) and failure are highlighted as the two main reasons for the removal of Valve Housing which was verified by operating Squadron maintenance personnel. Of the 56% of valve housings removed and forwarded to a maintenance facility for repair, 58% were found to be still serviceable. This was attributed to the complexity of the Valve Housing and the time required to fault find. Bot of these factors have led to a perception that it is quicker and easier to remove and replace the Valve Housing when a fault is indicated. Furthermore, 22% of the Valve Housings forwarded for maintenance have actually failed; over half of these failures were attributed to electrical components and only 7% attributed to mechanical component failures.

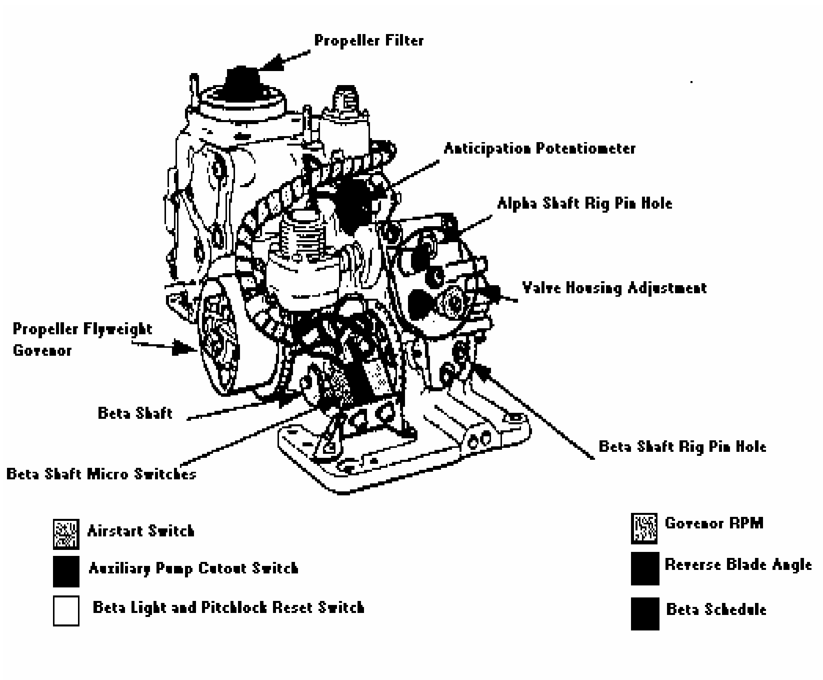

Figure 64: Valve Housing (Part No 780085-1)

Data Provided on Valve Housing (Part No 780085-1)

MPSPO provided data for 2 individual Value Housing assemblies; specifically Serial No 1244 and Serial No 10484. The Failure Logs for both components are provided at Appendix 2 – Case 4A Data for Valve Housing (Part No 710085-1) – Serial No 1244 and Appendix 3 – Case 4A Data for Valve Housing (Part No 710085-1) – Serial No 10484. The description of the various Failure Log descriptors is provided at Appendix 4 – Codes for Maintenance Management System for Case 4A Data – Valve Housing (Part No 710085-1). Additionally, MPSPO were able to provide a fleet wide

MTBF versus time based on the simple non-parametric analysis provided in Equation 55, a copy of which is provided at Figure 65.

$$MTBF = \frac{Total\_Operating\_Hours}{Total\_Failures}$$

Equation 55: MTBF Equation

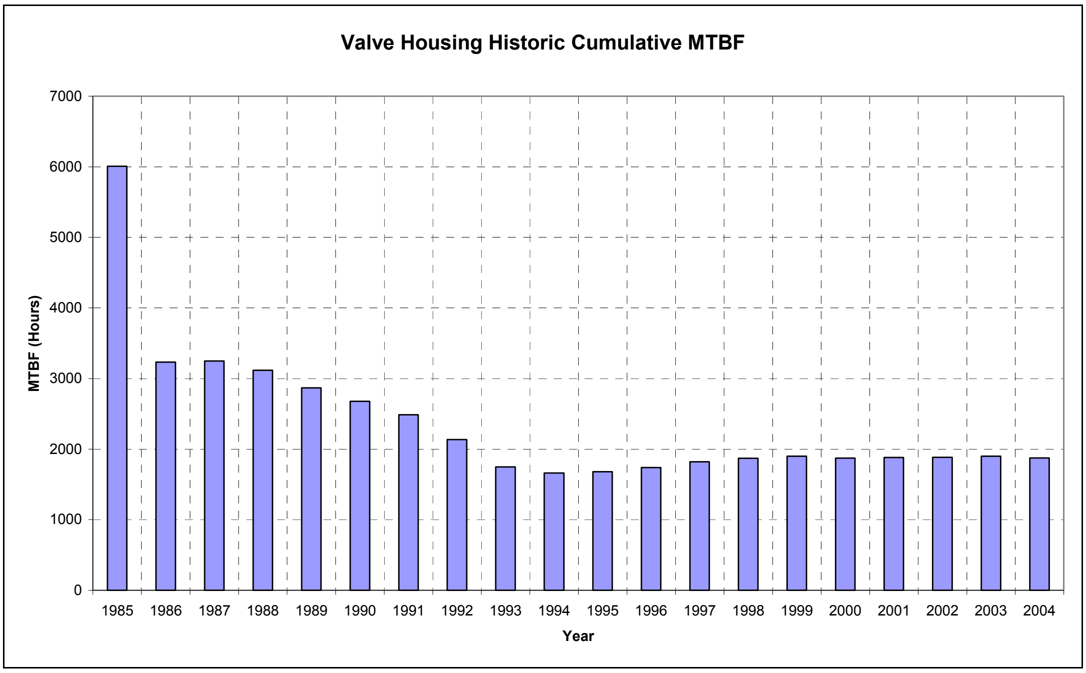

Figure 65: Valve Housing (Part No 710085-1) Historic Fleet MTBF

From this data it was also possible to calculate the 90% upper and lower Confidence Limit MTBF using the equation at Equation 56: This was completed and is attached at Figure 66.

$$MTBF_{CL} = \frac{2 \cdot T}{\chi^2_{(1-\alpha;2 \cdot r+2)}}$$

$$\begin{aligned}
&where \\
&T = Total_Operating_Hours \\
&\alpha = 1 - Confidence_Level \\
&r = Total_Failures
\end{aligned}$$

Equation 56: Percentile Confidence Limit for MTBF

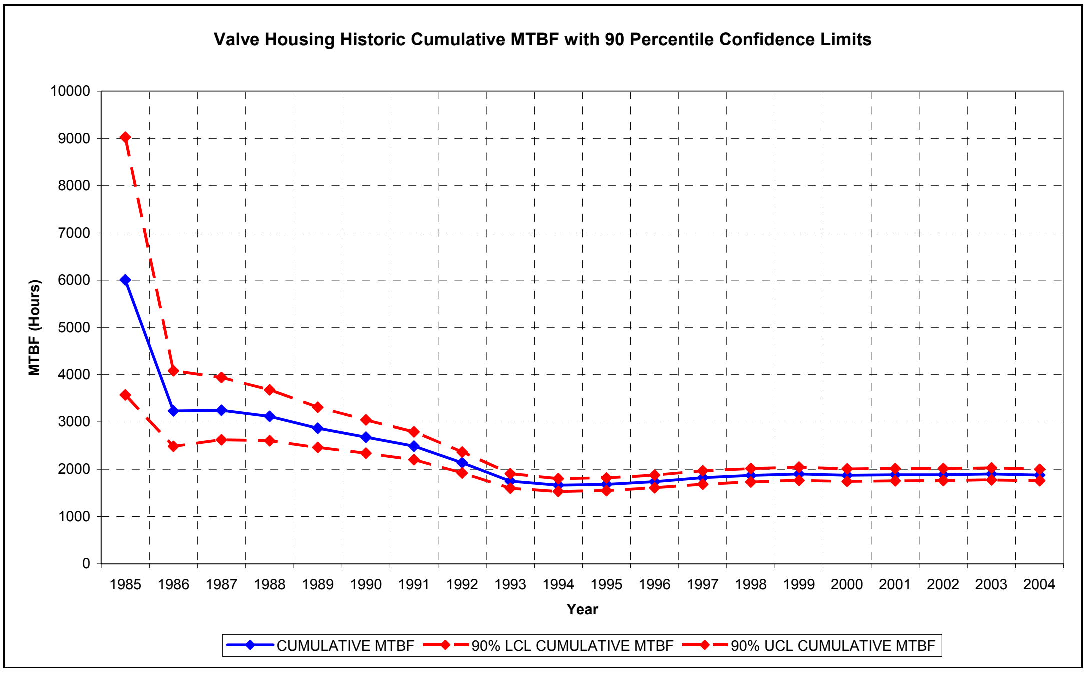

Figure 66: Valve Housing (Part No 710085-1) Historic Fleet MTBF with 90 Percentile Confidence Limits

General Principles for the Data Analysis for Valve Housing (Part No 780085-1)

To ensure consistency in the analysis of the Valve Housing data, a procedure was developed and is attached at Figure 68.

Data Analysis for Valve Housing (Part No 780085-1), Serial No 1244

Following the procedure provided at Figure 68 an analysis of Value Housing (S/No 1244) was undertaken. To allow a comparison to be made from the failure data and the future prediction capability of the method, only 8 of the 11 data points were used by the Parameter Estimator to allow the comparison from the CIF simulation with the remaining 3 data points. A CIF plot of the data for Value Housing (S/No 1244) is at Figure 67.

Data Analysis for Valve Housing (Part No 780085-1), Serial No 1244

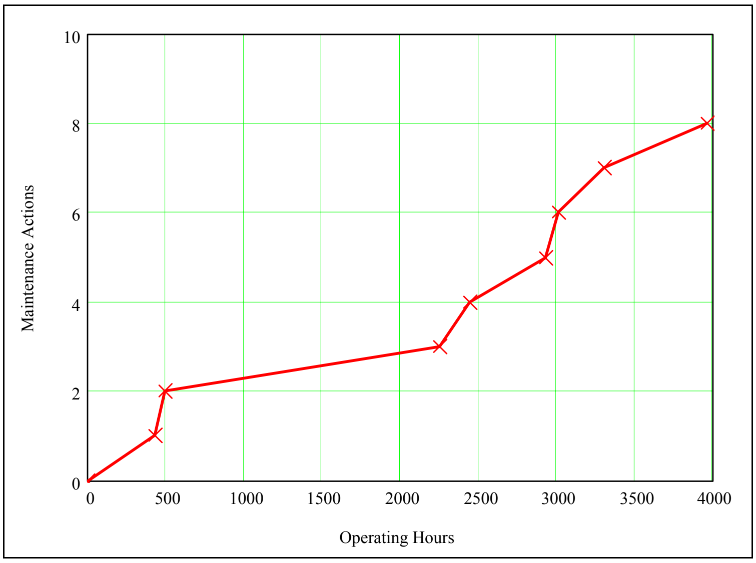

Figure 67: CIF Plot for Value Housing Serial No 1244

Step 1 – Test of Recurrence Rate Trend and Independent Interrecurrent Time (Serial No 1244)

Based on the procedure provided in paragraphs 16.5.1 and 16.5.2 of MEEKER and ESCOBAR [83] it was possible to evaluate the interrecurrent times for Value Housing (S/No 1244) for checking point-process model assumptions. This is shown through:

- Graphical review of Hours Between Maintenance Actions versus Maintenance Action as shown in Figure 69, and
- Review of Serial Correlation between adjacent interrecurrent times by plotting the Hours Between Maintenance Actions versus Lag-1 Hours Between Maintenance Actions shown in Figure 70. Additionally, it was possible to calculate *Pearson's r correlation coefficient* as a measure of the serial correlation of the Hours Between Maintenance Actions data. For Value Housing (S/No 1244) this was calculated as -0.4038.

[83] MEEKER, W.Q. and ESCOBAR, L.A., loc cit.

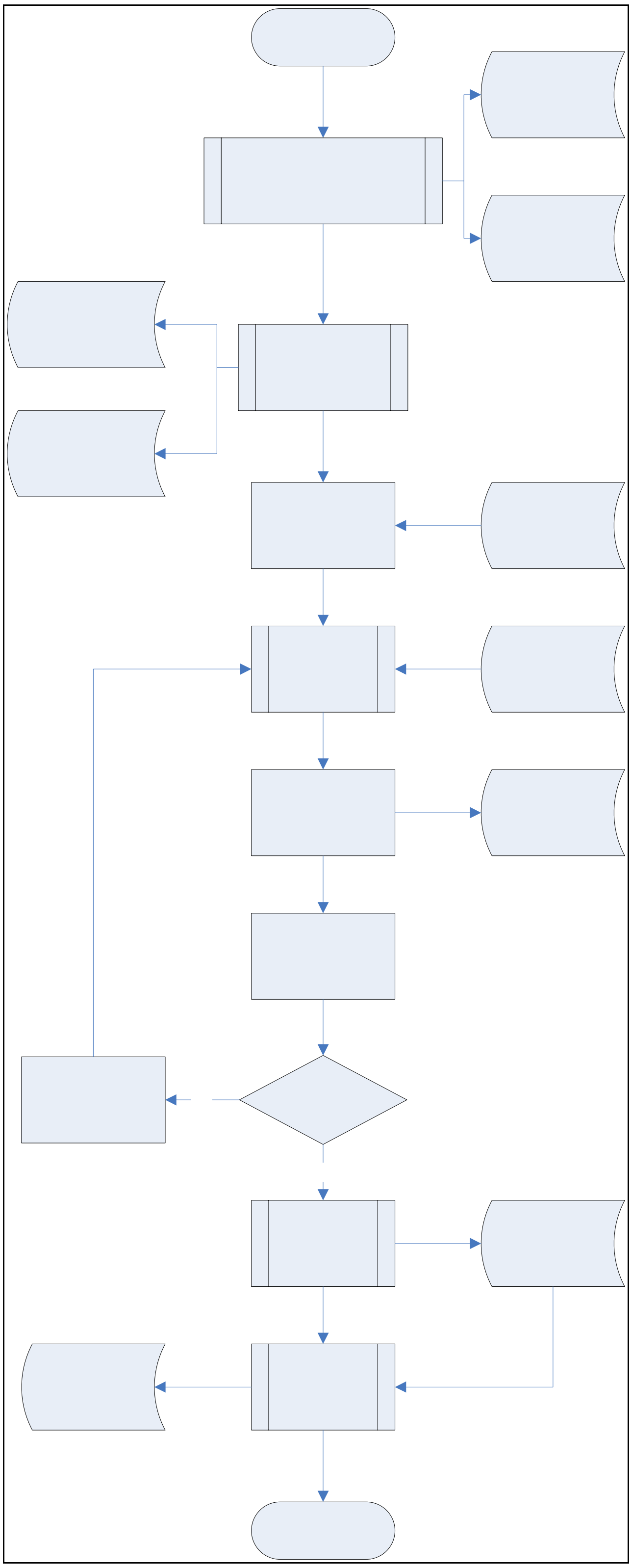

Figure 68: Case 4A Data Analysis Flowchart

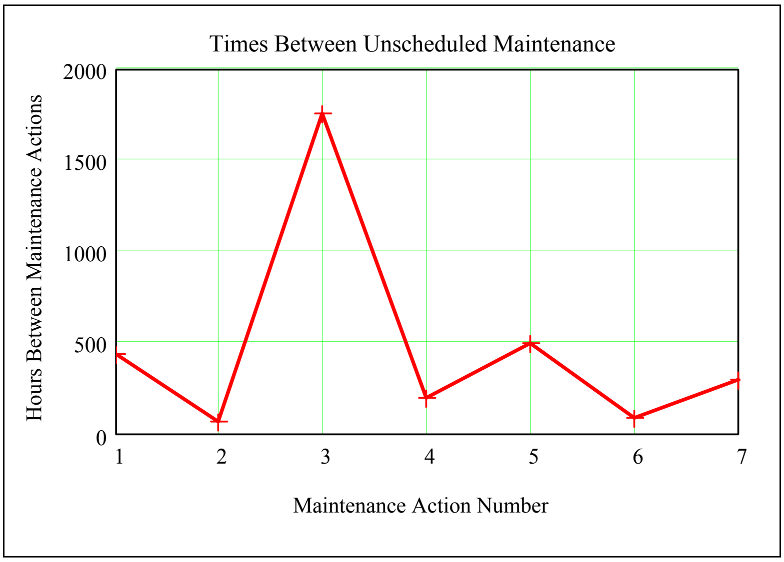

Figure 69: Hours Between Maintenance Actions versus Maintenance Action (S/No 1244)

Based on the results from Figure 69 and Figure 70 it was unclear whether the Valve Housing S/No 1244 has independent interrecurrent times. However, *Pearson's r correlation coefficient* of -0.4038 appears to indicate that there is some dependence.

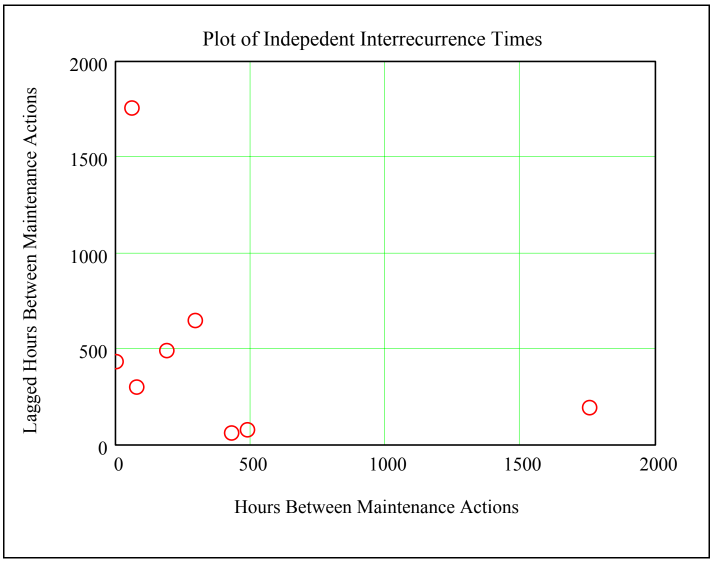

Figure 70: Hours Between Maintenance Actions versus Lag-1 Maintenance Action (S/No 1244)

Step 2 – Implementation of an ORP and NHPP Solution

Regardless of this result the implementation of an ORP and NHPP solution to the Value Housing (S/No 1244) was undertaken to help facilitate a comparison of the results of the model.

The ORP solution was based on a simple 2-parameter Weibull estimation of the failure only data, noting there was only a single OH in the data. This failure/suspension data was entered in Reliasoft Weibull++ (V5) software to estimate α and β using the Most Likelihood Estimators (MLE) option. A copy of the Weibull++ solution for Value Housing (S/No 1244) is provided at Figure 71.

Additionally, since the *Pearson's r correlation coefficient* of -0.4038 appears to indicate that there is some dependence, a HPP solution cannot to apply. Accordingly, a NHPP estimation procedure was undertaken based on MLE for α and β using the formula from MEEKER, et al[84] as shown in Equation 57 and Equation 58.

[84] MEEKER, et al, op cit, pg 413

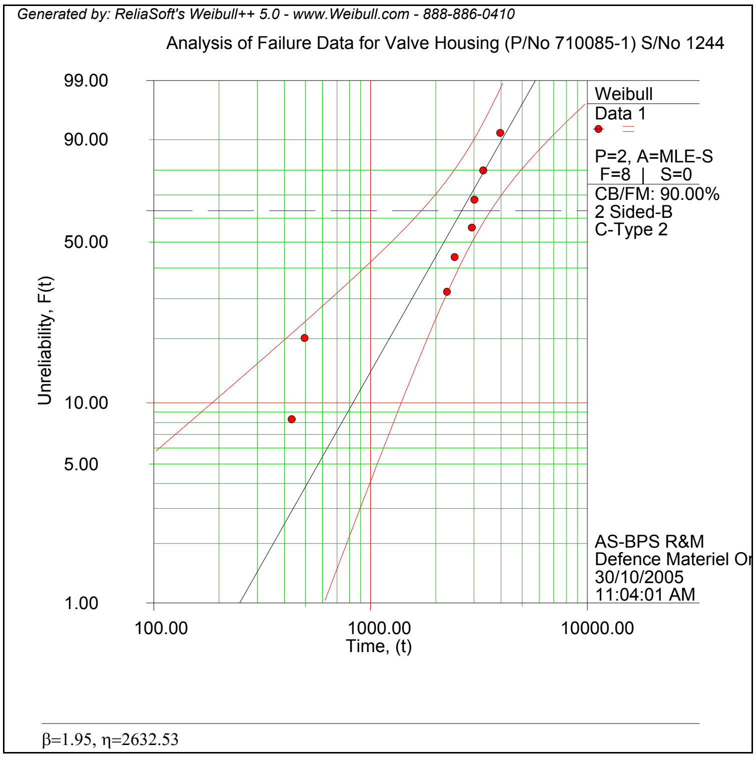

Figure 71: Weibull++ (V5) MLE of α and β for Valve Housing (S/No 1244)

$$\hat{\alpha} = \frac{t_a}{r^{\frac{1}{\hat{\beta}}}}$$

$$where$$

$$r = \sum_{j=1}^{m} d_j$$

$$d_1 \cdots d_m = non\_overlapping\_interval$$

$$t_0 = 0; t_m = t_a$$

Equation 57: MLE for α

$$\hat{\beta} = \frac{r}{\sum_{j=1}^{r} \ln\left(\frac{t_a}{t_j}\right)}$$

Equation 58: MLE for β

The results for the ordinary Renewal Process (RP) and a NHPP solution, both based on the assumption that the underlying TTF distribution is a 2-parameter Weibull are presented at Table 17.

Parameter Estimates	2-Parameter Weibull Distribution	Power Law NHPP
α	2632.53	766
β	1.95	1.184

Table 17: Parameter Estimates for α and β for Valve Housing (S/No 1244)

Based on the parameters in Table 17 it is possible to compare the model to the ORP and NHPP results through a simulated ORP and NHPP CIFs.

Step 3 – Selection of α_{min}, α_{max} and α_{guess}

Based on guidance provided in Table 7 for the selection of α_{min} and α_{max} and Table 9 for the selection of α_{guess} it was possible to select an initial boundary for α as shown in Table 18.

Parameter	Value	Rationale for selecting Value
α_{min}	1	Since the data doesn't show a lower boundary, set to the most extreme value
α_{max}	3800	Based on 2xMTBF where MTBF= α_{guess}
α_{guess}	1900	Given the Fleet MTBF versus time is constant it is possible to assume β = 1 and therefore it is possible to use α_{guess} = MTBF of the fleet data from Figure 65. Furthermore, since the point estimate MTBF, which is very close to the 90% lower confidence limit, it is possible to just use the point estimate MTBF of the fleet data from Figure 65.

Table 18: Initial Selection of α_{min}, α_{max} and α_{guess} for Valve Housing (S/No 1244)

Step 4 – Initial Run Parameter Estimator

The next step was to run the parameter estimator using the parameters from Table 18 with an Interleave = 1 for 1000 iterations providing the results in Table 19.

	Mean	Standard Deviation
α	1077	326
β	1.569	0.305
q_{PM}	0.825	0.386
q_{CM}	0.775	0.402

Table 19: Initial Run Parameter Estimator for Valve Housing (S/No 1244)

Step 5 – Review the Autocorrelation Chart and Choose Interleave Parameter Value

Based on the autocorrelation values for the data set as shown in Figure 72, an Interleave value of 20 is recommended to reduce the possible effects of autocorrelation.

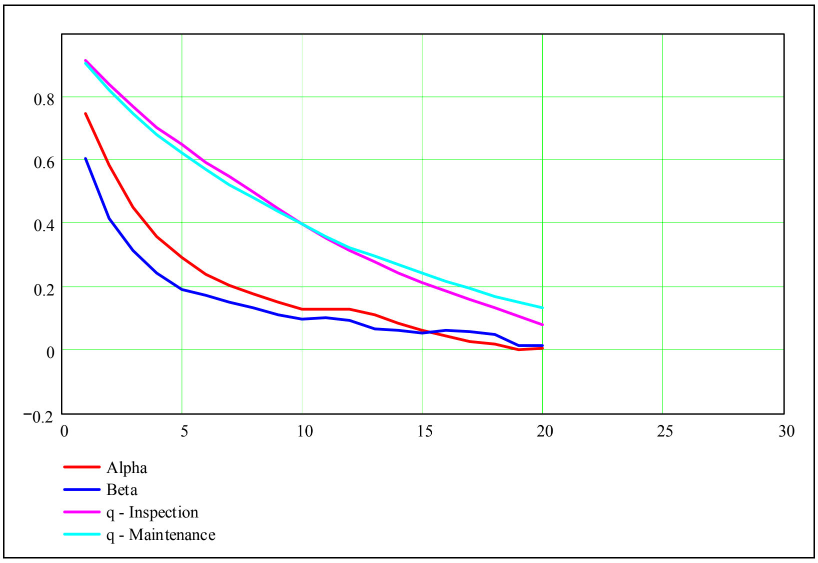

Figure 72: Autocorrelation Graph for Valve Housing (S/No 1244)

Step 6 – View α Coverage

Figure 73 shows that the initial values for α were too large and therefore they can be reduced in order to reduce computation time.

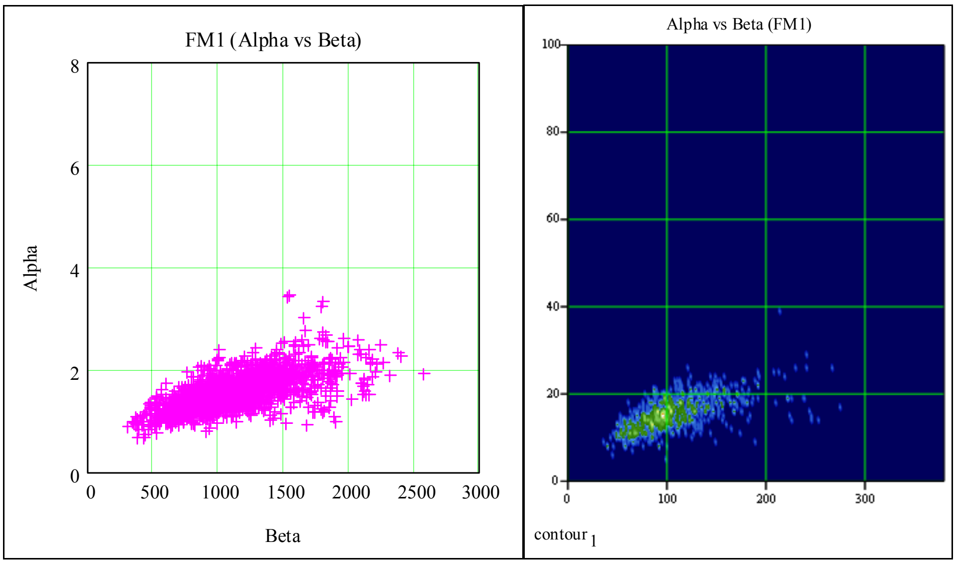

Figure 73: α Coverage for Valve Housing (S/No 1244)

Accordingly, the initial boundary for α as shown in Table 18 is modified as shown in Table 20.

Parameter	Initial Values	Extreme Left/Right Data Points from Figure 73	Value
α_{min}	1	290	200
α_{max}	3800	2581	2600
α_{guess}	1900	1100	1100
Interleave	1	n/a	20

Table 20: Final Selection of α_{min}, α_{max} and α_{guess} for Valve Housing (S/No 1244)

Step 7 – Re-run Parameter Estimator

The next step was to re-run the parameter estimator using the modified parameters from Table 20 with an Interleave = 20. As described in Chapter 4: Mathematical Set-up of Each Case the parameter estimator output's a number of sets of <α, β, q_{PM} and q_{CM}> data. This iterative nature of the results can be seen in Figure 74, Figure 75, Figure 76 and Figure 77. A statistical summary of these data sets is provided at Table 21.

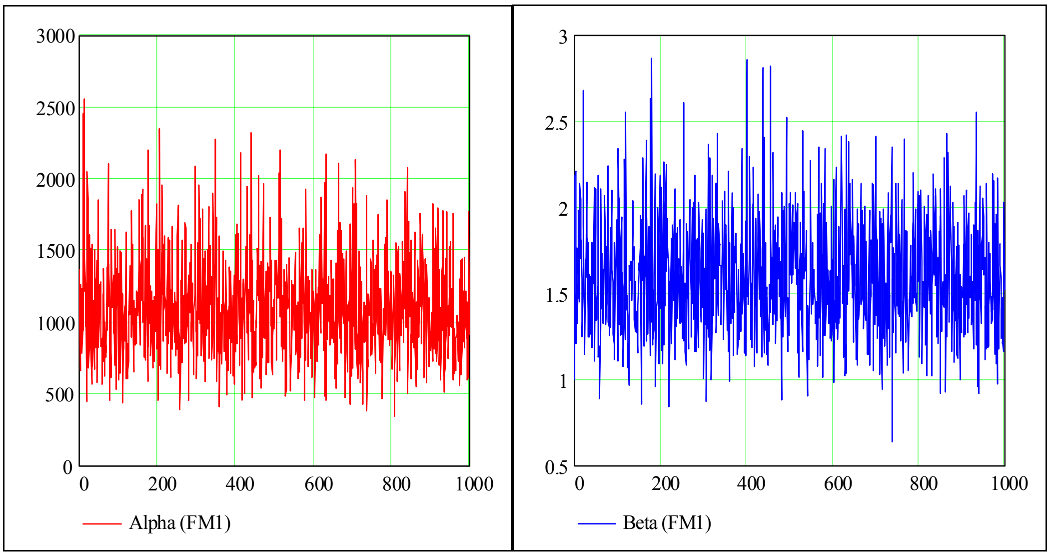

Figure 74: Iterative Variation of α and β for Valve Housing (S/No 1244)

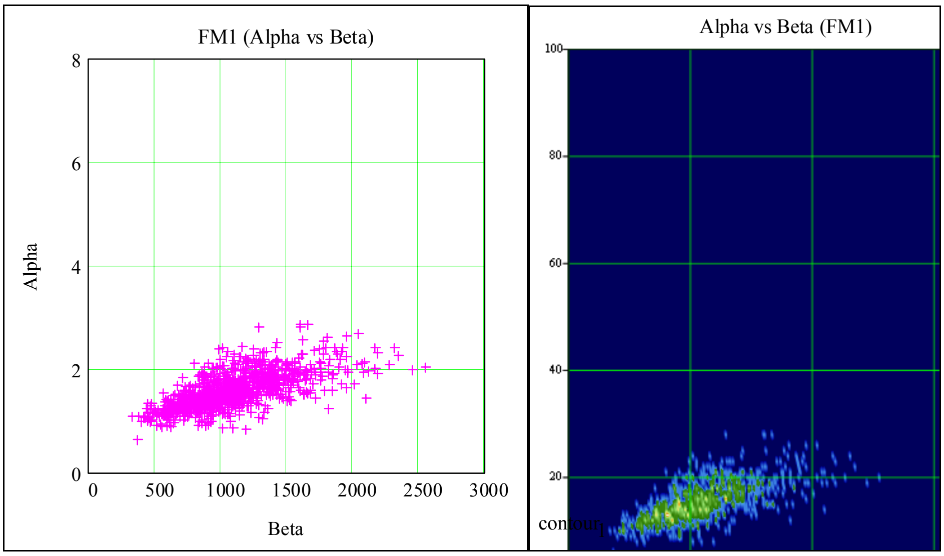

Figure 75: Iterative Variation of α versus β Graph for Valve Housing (S/No 1244)

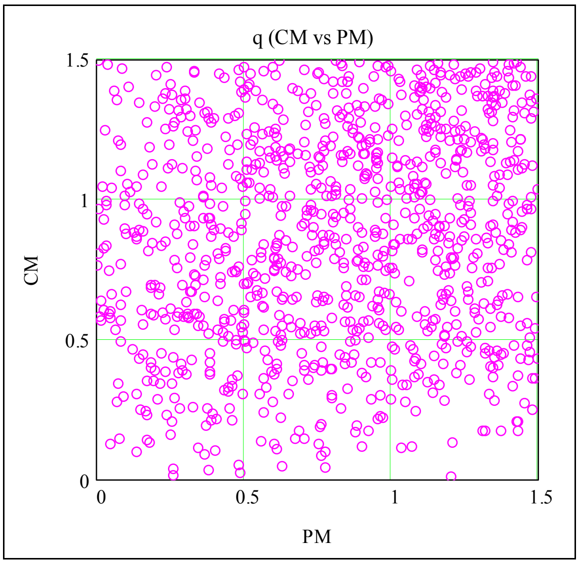

Figure 76: Iterative Variation of q_{CM} versus q_{PM} for Valve Housing (S/No 1244)

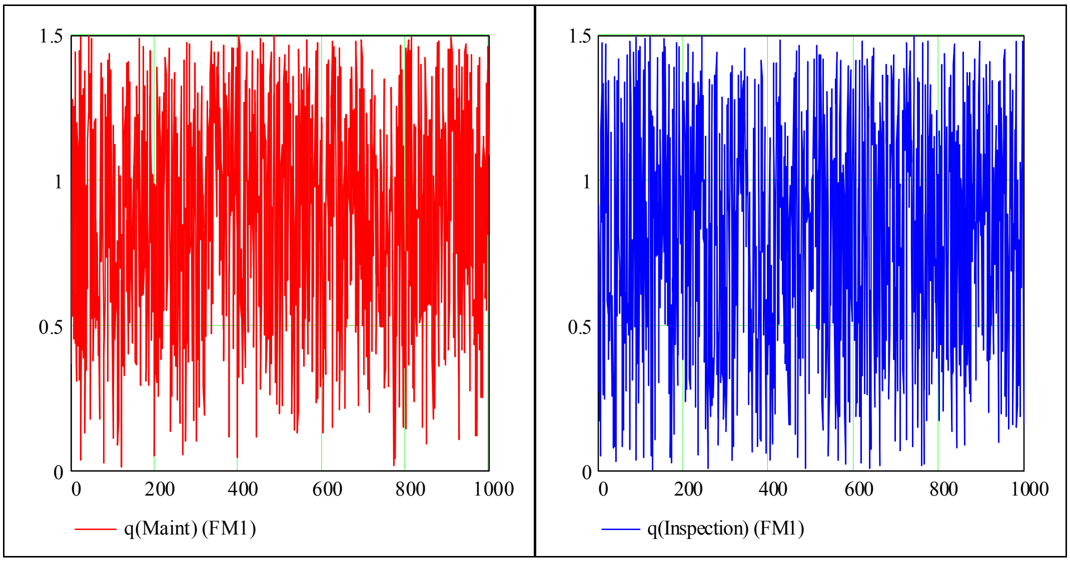

Figure 77: Iterative Variation of q_{CM} and q_{PM} for Valve Housing (S/No 1244)

	Mean	Standard Deviation
α	1096	347
β	1.587	0.339
q_{PM}	0.806	0.408
q_{CM}	0.865	0.379

Table 21: Final Run Parameter Estimator for Valve Housing (S/No 1244)

Step 8 – Re-run the CIF Simulator

Based on the number of sets of <α, β, q_{PM} and q_{CM}> data from the parameter estimator it is possible to provide a CIF curve of Valve Housing (S/No 1244), including the non-parametric 90% confidence limits. A graphical representation of the average CIF curve, including the non-parametric 90% confidence limits initial data input into the model, ORP (2-parameter Weibull) and NHPP (Power Law), is provided at Figure 78:.

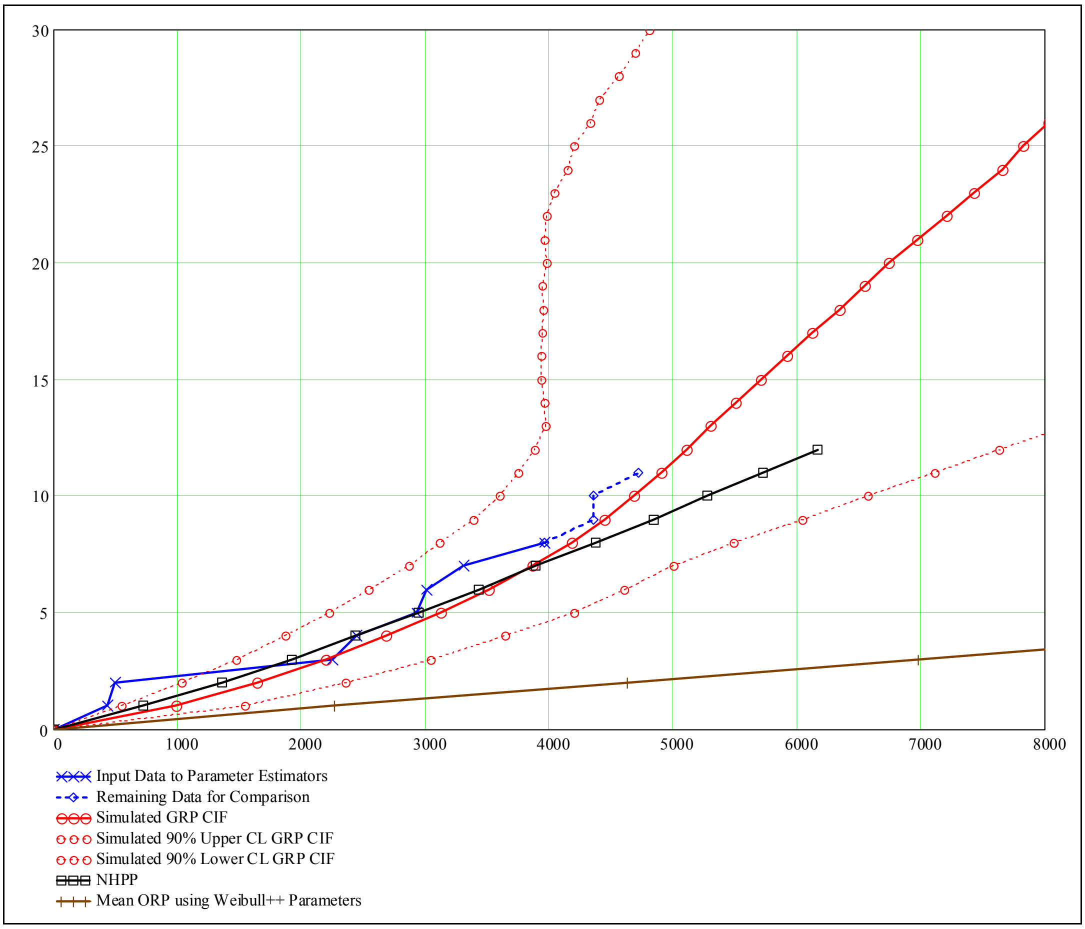

Figure 78: CIF Curve for Valve Housing Serial No 1244

As can be seen from Figure 78 the simulated GRP CIF was quite accurate in identifying the next TTFs, especially when compared to the NHPP and the RP model outcomes. Furthermore, it is interesting to observe that both the q associated with the preventative maintenance was very similar to the corrective maintenance. The value of q highlighted the fact that the repairs appear to be less effective at rejuvenating the component to a state that was only slightly better than the NHPP assumption of "*as-bad-as-old*".

Data Analysis for Valve Housing (Part No 780085-1), Serial No 10484

Following the procedure provided at Figure 68, an analysis of Value Housing (S/No 10484) was undertaken. To allow a comparison to be made from the failure data and the future prediction capability of the method, only 8 of the 9 data points were used by the Parameter Estimator to allow the comparison from the CIF simulation with the remaining data point. Unfortunately, due to the close proximity of the OH, only a single (in lieu of 3 for S/No 1244) data point could be projected. A CIF plot of the data for Value Housing (S/No 10484) is at Figure 79.

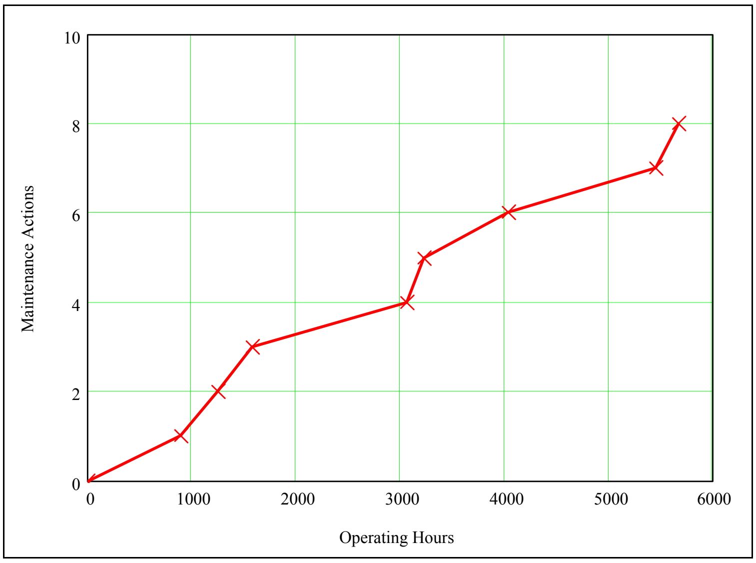

Figure 79: CIF Plot for Value Housing Valve Housing Serial No 10484

Step 1 – Test of Recurrence Rate Trend and Independent Interrecurrent Time

Based on the procedure provided in paragraphs 16.5.1 and 16.5.2 of MEEKER et al[85] it was possible to evaluate the interrecurrent times for Valve Housing (S/No 10484) for checking point-process model assumptions. This is shown through:

---

85 ibid

- Graphical review of Hours Between Maintenance Actions versus Maintenance Action as shown in Figure 80, and
- Review of Serial Correlation between adjacent interrecurrent times by plotting the Hours Between Maintenance Actions versus Lag-1 Hours Between Maintenance Actions shown in Figure 81. Additionally it was possible to calculate *Pearson's r correlation coefficient* of the Hours Between Maintenance Actions data. For Valve Housing (S/No 10484) this was calculated as –0.5399.

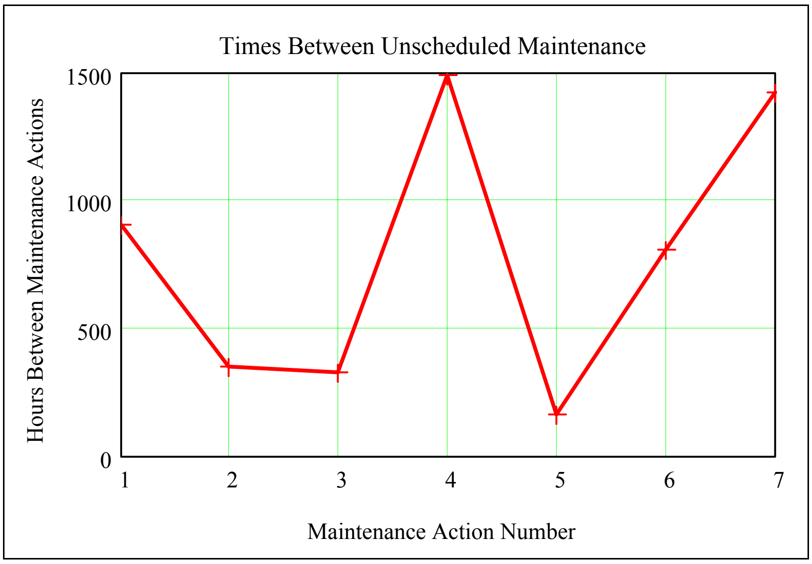

Figure 80: Hours Between Maintenance Actions versus Maintenance Action (S/No 10484)

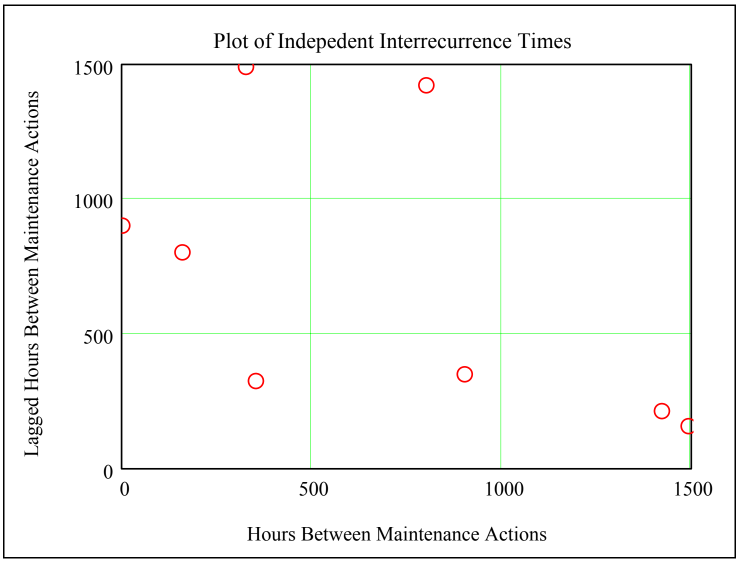

Figure 81: Hours Between Maintenance Actions versus Lag-1 Maintenance Action (S/No 10484)

Based on the results from Figure 80 and Figure 81 it was unclear whether the Valve Housing S/No 10484 has independent interrecurrent times. However, *Pearson's r correlation coefficient* of –0.5399 appears to indicate that there is some dependence.

Step 2 – Implementation of an ORP and NHPP Solution

Notwithstanding this result the implementation of an ORP and NHPP solution to the Valve Housing (S/No 10484) was undertaken to help facilitate discussion of the results of the model.

The ORP solution was based on a simple 2-parameter Weibull estimation of the failure only data, noting there was only a single OH in the data. This data was entered in Reliasoft Weibull++ (V5) software to estimate α and β using the MLE option. A copy of the Weibull++ solution for Value Housing (S/No 10484) is provided at Figure 82.

Additionally, since the *Pearson's r correlation coefficient* of –0.5399 appears to indicate that there is some dependence, a HPP solution cannot be used to analyse this data. Accordingly, a NHPP estimation procedure was undertaken based on MLE for α and β provided in paragraphs 15.2.1 and 15.2.2 of MEEKER et al[86] as shown in Equation 57 and Equation 58. The results are presented at Table 22.

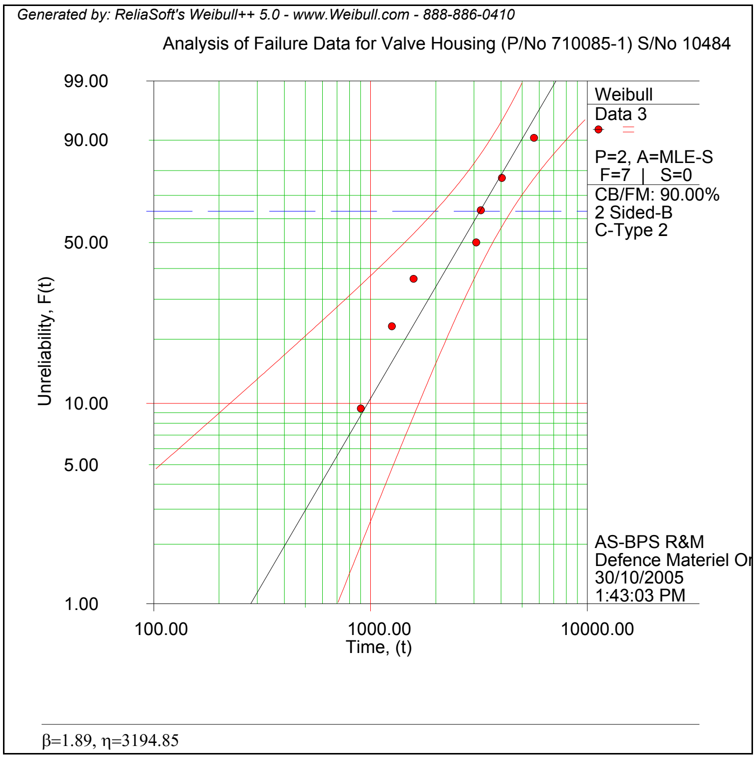

Figure 82: Weibull++ (V5) MLE of α and β for Valve Housing (S/No 10484)

86

Parameter Estimates	2-Parameter Weibull Distribution	Power Law NHPP
α	3194.85	1028.6
β	1.89	1.139

Table 22: Parameter Estimates for α and β for Valve Housing (S/No 10484)

Based on these the parameters in Table 22 it was possible to compare the model to the RP and NHPP results through a simulated RP and NHPP CIFs.

Step 3 – Selection of $\alpha_{min,}$ α_{max} and α_{guess}

Based on guidance provided in Table 7 for the selection of α_{min} and α_{max} and Table 9 for the selection of α_{guess} it was possible to select an initial boundary for α. This initial analysis was the same as conducted for Serial No 10484 as shown in Table 18. Accordingly, Table 18 data was also used as the initial boundary for α for Serial No 10484.

Step 4 – Initial Run Parameter Estimator

The next step was to run the parameter estimator using the parameters from Table 18 with an Interleave = 1 providing the results in Table 23.

	Mean	Standard Deviation
α	1544	442
β	1.825	0.468
q_{CM}	0.392	0.375
q_{PM}	0.836	0.386

Table 23: Initial Run Parameter Estimator for Valve Housing (S/No 10484)

Step 5 – Review the Autocorrelation Chart and Choose Interleave Parameter Value

Based on the autocorrelation values for the data set as shown in Figure 83, an Interleave value of 20 is recommended to reduce the possible effects of autocorrelation.

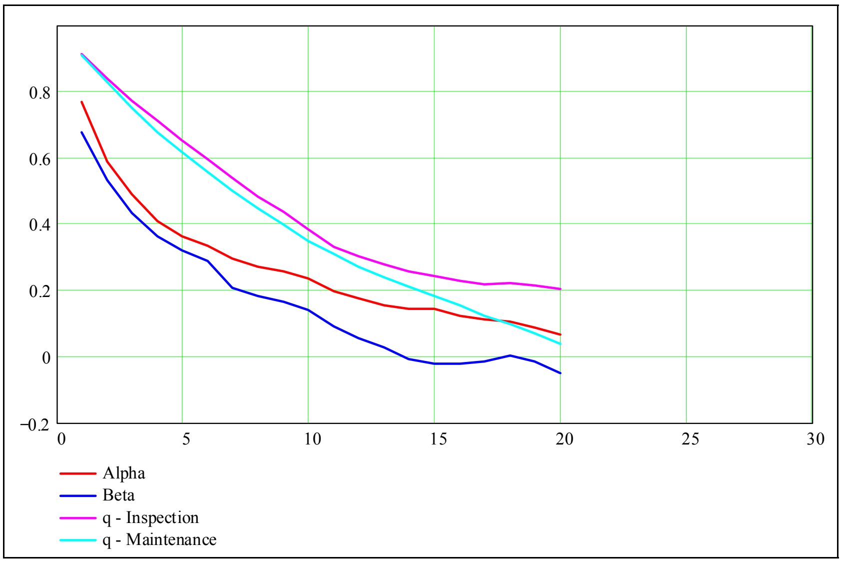

Figure 83: Autocorrelation Graph for Valve Housing (S/No 10484)

Step 6 – View α Coverage

Figure 84 shows that the initial values for α were too large and therefore they can be reduced in order to reduce computation time.

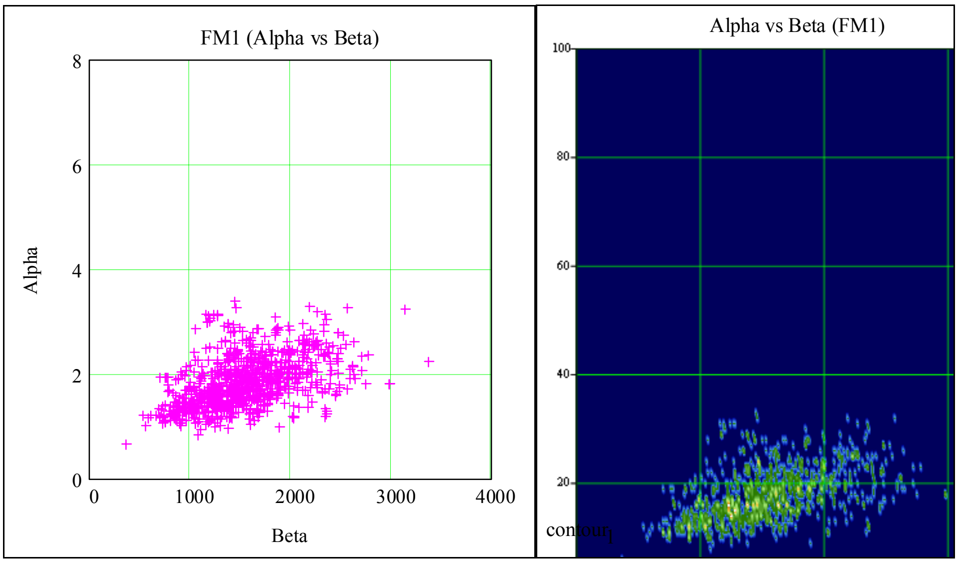

Figure 84: α Coverage for Valve Housing (S/No 10484)

Accordingly, the initial boundary for α as shown in Table 18 was modified as shown in Table 24.

Parameter	Initial Values	Extreme Left/Right Data Points from Figure 84	Value
α_{min}	1	377	350
α_{max}	3800	3378	3400
α_{guess}	1900	1544	1544
Interleave	1	n/a	20

Table 24: Final Selection of α_{min}, α_{max} and α_{guess} for Valve Housing (S/No 10484)

Step 7 – Re-run Parameter Estimator

The next step was to re-run the parameter estimator using the modified parameters from Table 24 with an Interleave = 20. As described in Chapter 4: Mathematical Set-up of Each Case the parameter estimator output a number <α, β, q_{PM} and q_{CM}> data sets. This iterative nature of the results can be seen in Figure 85, Figure 86,

Figure 87 and Figure 88. A statistical summary of these data sets is provided at Table 25.

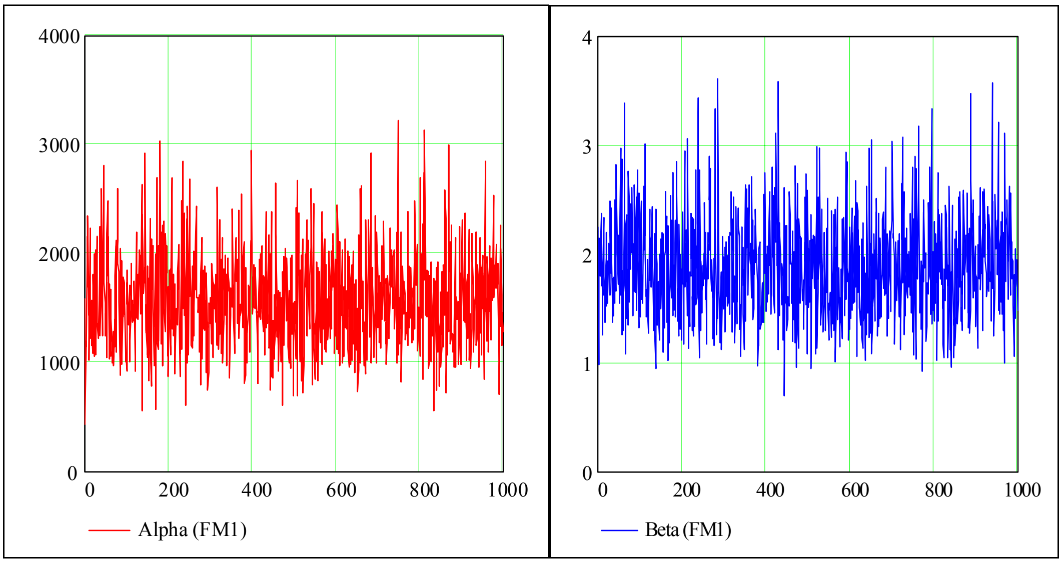

Figure 85: Iterative Variation of α and β for Valve Housing (S/No 10484)

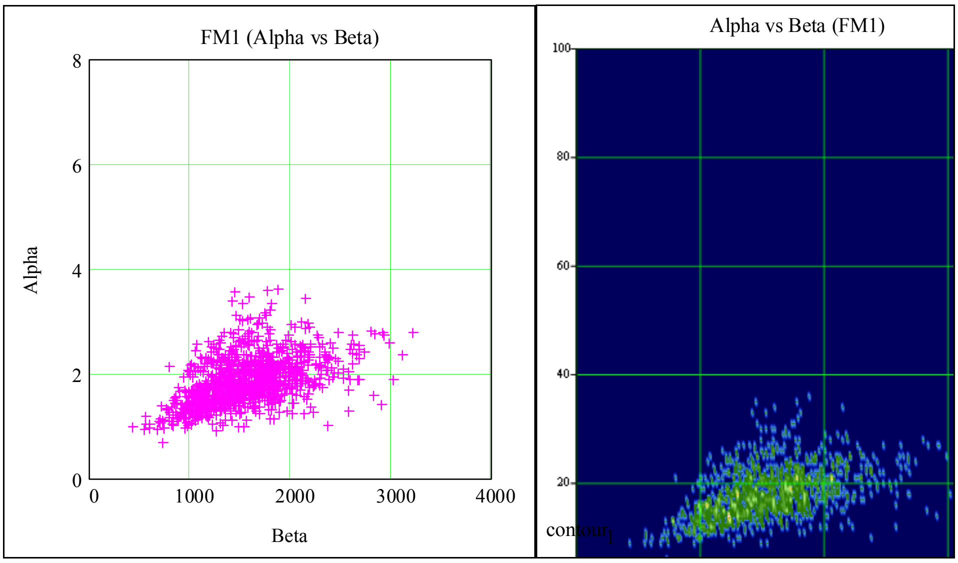

Figure 86: Iterative Variation of α versus β Graph for Valve Housing (S/No 10484)

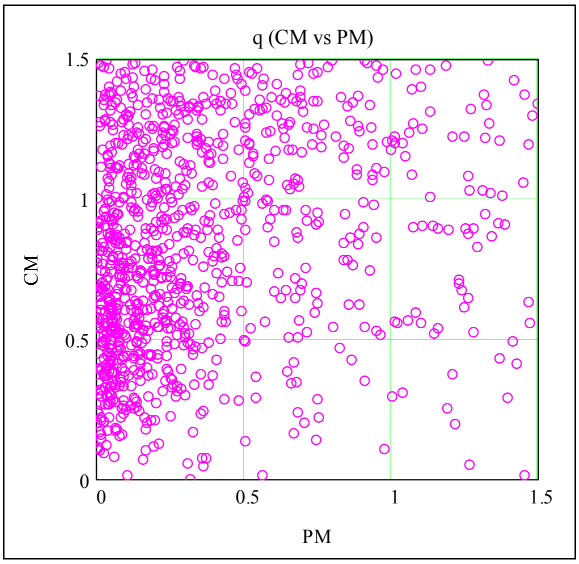

Figure 87: Iterative Variation of q_{CM} versus q_{PM} for Valve Housing (S/No 10484)

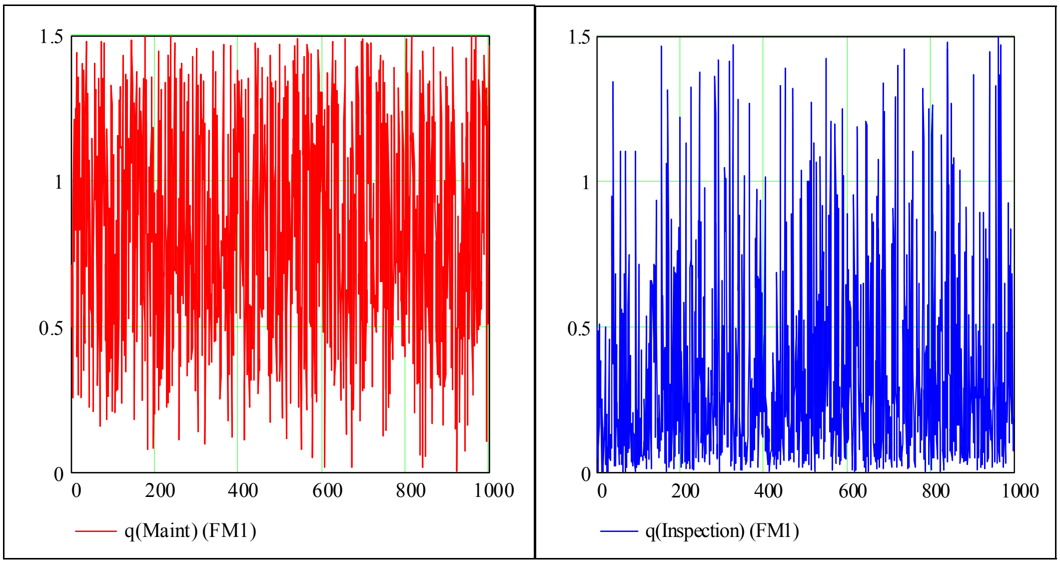

Figure 88: Iterative Variation of q_{CM} and q_{PM} for Valve Housing (S/No 10484)

	Mean	Standard Deviation
α	1570	431
β	1.873	0.46
q_{PM}	0.343	0.352
q_{CM}	0.831	0.379

Table 25: Final Run Parameter Estimator for Valve Housing (S/No 10484)

Step 6 – Re-run the CIF Simulator

Based on the number of sets of <α, β, q_{PM} and q_{CM}> data from the parameter estimator it was possible to provide a CIF curve of Valve Housing (S/No 10848), including the non-parametric 90% confidence limits. A graphical representation of the average CIF curve, including the non-parametric 90% confidence limits, initial data input into the model, RP (2-parameter Weibull) and NHPP (Power Law), is provided at Figure 89.

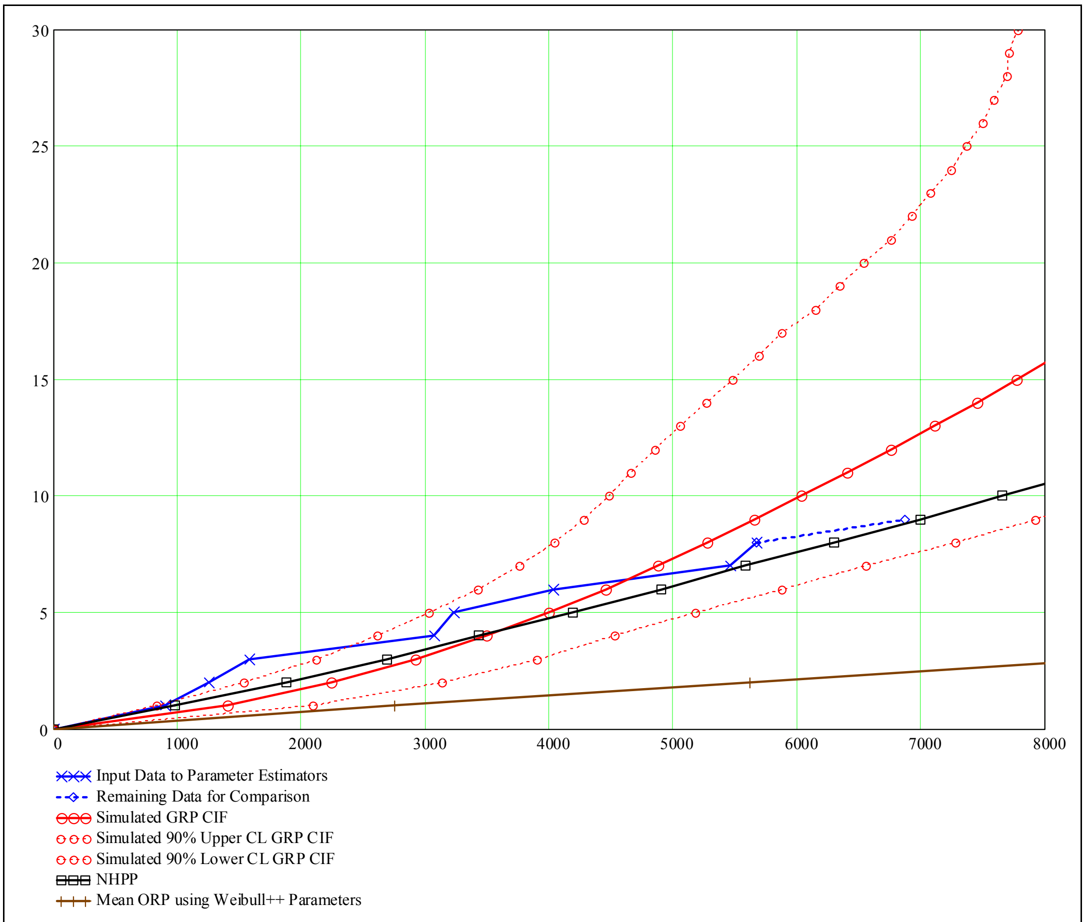

Figure 89: CIF Curve for Valve Housing (S/No 10484)

As can be seen from Figure 89 the simulated GRP CIF is more accurate in identifying the next TTF'\s, especially when compared to the RP model outcomes. Furthermore, it was interesting to observe the large difference between the *q*'s associated with the preventative maintenance (e.g. q = 0.343) which was significantly lower than the corrective maintenance (e.g. very similar q = 0.831). This difference in q highlighted the fact that the repairs appear to be less effective at rejuvenating the component to a state that was only slightly better than the NHPP assumption of "*as-bad-as-old*".

Case 4A Solution

Background

For the reasons previously stated the Case 4A results are based on simulated data for a repair item with two distinct failure modes which are not independent. The input to the data simulator is provided in Table 26.

Failure Mode 1	**Failure Mode 2**
α_{FM1}= 150 hours β_{FM1} = 1.5	α_{FM2} = 300 hours β_{FM2} = 3.5
$q_{inspection\_FM1}$ = 0.5	$q_{inspection\_FM2}$ = 1
$q_{maintenance\_FM1}$ = 0.7	$q_{maintenance\_FM2}$ = 0.2
$q_{maintenance\_FM1-2}$ = 1.2	$q_{maintenance\_FM2-1}$ = 0.2
Scheduled Inspection every 400 operating hours	

Table 26: Input to Data Simulator for Case 4A

To allow comparison of the model to the data, the whole set of data less the last 5 points was used by parameter estimator, while the simulator predicted the whole data set. A copy of the simulated data is provided at Appendix 5 – Case 4A Data.

Parameter Estimation

The estimator was run for 5,000 iterations with an interleave value of 5 resulting in 1,000 parameter sets of the various parameters. The initial guesses for the values are provided in Table 27.

Failure Mode 1	Failure Mode 2
$\alpha_{FM1} = 1$ $\beta_{FM1} = 1$	$\alpha_{FM2} = 1$ $\beta_{FM2} = 1$
$q_{inspection\_FM1} = 1$	$q_{inspection\_FM2} = 1$
$q_{maintenance\_FM1} = 0.5$	$q_{maintenance\_FM2} = 0.5$
$q_{maintenance\_FM1-2} = 1$	$q_{maintenance\_FM2-1} = 1$

Table 27: Case 4A Guess Values for Parameter Estimator

The results from the parameter estimator, including the variation over their individual space can be seen in Figure 90. From Figure 90 it possible to observe the variation of the two dependent failure modes.

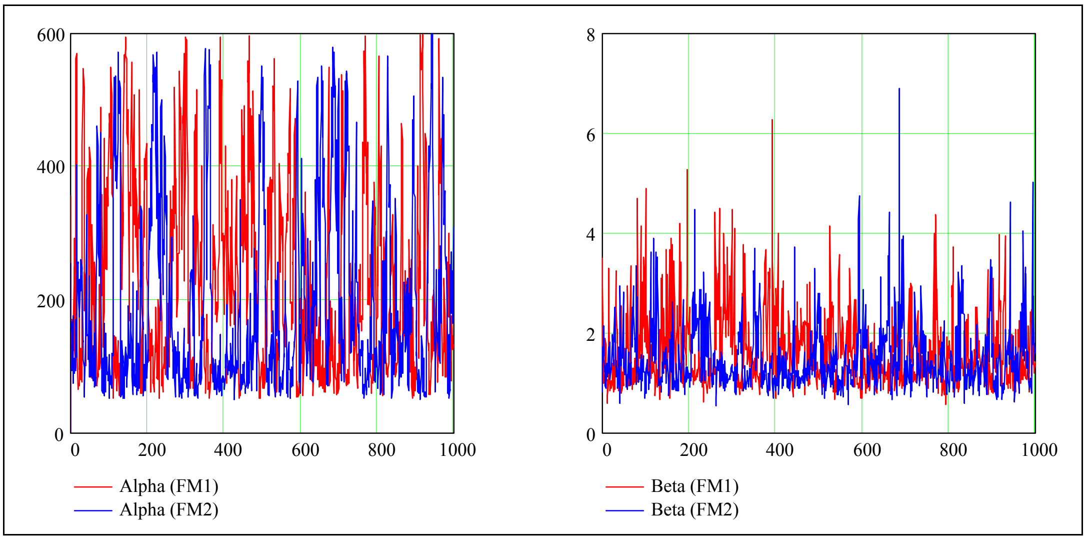

Figure 90: Variation of α and β Parameters for Case 4A Simulated Data

The variation in the α and β parameters for each failure mode can be observed better in Figure 91 and Figure 92 respectively.

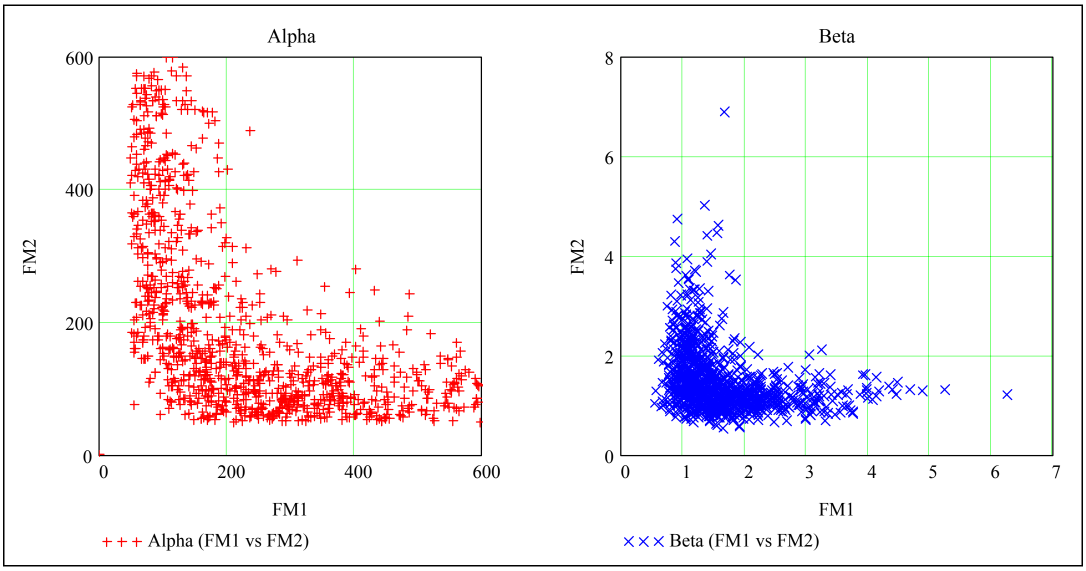

Figure 91: Comparison of α and β Parameters by Failure Mode for Case 4A Simulated Data

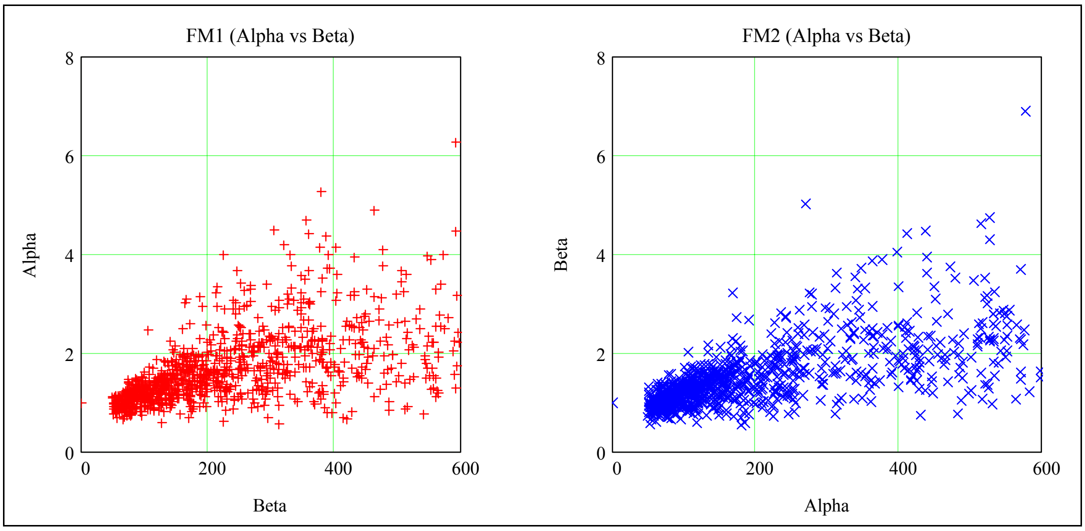

Figure 92: α and β Parameters Sets for Case 4A Simulated Data

Given the set-up of Case 4A it was also possible to observe the values of the q parameter for each failure mode for:

- Inspection,
- corrective maintenance (CM), and
- dependant q values for the CM activity.

Figure 93 provides a graphical representation of the variation of q for each of these factors while Figure 94 provides a comparison of q by failure mode.

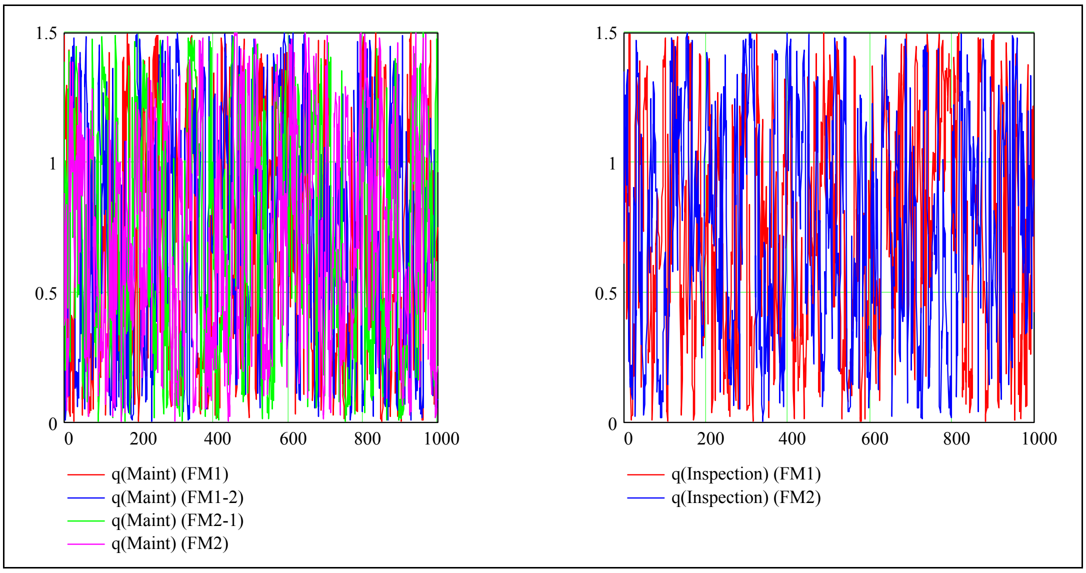

Figure 93: Variation of 'q' Parameters for Case 4A Simulated Data

As part of the results from the parameter estimator for α, β and q each of the parameters was assumed to be normally distributed and a mean and standard deviation calculated including *Pearson's r correlation coefficient*. The resulting values are provided in Table 28.

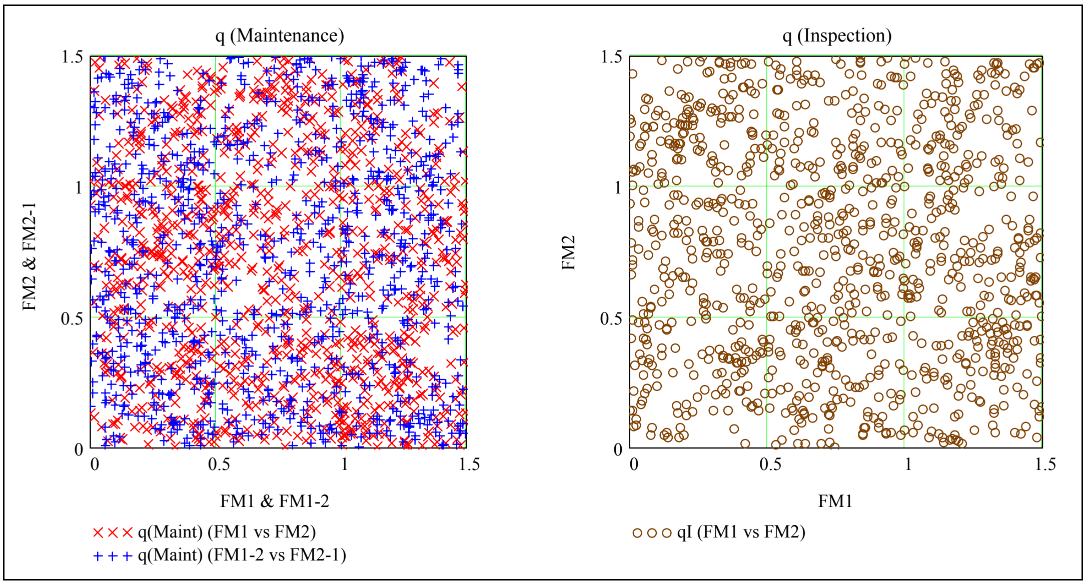

Figure 94: Comparison of 'q' by Failure Mode for Case 4A Simulated Data

Parameter	Mean	Standard Deviation	Pearson's r Correlation Coefficient
α_{FM1}	230.161	141.239	-0.147
α_{FM2}	196.247	141.207	0.07
β_{FM1}	1.657	0.741	-0.123
β_{FM2}	1.49	0.657	0.029
$q_{FM1\_Inspection}$	0.751	0.435	0.062
$q_{FM2\_Inspection}$	0.759	0.425	0.018
q_{FM1_CM}	0.7	0.437	0.031
$q_{FM1 \text{ due to } FM2}$	0.732	0.445	-0.097
q_{FM2_CM}	0.718	0.446	-0.046
$q_{FM2 \text{ due to } FM1}$	0.741	0.415	0.08

Table 28: Summary of Parameter Estimators for USS Grampus Data

CIF Simulation

Each of the set from the parameter estimator were then simulated 100 times and the averages recorded resulting in 1,000 CIF curves. The 1,000 CIF curves were then averaged to find the average CIF curve for all parameter sets, and the non-parametric 90% upper and lower confidence limits. The resulting CIF curve is provided at Figure 95.

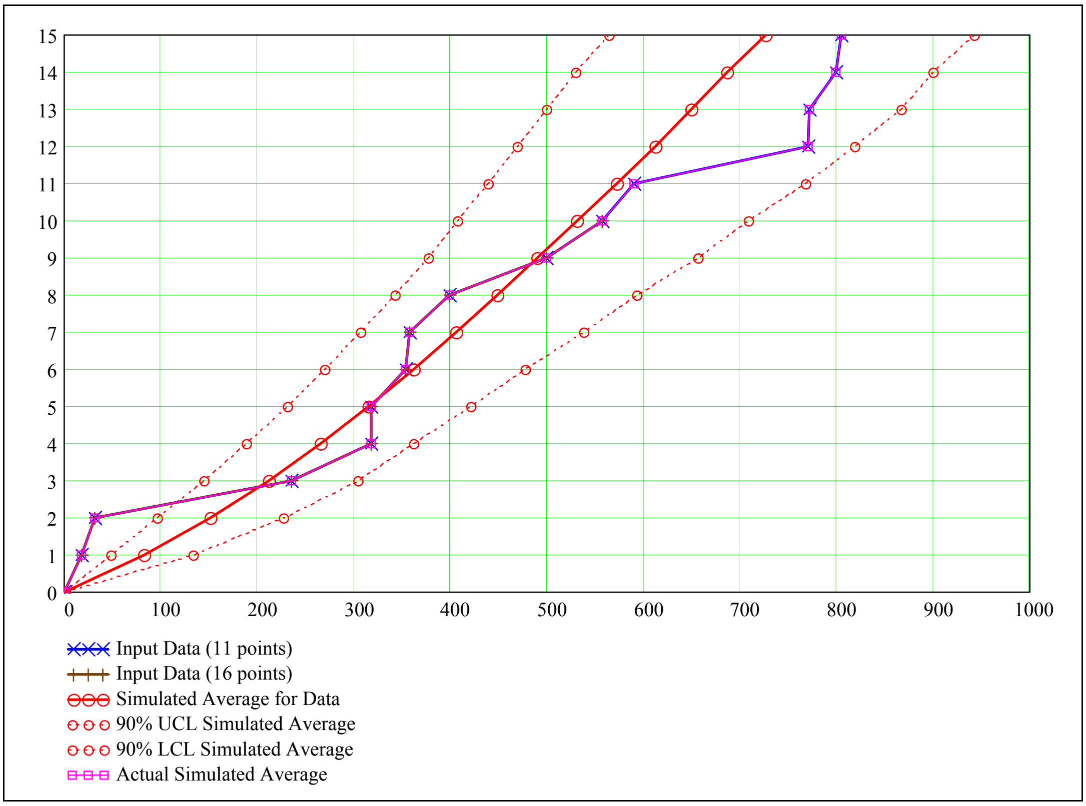

Figure 95: CIF Curve for Case 4A Simulated Data

As can been seen from Figure 95, the results predict the additional 5 data points, and the non-parametric ninety percentile upper and lower confidence limits effectively bound the simulated data.

Chapter 8: Conclusion

Summary

Over the duration of this research (since June 2002) I have seen the concept of the General Renewal Process (i.e. introducing *Virtual Age* into the Stochastic Point Processes to enable them to represent the full spectrum of repair assumptions) appears to have emerged at the forefront of academic literature. Furthermore, while there is a wide variation in potential models, a number of these models utilise an "age reduction" technique, (typically referred to as GRP), which is now widely accepted. As such, the Reliability Engineering community is beginning to see the benefit of moving away from the unrealistic maintenance assumptions of either the Ordinary Renewal Process (ORP) (i.e. *as-good-as-new*) or the Non-Homogenous Poisson Process (NHPP) (i.e. *as-bad-as-old*). Moreover, KAMINSKIY, et al[87], YANEZ, et al[88], METTAS, et al[89] and JACK[90] have all developed Maximum Likelihood Estimator (MLE) approaches to the single failure mode problem, some of which are implemented in Reliability software[91]. Additionally, HURTADO et al[92] provided an alternative to the MLE through the application of a Genetic Algorithm (GA).

---

87 KAMINSKIY, M. and KRIVTSOV, V., loc cit.

88 YANEZ, et al, loc cit.

89 METTAS, et al, loc cit.

90 JACK, N., loc cit.

91 Weibull++ (V7) by Reliasoft (http://www.reliasoft.com/Weibull/index.htm) and Bayesian reliability assessment tool (BRASS) (V1.2) by Prediction Technologies (http://www.prediction-technologies.com/products/brass.htm) for additional information.

While these solutions offer resolution of the maintenance assumption, they do not address the full spectrum of complexities that exists either in the Aviation industry, or in wider reliability community. Specifically, these complexities include the simultaneous ability to address:

- imperfect corrective and/or imperfect preventative maintenance for multiple failure modes existing in a single component;
- failure mode dependencies (e.g. repair of failure mode 1 may effect the *Virtual Age* of failure mode 2 by making the future failure earlier or later);
- imperfect inspection for multiple failure modes for a single component;
- data uncertainty in terms of unknown failure times (i.e. observe a failure at next inspection but cannot establish exactly when the failure occurred within the inspection period); and
- use of "soft-data" (e.g. data from similar equipment such as previous models, engineering judgement, etc) as an input to model.

Despite this trend the current engineering literature does not include any discussion on either the implementation or interpretation of the results (e.g. What does q = 0.67 mean? What should I do and why should I care?). Consequently, there is a potential that without an understanding of the underlying GRP methodology and subsequent

---

[92] HURTADO, et al, loc cit.

meaning and sensitivity of all the GRP variables, the GRP simply becomes a different type of 3-parameter Weibull equation for an analyst to use.

One of the reasons for the increasing interest in GRP is the desire for a more accurate model which may lead to a reduced Total Cost of Ownership (TCO). There is a high level of interest in the aviation industry which is dependent on the accuracy of failure prediction to determine spares holdings to maximise Operational Availability (A_o). When accuracy is assured profits are maximised through optimal utilisation of the individual aircraft. To achieve this, aviation operators (civil and military) the airlines will often purchase additional "insurance" spares to ensure the ALDT, specifically the delay due to a lack of a spare, is minimised. However, the cost of these "insurance" spares, both in terms of initial purchase and on-going repairs can represent a significant portion (up to 10%) of the TCO. For example, assuming a TCO for a major defence system is at least 500 million dollars (usually 10 times this), the management of RI's is therefore critical to ensure efficient and effective use of government, and ultimately, taxpayer, monies. Moreover, given the negligible profit margin for the commercial Aviation industry in the post 911 era, dependable RI model that more accurately reflects the aviation environment is clearly warranted.

Regardless of this need there are currently no solutions that simultaneously address the combined complexities of imperfect maintenance of multiple, dependent failure modes, imperfect inspections, data uncertainty and allow the contribution of various soft-data. Accordingly, the goal of this research was to address these complexities through completion of the following objectives:

- Develop a more "realistic" GRP model which addresses imperfect maintenance of multiple, dependent failure modes and imperfect inspection.
- Enable the use of a broader range of information type (i.e. engineering judgement, uncertain data, etc) with the explicit representation of all uncertainties, possibly through a Bayesian implementation.
- Provide an insight into behaviour of the model with changes in parameters through exploring the meaning of the model parameters including relating these parameter to operational and environmental factors, and applying the model to "real" data.

Research Contributions

In response to this demonstrated need, research was undertaken to meet the above objectives above were conducted to address both the development and implementation of a GRP model which realistically represents the life of an RI. The following summarises the research undertaken and illustrates the contributions to the management of RIs in the Aviation environment, and wider Reliability community.

Contribution 1 – Reformulate the GRP Model

The first contribution was the adaptation of the GRP model to address the realistic life of an RI. Specifically the transformation of the original single parameter, single failure mode KIJIMA Type I GRP model to a multivariate KIJIMA Type I GRP Model with the ability to manage:

- *Multiple dependant failure modes* – it is highly unlikely that any component will have only one failure mode, let alone failure modes that are independent (e.g. failure of a mechanical bearing will increase the heat within a component and may increase the probability of future "heat related" failure modes);
- *Imperfect corrective maintenance/preventative maintenance/inspection* – maintenance activities are conducted by a human and, by it's very nature, there is a reasonable likelihood of incorrect maintenance; and
- *Uncertainty in failure times* – given there are components where a failure is not observable during operation but only observed, and therefore repaired, during scheduled inspection point and it is reasonable that both are included in any model.

To allow the simple single parameter, single failure mode KIJIMA Type I GRP model to cater for these realistic additions, 10 cases were developed as part of this research allowing the analyst a board range of models that can be utilised in the modelling of any aviation RI based on:

(1) complexity of the component, and/or

(2) accuracy of failure/maintenance data.

The contribution from this part of the research was the development of a new GRP based model which has the ability to simulate the CIF of a representative life of an RI including imperfect maintenance of multiple, dependent failure modes, imperfect inspections and delays in repair actions.

Contribution 2 – Develop Bayesian Parameter Estimation Procedure

Given one of the objectives of the research was to ensure that any solution was able to utilise a broader range of information type (i.e. engineering judgement, uncertain data, etc) with the explicit representation of all uncertainties a Bayesian solution to the 10 Cases above was developed. The development of the Bayesian solution allows:

- Use of prior knowledge including engineering judgement; and
- Ability to manage uncertainty in the data (e.g. failure times of various individual failure modes, etc) and possible dependencies between failure mode (e.g. repair of failure mode 1 may effect the *Virtual Age* of failure mode 2).

The contribution from this part of the research was the development of Bayesian estimation procedure as the solution to the new GRP models which addressed the realistic life of an RI.

Contribution 3 – Develop a Numerical Procedure to Solve Bayesian Parameter Estimation Procedure

Given the GRP model produced was mathematically intractable, the research led to the development of a numerical estimation procedure to estimate the parameters for the Bayesian GRP model described above. As part of the development of the numerical estimation procedure an alternative sampler, known as the *Slice Sampler*, developed by NEAL[93] was utilised in lieu of the mode widely used Gibbs sampler or Metropolis-Hasting algorithm. The selection of the *Slice Sampler* was due to its unique ability to work with little to no tuning, or knowledge of an appropriate distribution. Furthermore, the *Slice Sampling* technique has the ability to:

- evaluate a "black-box" function that is proportional to its density, and in some cases, to also evaluate the gradient of this function; and
- include a Bayesian prior to facilitate the input of soft-data.

Unfortunately, the implementation of the *Slice Sampler* was not without difficulty. The two main challenges were (1) establishing an *f(x),* and (2) limited guidance of the

[93] NEAL, R, loc cit

implementation since, although the *Slice Sampler* has been informally published in 2003, there is no literature of implementation of this sampling technique.

Contribution 4 – Insight into Behaviour of the Model with Changes in Parameters

The final contribution of this research was insight into the behaviour of the GRP model for all cases, simple and complex, which has been missing from engineering literature. This insight allows the reader to answer the traditional question of "so what?". Should I spend my limited budget on fixing imperfect inspection or imperfect maintenance? Are there some rules of thumb to support these questions? Which GRP model should I use and why? Without acknowledging the methodology there is the potential that the results, and potentially the decision(s) that may result from the analysis to be in error. For example, it has been observed that the Time To Failure (TTF) of the KIJIMA Type I GRP model is:

- very sensitive to variation of low values of q (e.g. $0 \leq q \leq 0.2$); and
- very sensitive to variation in the value of β.

Furthermore, when examining the effect on multiple q, whether representing change $q_{inspection}$ or $q_{maintenance}$, there is a significant difference in effect based on the link to the dominant failure mode. In this circumstance the dominant failure mode is the one that results in the most renewals. Specifically that slight variations to the dominant failure mode will have comparatively larger impact on the CIF curve. Therefore, any resource (i.e. personnel and/or funding) consideration should be aligned to "fixing" the dominant failure mode.

Future Area(s) of Research

Not being content with this representing the end of the journey there are some facets of this research that should be continued. They are as follows:

Access to Aviation Datasets

Given the issue with data at the time of writing the main aim of the additional work is to apply this technique to a number of actual Australian Department of Defence (DOD) aviation datasets for a series of parts to examine the variation of the GRP parameters. There is particular interest in comparing q between items due to operational factors such as the operating location, maintenance facility/staff, maintenance tools/manuals/procedures, incorporation of a design change/modification, mission profile, etc.

The ability to get access to high fidelity datasets based on individual serial number is assessed as likely since there are a number of large acquisition contracts[94] which require Reliability Demonstration Tests as part of their contracts.

94 Project AIR 5077 – Airborne Early Warning & Control (AEW&C), Project AIR 5402 – Multi-Role Tanker/Transport and Project AIR 9000 Phase 1A – Additional Troop Lift Helicopter

Transfer to to C++ Windows® based environment

While not essential, one area to be completed in the transfer of the algorithms for the individual cases from development environment, MathCad®, to C++ Windows® based environment including optimising the code for speed. This development would be expected to aid the model's commercial application/acceptance.

Use of *q* as a Metric within Performance Based Logistic (PBL) Contracts

One area of significant interest to the author, and area of work for the next 2 years (i.e. January 2006- December 2007) is the possible use of the GRP equations as a measure of the effectiveness of maintenance activities. Given the Australian DOD desire, reflecting the majority of Western militaries, to outsource "non-core" activities, in this case Deeper Maintenance (DM) and RI Maintenance, new contractual frameworks are being constructed to focus on achievement of contract outcome rather than monitoring the process. Specifically recent Australian DOD research[95] has shown that while the outcomes are aspirational statements of military priorities, they are underpinned by physical performance characteristics. Accordingly, the RAM characteristics of Availability, Reliability, Maintainability and Supportability of an RI provided a framework for developing ASD outcomes (see Figure 96) for all systems (e.g. defined at a whole of aircraft level) and RIs.

---

95 RICHARDSON, D. and JACOPINO, A., "Use of R&M Measures in Australian Defence Aviation Performance Based Contracts", Reliability, Availability and Maintainability Symposium (RAMS), Newport Beach, CA, USA, 2006

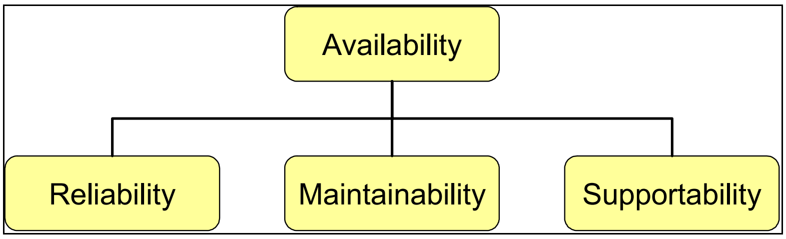

Figure 96: Relationship between Availability and Reliability, Maintainability & Supportability

As a part of this activity Strategic [Australian] Defence and Aviation doctrine was then examined to align system level characteristics to Defence priorities. Ultimately, *Systems Readiness* (Availability), *Mission Reliability* (Reliability), *Light Footprint* (Maintainability) and *Assurance of Supply* (Supportability) were chosen and are defined in Table 29. These metrics are defined in detail, including their implementation, in the Australian DOD Aviation System Division (ASD) Performance Based Contract (PBC) Handbook[96], which was a co-authored by the author of this paper.

Where the use of q has the greatest potential to benefit is in the management of the Deeper Maintenance and/or RI contracts. Additional Australian DOD research has shown that the performance at this level can be defined in terms of three outcomes as follows:

- Timeliness of maintenance/repair;
- Quality of Workmanship, and
- Consistency of maintenance/repair.

---

96 Aviation System Division (ASD) Performance Based Contract (PBC) Handbook – *Guiding Principles and Performance Framework*, 1st Ed., Australian Department of Defence, Canberra, Australia, 2005

Clearly the GRP framework by definition lends itself to a measurement of the *Quality of Workmanship* metric, however, the key to its utilisation within a contractual framework is linking the value of q to the extent of the maintenance/repair Contractor's responsibilities. That is to ensure that the maintenance/repair Contractor can control this value. This is a non-trivial exercise especially considering that under current Australian DOD policy, approximately 30% of the *At Stake margin*[97] of these contracts may be linked to the performance of q.

Outcome	**Explanation**
Systems readiness	The state of readiness of systems required to perform a specified mission or task.
Mission Success	A measure of the ability of an item to perform its specified mission under stated operating conditions.
Light footprint	Minimising the logistics support required for Weapon Systems in order to reduce vulnerability to attack and dependence on transportation.
Availability of Parts	Confidence in the provision of the right materiel and services, at the right place, at the right time and with the right quality, and to sustain that support over time.

Table 29: Summary of ASD Sustainment Outcomes

[97] The At Stake margin typically is equal to the amount of profit of approximately 10% – 15% of contract price. For example, if the annual cost of an individual contract is $10,000,000 and has an At Stake margin – profit margin = 10%, then the *Quality of Workmanship* metric will be equal to $300,000 per year. This will clearly get the attention of the contractor; the whole idea of performance based contracting.

Appendix 1 – Case 1A Data[98]

Renewal Number	USS Grampus Data ('000 Hours)	USS Halfbeak Data ('000 Hours)
0	0	0
1	0.86	1.382
2	1.258	2.99
3	1.317	4.124
4	1.442	6.827
5	1.897	7.472
6	2.011	7.567
7	2.122	8.845
8	2.439	9.45
9	3.203	9.794
10	3.298	10.848
11	3.902	11.993
12	3.91	12.3
13	4	15.413
14	4.247	16.497
15	4.411	17.352
16	4.456	17.632
17	4.517	18.122
18	4.899	19.067
19	4.91	19.172
20	5.676	19.299
21	5.755	19.36
22	6.137	19.686
23	6.221	19.94
24	6.311	19.944
25	6.613	20.121
26	6.975	20.132
27	7.335	20.431
28	8.158	20.525
29	8.498	21.057
30	8.69	21.061
31	9.042	21.309
32	9.33	21.31
33	9.394	21.378

98 MEEKER, W.Q.et al, op cit, pg 395.

Renewal Number	USS Grampus Data (‘000 Hours)	USS Halfbeak Data (‘000 Hours)
34	9.426	21.391
35	9.872	21.456
36	10.191	21.461
37	11.511	21.603
38	11.575	21.658
39	12.1	21.688
40	12.126	21.75
41	12.681	21.815
42	12.795	21.82
43	13.399	21.822
44	13.668	21.888
45	13.78	21.93
46	13.877	21.943
47	14.007	21.946
48	14.028	22.181
49	14.035	22.311
50	14.173	22.634
51	14.173	22.635
52	14.449	22.669
53	14.587	22.691
54	14.61	22.846
55	15.07	22.947
56	16	23.149
57	-	23.305
58	-	23.491
59	-	23.526
60	-	23.774
61	-	23.791
62	-	23.822
63	-	24.006
64	-	24.286
65	-	25
66	-	25.01
67	-	25.048
68	-	25.268
69	-	25.4
70	-	25.5
71	-	25.518

Appendix 2 – Case 4A Data for Valve Housing (Part No 710085-1) – Serial No 1244

Date Raised	Serial Number	LIFE SINCE OH ENHRS	LIFE SINCE NEW ENHRS	RR	Fault Symptom	WFD	USC	Unserviceability Details	FF	MAT	Maintenance Comment
24 Mar 86	1244	432.9	432.9	01	28 DEG MICRO ON ALPHA SHAFT WILL NOT ACTUATE	28	03	28 DEG MICRO ON ALPHA SHAFT WILL NOT ACTUATE	03	02	MICRO REP WITH A SERV ITEM
18 Apr 86	1244	497.0	497.0	01	28 DEG SW TO BE CALIBRATED AND TESTED	27	06	28 DEG SW TO BE CALIBEATED AND TESTED	07	03	MICRO ADJUST CHECK SERV
10 Feb 92	1244	2253.7	2253.7	01	NO FEATHER	01	02	FAILED FEATHER MICRO	03	02	
03 Jun 92	1244	2444.5	2444.5	01	WONT PULL REVERSE HORSEPOWER	02	07	METS SUSPECT STICKY PILOT VALVE	02	02	BB
04 Jun 93	1244	2444.5	2444.5	01	PITCHLOCK RESET OUT OF ADJUSTMENT - FOUND DURING INSTALLATION	27	06	PITCHLOCK RESET SWITCH OUT OF ADJUSTMENT	09	02	BB
12 May 94	1244	2935.1	2935.1	01	TWENTY EIGHT DEGREE SW MADE CONTINUALLY	02	03	FAILED SW	03	02	AA ALPHA SHAFT SWITCH REPLACED
07 Nov 94	1244	3015.4	3015.4	01	BETA LIGHT FAILS TO ILLUMINATE IN GROUNG ANGE	02	11	BETA LIGHT INOP	03	02	BB
01 Aug 95	1244	3313.4	3313.4	10	FLUCTUTATIONS BEYOND SERV LIMITS	02	02				OH CONDUCTED
01 Aug 95	1244	3313.4	3313.4	03		00	00		01	07	BB
01 Mar 99	1244	651.1	3964.5	01	ELEC FAIL	31	03		03	02	BETA SWITCH REPLACED WITH SERV ITEM
12 May 00	1244	1044.4	4357.8	01	OVERSPEED TO 102 PERCENT DURING NTS CHECK	01	06	MECHANICAL GOVERNING	09	02	AA
28 Oct 00	1244	1051.5	4364.9	01	OVERSWING PLUS MINUS 3 PERCENT	02	02	SUSPECT GOVERNOR	15	02	AA
08 Apr 02	1244	1408.0	4721.4	01	NO CHANGE INDICATED WHEN REVERSE HP ADJUSTED	02	02	RAN OUT OF REVERSE HP ADJUSTMENT	15	02	AA

Appendix 3 – Case 4A Data for Valve Housing (Part No 710085-1) – Serial No 10484

Date Raised	Serial Number	LIFE SINCE OH ENHRS	LIFE SINCE NEW ENHRS	RR	Fault Symptom	WFD	USC	Unserviceability Details	FF	MAT	Maintenance Comment
27 Jul 84	10848	902.5	902.5	01	NTS INOP LT AT FEATHER	01	03	AIR START MICRO SW CONTINUALLY MADE	07	03	AIR START SWITCH ADJUSTED
05 Aug 85	10848	1254.8	1254.8	01	FAILED	26	06	OUT OF TOLERANCE	01	04	FEATHER LIGHT TX
12 Nov 86	10848	1581.3	1581.3	01	NO FEATHER LIGHT	01	03	MICRO SWITCH FAILURE	09	02	
08 Jun 90	10848	3073.4	3073.4	01	NTS LIGHT INTERMITTANT	02	10	FEATHER MICRO ADJUSTED	07	01	
15 Oct 90	10848	3232.0	3232.0	01	POWERLEVER TO REVERSE ENG RPM DECAYED SECURED ENG	02	10	FAULT COULD NOT BE REPRODUCED	02	02	
05 Aug 92	10848	4036.8	4036.8	10	ENG OSPEED WHEN SYNC ON	02	06	SPEED BIAS MOTOR IRRATIC	02	02	BB
07 Aug 98	10848	5461.3	5461.3	03					01	07	AA
24 Nov 99	10848	216.7	5678.0	01	NIL FEATHER VALVE LITE DURING NTS CHECK	01	02	INOPERATIVE FEATHER VALVE MICRO	03	02	AA FEATHER VLV MICRO REPLACED
28 Nov 02	10848	1410.3	6871.6	01	ELECTRICAL FAILURE	04			03	02	REPAIR
24 Aug 05	10848	1566.7	7028.0		CURRENT LIFE STILL SERV						

Appendix 4 – Codes for Maintenance Management System for Case 4A Data – Valve Housing (Part No 710085-1)

Fault Found
A set of mutually-exclusive codes that describe the nature of any fault found (if any) on an item or MMI during the course of a Job or Arising. These codes are listed and defined below and can be found on the reverse side of the EE435 form or the back page of a blank CAMM2 Travel Tag.

01	No Fault	06	Moisture	11	Faulty Lubrication	16	Faulty Ordnance
02	Mechanical Component Fail	07	Bad Adjust/Align	12	Corroded	17	Ordnance Feed/ Release Fault
03	Electrical Component Fail	08	Damage	13	Faulty Manufacture	18	Software/Data Fault
04	Open Circuit	09	Out of Tolerance	14	System Tolerance High/Low		
05	Short Circuit	10	Contaminated	15	Expected Deterioration		

Maintenance Action Taken
A set of mutually-exclusive codes that describe the type of preventative or corrective maintenance performed on an item or MMI in order to resolve or complete a Job or Arising. These codes are listed and defined below and can be found on the reverse side of the EE435 form or the back page of a blank CAMM2 Travel Tag.

01	Repair in Situ	04	Check/Test Serv	07	Overhaul	10	Calibration
02	Repair	05	ESA/Throwaway	08	Mod/STI Incorp	11	Special Servicing
03	Adjust/Align	06	Bay Service	09	Throwaway Storage		

Reason for Report
A set of mutually-exclusive codes that describe the original reason why a Job or Arising was initially raised or opened on an item or MMI. These codes are listed and defined below and can be found on the reverse side of the EE435 form or the back page of a blank CAMM2 Travel Tag.

01	Failure	06	Calibration Due	11	FOD	16	Pre-Installation Maint
02	Bay Service Due	07	Scheduled System Performance Monitoring	12	Damaged	17	Reduce to Spares
03	Overhaul Due	08	Mod/STI Required	13	Removed for Access	18	Special Servicing Due
04	Throwaway Due	09	Cannibalisation	14	Configuration Change		
05	Scheduled Functional Check/Test	10	Abnormally Operated	15	Fault Finding		

Unserviceability Code
A set of mutually-exclusive codes that describe the nature of the unserviceability identified (if any) against an item or MMI during the course of a Job or Arising. These codes are listed and defined below and can be found on the reverse side of the EE435 form or the back page of a blank CAMM2 Travel Tag.

01	Damaged/Cracked	06	Out of Tolerance	11	Inoperative	16	Worn/Frayed
02	Mechanical Failure	07	Binding	12	Contaminated	17	Delaminated/Eroded
03	Electrical Failure	08	Blocked	13	Corroded	18	Noisy/Vibrations
04	Overheated	09	Leaking	14	Deteriorated	19	System Investigation
05	Overspeed/ Overstressed	10	Intermittent	**15**	**NO LONGER USED**		

When Failure Discovered
A set of mutually-exclusive codes that describe at what point a Failure was discovered against an item or MMI at the commencement or during the course of a Job or Arising. These codes are listed and defined below and can be found on the reverse side of the EE435 form or the back page of a blank CAMM2 Travel Tag.

01	In Flight	10	R3 Servicing	19	D Servicing	28	Higher Assembly Maintenance
02	During Operation	11	R4 Servicing	20	E Servicing	29	During Mod/STI
03	During Standby	12	Other R Servicing	21	Pre-Deployment Servicing	30	During Cannibalisation
04	Aircrew B/F	13	Special Servicing	22	Post-Deployment Servicing	31	During Access
05	Technical B/F	14	Analytical Condition Inspection	23	System Performance Monitoring	32	During Fault Finding
06	Turnaround	15	Depot Level Maintenance	24	Calibration	33	During Config Change
07	After Flight	16	A Servicing	25	Other Scheduled Servicing	34	During Flex Op Servicing
08	R1 Servicing	17	B Servicing	26	Pre-Installation Maint	35	During Reduction to Spares
09	R2 Servicing	18	C Servicing	27	Functional Check/ Test	**99**	**No Fault (U/S's ONLY)**

Appendix 5 – Case 4A Data

Renewal No	0	1	2	3	4	5	6	7	8	9	10	11	12	13	14	15
Time To Failure	0	19	33	236	318	318	354	359	400	500	558	591	771	773	800	805
Activity	-	CM FM1	CM FM1	CM FM2	CM FM1	CM FM2	CM FM1	CM FM2	I	CM FM2	CM FM1	CM FM2	CM FM1	CM FM2	I	CM FM1

Where:

I = Inspection

CM FM1 = Corrective Maintenance – Failure Mode 1

CM FM2 = Corrective Maintenance – Failure Mode 2

Glossary

Administrative Delay Time	ADT	The accumulated time during which an action of corrective maintenance on a faulty item is not performed due to administrative reasons. Typical examples of ADT include time raising paperwork for the job, time assigning personnel priorities, Labour strike, time taken to travel to equipment site, time taken to complete paperwork to release equipment from maintenance, etc.
After Flight	AF	The maintenance, including inspection, conducted by the Operational Level maintenance personnel after a flight had been completed.
Before Flight	BF	The maintenance, including inspection, conducted by the Operational Level maintenance personnel before an aircraft is release for a flight. May be equivalent to the TA maintenance.
Carried Forward Unserviceability	CFU	The RAAF terminology for the delay in repair of a component before the next flight to allow the aircraft to complete a scheduled mission. A CFU is only allowed on certain components that do not affect safety, and can only be authorised by specifically appointed personnel.
Corrective Maintenance	CM	
Cumulative Intensity Function	CIF	
Cumulative Distribution Function	CDF	
General Renewal Process	GRP	
Genetic Algorithm	GA	
Logistics Time Delay	LTD	The accumulated time during which a maintenance action cannot be performed due to the necessity to acquire maintenance resources, excluding any administrative delay. LDT includes time waiting for a Spare to become available, time waiting for an item of test equipment, time waiting for transportation, time waiting to use a facility, etc. LDT may also be referred to as Supply Delay Time.
Non-Homogenous Poisson Process	NHPP	Repairable Item model which uses *as-bad-as-old* repair assumption.
Ordinary Renewal Process	ORP	Repairable Item model which uses *as-good-as-new* repair assumption.
Preventative Maintenance	PM	

Royal Australian Air Force	RAAF	Information on the RAAF can be obtained from the official web site located at http://www.defence.gov.au/raaf/main.htm.
Rectification		Any corrective maintenance that requires the aircraft to be removed from the Flight Line as a result of failures that were identified either during the previously flight or during a pre/post flight inspection (e.g. BF, AF or TA).
Repairable Item	RI	*An item which can be restored to perform all of its required functions by corrective maintenance*, Military Standard 721C (MIL-STD-721C), Definitions of Terms for Reliability and Maintainability, 12 June 1981, pg 9
Serviceable		The RAAF terminology use to describe when an aircraft, system or sub-system is in a working or operational state.
Turn-Around	TA	The maintenance, including inspection, conducted by the Operational Level maintenance personnel between successive flights on the same day.
Time-To-Failure	TTF	
Unserviceable	U/S	The RAAF terminology use to describe when an aircraft, system or sub-system is in a failed state.

Bibliography

[United Kingdom Ministry of Defence (MOD)] Defence Standard (DEFSTAN) 02-45 (NES 45), *Requirements for the Application of Reliability-Centred Maintenance Techniques to HM Ships, Submarines, Royal Fleet Auxiliaries and other Naval Auxiliary Vessels - Category 2*, Issue 2, UK Ministry of Defence, 14 July 2000

[United States] Military Standard (MIL-STD) 1309D, *Definitions of Terms of Testing, Measurement and Diagnostics*, 12 February 1992

[United States] Military Standard (MIL-STD) 721C, *Definitions of Terms for Reliability and Maintainability*, 12 June 1981

MathCad 2001 - User's Guide with Reference Manual, Mathsoft, USA, 2001

ABDEL-HAMEED, M., Inspection, Maintenance and Replacement Models, *Computers & Operations Research*, Vol 22, No. 4, Apr, 1995, pp 435-441

Aviation System Division (ASD) Performance Based Contract (PBC) Handbook – *Guiding Principles and Performance Framework*, 1st Ed., Australian Department of Defence, Canberra, Australia, 2005

ASHER, H. and FEINGOLD, H., Repairable Systems Reliability, Marcel Dekker, New York, USA, 1984

COLLINS, J.A. *"Failure of Materials in Mechanical Design – Analysis, Prediction, Prevention"*, 2nd Ed., John-Wiley & Sons, USA, 1993

DAGPUNAR, J.S., *"Renewal-type equations for a general repair process"*, Quality and Reliability Engineering International, Vol 13, No 4, July-Aug. 1997, p. 235-45

ELBING, *"An Introduction of Reliability and Maintainability Engineering"*, McGraw-Hill, USA, 1997

GRALL, A., DIEULLE, L., BÉRENGUER, C., ROUSSIGNOL, M., Continuous-Time Predictive-Maintenance Scheduling for a Deteriorating System, *IEEE Transactions on Reliability*, Vol 51, No.2, June 2002

GROEN, F., "*Bayesian Framework for General Renewal Process Modelling Report*", Technical Paper, University of Maryland, 2002

GROEN, F., *"Supplement to 'Bayesian Data Analysis for General-Renewal Process'"*, Technical Paper, University of Maryland, 2003

HOSSEINI, M.M., KERR, R.M., RANDALL, R.B., Hybrid Maintenance Model with Imperfect Inspection for a System with Deterioration and Poisson Failure, *Journal of the Operational Research Society*, 50, 12, Dec 1999, p 1229-1243

HOYLAND, A. and RAUSAND, M., System Reliability Theory, John Wiley and Sons, USA, 1994

HURTADO, J.L., JOGLAR, F. and MODARRES, M., "*Generalized Renewal process: Models, Parameter Estimation and Applications to Maintenance Problems*", International Journal of Performability Engineering, Vol1, No. 1, July 2005, pp 37-50

JACK, N., "*Age Reduction Models for Imperfect Maintenance*", Mathematical Sciences Division, School of Informatics, University of Abertay, Dundee, Scotland

JACK, N., "*Analysing Event Data from a Repairable Machine Subject to Imperfect Preventative Maintenance*", Mathematical Sciences Division, School of Informatics, University of Abertay, Dundee, Scotland

JACOPINO, A., GROEN, F. and MOSLEH, A., Behavioural Study of the General Renewal Process, *Reliability, Availability and Maintainability Symposium (RAMS)*, Los Angles, CA, USA, 2004

KAMINSKIY, M. and KRIVTSOV, V., *"A Monte Carlo Approach to Estimation of G-Renewal Process in Warranty Data Analysis"* 2nd International Conference on Mathematical Methods in Reliability, Bordeaux, France, 4-7th July 2000

KAMINSKIY, M. and KRIVTSOV, V., *"A Monte Carlo Approach to Repairable System Reliability Analysis"* in *Probabilistic Safety Assessment and Management*, Springer-Verlag London Ltd, 1998, pp 1063-1068

KAMINSKIY, M. and KRIVTSOV, V., "*G-Renewal Process as a Model for Statistical Warranty Claim Prediction*", 2000 Reliability and Maintainability Symposium, 24-27th January 2000, Los Angeles, California, USA

KIJIMA, M. and SUMITA, U., *"A Useful Generalisation of renewal Theory: Counting Processes Governed by Non-Negative Markovian Increments"*, Journal of Applied Probability, #23, 1986, pp. 71-88

KIJIMA, M., "*Some Results for Repairable Systems with General Repair*", Journal of Applied Probability, #20, 1989, pg 851 - 859

LAW, A.M. and KELTON, *Simulation Modelling and Analysis*, 3rd Ed., McGraw-Hill Higher Education, USA, 2000

MEEKER, W.Q., ESCOBAR, L.A., *Statistical Methods for Reliability Data*, Wiley Interscience, USA, 1998

METTAS, A. and ZHAO, W, Modeling and Analysis of Repairable Systems with General Repair, *2005 Proceedings Annual Reliability, Availability and Maintainability Symposium (RAMS06)*, Alexandria, VA, USA, 24-27 Jan 2005

MODARRES, M., KAMINSKIY, M. and KRIVTSOV, V., *Reliability Engineering and Risk Analysis – A Practical Guide*, Marcel Dekker, Inc, New York, USA, 1999

MOSLEH, A., *ENRE655 – Advanced Reliability Modelling Course Notes*; University of Maryland, USA, 2005

NEAL, R. M., *Slice Sampling*, The Annals of Statistics, Vol 31, No. 3, 2003

NELSON, W. B., Accelerated Testing : Statistical Models, Test Plans, and Data Analysis, Wiley Series in Probability and Statistics, Wiley-Interscience, USA, 1990

RICHARDSON, D. and JACOPINO, A., “Use of R&M Measures in Australian Defence Aviation Performance Based Contracts”, *Reliability, Availability and Maintainability Symposium (RAMS)*, Newport Beach, CA, USA, 2006

SRIVASTAVA, M. S. and YANHONG, W., Estimation & Testing in an Imperfect-inspection Model, *IEEE Transactions on Reliability*, v 42, n 2, Jun, 1993, p 280-286

WALL, M., Modelling of Inspection Reliability, *IEEE*, 1996

YANEZ, M., JOGLAR, F, and MODARRES, M., “Generalized renewal process for analysis of repairable systems with limited failure experience”, Reliability Engineering and System Safety, Vol 77, USA, 2002